Geology, Geochemistry and Tectonic Setting of Conglomerates and Quartzites of the Bababudan Schist Belt, Karnataka Nucleus, India

ABSTRACT OF THE
THESIS SUBMITTED IN PARTIAL FULFILMENT OF THE REQUIREMENT
FOR THE AWARD OF THE DEGREE OF

DOCTOR OF PHILOSOPHY

IN

GEOLOGY

BY

Mukesh Arora

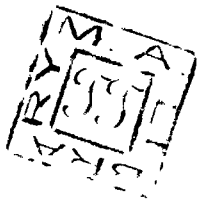

FACULTY OF SCIENCE
DEPARTMENT OF GEOLOGY
ALIGARH MUSLIM UNIVERSITY
ALIGARH

1991

A B S T R A C T

Greenstone belts of the Dharwar Craton (DC), Karnataka nucleus (KN) are one of the most important volcano-sedimentary rocks of Archaean eon for the understanding of crustal evolution of the early Earth. These belts have been divided into older and younger greenstone belts. Younger greenstone belts rest with a pronounced unconformity on an older crust made up of tonalite - trondhjemite gneisses (TTG), granodiorite and older greenstone belts comprise of mafic-ultramafic spinifex textured komatiite flows and chemogenic sediments. The volcano-sedimentary sequence in the younger greenstone belts, is subdivided into the Bababudan Group and the Chitradurga Group. The present thesis is devoted to the sedimentary constituents of the Bababudan Group exposed in the Bababudan schist belt, which is its type area. Volcanic sequence of this belt has been studied in fair detail by earlier workers (Bhaskar Rao and Naqvi, 1978; Bhaskar Rao, 1980). Sedimentary structures and depositional environment of the QPC and quartzites have been studied by Srinivasan and Ojakangas (1985). However, geochemistry of the sedimentary rocks had not been studied in detail . A comprehensive attempt has been made to study the sedimentological and geochemical characters of the quartzites and conglomerates of the belt in the present work.

The Bababudan Group in the Bababudan schist belt is divided into four formations (Viswanatha and Ramakrishnan 1981). The subdivision has been made on homogeneity of lithologies or lithotectonic association which in ascending order are the Kalasapura, the Allampur, the Santaveri at the Mulaingiri

Formations. Chadwick et al.(1985a) have enlarged the previous subdivisions and redefined the younger subdivisions in terms of an additional formation, viz. the Mundre Formation. Major emphasis in the work has been on the Kalasapura Formation and the Mundre Formation which are made up of quartz pebble conglomerate(QPC), Quartzites and the Kaldurga Conglomerate(KCM) respectively. The objectives of this work are to (1) elucidate the evolution of the basin, (2) estimate the composition of the crust exposed during middle and late Archaean and (3) infer the nature or exogenic and tectonic processes at that time.

Large scale geological mapping in selected spots of the conglomerates and quartzites, palaeocurrent measurements based on current bedding quartzites and imbrication of pebbles in the Kaldurga Conglomerate were carried out in the field. Thirty samples of the basal QPC , twenty samples of quartzites associated with QPC, and forty nine samples of the Kaldurga Conglomerate were collected from fresh and unaltered exposures. Statistical analyses of palaeocurrent data and grain size distribution of QPC and associated quartzites indicate that these are mineralogically and texturally mature sediments and that were deposited in a fluvial regime of a stable platformal environment. The presence of rounded grains of pyrite in the matrix of QPC indicates their detrital nature, derivation and transport under anoxic atmosphere and deposition in a reducing environment.

Modal analysis of the QPC, quartzites and the KCM was carried out to measure different mineral constituents. QPC mainly consists of vein quartz pebble and in its matrix, detrital pyrite,

uraninite and gold along with quartz, fuchsite and other micas are found. Rounded to subrounded pebbles of vein quartz generally have contact framework and the matrix above stated is found in the voids in between these pebbles. Matrix in the quartzites of a few samples is made up of mica and feldspar. Few samples contain feldspar more than 10% as detrital grains. Fuchsite is also present in many current bedded quartzites. Zircon is not found abundant in the quartzites sampled by the author, but Fareeduddin (1988) has reported fairly good amount of zircons from these quartzites.

The Kaldurga Conglomerate is a polymictic conglomerate consisting of boulders, cobbles and pebbles of TTG, granodiorite, quartzite, BIF, amphibolite, carbonate rock, vein quartz. etc. The rock is characterised by disrupted framework texture and the matrix/pebble ratio is high. The matrix consists of angular fragments of quartz, plagioclase, K-feldspar, rock fragments set in a fine grained matrix, mainly made up of fine grained chlorite, amphibole, plagioclase and mica. Detrital kyanite and zircon are seen in secondary plagioclase and quartz, which are formed due to recrystallization of the muddy matrix . Along some horizons of the Kaldurga Conglomerate, pebbles show prefered orientation showing a palaeoflow direction from NE to SW.

Model analysis of the matrix [M_1] of the Kaldurga Conglomerate shows that it is made up of angular fragments of quartz, plagioclase, K-feldspar and rock fragments like quartzite chert and phyllite. These fragments are set in a matrix (M_2) which is made up of fine grained quartz, plagioclase, chlorite amphibole and mica with occasional carbonate minerals.

The matrix (M_2) is recrystallized and contains secondary quartz and feldspar with inclusions of kyanite, zircon, chlorite, amphibole and mica.

Major,trace and REE analysis (42 elements) of each sample of QPC, quartzite and KCM have been carried out on XRF, AAS and ICP-MS. From ten samples of QPC, pyrite was separated and analysed for trace elements, REE and Sulphur isotopes. Composition of the plagioclase present in KCM was determined with the help of EMPA. These data, were processed on a computer for obtaining correlation coefficients between various components of each suite.

Sand size matrix of the QPC (MQPC) is characterized by enrichment in Cr, Co, Ni, Zr, Hf, V, Y and Rb; and depletion in ΣREE with pronounced negative Eu anomalies. It also contains higher U and Th. The mineralogical maturity is reflected in all geochemical data. Elevated Cr concentrations are situated in fuchsite and those of Co and Ni in detrital pyrite. K, Rb and Ba abundances reflect the micaceous content of the matrix. Most of the geochemical data indicate that QPC are the product of intense chemical disintegration and strong high energy hydrodynamic processes. Quartzites following QPC and also occuring interbedded with volcanic rocks at various stratigraphic levels are mature arenites extremely depleted in almost all trace elements and REEs. They also generally show strong negative Eu anomalies. Geochemical and mineralogical data from these quartzites also suggest their derivation from a continental crustal source which was subjected to intense chemical weathering and strong hydrodynamic processes. Detrital pyrite of MQPC exhibits enrichment in Co, Ni, Cu, and Zn. It has depleted to moderate

ΣREE with strong negative Eu anomalies. Geochemical characteristics of the pyrite are altogether different from the pyrite of sulphide facies BIF. $\delta^{34}S$ of this pyrite, from the matrix of QPC, indicate that the pyrite grains have been derived from a vein or porphyry type sulphide deposits.

Volcanic rocks of the Bababudan schist belt show geochemical characteristics of within plate type basalt or mid oceanic ridge basalt. BIFs are very important and abundant sedimentary constituents of the Bababudan Group. Geochemical work indicates that these BIF can be classified into cherty and shaly BIF (CBIEF *and SBIF). They are generally characterized by low level of* abundances of all elements. CBIF , in particular, are depleted in Cr, Co, Ni, Zr, Hf, Rb, Sr, V, Sc, ΣREE and exhibit strong positive Eu anomalies with enrichment in La. These data indicate that the BIFs were deposited from an ocean water in which hydrothermal solutions at MOR vent sites, brought the FeO, SiO_2 and REE. Contamination from simultaneous terrigenous clay and volcanic ash deposition has produced the observed variation. εNd = $^{143}Nd/^{144}Nd$ data from elsewhere from the BIF has indicated that these hydrothermal solutions were derived from depleted Archaean *mantle.*

Geochemical data like K_2O/Na_2O, Eu/Eu^*, ΣREE, HREE/LREE, La/Lu, Gd/Yb, U/Th, Th/Sc and Ni, Cr and Co abundances indicate that KCM is an active continental margin turbidite. MgO content of the KCM shoots upto 25% and the Cr content upto 1700 ppm. These data indicate that KCM was derived from a source which consisted of about 50% TTG and 50% mafic-ultramafic and sedimentary rocks. Debris of these rocks was transported in a

viscous media like slurry of mud flow or gravity flow. It indicates that at the time of deposition of the KCM , tectonic setting of the basin drastically changed from stable platformal to active continental margin type.

Structural work carried out by earlier workers and the map pattern of the belt cannot be explained unless large scale multiple deformation - folding, and crustal shortening as a result of horizontal compression is invoked. Observed geological, structural, mineralogical, sedimentological and geochemical characteristics of all rock types exposed in the belt are explained by a modified plate tectonic model with greater ridge length, faster ocean floor spreading and subduction and smaller plates. This mode is consistent with the global heat flaw data for the Archaean era, which was about 3 times more than present.

CONCLUSIONS:

On the basis of geological and geochemical work carried out on the sedimentary and volcanic rocks of the Bababudan schist belt, the following conclusions are made, which will be further strengthened with a study of palaeosols and other rock types of the adjoining areas:

i) A shallow depression was generated on the 3.0 Ga continental crust which evolved a shallow water basin. At the top of TTG and older supracrustal rocks, mature quartz pebble conglomerate,quartzites,shales and carbonates were deposited in this basin.

ii) These conglomerates and quartzites were produced through very

intense chemical (disintegration) and hydrodynamic activities operating on a middle-late Archaean crust made up of TTG and mafic-ultramafic rocks. The atmosphere in source area was anoxic, and the depositional environment was reducing shallow water not more than a few meter deep. The intense chemical disintegration leached and removed almost all mobile constituents, except restites,fuchsite mica and pyrite. Pyrite was not oxidized as oxygen was not present in the atmosphere at that time.

iii) Soon after the deposition of the basal QPC and quartzites a rift developed within the basin, through which, volcanism of "within plate" geochemical characteristics occurred. Lava was erupted into the basin in both subaqueous and subaerial conditions. At this time, spreading across the rift appears to have occurred and subsidence of the basin took place, resulting in relatively deeper shelf conditions, where deposition of CBIF, ferrugineous shale, shales and SBIF took place.

iv) The source for the silica and iron for BIF were hydrothermal solutions added to the ocean water at the site of rift which has become a mid oceanic ridge by that time. The deposition of BIF took place below wave base and photic zone, at the top of current bedded quartzites and volcanics. Volcanism continued even during the time of deposition of BIF as indicated by the interbedding of volcanic rocks with BIF. Simultaneous and alternate deposition of terrigenous shales, SBIF and CBIF indicates transgressional conditions. Spreading continued for a while as a very thick sequence of

BIF and ferruginous shales and volcanic ash was laid down.

v) After some time for which no geochemical evidence is available but which is a well recognized characteristic of "Wilson Cycle", the convection current directions were changed and compressional regime took over to produce subduction releted tectonic conditions during which the Kaldurga Conglomerate and other associated rock types were deposited. The geological, petrological and geochemical studies indicate that the Bababudan schist belt represents a geological terrain in which a shallow intracontinental basin evolved into an active continental margin related basin through a short time, and the reducing environment of basin changed into oxidizing environment. The intense chemical weathering gave way to dominant physical weathering and a transporting medium which was resposible for intense hydrodynamic activity was converted into viscous debris flow.

vi) The geochemical characteristics of the KCM suggest the multicomponent nature of the provenance, the configuration of various rock types and their mutual and probable mixing in different proportions. Transitional elements especially Cr, Ni, Rb and Sr have provided a fairly good base for computation of a mixing model of the source region and suggest a provenance area of 50% TTG, 35% ultramafic rocks, 10% mafic rocks and about 5% metasedimentary rocks, mainly quartzites. A comparative review of mafic - felsic ratios of upper continental crust of the Dharwar Craton, KN about 2.6 Ga ago and the composition of exposed crust during the early-middle Archaean conforms that the older Archaean

crust was significantly more basic. Geochemical signatures preserved in the KCM when compared with those of subsequent sedimentary strata suggest that the Bababudan schist belt represents a transitional stage in the unidirectional evolution of the Archaean continental crust from simatic to sialic.

vii) The geochemical characteristics and the structural geometry of the belt is best explained by a modified model of plate tectonics, in which smaller plates, larger ridge length (27 times), faster convection, faster production of oceanic crust and its destruction at low angle subduction zones are assumed. This model explains the observed features of all the rock types exposed in the belt. It is also suggested that during the Archaean "Wilson Cycle" was completed at a faster rate.

Geology, Geochemistry and Tectonic Setting of Conglomerates and Quartzites of the Bababudan Schist Belt, Karnataka Nucleus, India

THESIS SUBMITTED IN PARTIAL FULFILMENT OF THE REQUIREMENT FOR THE AWARD OF THE DEGREE OF

DOCTOR OF PHILOSOPHY

IN

GEOLOGY

BY

Mukesh Arora

FACULTY OF SCIENCE
DEPARTMENT OF GEOLOGY
ALIGARH MUSLIM UNIVERSITY
ALIGARH

1991

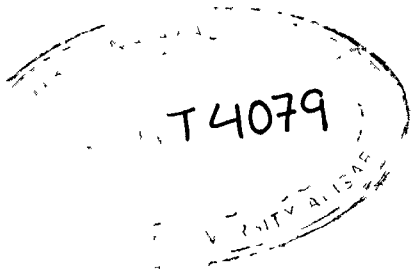

CERTIFICATE

This is to certify that the thesis entitled, "GEOLOGY, *GEOCHEMISTRY AND TECTONIC SETTING OF CONGLOMERATES AND QUARTZITES* OF THE BABABUDAN SCHIST BELT, KARNATAKA NUCLEUS, INDIA", is the record of bonafide research carried out by Mr. Mukesh Arora under our joint supervision at National Geophysical Research Institute, Hyderabad. We further testify that all the data presented in this thesis are based on his own observations.

PROF. S.M. CASSHYAP
Research Supervisor
Department of Geology
Aligarh Muslim University
A L I G A R H - 202 002.

11.10.91
DR. S.M. NAQVI, FNA
Research Supervisor
National Geophysical
Research Institute
H Y D E R A B A D - 500 007.

11/10/91
PROF. D. GUPTA SARMA,FNA
Director
National Geophysical Research Institute
H Y D E R A B A D - 500007

C O N T E N T S

ACKNOWLEDGEMENTS

This work has been carried out under the joint supervison and guidance of PROF. S.M. CASSHYAP and DR. S.M. NAQVI, FNA. I am deeply indebted to both of them for their efforts to make this work a reality.

I am extremely grateful to PROF. D. GUPTA SARMA, FNA, Director, National Geophysical Research Institute, Hyderabad, who has extended his kind support and encouragement and also made all facilities at NGRI available to me. DR. B.P. RADHAKRISHNA, FNA; DR. HARI NARAIN, FNA; PROF. K. NAHA, FNA; PROF. C. LEELANANDAM and PROF. K. GOPALAN, FNA, have been the source of inspiration throughout the work.

Dr. U. Raval, Dr. R. Srinivasan, Dr. V. Divakara Rao, Dr. B.L. Narayana, Dr. T.S.M. Hussain, Dr. Y.J. Bhaskara Rao, Dr. D.V. Subba Rao, Dr. B. Uday Raj and Dr.N. Charan have reviewed the manuscript at several times and made valuable suggestions.

Mr. Ravi Kaul, Director, AMD, Hyderabad; Dr. J.N. Gupta of AMD, Hyderabad have kindly provided the Sulphur isotopic data for the pyrite samples.

Dr. R. Natarajan, Dr. P.K. Govil, Dr. V. Balaram, Dr. D.S.N. Murthy, Dr. N. Charan, Mr. T. Gnaneswar Rao, Mrs. C. Manikyamba, Mr. S.L. Ramesh and Mr. K. V. Anjaiah have helped me immensely in carrying out analytical work at various laboratories of NGRI.

Continuous help extended by Mr. R.M.K. Khan, SRF, at all the stages of this work right from field work to preparation of the manuscript, is grately acknowledged. Without his help, completion

of this work within a limited time-frame would have been difficult. Mr. Ajay Manglik has also been kind enough to design softwares for the statistical and graphical representation of data.

I am thankful to Mr. K. Nageswara Rao and Mrs. Nancy Rajan for providing me with several draft of the manuscript; to Mr. Jamal-ud-din for excellant drafting and to Mr. C. P. Singh for reduction of the illustrations.

I am deeply indebted to my family for their patience, for not asking me too often when I might finish, and for not really noticing when I did! Last but not least, I acknowledge the silent encouragement extended by my elder brother Mr. N.K. Arora and my friend Mr. Arvind Bansal.

Financial assistance in the form of SRF from Council of Scientific & Industrial Research (CSIR), New Delhi is deeply acknowledged. This work forms part of the project on geochemistry of the Precambrian metasediments, supported by DST and NGRI.

10-10-91

HYDERABAD

(MUKESH ARORA)

CHAPTER-I

INTRODUCTION

1.1 SIGNIFICANCE OF GREENSTONE BELTS:

The early geological history of earth is preserved in Archaean Greenstone belts (Fyfe, 1990), which have developed in all major Archaean cratons. Their genesis has been a subject of great debate (Windley,1977;Condie,1981; deWit and Ashwal, 1986). During last 25 years, granite-greenstone terrains have been interpreted to represent a single tectonic environment; alternatively amalgalatam island arc (Condie, 1976), collapsed continental rift (Goodwin, 1981; Handerson, 1981) or back arc basin (Trank, 1976; Condie, 1976). A recent conclusion suggest that the development of granite - greenstone terrains has taken place in a variety of tectonic environment (West, 1980). Greenstone belts are characterised by rock types which represent platform deposits, MOR volcanics and also that of active continental margins (Goodwin, 1977; Fyfe,1980). "How does this model fit the complex Komatiite - tholeiite - andesite - rhyolite volcanic piles of the Archaean (Goodwin,1977), piles which appear to have all the rock type of a modern ridge and subduction zone combined ?" (Fyfe, 1980; p. 84). Application of plate tectonic model to greenstone belts has attracted the attention of Earth Scientists globally.

NOTE:- Following Radhakrishna and Naqvi (1986) greenstone belts have been referred as schist belts

Widespread shallow water environments in the Archaean are almost lacking (Banley et al.,1979). Quartz arenites and carbonates of the Archaean age have formally been regarded as rare lithounits with the exception in Dharwar Craton (Naqvi, 1976). However, recent work has shown that sediments belonging to the shallow water environment are also found in Australia, Canada and South Africa (Thurston and Chivers, 1990).

It is also a well established fact that 2/3rd of the continental crust was formed prior to 2.5 Ga (Moorbath,1975; 1977; Veizer,1976; Moorbath and Taylor 1981).Based on Sm-Nd, Lu-Hf, and Rb-Sr mass balance, Jacabsen (1988) has computed that ~ 40% of the present continental volume was formed by 3.0 Ga. Dia et al. (1990) based on $^{147}Sm/^{144}Nd$ ratios have proposed that the Archaean crust was composed of both granite (70%) and a mafic component (30%) which could have been komatiite. Genesis and nature of this crust has remained a subject of vigorous research during past 2 -3 decades (Feng and Kerrish, 1990; Naqvi, 1990; McLennan and Taylor,1991). Major emphasis has been towards the understanding of the volcanic rocks which are abundant in these belts (Drury et al. 1983). However, a considerable constituent of these belts are sediments of various kinds (Lowe,1982; Eriksson, 1980; Goodwin, 1990; Condie et al. 1991). While the volcanic constituents demonstrate the conditions and processes through which the volcanic and other magmatic rocks were produced, the sediments display informations regarding the intensity of exogenic processes operating at different times through out space and time. It is generally understood that fine-grained sediments sample the average composition of the source area, (Taylor and

McLennan,1985) and are effected by the conditions of transport, dispersal and environment of deposition (Naqvi et al. 1988). They further get modified by diagenesis and other subsequent processes including metamorphism. Therefore, the petrogenesis and geochemistry of sediments reflect the entire geological activity related with exogenic processes and also provide information about the tectonic setting of the basin in which they have been deposited (McLennan and Taylor, 1991).

The petrogenetic modelling of the volcanic rocks with the help of their geochemical characters, specially Sr and Nd isotopic signatures have been able to demonstrate vertical and lateral inhomogeneity in the mantle (Canlson, 1987). The ε Nd isotopic data established the compositional layering of the mantle. Two layers of mantle have been identified, the upper layer is depleted in ^{143}Nd, because it has taken part in formation of the crust. Nearly the entire crust has been provided by partial melting and fractionation etc. of this upper part of the mantle, and thus resulted in depletion of ε Nd (Depaolo, 1980; Allegre 1987, and Wasserburg, 1987). A depleted mantle was left after the formation of continental crust. The fractionation of the upper mantle has resulted in the concentration of SiO_2, Al_2O_3, K-group elements (LILE), LREE and upto certain extent MREE in the upper crust. The heat transfer in lower mantle takes place through conduction and the mass transfer takes place through plume activity. In the upper mantle i.e. depleted mantle, the heat and mass transfer take place by convection. This convection is believed to be responsible for adding the younger portion of the crust and accretion of the early formed continental crust.

1.2 STATEMENT OF THE PROBLEM:

The crust has been divided into lower and upper parts, the lower crust is exposed as high grade granulite terrains and the nature and composition of lower and upper crust exposed in the Archaean time could be studied through sediments, deposited in different time at different places in greenstone belts. It is quite well established that the sediments preserved in sedimentary basins represent the composition of first 10 kms. of upper crust (Taylor and McLennan, 1985; Taylor, 1991). Applying law of mass balance (Shibley and Wilband, 1977), it is shown that 100 gms. of granite is eroded on erosion get distributed into arenites, argilites and chemical sediments viz., material which goes into solution. But for 100 gms. of basalt there will be no arenite production and most of the mass will go as argiliites and dissolve load into the basins of deposition. Thus the study of the composition of sedimentary rocks is a very competent tool to decipher the compositional changes which have taken place throughout geological time. Especially since the time when hydrodynamic processes became active on the crust of the earth. In view of this, the greenstone belts of the Dharwar Craton provide an excellent opportunity as the sedimentary rocks preserved in these schist belts/greenstone belts represent a record of about 1 By from 3.5 to 2.5 Ga. Sediments of the older greenstone belts (Holenarsipur-Sargur Group) and the Chitradurga Group of younger greenstone belts have been studied earlier (Naqvi,1978;1983; Naqvi et al., 1983; 1988). However, sediments of the Bababudan Group of younger greenstone belts (3.0-2.8 By) have not been investigated in light of the facts mentioned above. In fact, the

study of this group of rocks could fill a major gap in our understanding about the geochemical evolution of the crust. In order to fill this gap in our knowledge a quantitative investigation of the Bababudan schist belt has been carried out. The sedimentalogical and geochemical aspects of metasediments of this belt were undertaken to address the following problems/questions.

i) What was the composition and nature of the pre Bababudan crust in Peninsular India?
ii) How it (crust) was formed?
iii) What changes it (crust) has seen subsequently?
iv) How the exogenic processes produced the first mature quartz pebble conglomerate and how the changes from stable plat formal conditions to unstable and deep water conditions in middle late Archaean occurred?
v) What was the nature of weathering processes?
vi) What was the nature of depositional environment and their atmosphere? and
vii) How the change from reducing environment to oxidizing environment and tectonic setting of the basin took place, within a short interval of time and space?

The above and some other related questions are one of the major controversies among the earth scientists working on Precambrian rocks. Through a detailed study of metasediments from the Bababudan schist belt, the present study provided a new data set and tried to interpret it in terms of changes in the

tectonothermal and chemical processes and summarise a model for the evolution of the basin, which in turn, reflects the mode of evolution of the upper continental crust of Dharwar Craton(DC).

Geology of Peninsular India and in perticular of its Dharwar region has been studied both extensively and intensively and many summaries have been reported in the literature during this period (Swami Nath and Ramakrishnan, 1981; Naqvi, 1981; Naqvi and Rogers, 1983, 1987; Radhakrishna and Naqvi,1986; Rogers,1986; Radhakrishna and Ramakrishnan, 1988, 1990). A region has been identified which does not seem to have witnessed any orogenic activity or metasomatism after 2.6 Ga. It has been designated as Karnataka Nucleus(KN). The geological history of a period between 3.5 - 2.5 Ga is preserved in these rocks. At least two main groups of greenstone belts can be identified namely older greenstone belts and younger greenstone belts punctuated by a very widespread crust forming event represented by Peninsular Gneisses (PG), which were dated at 3.0 Ga. (Swami Nath et al., 1976; Ramakrishnan et al., 1976; Naqvi and Rogers, 1987). Gold, silver, copper, arsenic, and Antimony are a few mineral deposits of the region. Older greenstone belts constitute 90% of mafic and ultramafic rocks (Komatiite) and about 10% of sedimentary rocks, whereas younger belts constitute 80% of sediments and 20% of volcanic rocks (Naqvi, 1983). The younger greenstone belts have been divided into Bababudan and Chitradurga Groups (Ramakrishnan et al., 1976; Swami Nath and Ramakrishnan, 1981). This area, thus represents a classical and representative case for the evolution of the Archaean crust, and hence, it has become one of the best studied regions among the Precambrian terrains of the world

(Newton and Anderson,1986; Drury,1988). One of the most distinguished and important constituents of greenstone belts of KN are their iron and manganese formations (Khan et al., 1991; Manikyamba et al., 1991; Gnaneswar Rao 1991). Recently stromatolites and microbiota have been found in association with the BIF in the chert-carbonate rocks (Naqvi et al.,1987; Venkatachala et al.,1991; Srinivasan et al., 1989; Vasudev et al.,1989).

1.3 THE GAP:

The sedimentary rocks of older greenstone belts have been studied by Naqvi et al (1983). Chitradurga sediments have also been studied in detail by Naqvi and Hussain (1972) and Naqvi et al. (1981). Primary sedimentary structures of the sediments of Bababudan Group have been studied by Srinivasan and Ojakangas (1986). Geochemistry of metavolcanics of this belt have been studied by Bhaskar Rao (1980), but the geochemical studies of metasedimentary rocks have not been carried out so far. Realizing the significance and importance of the geochemistry of these metasediments as stated above, this work has been taken up in this study and thus formed the major part of the present thesis.

Among the schist belts, The Bababudan Group does not consist the same type of lithologic sequence everywhere and therefore, based on the association with Mn formation Srinivasan and Sreenivas (1972) have further subdivided this group into Dodguni and Bababudan. The Bababudan Group in Chitradurga schist belt and Sandur schist belt which contain Mn formations and stromatolites have been studied by Gnaneswar Rao (1991) and Manikyamba et al.

(1991) respectively. The Bababudan Group in Kudremukh schist belt in which stromatolites have not been reported so far has been studied by Khan et al. (1991).

One of the main objectives of all these studies is to find the nature of exogenic processes and their results preserved in the Archaean sedimentary basins. For example, in the older schist belts the detrital material derived from the source rock having free plutonic quartz is very rare. Sedimentary processes have definitely been started by 3.9 Ga ago, as indicated by supracrustals of the Slave province, Canada (Bowring et al. 1989). Detrital zircons of 4.0 Ga are found in the siliciclastic sediments of the Pilbara region, Australia which indicate that exogenic processes operated even earlier (Compston and Pidgeon 1986). In spite of this antiquity of exogenic processes they have produced the mature Quartz Pebble Conglomerate (QPC) at the base of younger greenstone belts for the first time around 3.1 - 3.0 Ga. ago. This needs a convincing explanation, and author has tried to provide it in subsequent pages. Either vein quartz was not available before 3.0 Ga or the climatic conditions and hydrodynamic activities, then operating on the crust were of such type that they did not allow the production of QPC; or the depositional environments of earlier basins were not of such type which could allow to accommodate the QPC. Further more, it is a well established fact that there was no vegetation cover during Archaean time at the source area i.e. the primitive crust. It is also considered that in the Archaean time the duration of the day was very short (4 to 15 hours a day), 'Greenhouse effect prevailed' atmosphere was rich in CO_2, temperature of the ocean as

believed by some workers, was more than 80°C.(Costa et al.,1981; Holland,1984; Fyfe,1990). Combination of these factors would apperently result in a different style and rate of weathering and transportation. If delayed ocean degassing model (Towe 1983) is to be believed, then the effect of all parameters, as mentioned above, on sediment production and recycling indeed, would be markedly different from present and Phanerozoic time. If most of the hydrosphere was degassed around 4.0 Ga, its effects on sedimentary processes would be different. In the absence of dichotomy of oceans and continenents, a 2 km thick ocean would be covering the entire globe, really ruling out the detrital/clastic sedimentation (Hargraves, 1976, 1981; Shaw, 1980; Fyfe,1980; Nagy et al., 1983). These factors further enhance the uncertainity in the cause-effect-product relationship for the Archaean sediments and hence their interpretation becomes a very difficult task. Therefore, to understand the geological processes in the Archaean era, it is most meaningful to obtain more reliable geochemical data from appropriate settings. We are in a position to secure newer database of requisite precision with the help of modern analytical tools like ICP-MS, XRF, AAS, EPMA etc.

With the assumption of a different atmosphere and other physical and chemical parameters during early Archaean; combined with cooling of the earth crust, with higher heat flow rates, we propose a secular change in the rate, style, abundance, and composition of sediments. Such a secular change in composition of sediments reflects the change in composition of upper crust, which has supplied these sediments to the various basins. It is concluded that the Bababudan Group sediments represent a

transitional stage (3.0 Ga) of the unidirectional sima to sial crustal evolution between 3.5 to 2.5 Ga.

1.4 APPROACHES:

To address the questions raised above, the author has carried out the geological mapping of selected areas of the Bababudan belt. Primary sedimentary structures were studied for reconstruction of palaeoenvironment and palaeodirectional patterns. Statistical analysis of detrital components of the quartz pebble conglomerate, quartzites and the Kaldurga conglomerate was carried out to estimate the parameters of textural characteristics of these components.Detailed petrographical studies were carried out for the sand size matrix of QPC, quartzites and the graywacke matrix of the Kaldurga Polymictic Conglomerate (KCM). Some of mineral compositions were estimated on EPMA. Ninety samples of various metasedimentary rock types were analysed for their major, trace and rare earth elements on XRF, ICP-MS, AAS, and UVS. Ten samples of detrital pyrite, seperated from sand size matrix of QPC, were analysed for trace, REE and sulphur isotopes. These data were processed by means of software computer programmes e.g. GRAPHER, CORPCK, and TRIPLT to (a) obtain their binary and ternary relationships, and (b) determine their mean, range and correlation coefficient (r) between various elements. The data for forty two elements for each sample and related ratios are presented in following chapters.

1.5 ORGANIZATION OF THE THESIS:

The thesis presented here is divided into 14 chapters. Introduction which includes "Statement of Problem," and "approaches" forms Chapter-I.

Chapter-II provides brief discussion of a summary of the geology of Peninsular India with special reference to Dharwar Craton (DC), Karnataka Nucleus (KN). Various schemes of classification of supracrustals and interpretations for their possible origin have been reviewed. Brief description and mutual relationship of the rock suites exposed in DC,KN is discussed.

Chapte-III, deals with the geology of the Bababudan schist belt. Various hypotheses for the genesis of late Archaean volcano-sedimentary sequences, basement cover relationship and status of regional unconformity are discussed in this chapter. Lithostratigraphy of all rock types present in the Bababudan belt and nature of clastic metasedimentary rocks are outlined to facilitate the discussion on their geochemical characteristics.

Chapter-IV correlates the geology of DC with the global geological scenario with reference to the envisaged processes, which could have been operating during the Archaean time. Brief significant informations from early Precambrian rocks of Barberton, Pilbara, Zimbabwian, Canadian shield and Greenland, are included so that data from DC is understood in a global perspective.

Chapter-V contains the details of style of sedimentation in the Bababudan schist belt.

Chapter-VI includes the details of petrography and mineralogy of quartz pebble conglomerate(QPC),quartzites and graywacke matrix

of the Kaldurga Polymictic Conglomerate(KCM).

Chapter-VII describes the various techniques used to determine the chemical composition of different rock types, and also gives the procedure through which samples were collected in field.

Chapter-VIII gives the details of geochemical characteristics and behaviour of sand size matrix of QPC and quartzites. Interpretations of major, trace and REE constituents of these rock types form the framework of this chapter. Trace, REE and sulphur isotopic data obtained on detrital pyrite from QPC are also discussed in this chapter.

Chapter-IX deals with the geochemistry of volcanic rocks of the Bababudan belt. Data for this chapter were borrowed from the work of Bhaskar Rao and Naqvi (1978), Bhaskar Rao and Drury (1982) and Drury (1983). The main aim of this chapter is to deduce the constraints for the basin evolution from volcanic rocks of the basin.

Chapte-X provides the new interpretations of geochemical characteristics of oxide facies BIF which are very important constituents of Bababudan greenstone belt and are very significant rocks for the interpretation of the associated rocks. Data for BIF were borrowed from the similar and equivalent horizon of BIF of Kudremukh schist belt (Khan et al.,1991).

Chapter-XI presents the details and interpretation of geochemical studies of the graywacke matrix of the Kaldurga Conglomerate. Their major, trace and REE data were interpreted in terms of composition of provenance and the nature of exogenic processes. Clasts composition of the Kaldurga conglomerate are

also provided.

Chapter-XII, reconstructs the tectonic and depositional environment of the QPC, quartzites and the Kaldurga Conglomerate, with the help of the geochemical data obtained by the author and the data and interpretation available for volcanic rocks and Iron formations. A model for the evolution of the basin and its source area (the Middle Achaean Continental Crust) is proposed.

Chapter-XIII constitutes the synthesis and discussions on various aspects given in Chapter II to XII. Plausible interpretations and answers to the questions raised in Chapter I are discussed in the subsequent chapters.

Chapter-XIV summarizes and concludes present geological and geochemical work carried out by the author on metasediements of late Archaean Bababudan schist belt of Dharwar craton (Karnataka Nucleus), India.

The field, petrological and geochemical investigations, presented in this thesis, lead to suggest that the Bababudan schist belt and its metasediments represent transitional stage of sima to sial transformation. The basin started as a shallow water intracontinental basin in which a rift-ridge was developed. Spreading and volcanism along this ridge occurred. Through this ridge within plate type volcanic lava and hydrothermal solutions came up which gave rise to volcanic rocks and BIF. Sudden subsidence and change of convection current direction resulted in the change of the tensional regime to compressional regime. Ultimately it resulted in creation of orogenic conditions and deposition of unsorted, graywacke type sediments, characteristics of active continental margins, were deposited. Through this

process, a basin of highly stable tectonic conditions of passive margin or within plate rifting, was changed into rather unstable environment of active continental margin tectonic setting. In these sediments evidences are preserved to suggest that how intense conditions of chemical weathering and hydrodynamic activities gave way to the conditions of intense physical weathering and transport by viscous medium like slurry.

CHAPTER II

GENERAL GEOLOGY OF DHARWAR CRATON, KARNATAKA NUCLEUS

2.1 SUMMARY OF GEOLOGY OF SOUTHERN PENINSULAR INDIA (BELOW NARMADA-SON LINEAMENT):

The peninsular shield of India (Fig 2.1) has been divided into two main Protocontinents, i.e. i) Bundelkhand and, ii) Dharwar-Singhbhum Protocontinent (Radhakrishna and Naqvi, 1986). The Karnataka and Singhbum Nuclei (KN and SN) of the Dharwar-Singhbhum protocontinent consist of rocks older than 2.5 Ga. Similar rock types occur in Jeypore-Bastar nucleus (JBN), however, for this region radiometric age data are not yet available. At present this correlation is based on the lithologies of the Bengpal, Sukma and Iron ore groups of Jeypore-Bastar region (Crookshank, 1963), which are similar to those found in the Karnataka (KN) and Singhbhum (SN) Nuclei.

Within the Dharwar-Singhbhum Protocontinent, these nuclei are separated by the extensive tract of K-granites and other rock types of amphibolites(/green schist) facies. In this region to the east of Closepet granite, greenstone belt development is of subordinate order as compared to KN. K-granites are extensively developed here and they are relatively rare in KN. Their emplacement is more pronounced in the northern part of the protocontinent, and they form a garland around KN (Fig. 2.1). The southern portion shows extensive development of granulite facies rocks. A transition zone of about 50 km. width is found between the granulite facies in the south and amphibolite facies in the north, and it has been regarded as an Early Proterozoic

Fig. 2.1 : Generalized geological map of Peninsular India. KN, Karnataka nucleus; JBN, Jeypore-Bastar nucleus; SN, Singhbhum nucleus; EPMB, Early Proterozoic Mobile Belt; MPMB, Middle Proterozoic Mobile Belt; 1, Schist belts within nuclei; 2, tonalitic gneisses; 3, granodiorites, granodioritic gneisses, and granulites of EPMB; 4, K-granites in EPMB; 5, granulites and gneisses of MPMB; 6, Middle Proterozoic sedimentary basins; 7, Gondwana sediments in Godavari rift valley; 8, anorthosites emplaced along the EPMB-MPMB contact; 9, Eastern Ghat-Sukinda-Singhbhum thrust; 10, Deccan Trap cover.
Inset A shows different crustal elements of Peninsular India: 1, Dharwar-Singhbhum protocontinent; 2, Bundelkhand protocontinent; 3, Middle Proterozoic mobile belts of Eastern Ghats, Satpura, and Delhi (After Radhakrishna and Naqvi, 1986).
Inset B shows position of Karnataka State in India.

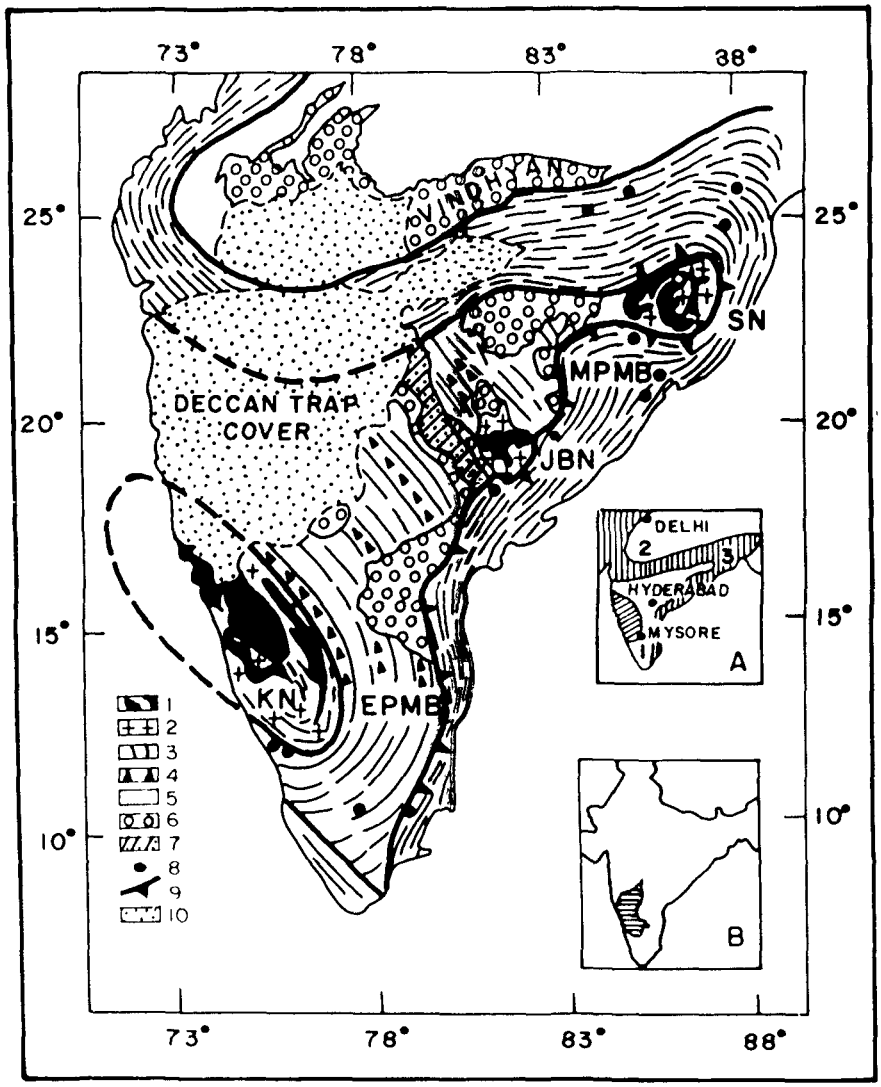
73°
78°
83°
88°
25°
20°
15°
10°
VINDHYAN
SN
MPMB
DECCAN TRAP
COVER
JBN
KN
EPMB
DELHI
2
3
HYDERABAD
MYSORE
A
B
1
2
3
4
5
6
7
8
9
10

Mobile Belts (EPMB). Consistent ages around 2.6 to 2.0 Ga characterize this belt (Radhakrishna and Naqvi,1986 ; Naqvi and Rogers,1987).

Bundelkhand and Dharwar-Singhbhum protocontinents on two sides are surrounded by the Middle Proterozoic Mobile Belts (2.0 to 1.5 Ga). The second mobile belts association (MPMB) of the Precambrian terrain of India constitute the Eastern Ghats province, Satpura orogenic province (Sausar Group); and the Aravalli-Delhi belt (Fig.2.1). Volcano-sedimentary schists of the Nellore and Khammam belts, charnockites, khondalites and related rocks including calc-silicates, mafic granulites, anorthosites and alkaline rocks, are some of the typical rock types of MPMB. Chattisgarh and Vindhyans are two important middle Proterozoic sedimentary basins (Radhakrishna and Naqvi, 1986). At the southern most tip of peninsular India, there is a zone of high grade granulites of Kerala and south TamilNadu. The granulite terrain is not composed solely of rocks of granulite facies, but gneisses and "supracrustal" rocks of amphibolite facies which are abundant. At places, some of these low grade metamorphic rocks may represent areas of retrogression from granulites (Naqvi and Rogers,1987). One suite of gneisses, near Madurai,TamilNadu, apparently formed by retrogression from charnockites. It has been dated at 550 Ma, and could be correlated with Pan-African orogeny (Hansen et al.,1985).

2.2 GEOLOGY OF DHARWAR CRATON, KARNATAKA NUCLEUS:

Dharwar craton, (Fig.2.2) a Precambrian greenstone-granite terrain, is the rigorously studied area of the Indian Shield.

Several summaries of the geology of this craton have been published recently (Swami Nath and Ramakrishnan, 1981; Naqvi, 1981; Radhakrishna,1983; Radhakrishna and Naqvi, 1986; Naqvi and Rogers, 1983, 1987; Radhakrishna and Ramakrishnan, 1990). This shield predominantly comprises the Archaean greenstone belts, gneisses, granites, and dyke swarms. Undeformed Proterozoic basin like Kaladgi and Bhima basin rest over this shield (Pichamuthu and Srinivasan, 1983 ;1984 ; Radhakrishna and Naqvi, 1986). The greenstone belts (GSB) are volcano-sedimentary sequences of several types formed at different time between 3.5(?) to 2.6 Ga. The gneisses surrounding/engulfing the greenstone belts are termed Peninsular Gneisses (PG). The term PG includes quartzo-feldspathic rocks with gneissic structure irrespective of chronology, genesis and metamorphic events. Similarly the term greenstone belt here is used as synonymous with Dharwar schists of Bruce Foote (1888). However, some workers have emphasized the inadequacy of the term greenstone belt for characterizing the essentially schistose and metamorphic status of the supracrustal rocks of the Indian Archaean. A suggestion was put forward to use terms like supracrustals or supracrustal association (Chadwick et al., 1981) but the old term schist belts seems to be more appropriate as it emphasizes the schistose character of the Archaean volcano-sedimentary sequence of India (Radhakrishna and Naqvi, 1986). The terrain dominated by schist belts passes through a transition zone to the high grade granulite terrain in the southern part of Dharwar Craton (Allen et al., 1983). Kaladgi and Bhima basins are major constituents of Proterozoic sedimentary basins (Radhakrishna, 1987). Differences in grade of

Fig. 2.2 : Geological map of western Dharwar Craton. P, Panjim; NK, North Kanara; SK, South Kanara; MA, Mangalore; D, Dharwar; BE, Bellary; DE, Davangere; C, Chitradurga; HO, Hoskere; S, Shimoga; A, Arsikere; T, Tarikere; CH, Chickmagalur; H, Hassan; B, Bangalore; M, Mysore; SA, Sargur (After Naqvi and Rogers, 1987).

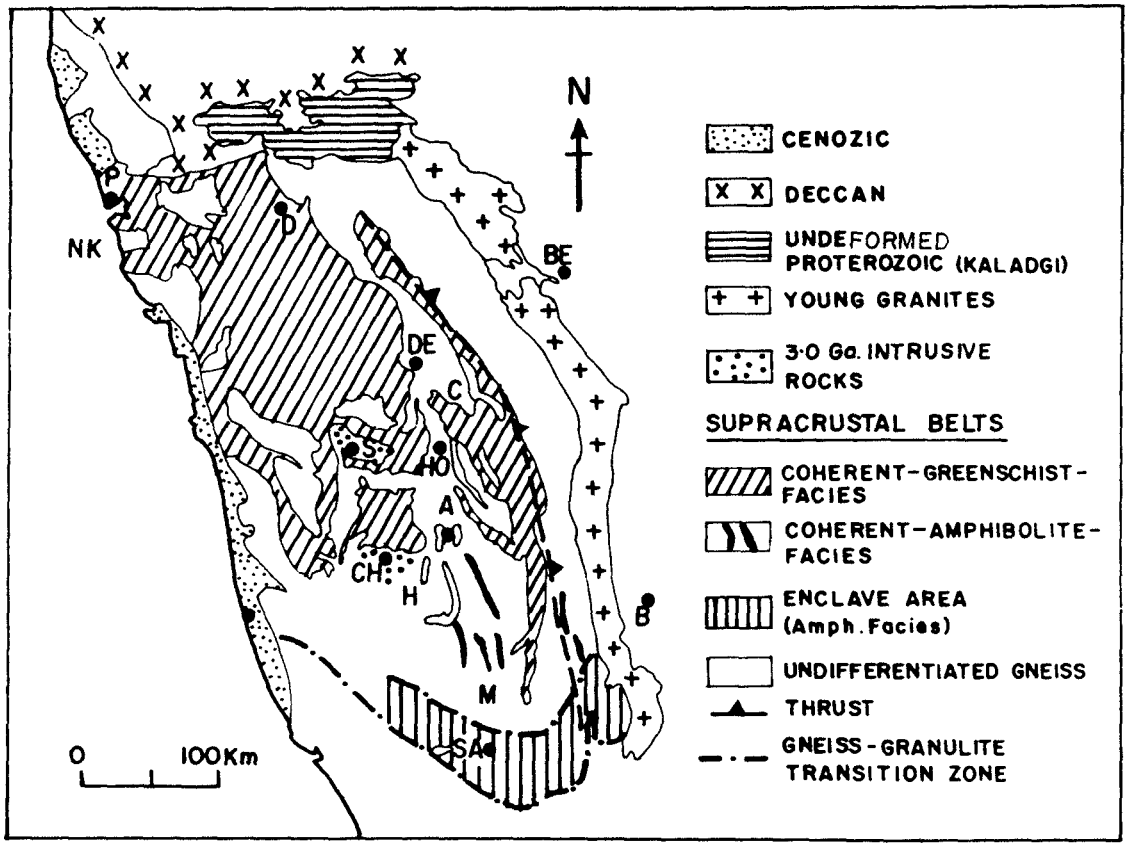
N
NK
P
D
BE
DE
C
S
HO
A
CH
H
M
SA
B
0
100Km
CENOZIC
DECCAN
UNDEFORMED PROTEROZOIC (KALADGI)
YOUNG GRANITES
3·0 Ga. INTRUSIVE ROCKS
SUPRACRUSTAL BELTS
COHERENT-GREENSCHIST-FACIES
COHERENT-AMPHIBOLITE-FACIES
ENCLAVE AREA (Amph. Facies)
UNDIFFERENTIATED GNEISS
THRUST
GNEISS-GRANULITE TRANSITION ZONE

regional metamorphism (within the craton) viz. low pressure type in the eastern area and intermediate pressure type in the western block of the Dharwar Craton have been noticed by Swami Nath and Ramakrishnan (1981). Consequently these differences in metamorphism brought the fundamental lithological distinction between the belts (Ramakrishnan et al.,1976; Swami Nath et al., 1976). These features along with the observation that greenstone belts are well developed in western block, whereas potassic granites are extensively intruded in eastern area of Dharwar Craton suggest a possible division of the craton into a western Dharwar Craton and an eastern Dharwar Craton. (Rogers, 1986; Naqvi and Rogers, 1987).

Eastern margin of western Dharwar craton is rather more uncertain, although, according to Naqvi and Rogers (1987) Closepet granite can be considered as a boundary between these two blocks. However, a major shear zone west of the Closepet granite could also be another possible eastern margin of western Dharwar craton. Drury and Holt (1980) and Drury et al. (1984) have recognized several "zones of high strain", and the lithological differences to the west and east of Closepet granite are distinct, the Closepet granite may be chosen as a margin of western Dharwar craton. Therefore this elliptical area with a garland of K-rich granite pluton on at least two sides has been regarded as Karnataka Nucleus (KN) (Radhakrishna and Naqvi, 1986) and its geology is discussed in detail.

2.3 DISTRIBUTION OF ROCK TYPES:

Geological map of Dharwar Craton (KN) shows six different

types of rock suites, viz. (1) undifferentiated gneiss-generally considered as Peninsular gneiss; (2) small enclaves of rock of amphibolite facies; (3) coherent belts of amphibolite and/or greenschist facies as a whole regarded as schist belts; (4) granodiorite tonalite trondhjemite (TTG) plutons or their metamorphic equivalents; (5) younger K-rich granites (~2.5 Ga. e.g. Closepet granite) and (6) undeformed Proterozoic sedimentary rocks, of Kaladgi and Bhima basins. These rocks are partially overlain by Deccan traps in the northern part of Karnataka nucleus.

2.3.1 Peninsular Gneisses:

The term "Peninsular Gneiss" was, and still is, applied to quartzo-feldspathic gneisses engulfing Dharwar schists. They exhibit extreme diversity of composition but most of the rocks are tonalites, trondhjemite and granodioritic gneiss (TTG) showing leucocratic-melanocratic banding, tygmatic folding, agmatitic structures and several other factors (Naqvi et al.,1983). Apart from these, inclusions of other rock types like ultramafic/mafic rocks are also present (Viswanatha and Ramakrishnan, 1981; Bhaskar Rao et al., 1983; Monrad, 1983; Radhakrishna and Naqvi, 1986) which cannot be distinguished on a small map scale (Fig.2.2).

Apart from their magmatic precursors, sedimentary precursors (meta-arkose) are also reported in them (Udai Raj, 1991). Therefore two types of gneisses namely the ortho and para gneissess are part of the PG (Naqvi and 13 others,1983). However, the low initial $^{87}Sr/^{86}Sr$ (0.701 to 0.702) ratios show that most

of the gneisses for which such data are available are mantle derived (Faure and Powell, 1972), or formed due to partial melting of amphibolites or primitive simatic crust (Arth and Hanson, 1975). The ortho Peninsular gneisses and related granotoids have intruded at various stratigraphic levels as implied by the intrusive contacts with the oldest as well as youngest member of Dharwar schist belts, without any obvious evidence of tectonic contact to discard their genetic affinity (Pichamuthu and Srinivasan, 1983). The representation of different components of PG as one mapable unit is caused by their quartzo-feldspathic nature. Mutual relationship between PG and schist belts has been debated since last 100 years (Radhakrishna and Ramakrishnan,1990). Dharwar schist were considered to be the oldest rocks of Peninsular India in which PG intruded. The other group thought that PG was the basement of schists (see Radhakrishna and Ramakrishnan, 1990 for historical development of ideas). Radhakrishna (1967) proposed that PG intruded one set of schist and formed basement for the other younger group. Swami Nath et al.(1976) and Ramakrishnan et al.(1976) substantiated this view and Naqvi (1981) proposed an interfingering stratigraphic relationship between various components of PG and schist belts formed at different times between 3.5 to 2.6 Ga. This model stratigraphy is presented in Fig. (2.3).

2.3.2 Mafic Schist Belts:

Schist belts, lying within sialic Peninsular Gneisses of Dharwar craton, show a distinctive variation in their i) grade of metamorphism, which varies from greenschist facies to amphibolite

Fig. 2.3 : Interfingering sequence model of greenstone belts and acid plutons wherein Dharwar greenstone belts and Peninsular Gneisses have been divided into 5 successive interfingering, lithostratigraphic and lithotectonic groups (After Naqvi, 1981).

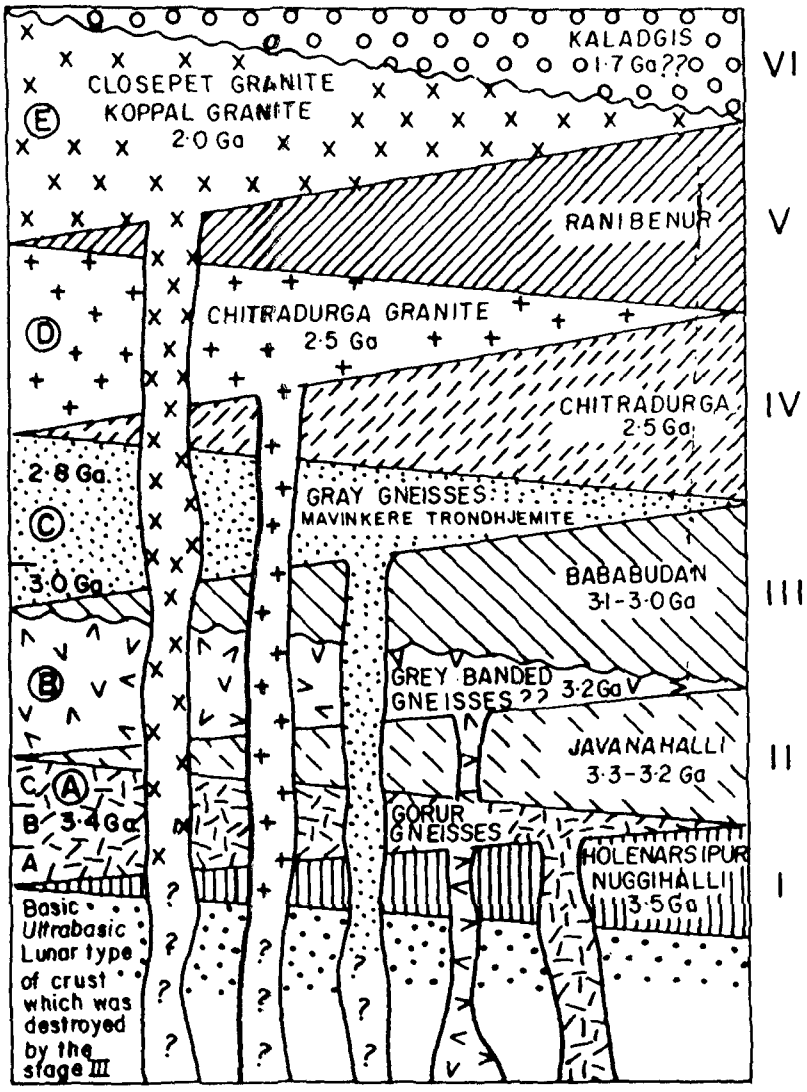
KALADGIS
1·7 Ga??
CLOSEPET GRANITE
KOPPAL GRANITE
2·0 Ga
RANIBENUR
CHITRADURGA GRANITE
2·5 Ga
CHITRADURGA
2·5 Ga
2·8 Ga
GRAY GNEISSES
MAVINKERE TRONDHJEMITE
3·0 Ga
BABABUDAN
3·1-3·0 Ga
GREY BANDED
GNEISSES ?? 3·2 Ga
JAVANAHALLI
3·3-3·2 Ga
GORUR
GNEISSES
HOLENARSIPUR
NUGGIHALLI
3·5 Ga
B 3·4 Ga
A
Basic
Ultrabasic
Lunar type
of crust
which was
destroyed
by the
stage III
VI
V
IV
III
II
I

facies; ii) ratio of volcanic rocks to the sedimentary rocks i.e. from 90:10 to 20:80; iii) Coherency of basins shape and dimension, which again ranges from small enclaves to extensively spreaded belts. Recent studies have led to further classification of these schist belts.Based on the available stratigraphic, structural and geochronological data schist belts may be grouped as (1) enclaves (2) older schist belts and (3) younger schist belts.

2.3.2.1 Enclaves of high grade mafic amphibolite facies:

Enclaves of high grade mafic schistose rocks in gneisses, which are abundant only in the southern part of the craton (Fig.2.2). These small enclaves range in dimension from a few meters to a km. in width and a few meters to about 10 kms. in length. Sometimes these are exposed in a form of narrow band hardly a meter wide. These enclaves, representing elongate and locally faulted synformal keels and antiformal hinge, are sometimes aligned to form a linear belt (Viswanatha and Ramakrishnan, 1981). These are referred to in literature as the metamorphics (Jayaram, 1907) and the Sargur schists (Rama Rao, 1940). Typical rock assemblages include amphibolites, mafic granulites, magnetite quartzites, calc-silicate rocks, and minor quartzites. Ultramafic-mafic anorthositic suites are found at a few places. Swami Nath and Ramakrishnan (1981) have grouped them in their Sargur group.

2.3.2.2 Coherent belts of amphibolite facies (older schist belts):

These belts consist of large outcrop area in comparison to the above discussed enclaves, but at the same time these are

relatively less extensive when compared with low grade younger schist belts.The Nuggihalli, Krishnarajpet, southern part of Holenarasipur belt etc. are some typical and relatively more studied examples of this type. Since the lithotypes of these belts are highly metamorphosed and disturbed, their stratigraphy is heatly debated among contemporaneous workers (Swami Nath and Ramakrishnan, 1981; Naqvi,1981). These belts are made up of mafic-ultramafic komatiites,amphibolites,kyanite-staurolite-mica-garnet-quartz schists, chloritoid - magnetite - corundum fuchsite-quartz schists, fuchsite quartzites and other rock types as described by Hussain and Naqvi (1983), Divakar Rao et al.(1983) and Jafri et al.(1983). They contain only 1.3% silicic rocks which are believed to be metachert on the basis of their oxygen isotopic data (Naqvi et al.,1981). In the absence of primary structures indicating top and bottom, stratigraphic sequence cannot be established and thus the uncertainty about the correlation of rock assemblages across isolated belts and enclaves suggests that they should be kept separated from other enclaves of same facies of metamorphism (e.g. Janardhan et al., 1979; Naqvi and Rogers, 1987).

2.3.2.3 Younger schist belts:

In general, the grade of metamorphism is of greenschist facies, but locally it has reached up to epidote amphibolite or lower amphibolite facies. These belts are typically characterized by large and consistent outcrops over a large area, abundance of clastic sedimentation and the relatively high ratio of sedimentary rocks to volcanic suites. The presence of quartz pebble

conglomerate as a major unconformity lying over the gneissic basement and current bedded and ripple marked quartzites is an indication of commencement of stable shelf/platformal environment of deposition (Srinivasan and Sreenivas,1972). Biogenic structures like stromatolite, and flysch type rock units e.g. graded bedded graywacke conglomerate are some more diagnostic properties of these schist belts. Since deformation has not been so intense and primary sedimentary structures are preserved, their stratigraphy can be established in subsequent sections. The Bababudan, Chitradurga, Shimoga and Western Ghat belts are some typical examples. These are the main belts of the Dharwar craton. These belts are mainly made up of the Bababudan and Chitradurga Groups.

2.3.3 3.0 Ga. Old Trondhjemites and Granulites:

As emphasized earlier, it is virtually difficult to distinguish various components of the Peninsular Gneiss (PG) on a mappable scale, because intermixing of various components is of rather small scale. The only variant of the PG that is separated in Fig.(2.2) is a suite of poorly foliated to massive, diapiric bodies with ages of about 3.1 to 2.9 Ga. For example, Sigegudda trondhjemites, Holekote trondhjemite, Chickmagalur granodiorite (Monrad,1983; Stroh et al.,1983; Chadwick et al.,1985a; Rama Rao et al.,1991). Other trondhjemite rock bodies with similar character are not shown in geological map. These bodies range in size from small dykes and sills to plutons with diameters of many kilometers. Chickmagalur granodiorite which is dated at ~ 3.1 Ga. (Taylor et al., 1984) is exposed on the southern margin of the Bababudan schist belt. Mineralogically it is a simple mixture of

quartz, plagioclase, biotite, K-feldspar, hornblende in variable proportion (Naqvi and Rogers, 1987).

2.3.4 Younger (K)-Rich Granites:

These include some diorites and granodiorites, but the major rock types are rich in K-feldspar (like Closepet, Arsikere, Banavar, Hosedurga and Chitradurga granites. These granites have been intensively studied by Divakar Rao and Rama Rao (1982), Divakar Rao et al. (1987; 1990) and Friend and Nutman (1991). Some bodies are diapiric although gradational margins are also observed. The compositional and textural properties are discordent with the surrounding Peninsular Gneisses. The Closepet granite is the best example of the rock suite, dated 2.4 to 2.5 Ga. (Crawford, 1969; Taylor et al.,1986; Friend and Nutman, 1991). Other examples are Chitradurga, Hosedurga, Hosepet granites, which were emplaced more or less at the same time in geological history of crustal evolution of Dharwar craton, Karnataka nucleus. Most of these are associated and emplaced with 2.6 Ga. orogeny.

2.3.5 Undeformed Proterozoic Basins:

Cuddapah, Kaladgi and Bhima basins are found resting on the rocks of KN and EPMB (Fig. 2.1). These basins represent middle and late Proterozoic era and some of them have been studied in detail (Radhakrishna,1987). In northern part of the Karnataka nucleus, the undeformed Proterozoic basin, viz. Kaladgi and Bhima basins are resting unconformably over the Ranibennur group, as described by Naqvi (1981).

2.4 CLASSIFICATION AND CORRELATION OF ARCHAEAN SCHISTOSE ROCKS IN DHARWAR CRATON AND ITS BEARING ON ARCHAEAN SEDIMENTATION :

Recently detailed investigations have led to a variety of classification of Dharwar schistose assemblages and the development of numerous new stratigraphic terminology. Some of the recent classifications are given in Table 2.1.

Jayaram (1910) Rama Rao (1924, 1940) and Radhakrishna (1967) suggested that schist belts like those of Holenarasipur and enclaves in the Peninsular Gneisses were older than the main Dharwar belts of Shimoga and Chitradurga. Viswanatha and Ramakrishnan (1976) have distinguished a separated group older than the Dharwar and named it the "Sargur Super Group". However, in their subsequent papers, the same sequence has been designated as Sargur schist complex (Ramakrishnan et al., 1976; Swami Nath and Ramakrishnan, 1981). According to this school of thought Peninsular Gneiss is the basement for Dharwar Supergroup, however, basement of older Sargur is not known fully.

With the progress of the work on the Dharwar Craton, it was gradually realised that the entire Dharwar greenstone sequence cannot represent one single system (Radhakrishna, 1954;1967) Detailed geochemical, petrological studies and geological mapping by Naqvi (1967;1974) and Naqvi and Hussain (1972) clearly demonstrated that before the deposition of main cycle of Dharwar schist one more cycle of sedimentation, volcanism, metamorphism and deformation was over. This concept was further substantiated and established by Viswanatha and Ramakrishnan (1976) where in they proposed the concept of "Rocks older than Dharwars". Swami Nath et al., (1976) and Ramakrishnan et al., (1976) proposed that

Table 2.1 : Classification of supracrustal rocks in Dharwar Craton, Karnataka nucleus.

Swami Nath et al. (1976)

	----------UNCONFORMITY----------	
Dharwar Supergroup	Chitradurga Group (2.3 - 2.5 Ga) ---------Unconformity---------- Bababudan Group (2.5 - 2.6 Ga)	Greenstone belts (Upper Archaean)
	----------UNCONFORMITY----------	
Peninsular Gneissic Complex	Migmatites, Gneisses and Granites	
Sargur Supergroup	Several unclassified groups of schist belts and enclaves	High grade schists (Lower Archaean)
	----------UNCONFORMITY----------	
(?) Sialic	Basement (?)	(as yet undifferentiated from PGC)

Naqvi et al. (1980)

YOUNGER BELTS	Bababudan, Chitradurga, Shimoga, etc., graywackes, quartzose sediments, shales, basalts to rhyolites, cherts, carbonates; greenschist facies.
INTERMEDIATE BVELT	Javanahalli; arkoses, amphibolites (metapelites) calc-silicates, metavolcanics; amphibolite facies.
OLDER BELTS	Nuggihalli, Krishnarajpet, southern part of Holenarasipur, etc., ultramafic/anorthositic suites (mostly volcanic), metapelites, cherts and iron formations, no clastic quartz; amphibolite facies.

Naqvi, 1981

	2.6 - 2.4 Ga Granitic activity.
CHITRADURGA GROUP	Chert, sericitic phyllite, metavolcanics, chlorite schist, graywacke conglomerates (K.M. Kere) Graywacke Graywacke Conglomerate (Aimangala) Arkose-grit Graywacke Conglomerate (Talya)
BABABUDAN GROUP	Kaldurga Conglomerates Quartzite (BMQ) Argillite schist Mafic flows Mafic flows with interlayers amphibole-garnet schist Chlorite schist Orthoquartzite (fuchsitic at places) Basal Conglomerate
	----------UNCONFORMITY----------

	Dykes
	Quartz veins
JAVANAHALLI	Pegmatites, granites
GROUP	Fuchsite-quartzite
	Ultramafic-schist
	Ortho and para amphibolites interbedded with Carbonate Parameters

(Tonalitic and Trondhzemitic activity {3.5 Ga})

	Dunite, Fuchsite quartzite, high Al, Mg sediments
HOLENARSIPUR	Hornblende schist, tremalite-actinolite schist,
GROUP	Serpentinite, Peridatite

? ? ? Basement ? ? ?

Swami Nath and Ramakrishnan (1981)

Kaladgi, Badami and Bhima Groups

--------UNCONFORMITY----------

DHARWAR	Chitradurga Group
SUPERGROUP	--Unconformity---
	Bababudan Group

--------UNCONFORMITY----------

PENINSULAR	Migmatites, gneisses,
GNEISS	granitaids
	Several unclassified
SARGUR GROUP	associations of
	supracrustal rocks

B A S E M E N T N O T S E E N
(3.4 Ga Old Gneisses)

Pichamuthu and Srinivasan (1983)

Chitradurga Subgroup:	graywackes, conglomerates, silicic volcanic rocks, banded iron formations
Dodguni Subgroup:	quartz conglomerates and sandstones, meta-pelites, carbonates, manganese and iron formations
Bababudan Subgroup:	quartz conglomerates and sandstones, basalts and rhyodacites, graphitic metapelites, banded iron formations
Nuggihalli Subgroup:	quartzites, metapelites, ultramafic/anorthositic intrusive rocks

---

Radhakrishna (1983)

Younger greenstones (Dharwar type):	quartzose clastic sediments, carbonates, cherts, iron formations, basalts and rhyolites; includes Shimoga, Chitradurga and Sandur basins
Ancient supracrustals (>3,000 m.y.):	mafic/ultramafic igneous rocks, rate clastic sediments; sediments consist of volcanic debris or chemical precipitates; includes Holenarasipur, Nuggihalli, Krishnarajpet, etc. belts; Javanahalli belt is of same age but contains quartzose clastic sediments
Ancient supracrustals (Sargur type):	occurs in transition zone to granulite facies at southern margin of craton; mafic/ultramafic/ anorthositic suites, aluminous metapelites, fuchsite quartzites, iron and manganese cherts, graphitic schists

Dharwar greenstone belts can be divided into two distinct group : a younger "Dharwar Supergroup" and an older prebasement gneiss "Sargur Group". The Dharwar Supergroup is further divided into the basal volcanic-rich Bababudan Group and the overlying shale/graywacke - rich Chitradurga Group. Radiometric age control limits the age of Bababudan and Chitradurga groups to the period of 3.0-2.55 Ga (Crawford, 1969; Venkatasubramanian and Narayanaswamy, 1974a; Beckinsale et al., 1980; Taylor et al., 1984). Peninsular Gneiss was recognised as the basement to the Dharwar Supergroup, although mineralogical mobilisation during the Dharwar orogeny had occurred. It was also pointed out that the Dharwar schists were deposited on a peneplained basement of Peninsular Gneiss as evidenced by the supermature basal quartz pebble conglomerate at the base of Bababudan Group which forms one of the main subject of this thesis. Sargur Supergroup is more complex, and regarded as an orthoquartzite-carbonate-pelite association, typical of ensialic basin. These belts are characterised by platformal assemblage and their relatively higher grade of metamorphism ranging from amphibolite facies to lower granulite facies. The older sialic basement which is indistinguishable from the rest of the gneissic complex is considered as the base of Sargur Supergroup. However, unconformity between Sargur group and older gneisses is not defined or exposed. The Holenarasipur, Krishnarajpet, Nuggihalli, Nagamangala belts are some typical examples of this Supergroup.

The "Peninsular Gneiss" together with these supracrustal remnants and enclaves forms the basement to the younger rocks overlying the basal unconformity. Since the major event of

"Peninsular Gneiss" intrusion is dated around 3.0 Ga, the Sargur rock probably belong to early-middle Archaean. Rocks overlying the regional basal unconformity marked by the uraniferous and pyritiferous conglomerate (oligomictic) exposed in the Bababudan, Western Ghat, Chitradurga and Sigegudda belts are classified under Dharwar Supergroup.

Naqvi et al. (1978 C and 1980) and Naqvi (1981) have subdivided the Dharwar schists into three types namely : (1) Holenarasipur-Nuggihalli type (or older schist belt) mainly consisted of ultramafic/ anorthositic suites (mainly volcanic), metapelite, cherts and iron formations; virtually no clastic (terrigenous) sedimentary rocks were formed. Metamorphism is upto amphibolite facies. Nuggihalli, Krishnarajpet, southern tip of Holenarasipur belts are a few classical examples of the same; (2) Javanahalli type, which has meta arkose (Paragneisses) at the base, and including arkose, amphibolite (metapelites), calc-silicates, metavolcanics and fuchsite quartzite (Naqvi et al., 1981). The status of this formation, which is manifested by only Javanahalli schist belt, in relation to other groups is uncertain because of the tectonic contacts and absence of unconformities. The Javanahalli group was recognised to be different in lithology and metamorphism from the Chitradurga Group and considered older (Sampat Iyengar, 1905). After the identification of high grade schist as forming a separate group, the Javanahalli rocks were correlated with the Bababudan Group (Iyengar, 1976) and with the high grade schists (Ramakrishnan et al., 1976). However, Ramakrishnan (1980) has since revised his opinion and considered it to be equivalent to the Chitradurga

Group. The lithologies of this group are comparable with Bababudan-Chitradurga Groups, whereas, metamorphic grade is equivalent with older Holenarasipur Group. Hence, Naqvi et al. (1980) and Naqvi and Rogers (1987) separated them as Intermediate belt; (3) Bababudan-Chitradurga type which is unconformably resting over Peninsular Gneiss. This regional unconformity is represented by uranium, gold and pyrite bearing oligomictic quartz-pebble conglomerate. Typical rock units are arenite, quartz sediments, shales, basalts to rhyolites, cherts, phyllites and carbonates. Bababudan, Shimoga, Chitradurga are the characteristic belt of this division and designated as younger belts (Naqvi and Rogers, 1987). In comparison to the older belts, these belts are rich in sedimentary lithounits over to volcanic suites and first time in the geological history, the craton undergone with extensive exogenic processes as indicated by terrigenous sedimentary rocks deposited under various flow regimes.

Naqvi (1981) proposed a interfingering model of stratigraphy of the Dharwar schist belts and acid plutons (Fig. 2.3). However, because of polymetamorphism and scanty isotopic age data there is no unanimity of opinion regarding their regional stratigraphy (Naqvi, 1982), but in absence of these unequivocal evidences, this model gives a more genetic sequential view of schist belts of Dharwar Craton. It is also clear from this model that as Dharwar schist belts are made up of volcano-sedimentary metamorphics of varying ages, the Peninsular Gneisses also consist of pluotonometamorphic rocks emplaced into stratigraphic succession of different ages at different times. Hence, any individual belt

is younger than any particular gneiss and may be older than other group of gneisses. It was a major contribution to the most controversial aspect of Precambrian geology of South India. In this attempt Naqvi (1981) divided the Dharwar schists into four groups viz. (1) Holnerasipur Group - older supracrustal group of the craton. In this group, precursors of the gneisses dated at 3.4 Ga by Beckinsale et al. (1980), are found intruding the belt. It consists of mafic-ultramafic schists and chemogenic argillaceous sediments, fuchsite quartzite, kyanite-staurolite-mica-garnet-quartz schist, graphite schists, and chloritoid-magnetite-garnet schist. No evidence was found for detrital sedimentation. It is followed by (2) Javanahalli Group - which mainly consists of sediments, including quartzite, metaarkose, para amphibolites, ironstones and cherts, intruded by sills and dykes (Naqvi et al., 1980, 1981; Narayana et al., 1983). One of the most significant features of this group is the first appearance of current bedded sediments, which is undoubtedly a sialic derivation. The Javanahalli Group is followed by (3) Bababudan Group - it commenced with a marked unconformity represented by quartz pebble conglomerate. The maximum age of this group is controlled by the age of Mavinkere trondhjemite (3.0 Ga.) and the age of Chickmagalur granite (3.1 Ga). It includes various type of metavolcanics, interbedded with current bedded quartzite, chlorite schist. Ferruginous schist and BIF are most prominent rock types of this group (Bhaskar Rao and Drury, 1982; Naqvi and Rogers, 1987). The Bababudan Group is followed by (4) Chitradurga Group - the existence of a break between Bababudan and Chitradurga Group is controversial. It consists of

metagraywackes, metapelites, calc- alkaline metavolcanics, various type of cherts and sulphides.

2.5 STRUCTURES:

Structures of three generations in hand specimen and outcrop are common in all the supracrustal rocks- banded ferruginous quartzite, mica schist and chlorite schist, marble and calc-silicate rocks (Naha et al., 1986; Mukhopadyay, 1986; Ghosh and Sengupta, 1985). Recently Naha and Mukhopadhyay (1990) synthesized the structural styles of whole Peninsular India and proposed structural evolution for Karnataka nucleus. Structures of the first generation comprise isoclinal folds on stratification (DhF_1) having long limbs and thickened hinges, with an axial planer cleavage. The (DhF_1) folds have been affected locally by near-coaxial upright folding (DhF_{1a}) during the second phase. These two sets of folds may represent structures formed at different stages of progressive deformation. Structure of the third generation (DhF_2) consist of upright folds with varying tightness, with the axial planes striking between NNW and NNE. The (DhF_{1a}) folds have affected the axial planes of the (DhF_1) folds with the fold axes remaining nearly constant. As a result, the (DhF_1) folds change from recumbent/reclined through inclined, to upright attitude.

Chadwick et al. (1978) reported approximate parallelism of fabrics in pre 3.0 Ga. greenstone belts (Sargurs) and younger sequences (Dharwar), Naha et al. (1986) also reported similar relationship. However, the correlation between the deformation episodes in the "Sargurs" and "Dharwars" is controversial and

relationship is not unequivocally established (Mukhopadhyay, 1986). Similarly of structural style brought out first by Chadwick et al. (1978) was interpreted by Mukhopadhyay (1986) as due to rotation of earlier "Sargur" structures into parallelism with the younger "Dharwar" structures.

2.6 PETROLOGY OF ROCK TYPE:

2.6.1 Petrology of Rocks in Enclaves and Coherent High Grade Belts:

2.6.1.1 Quartzite and iron stones:

Quartzose rocks are common in enclave suites but rare in coherent high grade schist belts. They occur in the enclaves as thin layers associated with other presumed metasediments such as calcareous rocks and aluminous mica schist (Naqvi and Rogers, 1987).Ironstones are quartz-magnetite or quartz-silicate rocks, containing minerals such as grunerite or hedenbergite.

2.6.1.2 Mica schist:

Mica schists are commonly referred to as "metapelites". Mineralogically it consists of a mixture of biotite, muscovite kyanite, staurolite and graphite.

2.6.1.3 Calc-silicates:

Calc-silicate rocks presumably are metamorphosed calcareous sediments. The major minerals are calcite, garnet, amphibolite,

diopside, anorthite, dolomite and quartz. Talc, serpentine and/or phlogopite (Naqvi and Rogers, 1987).

2.6.1.4 Manganese rich rocks:

Manganese rich rocks occur only locally, interbedded with quartzites and calc-silicate rocks (Janardhan et al., 1981). Principal Mn-ferous minerals are spessartite and Mn-bearing clino- and orthopyroxene, other than quartz and feldspars.

2.6.1.5 Amphibolites:

Amphibolites contain hornblende and plagioclase, generally with abundant garnet. Clinopyroxene is present in some rocks (Naqvi and Rogers, 1987; Viswanatha and Ramakrishnan, 1981).

2.6.1.6 Mafic granulites:

Mafic granulites consist primarily of plagioclase, both pyroxenes, garnet $\pm$ amphiboles. Some of the granulites may be part of layered or other intrusive bodies. A few granulites may represent higher grade equivalents of paramphibolites (Hussain and Naqvi, 1983).

2.6.1.7 Ultramafic/anorthosite rocks:

These are grouped together although their cogenetic nature is not well established. The high grade enclaves include metamorphosed ultramafic assemblages with variable proportion of olivine, serpentine, orthopyroxene, chromite, actinolite, talc, carbonate and chlorite (Naqvi, 1978).

2.6.2 Petrology of Rocks of Greenschist Belts:

Apart from various type of metavolcanic rocks and minor anorthositic ultramafic suites (which are similar to the high grade schist belts), clastic metasedimentary rocks constitute a well significant contribution to these younger schist belts. Their petrology, in brief is discussed below :

2.6.2.1 Metavolcanic rocks:

Most of the volcanic rocks in these schist belts are mafic, although significant amount of silicic rocks also occur but locally. The metabasalt commonly consist of a mineral assemblage of amphibole and plagioclase ± quartz ± garnet ± epidote as major mineral phase (Naqvi, 1972; Naqvi and Hussain, 1973a, 1973b; Drury, 1983).

2.6.2.2 Iron and manganese rocks:

The iron and manganese rich rocks of the low grade schist belts appear to be compositionally similar to those in high grade belts (Naqvi et al., 1981). Mukhopadhyay et al. (1980) summarized the mineralogy of banded ferruginous quartzites and argillites in the Bababudan schist belts. Magnetite, quartz and clay appear to be primary minerals in these rocks. Hematite formed secondarily although exact time is not clear. Metamorphic minerals in the quartzites include cummingtonite, grunerite, magnesieoribeckite and acmite. Siderite is present in some argillites. Pyritic chert and black shale are presumably deep water facies of the iron-oxide bearing rocks (ibid).

In manganese deposits, primary minerals are mostly pyrolusite and cryptomelane. Secondary mobilization forming both veinlets and conformable concentrations. There is apparently no relationship to volcanic rocks, indicating a sedimentary rather than volcanogenic origin (Naqvi, 1972; Naqvi and Hussain, 1972).

2.6.2.3 Chert and carbonates:

Thin beds of chert and carbonate rocks occur sporadically throughout the low grade schist belts. Most of the carbonates are dolomictic limestones (Devaraju and Anantha Murthy, 1984), although some pure limestone is also present. Recrystallization has formed fine grained quartzites from much of the chert and given a coarser crystalline texture to the limestone (Naqvi, 1967). Distinction between clastic quartzites (unless they are conglomeratic) and recrystallized chert is difficult. Kumar et al. (1983) found $\delta^{13}C/^{12}C$ ratios from +0.3 to -1.3 points per thousand, in Chitradurga carbonates, possibly indicative of organic activity.

2.6.2.4 Micaceous schists:

Schistose rocks consisting of quartz, minor feldspar, and high abundances of biotite, muscovite, and/or chlorite are generally regarded as metapelites. The major schist belts, such as Chitradurga have thick sequence of these fine grained rocks, although the greatest thickness of sedimentary accumulation seems to consist of graywackes. The abundance of micaceous schists indicates extensive development of clays in the source areas of the schist belts (Seshadri et al., 1981; Naqvi and Rogers, 1987).

2.6.2.5 Quartzites:

In low grade schist belts, quartzites are purely detrital, as it is exhibited by various primary sedimentary structures. Other than an appreciable amount of quartz, both mono and poly crystalline some ferrous metals, viz iron (magnetite or pyrite), manganese (generally as an oxide) and chromium (fuchsite) are also present in high concentration; plagioclase and other heavy minerals like zircon, rutile, epidote, garnet are also present. Microcline and orthoclase are also present but in very less quantity.

2.6.2.6 Conglomerates:

Both type of conglomerates, oligomictic and polymictic, are present in younger schist belts. Many oligomictic conglomerates contain only quartz pebbles, which indicate extreme weathering in a source area or on an erosional surface. Matrix, filling in intervening space, is also of quartz, but sometimes fuchsite quartzite is also present. In the southern margin of Bababudan schist belt, presence of quartz-pebble oligomictic conglomerates forms a regional unconformity and it is an uraninite, gold and pyrite bearing horizon. Pebbles are not only of pure quartz, but quartzitic pebbles are also reported (Chadwick et al.,1985a). In general, oligomictic sedimentary conglomerates are rare.

The polymictic conglomerates of the schist belts have a clay matrix and generally contain fragments of all underlying rock types (Naqvi and Hussain, 1972; Naqvi et al., 1978a; Ranganna et al., 1981; Arora et al.,1991), including debris from underlying

rocks within the schist belt in addition to those from surrounding terrains.

2.6.2.7 Graywackes:

Graywackes constitute thick sections of many low grade schist belts and virtually no occurrence has been reported from high grade older schist belts. Their average composition is about 40% quartz, 40% rock fragments (including lithic fragments) and micaceous matrix, 10% plagioclase, 5% K-feldspar, 5% chert and quartzites. They were commonly deposited late in the evolutionary history of the sedimentary basin and were clearly derived by erosion of the gneissic terrain including older mafic belts (Naqvi and Rogers, 1987; Argast and Donnely, 1986).

2.6.3 Petrology of Peninsular Gneisses:

Similar to all other gneissic complexes in the world, the Peninsular Gneiss of India is extremely difficult to investigate. A major problem is caused by of its great diversity, with variability on a scale ranging from hand specimens to mountain ranges (Pichamuthu, 1976). The general mineralogy of the Peninsular Gneisses is very simple. All rocks contain quartz, plagioclase and biotite in variable proportions. Most rocks also contain small amount of K-feldspar and muscovite or hornblende is present in some samples (Bhaskar Rao et al., 1983). The rocks are, therefore, the tonalitic/trondhjemitic "grey gneisses" of many Archaean terrains.

2.7 GEOCHEMISTRY:

In Dharwar craton, an extensive geochemical investigation has been carried out by many workers A general and overall review of geochemistry of various rocks type, constituting high and low grade schist belts, is discussed below.

2.7.1 The Holenarsipur Group:

On the basis of SiO_2 and REE abundances the metasediments of Holenarasipur Group (Naqvi, 1981) which include metapelites and schists (Naqvi et al., 1983; Hussain and Naqvi, 1983) have been classified into four groups (Naqvi, 1983). Group I is marked by low SiO_2, low alkalies and at least 10 times higher concentration of REE, than that of chondrites. Eu anomalies vary from +ve to -ve. Metapelites are enriched in Fe_2O_3, TiO_2, MgO, CaO, Cr, Co and Ni. Group II is characterised by higher SiO_2 and constant dilution of Fe_2O_3, TiO_2, MgO, CaO, Cr, Co and Ni. Group III exhibits high Al_2O_3 concentrations, and also contain large amount of Fe_2O_3 and Cr. LREE are more enriched in this group rather than I or II. Group IV, shows enrichment of HREE and +ve Eu anomalies. The high Al, high Cr and Ni and +ve correlation between Al_2O_3 and Cr, suggesting a probable common source for Al and Cr (Naqvi, 1983).

2.7.2 The Javanahalli Group:

Javanahalli Group (Naqvi, 1981) is mainly made up of metasediments, and about 10% of these metasedimentary rocks constitutes the paragneissic suites. Most of these paragneisses rocks have K_2O/Na_2O more than one. However, in some cases it is

less than one. Irrespective of the variation in alkali content, the paragneisses show REE patterns similar to some Archaean adamellites and granites and to Phanerozoic shales, quartzites and arkoses, showing LREE enrichment, large -ve Eu anomalies and relative flat HREE. No similarity was found between paragneisses and older sediments. The fact that both Na and K-rich paragneisses show similar REE patterns (Narayana et al., 1983) indicates that both type of arkoses were derived from underlying gneisses (Naqvi et al., 1980; Naqvi, 1983; Uday Raj, 1991). These paragneisses are overlain by para-amphibolites. Major element composition of the amphibolites is not diagnostic of their original nature. Trace and REE, however, can help to clarify the nature of original rocks. The Th/U, Ba/La and La/Th ratios, are significantly different from those of Archaean metavolcanic amphibolites. REE patterns are flat or LREE depleted and show +ve Eu anomalies, in general, which are different from the metabasalts of most of the Archaean terrain (Murali et al., 1979). The amphibolites are therefore regarded as a product of simultaneous argillaceous and carbonate sedimentation from a heterogenous terrain (Naqvi, 1983).

2.7.3 The Bababudan Group:

About 30-40% of exposed surface of Bababudan Group (Naqvi, 1981) is made up of detrital metasediments, and 10% constitute ironstones. Most of the metasediments except BIF are clastic by their nature. Derivation of the debris of these sediments from a source area of mixed composition is evident from variation in the Na_2O/K_2O ratios, and Cr, Co, Ni, Fe and Mg abundances (Naqvi,

1983; Arora et al., 1991).

2.7.4 The Chitradurga Group:

Metasediments of Chitradurga Group (Naqvi, 1981) cover about 80% of total exposed area of the craton, and constitutes predominantly graywackes, shales, quartzites and conglomerates. Limited geochemical work has been carried out in this area (Naqvi and Hussain, 1972; Naqvi et al., 1978a ; Naqvi, 1978; Naqvi et al., 1988). Again, geochemical studies confirm the multicomponent nature of provenance, which have provided the sediments to rocks of Chitradurga Group. Here also Fe, Mg, Ni and Cr are abundant, and high K_2O and K_2O/Na_2O ratios.

CHAPTER-III
GEOLOGY OF THE BABABUDAN SCHIST BELT

3.1 INTRODUCTION:

The Bababudan schist belt is named after the precipitous crescentic Bababudan hills located in the southwestern part of the Karnataka (Fig.3.1). The ring of hills encircles the densely wooded, picturesque Jagar valley to the west.

The schist belt (Fig.3.2) has the configuration of a broad basin, with arcuate indentations, irregular embayments and tongue like projections at the margins (Viswanatha and Ramakrishnan, 1981). The eastern, western and the northern boundaries of this schist belt are marked by prominent faults (Chadwick, et al. 1985a & b). Southern boundary of the Bababudan schist belt is marked by most prominent unconformity, represented by quartz pebble conglomerate (QPC). First mature arenites, and other sedimentary units derived from a continental crust were deposited in the geological history of Dharwar craton (Karnataka Nucleus). The QPC at the base of Bababudan represents the regional unconformity between underlying "Peninsular Gneisses", which includes migmatic, granitic gneisses (e.g. Chickmagalur granite) and granodiorite (2.9-3.2 Ga; Ramakrishnan et al., 1984; Taylor et al., 1984), and the Bababudan Group of Dharwar Supergroup (Swami Nath et al., 1976; Swami Nath and Ramakrishnan, 1981). However, at some places it is directly resting over palaeosols (Fig.3.3).

This late Archaean (Chadwick et al., 1985a) volcano-sedimentary sequence occupies a large area of about 2650 km^2, and form basal part of Dharwar Supergroup, i.e. Bababudan Group. The belt exposes one of the best geological

Fig. 3.1 : Geological map of the early Precambrian of Karnataka. AGD, Anagod; AH, Aladahalli; AMG, Aimangala; ARK, Arsikere; BBN, Bababudan; BNG, Bangalore; CHI, Chiknaikanahalli; CKM, Chickmagalur; CPT, Closepet; CTD, Chitradurga; DH, Dharwar; DHP, Dharmapuri; DNI, Dodguni; HNI, Honnali; HNP, Holenarasipur; JH, Javagondanahalli; JMD, Jogimardi; JPN, Jampalnaikankute; KBG, Kabbaldurga; KGF, Kolar Gold Field; KLI, Kondli; KMK, Kurubaramaradikere; KPK, Kempinkate; KPR, Kalasapura; KTR, Kartikere; KWA, Kumbarwada; MJB, Manjarabad; MK, Madadkere; MND, Munirabad; MYK, Mayakonda; NH, Nuggihalli; NK, Nerale Katte; PS, Pensamudra; PTN, Patna; SDR, Sandur; SGR, Sargur, SMG, Shimoga; SKT, Siranakatte; TKR, Tarikere; TYA, Talya.

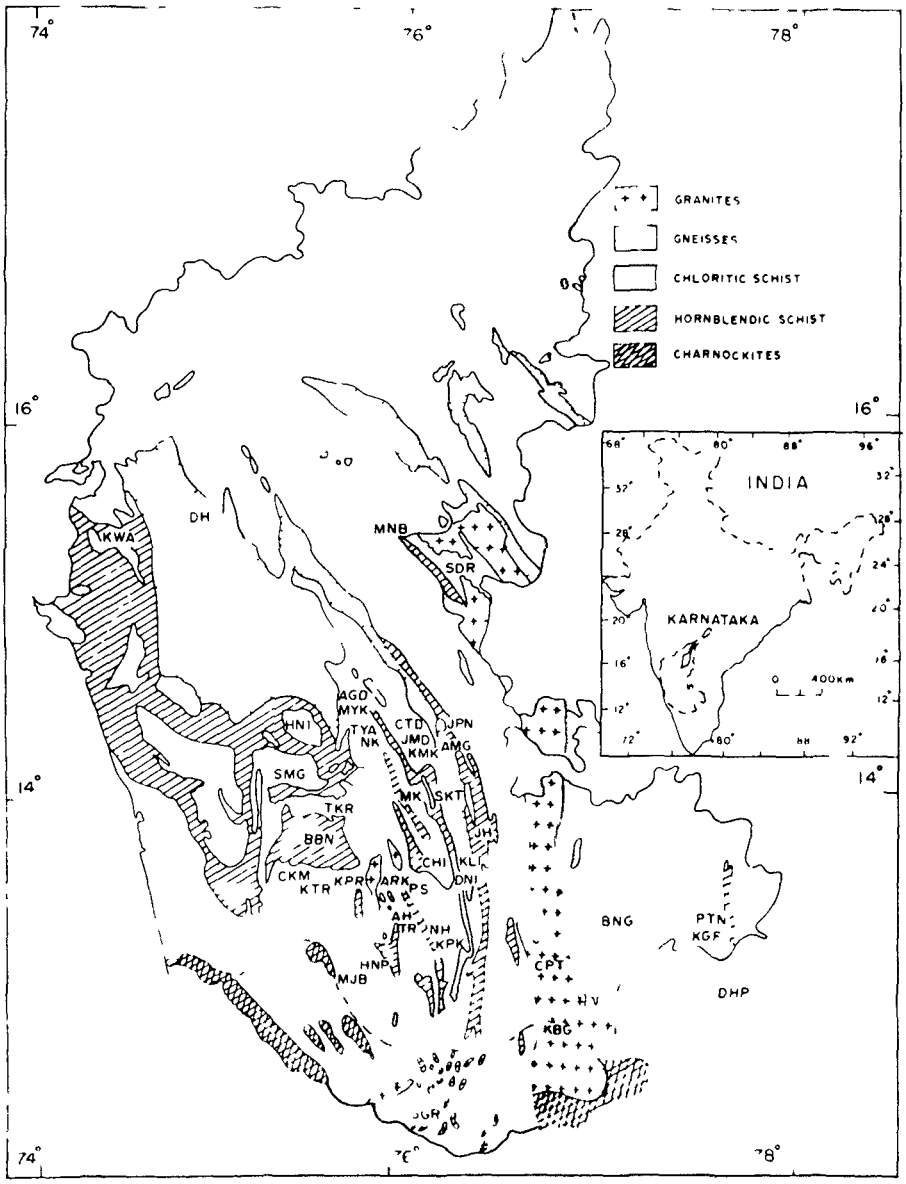
74°
76°
78°
16°
14°
GRANITES
GNEISSES
CHLORITIC SCHIST
HORNBLENDIC SCHIST
CHARNOCKITES
INDIA
KARNATAKA
400km
DH
KWA
MNB
SDR
AGD
MYK
TYA
NK
HNI
CTD
JMD
KMK
UPN
AMG
SMG
MK
SKT
TKR
BBN
CHI
KL
DNI
CKM
KTR
KPR
ARK
PS
AH
TR
NH
KPK
HNP
MJB
BNG
PTN
KGF
CPT
HV
KBC
DHP
SGR

Fig. 3.2 : Stratigraphic map of the Bababudan schist belt, Dharwar Craton, KN (After Chadwick et al., 1985 a).

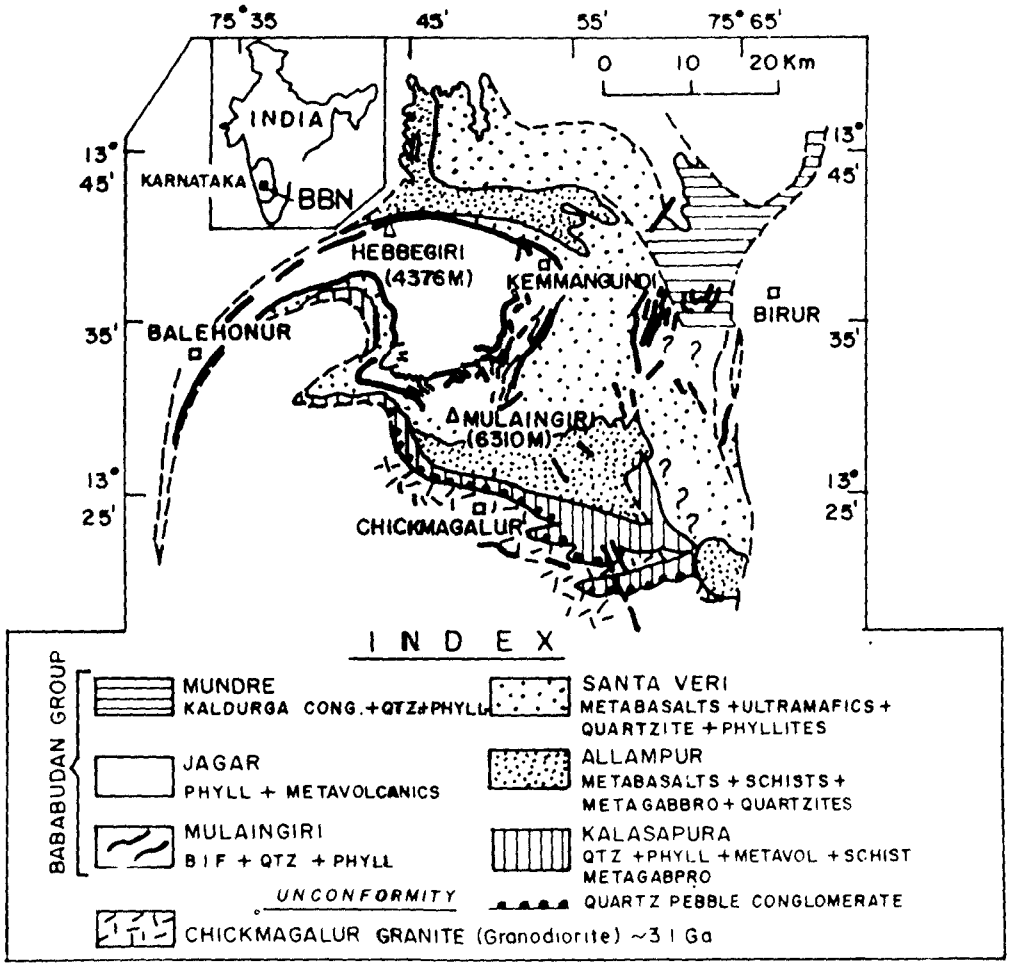
75°35
45'
55'
75°65'
0 10 20Km
INDIA
KARNATAKA
BBN
13° 45'
HEBBEGIRI (4376M)
KEMMANGUNDI
BIRUR
BALEHONUR
35'
MULAINGIRI (6310M)
13° 25'
CHICKMAGALUR
INDEX
BABABUDAN GROUP
MUNDRE
KALDURGA CONG.+QTZ±PHYLL
JAGAR
PHYLL + METAVOLCANICS
MULAINGIRI
BIF + QTZ + PHYLL
SANTA VERI
METABASALTS +ULTRAMAFICS + QUARTZITE + PHYLLITES
ALLAMPUR
METABASALTS + SCHISTS + METAGABBRO + QUARTZITES
KALASAPURA
QTZ +PHYLL +METAVOL +SCHIST METAGABPRO
UNCONFORMITY
QUARTZ PEBBLE CONGLOMERATE
CHICKMAGALUR GRANITE (Granodiorite) ~3.1 Ga

Fig. 3.3 : Quartz Pebble Conglomerate is unconformably resting on underlying Palaeosols. Location about 500 mts. South of Lakya.

Fig. 3.4 : Model Stratigraphic sequence of the Bababudan Schist belt.

3.3

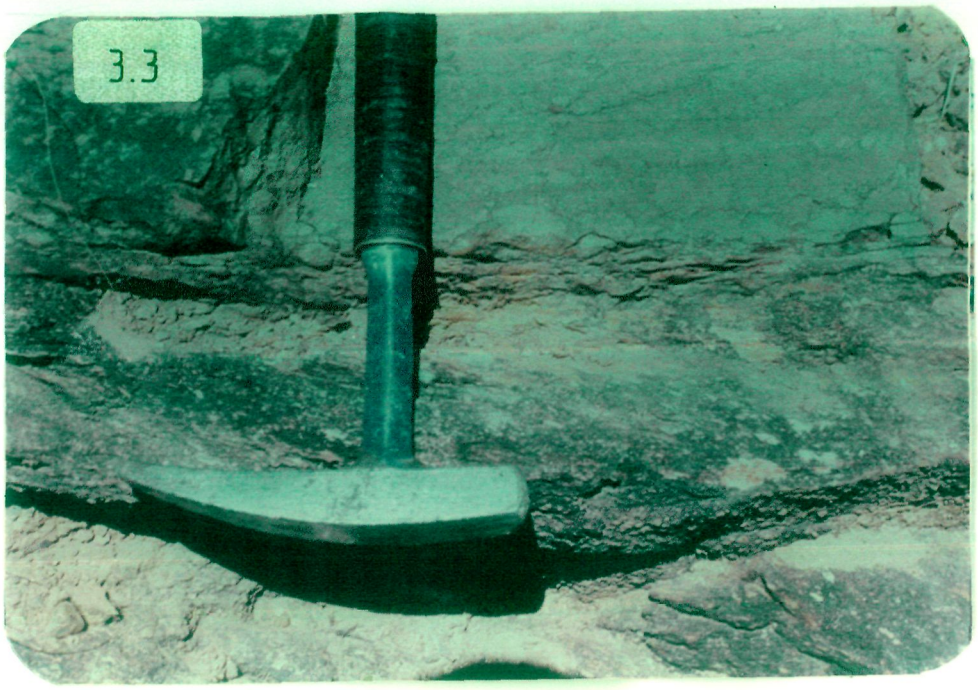

3.4

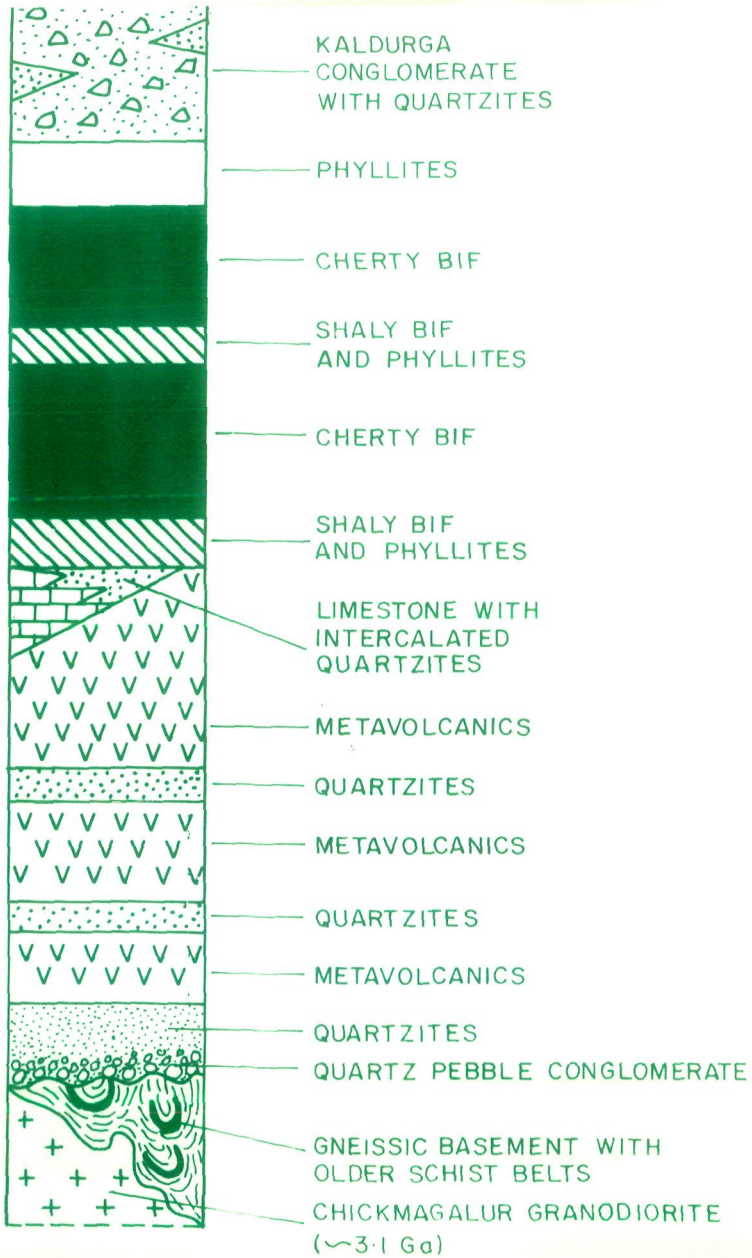
KALDURGA CONGLOMERATE WITH QUARTZITES
PHYLLITES
CHERTY BIF
SHALY BIF AND PHYLLITES
CHERTY BIF
SHALY BIF AND PHYLLITES
LIMESTONE WITH INTERCALATED QUARTZITES
METAVOLCANICS
QUARTZITES
METAVOLCANICS
QUARTZITES
METAVOLCANICS
QUARTZITES
QUARTZ PEBBLE CONGLOMERATE
GNEISSIC BASEMENT WITH OLDER SCHIST BELTS
CHICKMAGALUR GRANODIORITE (~3·1 Ga)

section of the Bababudan Group and thus constitutes its type area.

3.2 DISTRIBUTION OF ROCK TYPES:

Most part of the Bababudan basin is occupied by (i) metavolcanics, mainly basaltic and associated mafic-ultramafic rocks; (ii) a range of detrital metasedimentary sequences including oligomictic quartz-pebble-conglomerate, associated orthoquartzite (quartz arenite), graywackes and phyllites; (iii) an important deposit of economic potential particularly iron-ores in the form of banded ferruginous cherts (BIF) and (iv) argillaceous schist (Viswanatha and Ramakrishnan, 1981; Chadwick et al., 1985a). Geological map of the Bababudan schist belt (Fig.3.2) shows the distribution of above stated rock types. A brief description of various rock types is discussed below :

3.2.1 Metavolcanics and Related Rocks:

In the Bababudan schist belt, predominant metavolcanics are present with many concordant and discordant ultramafic-ultrabasic igneous bodies. Several repetitive cycles of volcanic and sedimentary rocks are exposed throughout the stratigraphic column, in which volcanic rocks are more predominant than sediments particularly in the lower and middle sections (Fig.3.4). Though the rocks show mineral assemblages of upper greenschist to lower amphibolite facies, their primary structures including columnar, amygdaloidal, columnar and variolite structures are more or less well preserved (Bhaskar Rao, 1980; Viswanatha and Ramakrishnan, 1981; Bhaskar Rao and Drury, 1982).

Metavolcanics of this basin, show a wide compositional

spectrum from basic to siliceous through intermediate varieties. Common rock types are basalt, basaltic andesite, andesite, rhyodacite, rhyolites etc. In general, all volcanic suites display distinct tholeiitic affinity. From stratigraphically "low" to "high", there is marked decrease in iron enrichment in basaltic andesites; suggesting a progressive increase in their calc- alkaline affinity (Bhaskar Rao, 1980). The volcanic suites associated with the BIF are probably calc-alkaline. The associated ultramafic-ultrabasic rocks, showing the same grade of metamorphism, form structurally conformable schist bands. Compositionally, they range from gabbro, olivine-gabbro to pyroxenite-peridotite (Srinivasan and Sreenivas, 1972; Pichamuthu, 1982).

3.2.2 Banded Iron Formation (BIF):

Most of the banded ferruginous cherts in the Bababudan schist belt are banded iron formation (Chadwick et al., 1985a) in the sense of definitions reviewed by Eichler (1976) and Trendall (1983), i.e. iron should not be less than 15%. The BIFs are exposed in the main Bababudan range (the Bababudan arc of mountains) in the central-western part of the belt and the Birur range of hills along the eastern- north eastern parts of the basin (Fig. 3.5).

In the lower portion, BIFs are overlying the phyllites, and are commonly interstratified with chloritic schists. The iron stone is often cherty and rich in magnetite (Viswanatha and Ramakrishnan, 1981). It contains several parallel seams of amosite asbestos (Bruce Foote, 1900;Radhakrishna and Venkoba Rao,

Fig. 3.5 : Thick sequence of Oxide facies Banded Iron Formation in the Bababudan schist belt. Location near Bababudan shrine at Mulaingiri hills.

Fig. 3.6 : Small xenoliths of amphibolite of older schist belts, trapped within the Chickmagalur granodiorite (~3.1 Ga), show the recycling of early formed crust for generation of granodiorite. Location near Marle.


3.5

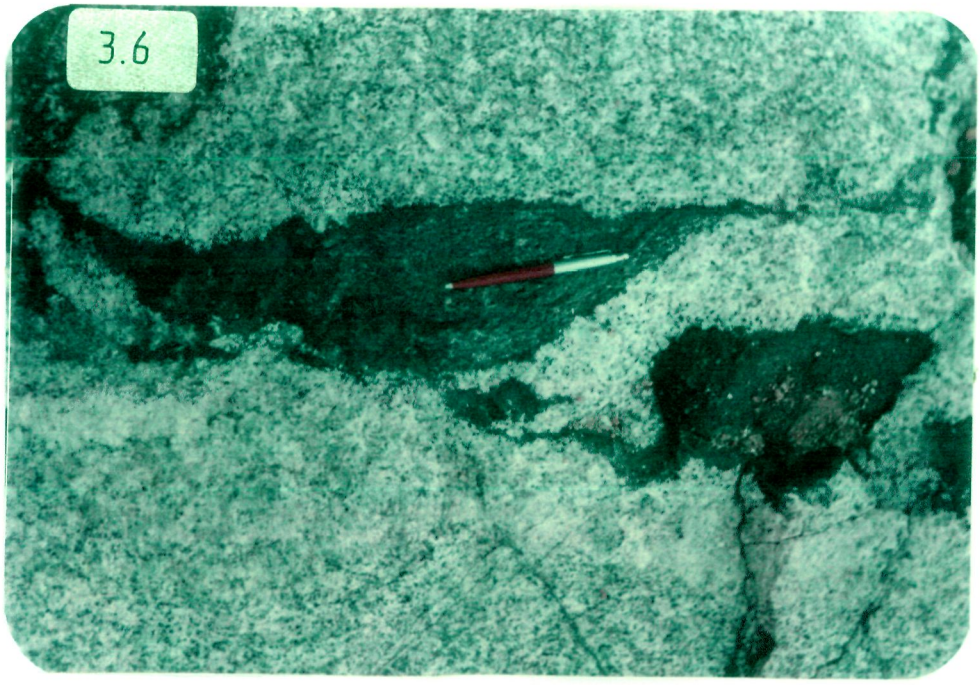
3.6

1967). Sreeramachandra Rao (1977) observed that the iron formations and the iron rich lithotypes range from 5 to over 200 mts. in thickness and are essentially of non-oolitic magnetite facies and silicate facies comprising amphiboles. Sulphide facies (James, 1954) is rather insignificant. Mutually transitional and intermixed mafic-felsic volcanics, volcaniclastics and chemical derivatives-aluminosilicate schists, magnesian iron silicate schists, cherts and iron oxide form successive rhythmic layers in the iron formations (Sreeramachandra Rao, 1977). Bhaskar Rao (1980) found that the protore in iron formation of all areas is magnetite and that the rocks in Bababudan and Kodachadri areas are of greenschist facies while those in Kudremukh are of epidote-amphibolite facies of metamorphism.

3.2.3 Conglomerates and Associated Quartzites:

Metasedimentary units in the Bababudan schist belt consist of a basal oligomictic quartz-pebble-conglomerate, associated quartz arenite, quartzites at various stratigraphic horizons, polymictic Kaldurga Conglomerate and phyllites.

Quartz-pebble-conglomerate with orthoquartzites is exposed along the southern boundary of the belt and occupies prominent peaks. The total length of the exposure is about 85 km. The persistent strike wise exposure right from Kalasapura to further west of Chickmagalur town, is a remarkable feature which could be a result of repetition of folds trending E-W, with axial plane dipping towards north. Thickness of this horizon varies considerably from place to place from about 2 mts. to 30 mts. Quartz pebble conglomerate beds are generally massive, hard and

brown. This conglomerate is known to be uraniferous, auriferous and pyritiferous (Narasimhan and Viswanatha, 1970a; Rama Rao, 1974; Swami Nath et al., 1974; Sreenivas and Srinivasan, 1974; Fareeduddin, 1988).

Quartzites associated with QPC and other quartzites interbedded with volcanic rocks, which are present at various stratigraphic levels of the Bababudan schist belt, are characterized by the presence of a number of primary depositional sedimentary and deformational structures. These quartzites are generally medium grained, compact and grey to brown in colour. Fuchsite quartzite with its peculiar green colour is also present at many places.

The Kaldurga Polymictic Conglomerate, with graywacke matrix is another important and predominant sedimentary sequence of this volcano sedimentary schist belt. Its matrix shows the effect of metamorphism to amphibolite facies. Chlorite is often present as retrograde mineral (Arora et al., 1991).

3.2.4 Peninsular Gneisses:

Peninsular Gneisses include quartzofeldspathic gneisses mainly tonalitic-trondhjemitic (TTG), migmatites and associated syntectonic tonalites or trondhjemites, rich in enclaves or remanents of older Sargur Group or its equivalents. The gneiss surrounds the Bababudan belt from all sides (Viswanatha and Ramakrishnan, 1981). Common components of the gneisses include both concordant and discordant sheets and patches of mafic to ultramafic amphibolites of both massive and schistose type. Small sheets and veins of granitoid rocks range in texture and

granularity from aplite to pegmatite. Chickmagalur granodiorite, more precisely a granitoid gneiss, has broadly the configuration of an inverted triangle with its base along the southern margin of the Bababudan basin. Three prominent embayments are seen at the north eastern corner of the granite (Chadwick et al., 1978; Viswanatha and Ramakrishnan, 1981). The rock is leucocratic, coarse grained and commonly show a feeble lineation or a streaky foliation. The gneisses and the granites are well exposed all along the southern slopes of the conglomerate-quartzite band. All along the southern contact with the gneisses, the granite has sent out apophyses and granitic veins into the gneisses and has thus, enclosed numerous xenoliths of banded gneisses, ultramafic rocks and amphibolites (Fig.3.6).

3.3 LITHOSTRATIGRAPHY OF THE BABABUDAN SCHIST BELT:

The Bababudan Group of the Bababudan schist belt (Swami Nath et al., 1976) is dominantly made up of metavolcanics, therefore it is difficult to subdivide this volcano-sedimentary sequence on the basis of field characteristics of metavolcanics only (Chadwick et al., 1985a). Viswanatha and Ramakrishnan (1981) suggested that the reconstruction of the stratigraphy of this belt is mainly dependent on the identification of depositional margin. Stratigraphy of the Bababudan schist belt could be erected after identification of quartz pebble conglomerate at southern margin of the belt as anerosional unconformity. Thus depositional margin of the belt (Iyengar, 1976; Viswanatha, 1976) and recognition of comparatively thin sedimentary unit (quartzites) within the metabasalts as a basal member are key factors of the tentative

subdivision of the belt into various subgroups as proposed by Chadwick et al.(1985 a) and given in Table 3.1.

Along the southern contact, the quartz pebble oligomictic conglomerate truncates the foliation and banding of the gneissic complex. At the Chickmagalur tankbund the low dipping (~30°N) conglomerate beds are underlain by a palaeosols about a meter thick. However at south of Lakya village (at a road cutting), palaeosole horizon is as thick as 10 mts (see Fig. 3.3, sec 3.1). This horizon of palaeosol is not found between Chickmagalur granite and overlying QPC. It is developed on gneisses only and a gradation from unweathered gneisses to palaeosole is clearly seen around the Lakya section. These features suggest that the southern margin marks a distinct erosional unconformity between the Bababudan Group and Peninsular Gneiss, including Chickmagalur granite. Viswanatha and Ramakrishnan (1981) worked out the succession of the belt on the basis of order of superposition aided mainly by primary sedimentary structures like ripple marks and cross beddings in quartzites, and vesicular tops of weakly deformed volcanics. No large scale inversions have been found, thereby indicating right side up succession. It has also been found that there is neither prominent imbrications at the basin margin as in Labrador Trough (Dimroth, 1970; 1972), nor large scale early nappes as reported from the western Ghat belts (Drury and Holt, 1980; Viswanatha and Ramakrishnan, 1981), to distort the Bababudan stratigraphy. Since the basis of this classification is lithology, therefore, it has been referred as lithostratigraphy. They (ibid) recognised another unconformity between the Bababudan and the Chitradurga Group in the the Bababudan belt, which is

Table 3.1: Stratigraphic sequence of the Archaean Bababudan schist belt, Dharwar Craton, India (After Chadwick et al. 1985).

NORTHWEST, SOUTHWEST AND SOUTHEAST BABABUDAN	NORTHEAST BABABUDAN
	Local granitic intrusions
JAGAR FORMATION (? up to 2000 m) (restricted to Jagar depression)	MUNDRE FORMATION (min. c.7000m) Kaldurga Conglomerate:
Metabasalts and siliceous phylites.	Upper division: clasts of basement dominant; Lower division: clasts of cover and basement in upper horizon; clasts only of cover in lower horizon; calcareous quartzite in the upper horizon of lower division; Lateral equivalents of Kaldurga conglomerate are cross-bedded quartzite interbedded with phyllites; Metabasites and quartzites overlie the Sarasvatipura conglomerate which is unconformable on the basement in the east Bababudan.
MULAINGIRI FORMATION (200-1500m)	
Interbedded banded ferruginous cherts and phyllites with rare metabasites and ultramafic schists.	
SANTAVERI FORMATION (0-? 2000m)	
Metabasites, local rhyolites, tuffs and agglomerates; serpentinites common in NW Bababudan; basal Tanigebail quartzite in north is presumed to be the equivalent of the basal Kaimara quartzite in the south.	
ALLAMPUR FORMATION (0-? 2000m)	
Metabasites, metagabbros, ultramafic schist; local banded ferruginous cherts and interbedded phyllites; basal Lakya quartzite in south; base not seen in north Bababudan.	
KALASAPURA FORMATION (up to ? 2000m)	
Metabasalts, metagabbros, ultramafic schists; local phyllites and interbedded quartzites; basal quartz-pebble-conglomerate (QPC) unconformable on peninsular gneiss basement in southern Bababudan.	

PENINSULAR GNEISS BASEMENT (c. 3.1 Ga) includes the Chikmagalur Granite (granodiorite), found along most of the southern unconformable boundary, other granodioritic masses and banded migmatic orthogneisses. Extensive tracts and enclaves of the Sargur supracrustal association are common in the gneisses.

represented by the Kaldurga Polymictic Conglomerate. Its stratigraphic position and origin has been a matter of serious debate. Naqvi et al. (1978b) suggested that this polymictic conglomerate with graywacke matrix is not a marking horizon for an unconformity and thus not a representative of a stage of non-deposition. Alternatively they suggested that it indicates a condition of intense sedimentation. The Tarikere Formation of the Chitradurga Group in the Bababudan belt is lying above this so called unconformity. Author's work also on this rock suite indicates that the Kaldurga Conglomerate is a fanglomerate and can not be taken as an unconformity.

Chadwick et al. (1985a) have slightly modified the lithostratigraphy of the belt, because they found that descriptions and estimation of thicknesses of various formations of the belt, made by Viswanatha and Ramakrishnan (1981), were based mainly on the occurrence of the formation in the southern part of the belt and did not provide clues about the possible regional variations in thickness and lithofacies. In order to provide a more comprehensive description of the lithostratigraphy of the whole basin, Chadwick et al. (1985a) enlarged the definition of previous subdivisions and redefined the younger subdivisions of the Bababudan Group. They (ibid) added an additional formation namely, the Mundre Formation, which includes the prominent Kaldurga Polymictic Conglomerate in north-eastern part of the basin. The Jagar Formation which overlies the Mulaingiri Formation and consists of phyllites, seems to be a lateral equivalent of the Mundre Formation. The Allampura and the Santaveri Formations have also been extended after including major

lithostratigraphic divisions in the north of the belt, on the basis of spatial relations as indicated by way-up criteria on (Chadwick et al., 1985a). Due to these modifications in the interpretation of the stratigraphy, the rocks in north east of Bababudan, which were regarded earlier as a part of the Chitradurga Group, have now been included within the Bababudan Group. Thickness of individual formations, their typical lithologies and genetic associations are given in Table 3.1.

3.4 STRUCTURES:

As far as structural studies of the Bababudan belt are concerned, Pichamuthu (1935, a,b,c) for the first time noted the synclinal structure (Kaldurga syncline) and an "over fold" in the Nandi valley in the northeast and he later suggested (Pichamuthu, 1961) the existence of a refolded syncline which has resulted in the present shape of the basin. According to Naha and Chatterjee (1982) and Naha et al. (1986) the Bababudan hill ranges show three generations of folding on all scales. The isoclinal first folds (F_1) on westerly plunging axes were overprinted by nearly coaxial, upright, open folding (F_2), which caused a swing in strike not only of the bedding planes but of the axial planes of the F_1 folds also. These refolded folds were affected in the final phase by upright folds, of the F_1-F_2 axes. Superposition of F_2 folding on F_1 folds has resulted in hook-shaped interference patterns with double closers (Fig. 3.7a). Superposition of F_3 folding on F_2 folds has led to dome - and - basin structures (Fig.3.7b). Chadwick et al (1985b) proposed that the structures within the basin are dominated by steep fault and

Fig. 3.7(A): Simplified map of the Bababudan schist belt showing the pattern given by the banded iron formation (After Sampat Iyengar, 1912).

(B): Dome-and-basin interference pattern (type-I) on axial planar cleavage of F_1 generation in BIF due to superposition of F_2 and F_3 open folding.

(C): Hinge zone of an isoclinal F_1 fold in quartzite with gently dipping axial plane. Slight fanning of axial plannar cleavage is noticed. Location on the Chickmagalur - Kadur road; 11th Km from Chickmagalur town.

(D): Field photograph showing the isoclinal fold in banded ferruginous cherts.

A

B

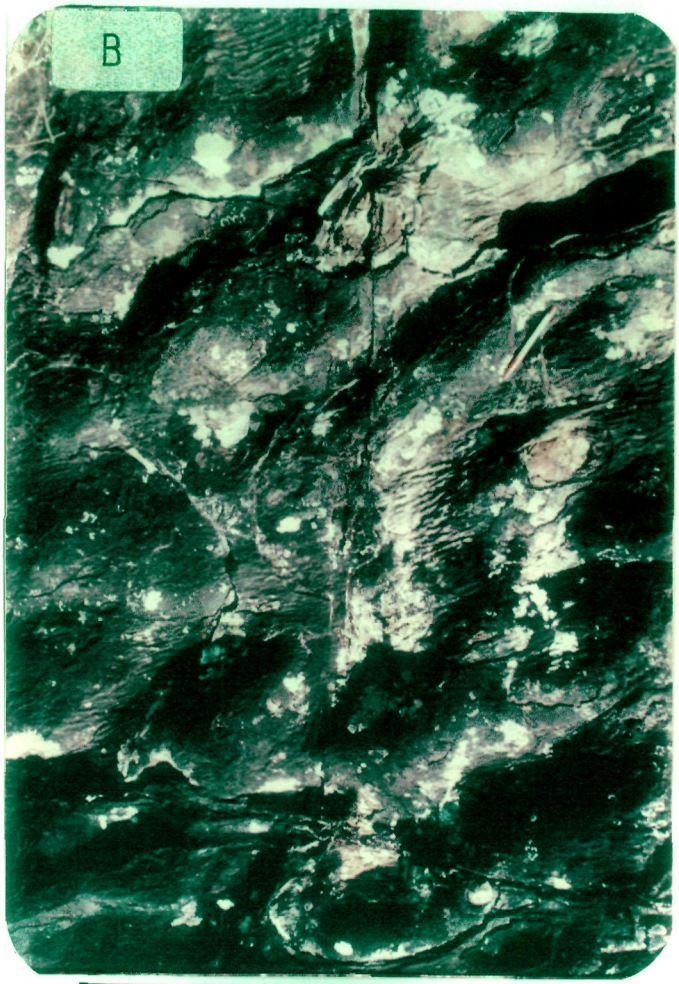

C

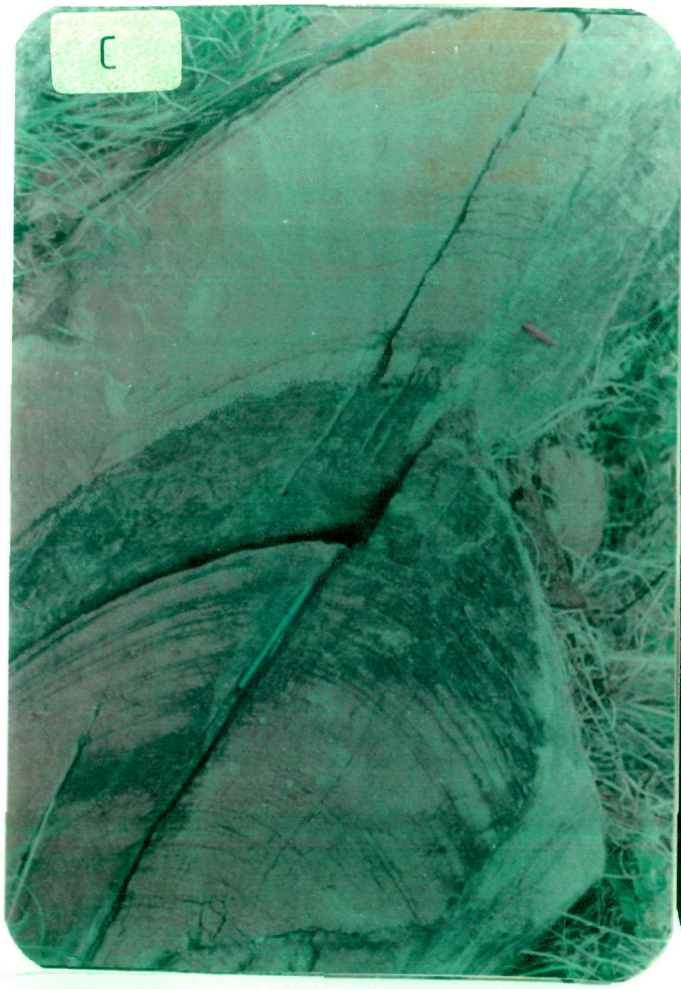

D

upright open folds with strongly curved hinge lines within steep axial surfaces (Fig. 3.7c). The Bababudan syncline is an open east-west fold which curves gently westward into a tight cusp trending north, parallel to the western boundary fault. East of the syncline the structure is dominated by the upright open arch and complex saddle zone of the Santaveri anticline. Synchronous refolding and rapid variations in the style of small scale folds are common especially in the multilayered complexes of banded ferruginous cherts (Fig. 3.7d). Chadwick et al. (1985b) regarded the folds illustrated by Naha and Chatterjee (1982) as products of the same period of deformation and not as effects of distinct phases.

3.5 PETROLOGY OF ROCK TYPES:

Apart from various types of metavolcanic suites, the Bababudan schist belt is comprised of both clastic and nonclastic metasedimentary rocks also, including conglomerates, quartzites, phyllites and banded iron formations.

3.5.1 Metavolcanics:

The metavolcanics of the belt consist of a wide variation of suites ranging in composition from basalt to rhyolite. Metamorphic grade varies from upper greenschist to lower amphibolite facies. This variation of metamorphic grade is also exhibited by the associated ultramafic-ultrabasic bodies. Some of these UM+UB bodies are clearly intruding into the mafic volcanics, whereas some of them may be volcanic flows but spinifex texture has not been noticed as yet. Mineral assemblages and geochemistry

of the volcanic suites and related mafic-ultramafic rocks and schists are studied by Bhaskar Rao (1980), Bhaskar Rao and Naqvi (1978), Bhaskar Rao and Drury (1982) and grouped as follows :

Mafic rocks	: Chlorite, actinolite, plagioclase, quartz, epidote, calcite, ankerite, hematite, tremolite. Clinopyroxenes are rarely present.
Schists	: Chlorite, sericite, muscovite, biotite, carbonates, quartz, actinolite, clinozoisite
Ultrabasic association	: Tremolite, actinolite, chlorite, antigorite, zeolite, clinopyroxene, oligocls (very rare).

Textural obliteration and overprinting in metavolcanics is a function of grain overgrowth, penetrating deformation and hydration reactions. At very low temperature, mineral nucleation is induced leading to growth of new metamorphic mineral assemblages, as replacement of the "primary" minerals. The higher temperature results in the abundance of the new phases. Metavolcanics of the belt display a complex interplay of all these phenomenon, but it is interesting to note that in most rock samples, even in many highly altered specimen, secondary phases did not grow acorss the primary grain boundaries. As a result, relict primary structures and textures like anygdolidal and porphyritic structures (micro variolitic and spherulitic) etc. are often preserved (Bhaskar Rao, 1980).

3.5.2 Banded Iron Formation:

Major part of the Mulaingiri Formation of the Bababudan

schist belt constitute of banded iron formation of the belt (Viswanatha and Ramakrishnan, 1981; Chadwick et al., 1985a). Mineralogy and texture of BIF of this belt has been described in detail by Chadwick et al. (1986). In general magnesioriebeckite (Bababudanite- Smeeth, 1908; Pichamuthu, 1936) is a well known mineral, especially as asbestiform crocidolite, in BIF. In Bababudan hill range, BIF include nine other species of minerals of which quartz and magnetite are the most abundant. Magnesioriebeckite and aegirine are essential components, whilst magnesian siderite (var. pistomestite) is an important accessory. Minor accessory minerals include apatite, pyrite, hematite and hydrous iron oxides (Chadwick et al., 1986). Similar mineralogy has been reported from Kudremukh belt by Khan et al. (1991).

The BIF of this belt and host to magnesioriebeckite and aegirine is finely layered, principally with seams of magnetite $\pm$ quartz $\pm$ carbonate, varying from 0.1 to 10 mm in thickness interbedded with seams of comparable thickness, rich in quartz with other silicates and carbonate. Layers of this type in BIF have been described as mesobands (Trendall, 1983), and known as chert layers. Quartz in those parts of cherty layers, is least affected by deformation and has a fine grained, equidimensional granoblastic-polygonal texture. The uniform or weak undulose extinction indicates that the quartz grains are relatively strainfree. In deformed parts of some chert layers quartz grains are coarser and commonly elongate with a preferred dimensional orientation parallel to long needles of magnesioriebeckite. Undulose extinction is more intense than in quartz in least deformed parts, although deformation bands are not common and

grain boundaries are only weakly sutured (Chadwick et al., 1986).

3.6 GEOCHEMISTRY:

As described in earlier sections that metavolcanics, clastic metasedimentary rocks and banded iron formation are three major rock types in the Bababudan schist belt. Geochemistry of clastic metasediments constitutes a major part of this thesis and is described in details in subsequent chapters. Geochemical characters of metavolcanics carried out by Bhaskar Rao and Naqvi (1978), Bhaskar Rao (1980), Bhaskar Rao and Drury (1982), Drury (1983) are briefly discussed in Chapter IX. However, geochemistry of BIF of the Bababudan Schist belt has not been studied so far. Since Kudremukh BIF are supposed to be an equivalent of Bababudan BIF, therefore, geochemistry of BIF from the Kudreamukh schist belt, carried out by Khan et al.(1991), may give a preliminary perception regarding the genesis of Bababudan BIF as discussed in Chapter X.

CHAPTER - IV

DHARWAR GEOLOGY IN A GLOBAL CONTEXT

The Archaean greenstone belts of KN have a very special and significant place in the understanding of the Archaean geological processes (Lowman(Jr), 1989). Greenstone belts of KN, represent a geological history of one Ga, which is not so well preserved and exposed in other regions. For example in Canadian shield, greenstone belts older than 3.0 Ga are rarely found. In Greenland, the Isua and Mallena supracrustal rocks which are somewhat high grade equivalent of greenstone belts, represent early and middle Archaean. In South Africa also the Onwarwacht, Moodies and Fig Tree Groups represent relatively short span from early to middle Archaean. In Australia the greenstone belts of Pilbara are of early Archaean age and the belts of Kalgoorlie-Kambalda region are of middle and late Archaean age (Condie, 1981). In Dharwar Craton, despite of limited support from radiomatric age data, geological evidence have demonstrated that the greenstone belt development processes have operated from 3.5 to 2.5 Ga. Further, the variety and abundances of sediments in greenstone belts are exemplary and unique. For example no other Archaean greenstone belt in the world has a basal uriniferous, pyritiferous and Gold bearing QPC, which has been derived from a source area exposed to anoxic atmosphere and deposited in a reducing environment. In no other greenstone belt such enormous amount of quartzite, carbonates, stromatolitic carbonates and BIFs have been deposited. Therefore these

greenstone belts of Dharwar Craton, have a special place and significance as pointed out by Drury (1988) in his review of Naqvi and Rogers (1987).

The age of the oldest continental rock is 3.8 Ga (Moorbath et al., 1972), the age of the detrital zircons from Pilbara is 4.0 Ga. (Compston and Pidgeon 1986). Nd isotopic data have shown that by 3.8 Ga. ago atleast 40% of the continental crust by volume was present (Jacobsen 1988). Atleast 2/3rd of the continental crust was formed by 2.5 Ga ago (Moorbath and Taylor, 1981). This shows great antiquity of continental crusts, whereas, oceans are not more than 200 Ma old. Therefore the maximum age of survival of oceanic crust can be taken as 200 Ma only. The presence of the sediments of similar characteristics in the Archaean to those found in the Phanerozoic, suggest that the existance of oceans and seas in Archaean time cannot be disputed. If Plate Tectonics has governed the entire geological activity of the Phanerozoic era, there is no appreciable scientific basis to assume that such processes were not operating in the remote past of the earth history. There could be some modifications, because of differences in thermal and pressure regimes prevailing during early Precambrian, but the destruction of ocean which were present during the Archaean cannot be overemphasised. The remnants of the Archaean oceans can be discovered in greenstone belts, and high grade granulite belts where sediments and subaqueous volcanic rocks are present. The greenstone belts of India have a very large and widespread horizon of BIF (2.8 to 2.9 Ga), extensively thick sequences of graywackes, graywacke conglomerates, and also volcanic rocks. The interpretation of tectonic setting from the

geochemical data available on these belts indicate that most probably plate tectonic theory in modified form can be applied to these rock types (Fyfe, 1980, 1990). For example, the Chitradurga schist belt is suspected as a suture zone (Naqvi, 1985). Kolar schist belt is also considered a suture zone (Rajamani et al., 1985). The enormous quantity of iron in the form of BIF, is believed to be provided from hydrothermal vents situated in oceanic ridges present at that time (Jacobsen and Pimental - Klose, 1988; Derry and Jacobsen, 1990; Manikyamba et al.,1991; Gnaneswar Rao, 1991). Therefore the collection and interpretation of trace element and isotopic data on rocks of greenstone belts of India shall definitely provide certain constraints on the Archaean tectonic regime and crustal evolution.

The study of these greenstone belts has contributed significantly towards the major aspects concerning the history of the earth during Precambrian time (Radhakrishna and Naqvi, 1986). It appears that the present division of crust into two contrasting components i.e. continental and oceanic with definite shape, geometry and other physico-chemical parameters, came into existence at a very early evolutionary stage of earth's development. The material comprising these continents had rapidly changed and the 2/3rd mass of the continent came to surface by 2.5 Ga. Using several isotopic parameters, geochemists have proposed various growth rates (Fig. 4.1A), but most of these models suggest that the 80% of the crust had definitely formed before 2.5 Ga, however, Hurlay (1968), Hurlay and Rand (1969) are of the view that the crust forming processes have been continued even after 1.0 Ga. Although, the later work (Jacobsen, 1988) has

Fig. 4.1 A: Various crustal growth models. Most of these models propose that most of the continents differentiated from the mantle early in earth history. The concept of continuous or quasi-continuous growth of the continental crust has received much support from the isotopic studies.

Fig. 4.1 B: Generalized model for the growth of the continental crust throughout geologic time. The initiation of crustal growth is assumed to be at 3.9 Ga. This model shows that continents grew rapidly till 2.5 Ga. (After Taylor and McLennan, 1985)

Fig. 4.1 C: Diagram illustrating the relative abundance of rock types at different times in Southern Peninsular India. It shows that there are some remarkable correlations in the abundances of the rocks in different geological environments (After Naqvi et al., 1978a). Predominance of siliciclastic rocks and orthoquartzites is noted in Proterozoic sedimentary basins.

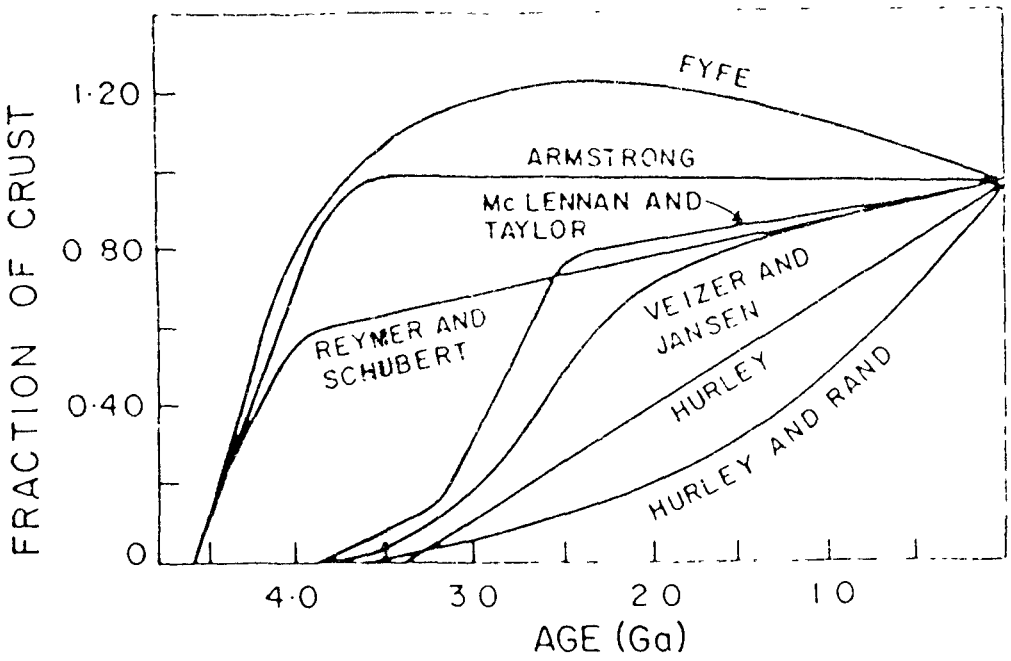
FRACTION OF CRUST
1·20
0 80
0·40
0
FYFE
ARMSTRONG
Mc LENNAN AND TAYLOR
REYNER AND SCHUBERT
VEIZER AND JANSEN
HURLEY
HURLEY AND RAND
4·0
3 0
2 0
1 0
AGE (Ga)

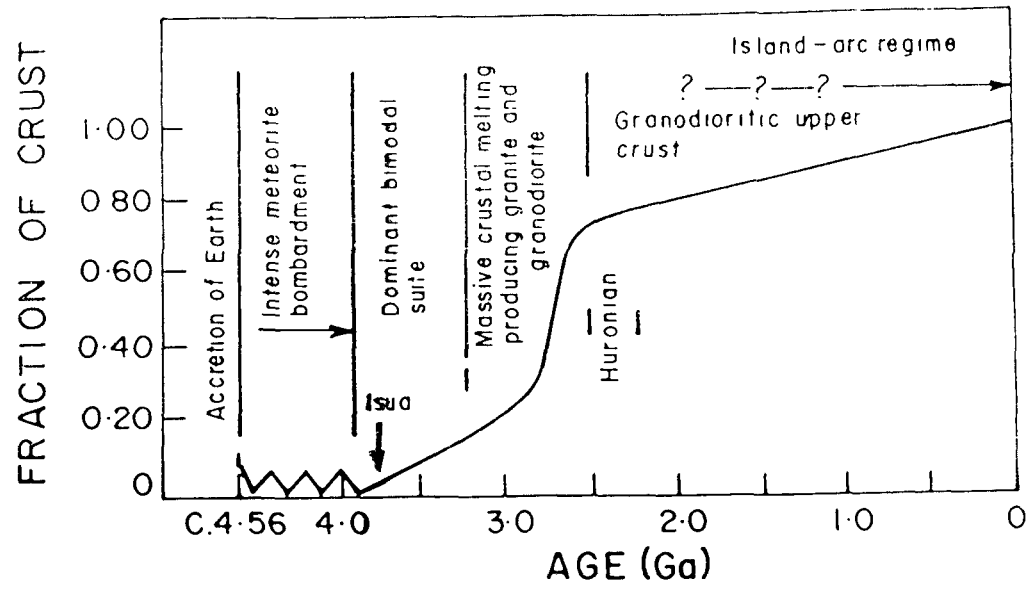
FRACTION OF CRUST
1·00
0 80
0·60
0·40
0·20
0
Island – arc regime
? —? —?
Granodioritic upper crust
Accretion of Earth
Intense meteorite bombardment
Dominant bimodal suite
Massive crustal melting producing granite and granodiorite
Huronian
Isua
C.4·56
4·0
3·0
2·0
1·0
0
AGE (Ga)

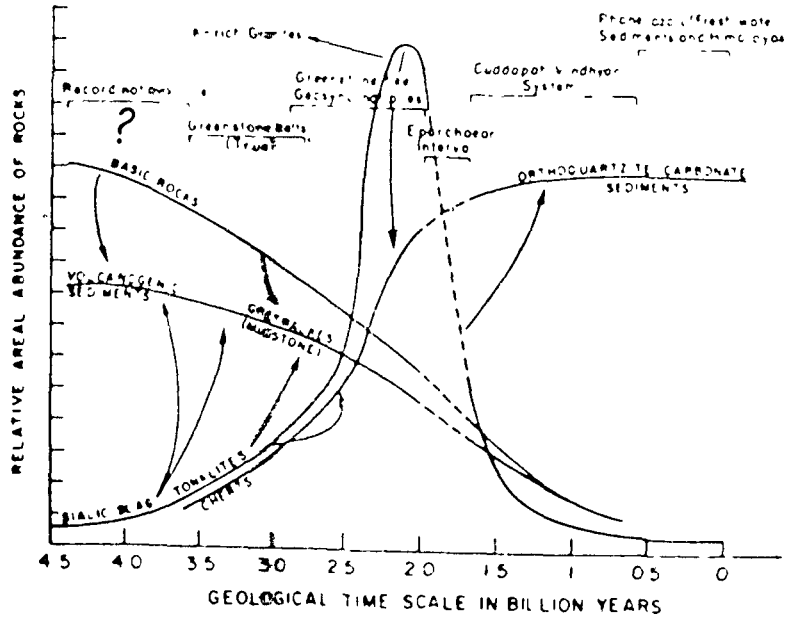
RELATIVE AREAL ABUNDANCE OF ROCKS
?
BASIC ROCKS
ORTHOQUARTZITE CARBONATE SEDIMENTS
TONALITES
CHERTS
4·5
4·0
3·5
3·0
2·5
2·0
1·5
1
0·5
0
GEOLOGICAL TIME SCALE IN BILLION YEARS

demonstrated that the major part was formed by 2.5 Ga. The model proposed by Taylor and McLennan (1985), given in Fig.(4.1B), appears to explain many of the observed chemical characteristics of the greenstone belts all around the world, and the model given by Naqvi et.al. (1978b) still appears to hold good in a broader sense for the growth of the continental crust for Indian sub-continent (Fig. 4.1C). Shaw (1980) has argued that it can be accepted that the Earth was at one time largely molten, then heat conduction from the interior, aided by convection and surface radiation, would have initially led to crystallization upwards from the base of the mantle. This would have been followed by crystallization downward from the surface. Sometime after the rate of supply of heat from the interior was exceeded by the rate of surface radiative heat loss, at this time the molten geoid would begin to secrete its first crust. According to Shaw (1980) this first crust was worldwide unstable and composed of polygonal segments or rafts of crystals, remelting and resolidifying in response to local heat variations, floating on residual convecting magma beneath. Summarising Shaw (1980), proposed that the proto Archaean era was characterised by a universal brecciated and cratered crust of rather subdued relief, mostly submerged below a premitive universal ocean. There was at this time no meaning of the present day terms "continental crust" and "oceanic crust", and the entities which we call continents and ocean basins did not exist. Plate tectonics consequently had no meaning at that time. From that proto Archaean era, by 3.8 or 4.0 Ga it is evidenced that some part of the continental crust came into existance.

QPC at the base of the Bababudan Group around 3.0 Ga. along

with the cross bedded and ripple bedded quartzite indicates the stability of the basin. It is also apparent that extensive magmatic activity, with consequent generation and stabilization of parts of continental crust had occurred during the period between 3.8 to 3.0 Ga. It appears that middle Archaean exogenic and endogenic processes became somewhat similar to those which were operating in subsequent geological periods. It is almost agreed by most of the precambrian geologists and geochemists that the plate tectonic processes have grown in scale from the proto Archaean to the present time, and did not operate at all until earth developed, continental nuclei and incipient oceans. The development was gradual and probability in stochastic response to mantle convection pattern. Although, there is little evidence for the Phanerozoic type plate tectonics in early Archaean, the evidence provided from different areas during last few years, are strengthening the view that it can be applicable in middle - late Archaean period (Shaw,1980). Since one Ga of geologic history is exposed in greenstone belts of Dharwar Craton, their geochemical data are extremely useful in understanding the global processes controlling the development of outer sphere during early stages. It is gradually being realised that these greenstone belts repesents a "Wilson Cycle" in modified form.

According to Fyfe (1980) there is an increasing evidence for a major change in the conduction style of the earth near the Archaean - Proterozoic boundary. Models of these changes are imperfect, but the changes from viscous drag subduction to negative buoyancy subduction which was earlier proposed by Hargraves (1976) is getting support. Fyfe (1980) believes that

during early heating and degassing of our planet, the hydrosphere must have played a critical role, and water would have controlled the nature of the early crust, its thickness and thermal regime. According to Fyfe (1980) crustal models can be grouped into two types; in the first type proposed by Moorbath (1978), McCulloch and Wasserburg (1978), continental type crust is considered to be formed episodically and irreversably; it assume a slow rate of growth of continental crust. Another model proposed by Hargraves (1976; 1978), Fyfe (1978), continental crust is mostly submarine and formed early but it reworked and preservation is accidental. One of the major problems of greenstone belts is to construct a model which may explain the complex komatiite, tholelite, andesite, rhyolite volcanic piles and diverse nature of sediments found in them. These belts appear to have all the rock types of a modern ridge and subduction zone complex. Some of them even contain platformal sediments, furthermore they invariably contain BIF. The Fe, Si and REE and Nd isotopic abundances of BIF very strongly suggest that the BIF are a consequent of hydrothermal activity along the Archaean MOR. BIF in many Archaean greenstone belts are deposited along shallow shelf. Therefore a combination of various tectonic settings juxtaposed to each other appears to have generated greenstone belts. The Archaean greenstone belts and the surrounding gneisses of the KN became tectonically inactive at about 2.6 Ga, due to this reason the crustal evolution process clearly sets the Archaean apart from later tectonic regimes.

West (1980) has suggested a tectonic model for early Precambrian in which widespread, sporadic episodes of mafic

volcanism from the upper mantle build up on a submarine protocrust containing a sialic component. A sufficiently thick layer of volcanics acts as a thermal blanket, causing softening of the substratum; the protocrust then partially ingests the volcanics by diapiric action. Irregularly, but gradually, the protocrust thickens. Meanwhile, gradual cooling of the mantle thickens the lithosphere and increases its mean density. Eventually, subduction of high-density parts of the lithosphere begins, while more sialic, hotter, softer portions are compressed laterally and thickened. Water drains into new ocean basins. Uplifted continental surfaces are deeply eroded and stabilized by the loss of a substantial part of their radioelement content into sediment.

With the variety of models and the explanations as available for the different set of greenstone belts of KN, the one most important factor i.e. presence of both rock types, characteristics of subduction and ridges, need an explanation. The available data and evidences presented in subsequent pages show that most of the late Archaean greenstone belts have started as rifts on a thin continental crust and with the change of convection current direction they have closed through modified subsudction process. Understanding of this process requires the understanding of heat transport process. According to Fyfe (1990), perhaps all the change in the system is related to changes in the power supply of the system under study. It is the understanding of change in the power supply and cooling of system, that are required to understand the record of the greenstone belts.

The dichotomity in the greenstone belts as they have both ridge and subduction related rock types, and sometimes even the

rock types which are characteristic of shallow water basin (Banley et al.,1979), as in the Bababudan schist belt, require a faster completion of "Wilson Cycle" for which faster spreading and greater ridge length in the Archaean is essential. Assumption of faster spreading, larger ridge length, smaller size of convection currents, large number of plates of smaller size explains almost all attributes of greenstone belts of India as well as other parts of the world. These assumptions provide great constraint for the formation of BIF in juxtaposition and stratigraphically above the rock association of quartzite and QPC, and, also, their being overlain with different type of volcanic rocks, graywackes, conglomerates which are characteristic rocks of active continental plate margin. Because of these characteristics the greenstone belts of KN are, possibly, one of the most significant suite of rocks, and provide an opportunity to study the geologic processes operating during middle - late Archaean.

The QPC, quartzites, stromatolitic carbonates-chert, BIF sequence is deposited in a shallow shelf and the iron of BIF was provided by hydrothermal solutions from vents of mid-oceanic ridges. To transport this iron from deeper part to shelf area, shorter distance between site of deposition and site of addition is needed. This can be achieved only when ridge length is longer and spreading was faster. Earlier Hargraves (1986) has suggested that the younger oceanic lithosphere subducts more slowly. If this concept is applied to the Archaean then greater ridge lengths during the Archaean time may explain many observed facts. Based on computation of several data related to oceanic heat loss, Hargraves (1986) has derived a quantitative expression which

indicates that ocean heat loss is proportional to the cube root of ridge length. According to Hargraves (1986), if Archaean heat flow was three times greater than that of today, then 27 times as much ridge length would have been required, which would suggest that the Archaean crust was covered by many smaller plates moving slowly.

Both increased ridge length and rate of subduction were prevailing during the Archaean (Burke and Kidd 1978, Burke et al. 1981), a greater rate of accretion and subduction could have been achieved by faster spreading by greater ridge length equivalent to subduction zone. Burke et al. (1981) suggested, however, that substantially greater length of subduction zone was more likely in contrast to this conclusion. The first of these alternatives is apparently becoming the accepted mechanism. Dewey and Windley (1981) suggested a mini late Archaean relative plate motion which seems to be six times as faster as present rate. Nisbet and Fowler (1983) assumed a spreading rate of 40 cm per year. Windley (1984) reported that there is much agreement that a spreading rate in early Precambrian was several times faster than that of today. The area of the ocean floor during the Archaean cannot exceed the surface area of the earth which is generally presumed constant. To decipate the three times higher heat flow in the Archaean time, a ridge length of 27 times of present time is required (Hargraves 1986). Therefore plate tectonics at Archaean time would require the ridge length equal to $27 \times 5000 = 1.35 \times 10^6$ km. Maximum age of subducting lithosphere at trenches is 2.0 Ma and the average distance from a ridge to trench is around 225 km (maximum ~ 770 km). Widespread "shallow subduction" in the Archaean is a

tectonic style suggested by Dewey and Windley, Sleep and Windley (1982), Abbott and Hoffman (1984) and Abbott (1984) to the extent that dominant force driving the plate tectonics is considered to be "slab pull". Hargraves (1986) concludes that the Archaean plate tectonic regime require much more total ridge length and slower rather than faster spreading. The $L^{1/3}$ relation derived between heat loss and ridge length leads to the picture of an early earth with many smaller plates moving slowly.

Naqvi (1983) proposed a unidirectional transformation from simatic to sialic crust. For the evolution of Indian shield, Naqvi (1982) suggested that after initial differentiation of the earth, the process of sima-sial transformation has been governed mainly by exogenic processes. It is visualised that the global simatic crust was covered by a thin hydrosphere, soon after primary degassing of the earth. Emergence of basic islands in this hydrosphere created numerous shallow water basins and in these basins early Archaean greenstone belts were formed. Sedimentary components of these belts, which are mainly chemogenic, were provided by intense chemical weathering of the newly emergent basic islands, whereas the volcanic component was produced by shallow-high temperature partial melting of the protomantle. Partial melting of basaltic crust, thus, produced trondhjemites-tonalites and formed continental nuclei. Erosion of these nuclei and, deposition and volcanism between them have produced the younger greenstone belts. Windley (1981) suggested that middle Archaean (3.0 to 3.5 Ga) was a period of rigorous growth (accretion) and destruction (subduction) of oceanic lithosphere with consequent production of voluminous calc-alkaline

melts with tonalitic end products, deformed and metamorphosed into continental gneisses and granulites in lower crustal levels. Extensive rifting in marginal basins gave rise to multiple greenstone belts as proto-ophiolites. No stable craton formed at early proto-plate time (Windley, 1981). He identified five stages in earth history which are given in table (4.1). Hargraves (1981) recognised three following major uncertainties impeding classification of the Precambrian geologic record: i) thermal history, ii) the history of growth of continental crust, and iii) tectonic style. The only certainty is that average heat flow has declined. The mechanism for the plate tectonics is the pull associated with subduction of cold, negative buoyant oceanic lithosphere. Hargraves (1981) suggests that if this concept is valid then the subduction is less likely earlier in earth history when heat flow was higher. However, with high heat flow that rate of convective circulation in the mantle was faster and viscous drag forces at the base of lithosphere may have been stronger. He suggest following model which is divided into four stages:

1) Initially, in a vigorously convecting earth, the viscous drag forces were sufficient to drag buoyant crust back into the mantle (viscous drag subduction). No crust survived this recycling, but it enhanced the upward concentration of sialic components in the earth.
2) With cooling, slowing of convection and the passage of time, a buoyant, possibly continuous global scum-crust of intermediate composition would have developed. This crust was effectively decoupled from the juvenile mantle and was recycled as a result of volcanic addition on surface and

Table 4.1: The main stages in Precambrian crustal development in the context of earth history (after Windley, 1981).

---

1. 4.5 - 3.9 Ga

No rock record preseraved, therefore extreme speculation. Formation of proto-crust and proto-lithosphere of unknown thickness. Non-reducing atmosphere and hydrosphere evolve rapidly.

2. 3.9 - 2.7 Ga

High rate of radiogenic decay, vigorous small-scale mantle convection and new oceanic crust which was subducted to give rise to voluminous calc-alkaline melts with predominantly tonalitic end-products, deformed to gneisses. Extensive rifting in marginal basins gives rise to multiple greenstone belts as proto-ophiolites.

3. 2.7 - 2.3 Ga

Transitional and diachronous period during which much uplift and erosion of late Archaean thick continental crust gives rise to voluminous clastic debris. Stabilization of crust-lithosphere following aggregation of Archaean proto-plates. Many dykes and stratiform intrusions injected into stabilizing crust.

4. 2.3 - 0.6 Ga

Lower mantle temperatures and slower global spreading rate led to "normal" Wilson-cycle from early Proterozoic. Narrow geosynclines and mobile belts formed by Cordilleran-Himalayan collisional tectonics giving rise to extensive more stable plates.

5. 0.6 - present

Wilson cycle controls all geological phenomena.

remelting and removal at the base.

3) With further cooling crust became coupled to the mantle; the average density of lithosphere increased and ultimately buoyancy-powered subduction of crust could begin. Subduction of segments of the entire lithosphere, where crust was thin, initiated the contemporary plate-tectonic style and growth of the continent-ocean dichotomy. Simultaneously, decoupling and sinking of mantle lithosphere separated from crust caused intracontinental mobile-belt orogeny.

4) With continued decrease in continental heat flow the strength of the boundary between continental crust and the mantle has increased and decoupling has become more difficult; as a result intracontinental orogeny is now rare or impossible. This leaves only buoyancy-powered subduction of oceanic lithosphere as the predominant contemporary orogenic force.

Glikson (1981) believes that operation of plate tectonic (Wilson Cycle) in late Archaean is consistent with the isotopic and geochemical evidences for two stage mantle melting. However, in his opinion there is no intrinsic reason in these data to suggest modern type tectonic environments, and many features of Archaean rocks suggest temporarily unique conditions.

Goodwin (1981) has concluded that Archaean greenstone belts lying in granite-greenstone terrains contain mafic volcanic rocks and features low to medium grade metamorphic assemblages, yet otherwise display a great diversity in size, form, lithology, stratigraphy, age, basement-cover relations and structural deformation as indicated by consideration of four main granite -

greenstone belts in Peninsular India, South Africa, western Australia and southern Canadian shield. According to Goodwin (1981) greenstone belts development is attributed to the Archaean plate tectonic processes that involved limited movement of numerous small plates operating under a high geothermal gradient and thereby lacking conventional subduction zones. Thus the Archaean plate tectonic processes differ in significant respect from modern plate tectonics, yet provide similar volcanic and plutonic products. Goodwin (ibid) contends that during earth history the plate tectonic processes have taken several forms, all involving atleast some moving plates, of which the current is but the latest.

Regarding the nature of early crust, Anhaeusser (1981) discussed the evidence from Barberton Mountain land and concluded that oldest recognizable rock in this area are ensimatic in character (peridotite and basaltic komatiites, dated at 3.5 Ga; Glikson, 1980). These rocks are compositionally competable with the probable source material from which a large volume of intrusive, TTG was generated following partial melting at depth (Glikson, 1984). The early sialic additions both arose from and interacted with the supracrustal assemblages at deep and shallow crustal levels respectively to form complex migmatites and the protocontinental crust of the developing cratons. Anhaeusser (1981) mentioned that there is no evidence either in Barberton greenstone belts or the surrounding terrain to suggest that plate tectonics, in the modern sense of the term, may have been responsible for the development of the region. He claims that the ancient crust evolved as a response to vertical tectonics,

involving the sinking of simatic lithospheric slabs and diapiric upwelling of the succession of granotoides that commenced with early Na - rich phases, but later change into K - rich magma, for the final stage of Archaean crustal consolidation at 3.2 - 3.0 Ga ago. Evidences have been brought out to suggest that the Zimbabian craton has been a coherent tectonic unit with little internal deformation from atleast 2.6 Ga. Nesbitt et al. (1980) and Wilson and Nutt (1990) pointed out evidence from within the Zimbabian craton suggesting that continental nucleous had existed since early Archaean time. Main greenstone belt sequence were erupted at protocontinental crust. These authors believe that the Zimbabian craton has behaved as a plate since Archaean, but the plate tectonic regime may have been very different from that of today.

Slave province in the NW early part of Canadian shield is a crustal sediment dominated by Archaean granite-greenstones. According to Henderson (1981), these supracrustal rocks were deposited in a 10-15 my period, 2.6 Ga ago in a series of small fault bounded basins, that formed due to regional extension of the 3.0 Ga granitic to tonalitic basement.

Green (1981), based on the experimental work on the magma and melting temperature for komatiites, suggests that while it is possible that the lithosphere similar to that of modern earth and a similar pattern of plate tectonic existed in the Archaean, an alternative, preferred model predicts a thinner lithosphere, more active plate movements, instability of eclogite at deep crustal depths and an absence of subduction of oceanic crust.

The latest understanding about the Canadian shield is, that

in this region, several litho-stratigraphy and association in greenstone belts are found. These are: i) quartz arenite and carbonate stromatolite bearings sequences, ii) mafic-ultramafic volcanic sequence, iii) mafic-felsic volcanic cycles, iv) Timiskaming type sequence of fluvitile sediments and calc-alkaline - alkaline volcanics (Thurston and Chivers 1990).

Recently recognised quartz arenite bearing sequence, from bottom to top, in the Sachigo and Wabigoon sub-province, are as follows: quartz arenite + stromatolite bearing carbonate, oxide facies BIF, komatiites and tholeiites (Thurston and Chivers, 1990). Primary structures in the quartz arenite indicate shallow water deposition and represent mature sedimentation. Granotoid provenance of these association is postulated, based upon petrography of coarse arenite and clasts of associated conglomerates. A few dated super pre-quartz arenite bearing sequence are 2.85 Ga. The shallow water origin of primary structure and aerial extent of quartz arenite and carbonate bearing sequences invite comparison with platformal sediments at passive margin. Platformal sequence, unconformably lying over 3.0 Ga granotoides and older mafic volcanics. This sequence is almost identical and similar to that exposed in the Bababudan Group.

The above discussion clearly indicates the importance and significance of the debated geological and geochemical studies over Indian greenstone belts, directed towardes a global understanding of the exogenic processes operating during Archaean. The excellent exposure and the predominance of the sedimentary rocks in late Archaean provides the opportunity to understand them. The data and interpretation presented in subsequent pages

can be appreciated in a better way in the light of the above discussion which indicates that atleast during late Archaean, the observed characteristics of greenstone belts are best explained by application of a modified form of plate tectonics.

CHAPTER - V

SEDIMENTATION IN THE BABABUDAN SCHIST BELT

5.1 INTRODUCTION:

The abundance of different types of sedimentary rocks has changed through geological time. Ronov (1964) and Ronov and Migdisov (1971) have estimated the Vol % of different sedimentary rocks present in geological time scale (Fig. 5.1). The abundance variation in the volume of sedimentary rocks reflects, the source composition, tectonic and depositional environment and recycling which have produced these sediments during different era. A great difference, in nature and abundance of the sediments of greenstone belts of various ages and depositional-tectonic environment has been noticed by Naqvi (1983). Late Archaean "younger schist belts", like the Bababudan schist belt, are volcano sedimentary sequences. The individual schist belts include thick mafic to felsic volcanic accumulation with associated sedimentary sequences which generally occur near the top of volcanic cycles (Ojakangas, 1990). However, in the Bababudan belt, sequence starts with sedimentary units at the bottom which are also found interbedded with volcanic sequences. Their sedimentary structures, primary textures and mineralogies are commonly well preserved (Srinivasan and Ojakangas, 1986).

Sedimentological studies of greenstone belts of Karnataka started with the classical work by Pichamuthu (1935 a-c). In his pioneering work he tried to prove the sedimentological nature of some of the constituents of greenstone belts, as, at that time all

Fig. 5.1 : The compositional evolution of sedimentory rocks. It is clear from illustration that sandstones and shale form a more or less constant proportion after 2.5 Ga. The relative importance of graywacke has declined and that of quartz arenites has increased with time (After Ronov, 1964).

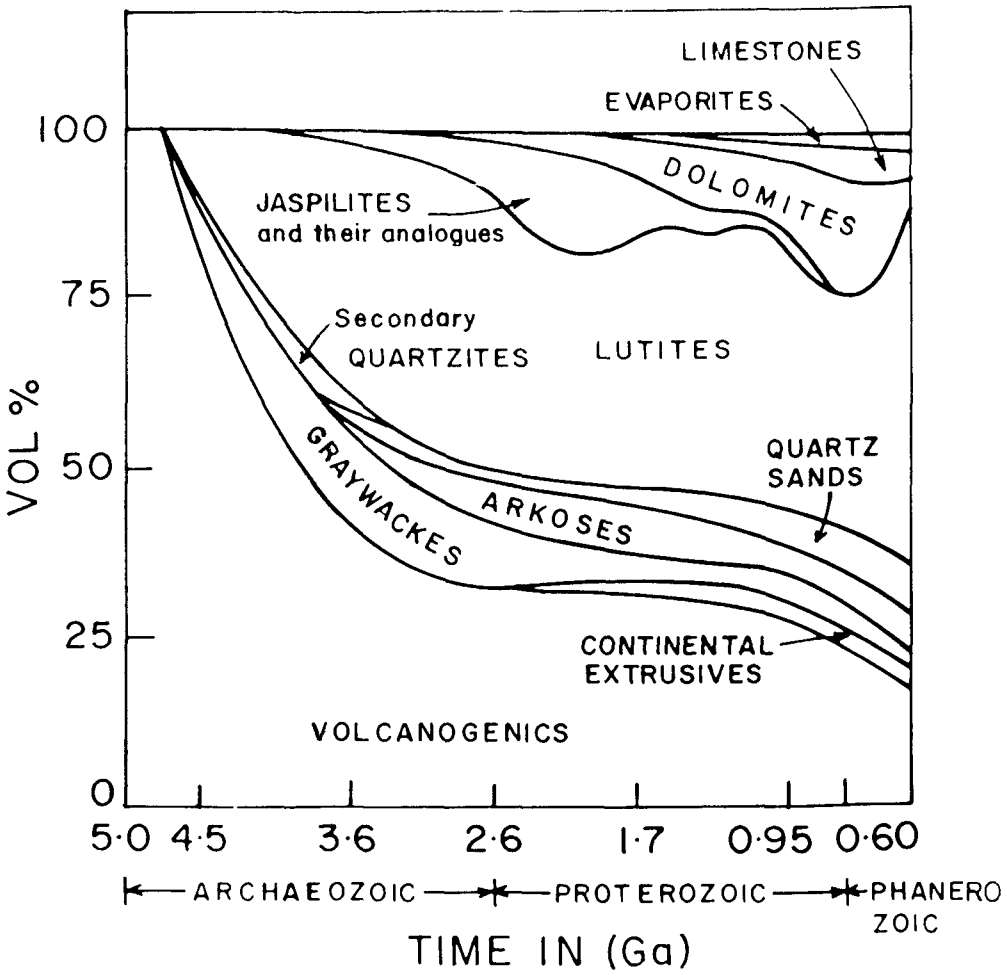
LIMESTONES
EVAPORITES
DOLOMITES
JASPILITES
and their analogues
Secondary
QUARTZITES
LUTITES
QUARTZ
SANDS
ARKOSES
GRAYWACKES
CONTINENTAL
EXTRUSIVES
VOLCANOGENICS
VOL %
100
75
50
25
0
5·0 4·5 3·6 2·6 1·7 0·95 0·60
ARCHAEOZOIC
PROTEROZOIC
PHANERO
ZOIC
TIME IN (Ga)

of them were thought to be of igneous origin (Smeeth, 1916). Sedimentary origin of several constituents of greenstone belts was further strengthened by Rama Rao (1940, 1964), Radhakrishna (1940, 1964), Pichamuthu (1967), Srinivasan and Sreenivas (1968, 1972), Naqvi and Hussain, (1972) Naqvi et al. (1978b), Srinivasan and Ojakangas (1986), Srinivasan and Naqvi (1990), Arora et al. (1991). From early 70's workers in the field of Precambrian Geology have tried to correlate sedimentation with its tectonic history. Subsequently, many detailed attempts have been made to relate sedimentation to the environment of deposition (Naqvi and Hussain,1972; Srinivasan and Sreenivas,1972; Naqvi, 1978; Naqvi, 1983; Naqvi et al 1978b, 1983, 1988).

This chapter, comprises of sedimentological work by the author on the clastic sedimentary rocks of the belt. The lithofacies analysis of conglomerates, both oligomictic and polymictic, associated quartzites (Quartz arenite), and fine clastics, including palaeocurrent analysis have two major objectives : (1) interpretation of the environments of deposition, and (2) determination of the direction of the provenance of the sediments.

4.2 LITHOFACIES ANALYSIS:

A facies is defined as a body of rock with specified characteristics (Reading, 1986). In case of sedimentary rocks, it is defined on the basis of colour, bedding, composition, texture, fossils and sedimentary structures. A facies should ideally be a distinctive rock that forms under certain conditions of sedimentation, reflecting a particular process or environment.

However, the term facies is used in many different sense. Facies may further be subdivided into subfacies or grouped into facies associations or assemblages.

"Lithofacies" should thus refer to an objectively described rock unit. That is, a group of sedimentary rocks, grouped on the basis of lithologic characters e.g. conglomerate, sandstone or fine clastics (or their metamorphic equivalents). Lithofacies have further been subdivided on the basis of primary sedimentary structures, present within the unit of rock.

Since clastic metasediments are well exposed and accessible in basal and uppermost formations. i.e. the Kalasapura and Mundre formation respectively. Lithofacies analysis and their interpretations are mainly confined to them. Due to discontinuous outcrop pattern and scarcity of exposures in the down dip direction, lithofacies interpretation is based on careful examination of critical outcrop and section along the strike. Strike wise persistency of the outcrop is a characteristic feature of the belt.

5.3 LITHOFACIES DESCRIPTION:

5.3.1 Kalasapura Formation:

In Kalasapura Formation broadly three lithofacies types are recognised viz. conglomerate (oligomictic), quartzites and fine clastic shales (phyllites) which lie successively as shown in columnar generalized and interpretive lithofacies section (Fig. 5.2). The lithofacies are coded by the capital letters, using a modified scheme of Miall (1983). Each facies has again been

Fig. 5.2 : Generalized and interpretive lithofacies section of the Kalasapura Formation, southern margin of the Bababudan schist belt. Three lithofacies are shown i.e. Conglomerate (Cg); Quartzite (S) and Phyllites/Fine clastics (F), which have further been subdivided into sub facies or associations. In all 11 sub facies are shown in the illustration.

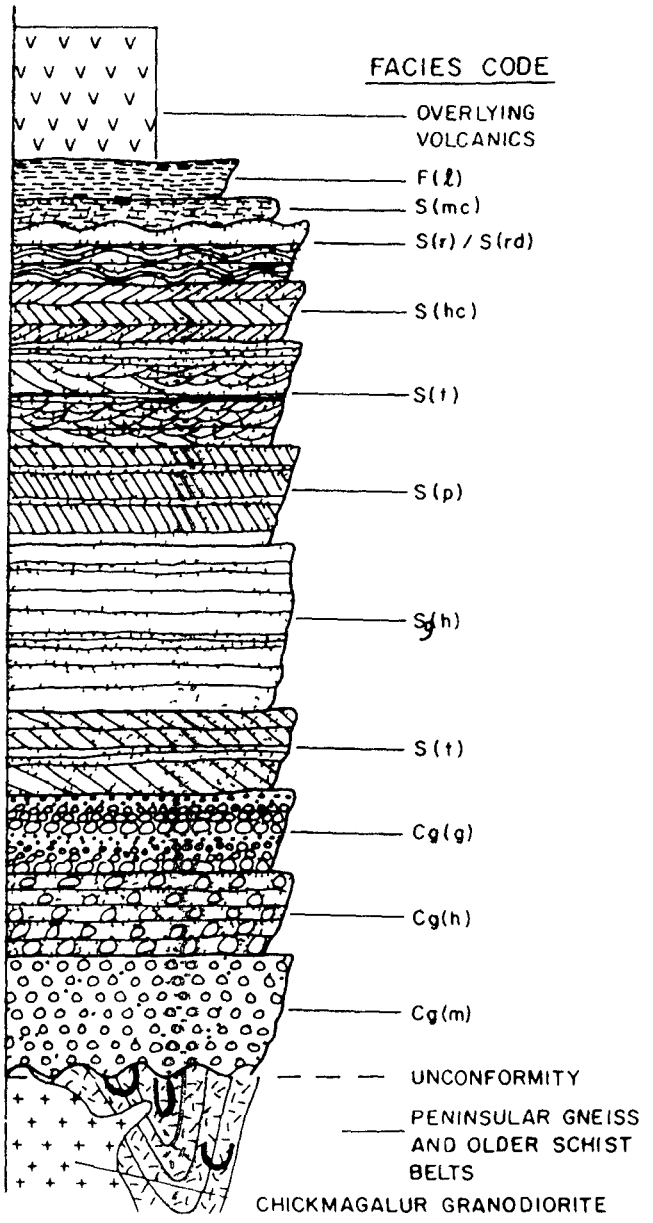
FACIES CODE
OVERLYING VOLCANICS
F(l)
S(mc)
S(r) / S(rd)
S(hc)
S(t)
S(p)
S(h)
S(t)
Cg(g)
Cg(h)
Cg(m)
UNCONFORMITY
PENINSULAR GNEISS AND OLDER SCHIST BELTS
CHICKMAGALUR GRANODIORITE

differentiated into subsurfaces, based on dominant texture and sedimentary structure, and designated using appropriate lower case letters. In this way a total of 11 lithofacies were recognised as listed in Table (5.1).

5.3.1.1 Conglomerate,Massive {Cg(m)}:

This facies occupies the southern margin of the belt and unconformably overlies the palaeosols (Fig. 5.3) and/or Chicknagalur granodiorite/ gneissic basement. The conglomerate is characterized by pebbles of vein quartz. It is massive in nature (Fig. 5.4) with an average thickness of 3 mts. In general the average size of clast is around 5 cm in diameter. However, bigger clast (as much as 10 cm in diameter) as well as granules are also present. Most of the clasts are sub-rounded to well rounded, showing smooth surface. Contact type or clast supported framework is preserved and represents original characteristic of deposition. Clasts are extending support to each other making rectangular lattice (Fig. 5.5), however, due to metamorphic stress this lattice gets often changed into rhombohedral, which is less stable (Fig. 5.6). Almost all the quartz pebble are smoky grey in colour; but a few are bluish also. Other than quartz pebbles, which themself make more than 95% of total population, clasts of fuchsite quartzite are also observed. The presence of the pebbles of fuchsite quartzite, though rare, but is an important observation and supports the presence of older supracrustals in the source area. In most of the cases the upper surface of clasts are cracked (Fig. 5.7). Fractures with right angle are developed on the outer surface which indicate non ductile i.e brittle

Table 5.1: Legend of lithofacies sequence in study areas.

Code	Lithofacies name
Cg(m)	Conglomerate, massive
Cg(h)	Conglomerate, stratified
Cg(g)	Conglomerate, graded
Sg(t)	Grity quartzites, trough crossbedded
S(h)	Quartzite, stratified
S(p/t)	Quartzite, planar and trough crossbedded
S(he)	Quartzite, heringbone crossbedded
S(r/rd)	Quartzite, ripple/ripple drift laminated
S(c)	Quartzite, mud crackes
F(l)	Phyllites, paper thin laminated

Fig. 5.3 : Quartz Pebble Conglomerate is resting unconformably over palaesols. Location about 500 mts. south of Lakya.

Fig. 5.4 : Massive quartz pebble conglomerate, (Cg(m)), this facies is about 3 mt. thick and consists of clasts of quartz, which are well rounded with an average size of 5 cm in diameter. Location near Kartikere, south-east of Chickmagalur.

Fig. 5.5 : Contact framework is very common in QPC. Each clast supports other clast. This field photograph shows the rectangular lattice, made-up of clasts of vein quartz. Location near Marle.

Fig. 5.6 : At some places, due to metamorphic stress, rectangular lattices have been changed into rhombohelral type of framework, as shown in this photograph. Location near Marle.

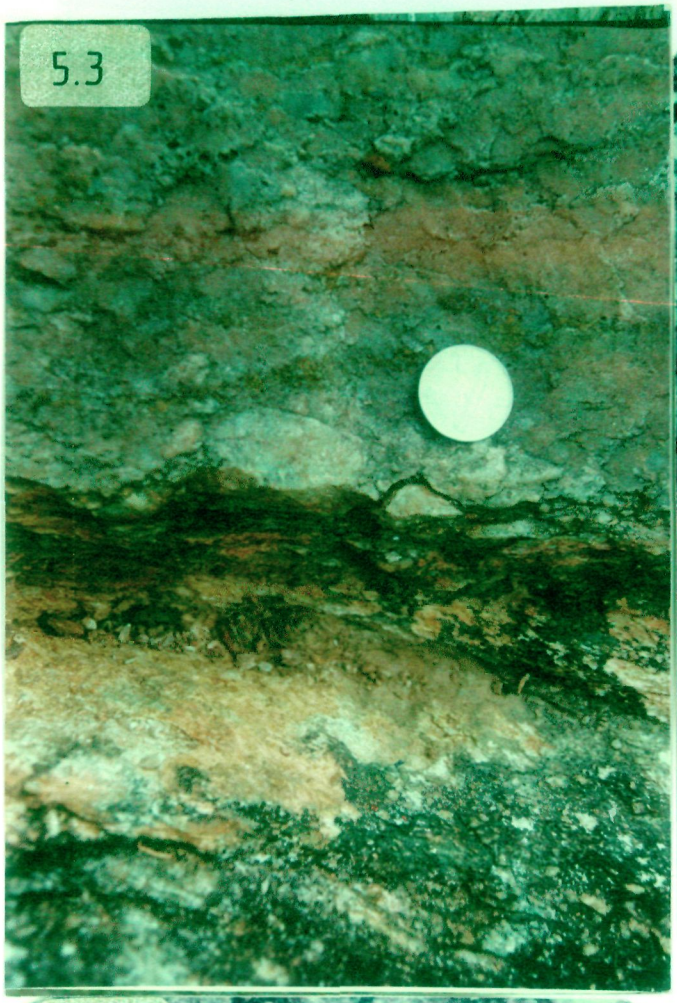
5.3

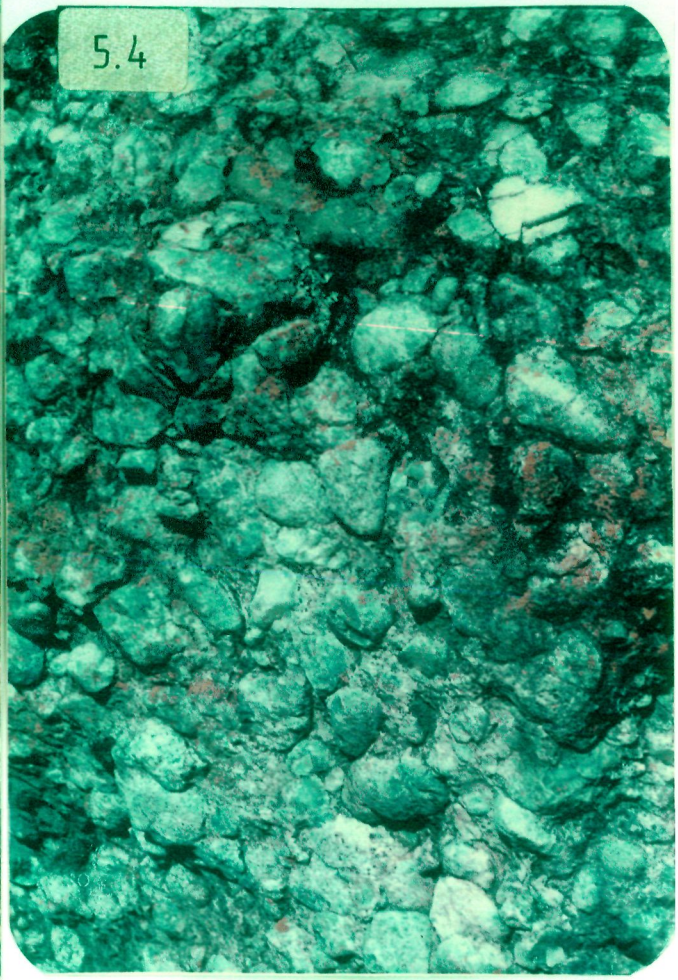
5.4

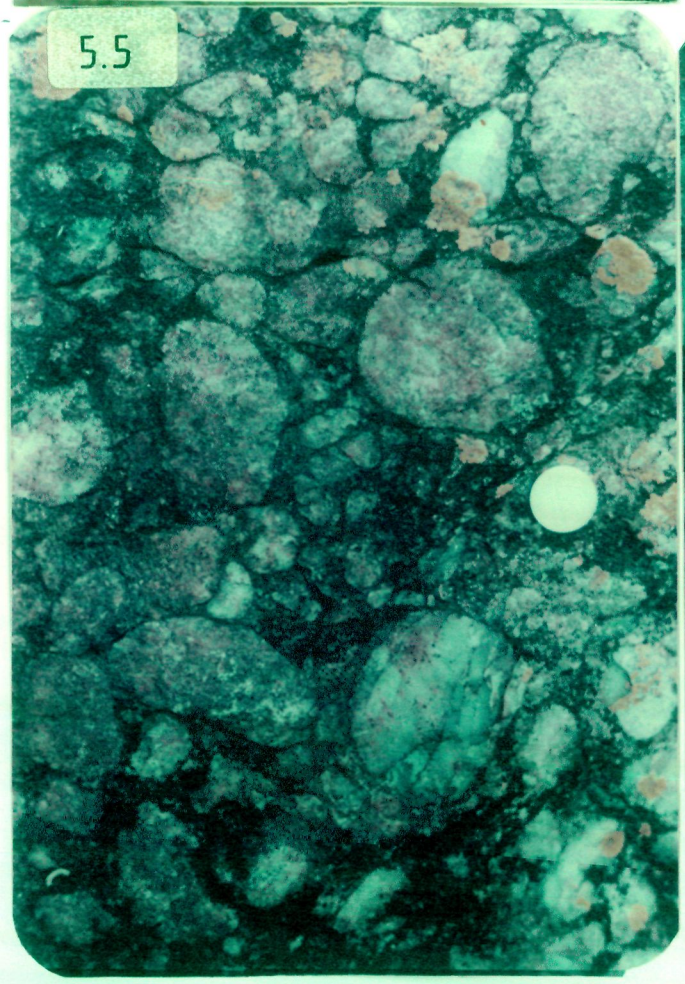
5.5

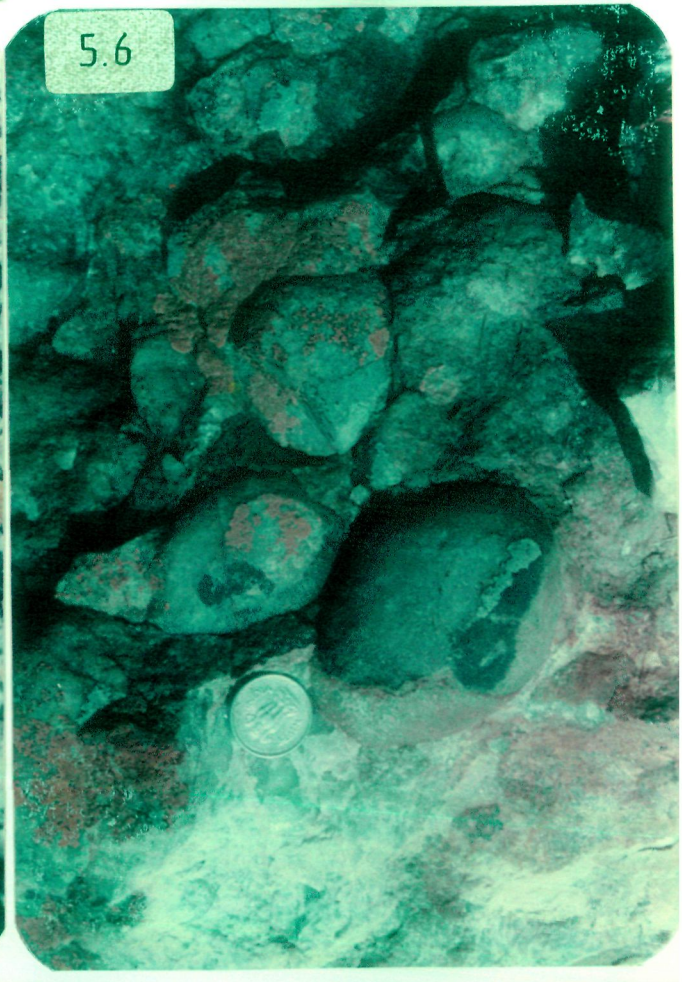
5.6

deformation of the pebbles which could not penetrate deeper into the pebbles.

Fine to medium grained sand particles form an essential part of the matrix. The matrix is usually quartzitic. Zircon, mica including fuchsite, pyrite, uraninite, rutile are some important accessories. These minerals have been reported from this horizon by Fareedudin et al.(1988). Our work does not indicate that much abundance of zircons as reported by Fareeduddin et al. (1988). Presence of pyrite and uraninite is one of the characteristic features of the matrix of quartz pebble conglomerate (Rama Rao, 1974; Aurora, 1985). Early workers have reported this unit to be auriferous also (Sampat Iyengar, 1906). At a few outcrops, relative enrichment of detrital pyrite between the vein quartz pebble has been observed fairly good (Fig. 5.8). Fuchsite specks are very clear in polished block sections (Fig. 5.9), its abundance is responsible for the greenish tinge of the fresh outcrop of the quartz pebble conglomerate, otherwise leaching of pyrite to limonite leaves brownish colour. Since pyrite and other sulphide minerals are more succeptiable to oxidation and the chemical weathering, consequent leaching leaves behind empty spaces in the outcrop with or without limonite. Selective weathering pattern is a characteristic of this horizon (Fig. 5.10). Uraninite is also present but rarely, as indicated by Th and U concentration. Generally in massive conglomerate clast-matrix ratio is very high (95:5).

Fig. 5.7 : Field photograph shows the development of various sets of fractures on the surface of quartz pebbles, which are consequence of brittle deformation. Location near Marle.

Fig. 5.8 : Matrix of QPC is pyriteferous, uraniferous and at some places auriferous also. Pyrite is most abundant mineral. Photographs illustrates its extraordinary enrichment at a fresh and unaltered outcrop. Location near Chickmagalur town on Chickmagalur-Kodur road.

Fig. 5.9 : Fuchsite is also present in fairly good amount in matrix of QPC. Green specks of fuchsite are clearly visible on this polished block of QPC.

Fig. 5.10 : A characteristic weathering pattern of QPC outcrop. This type of pattern is mainly because of selective chemical weathering. Pyrite grains, which are very susceptible for chemical weathering are eventually leached away. Location north-east of Kartikere.

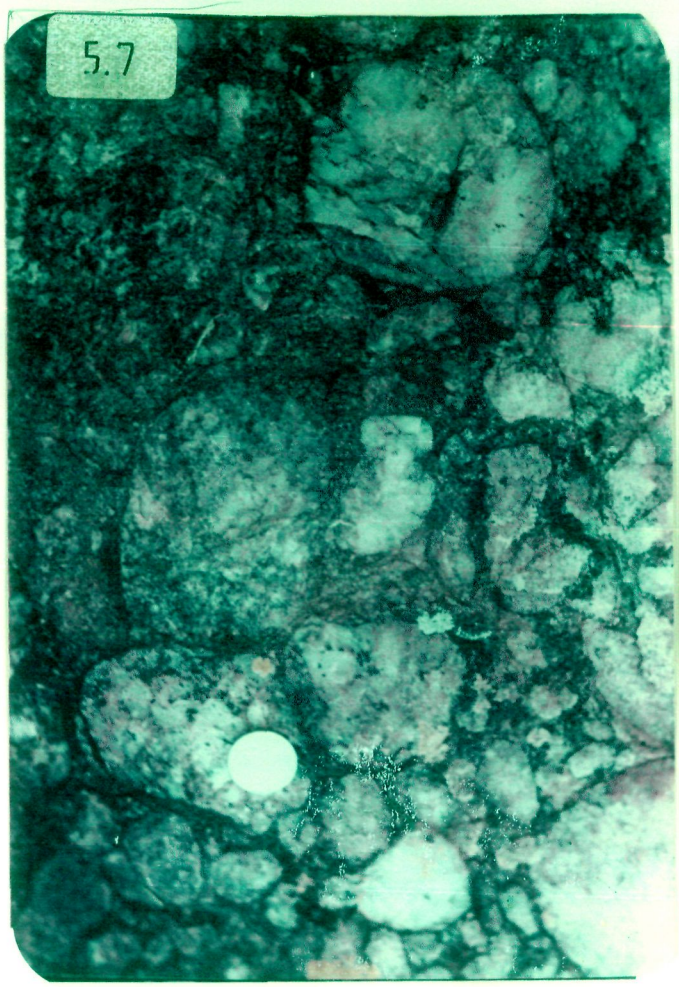
5.7

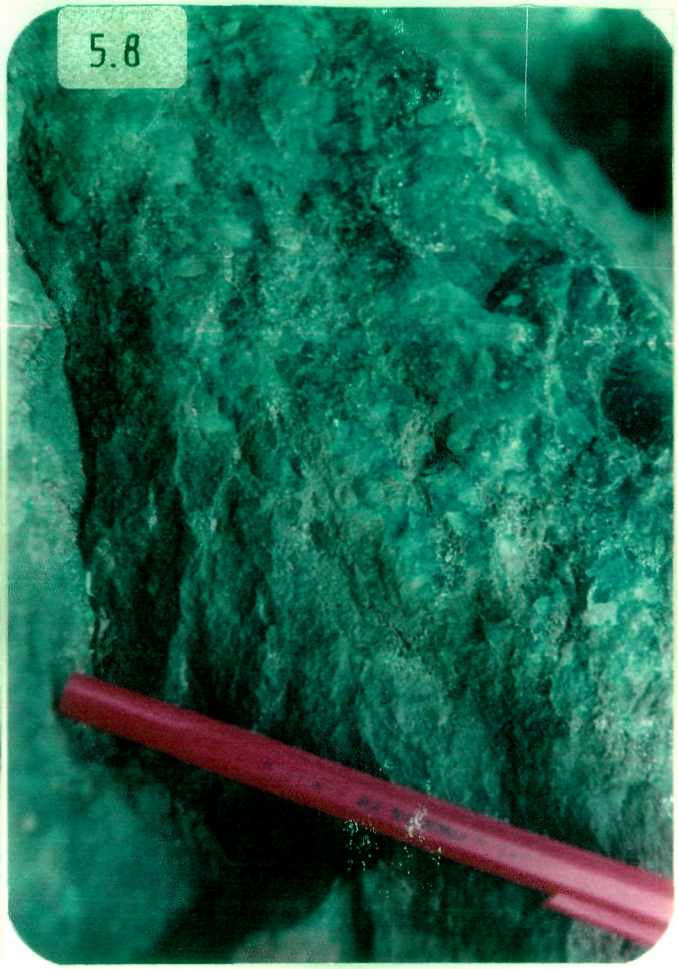
5.8


5.9

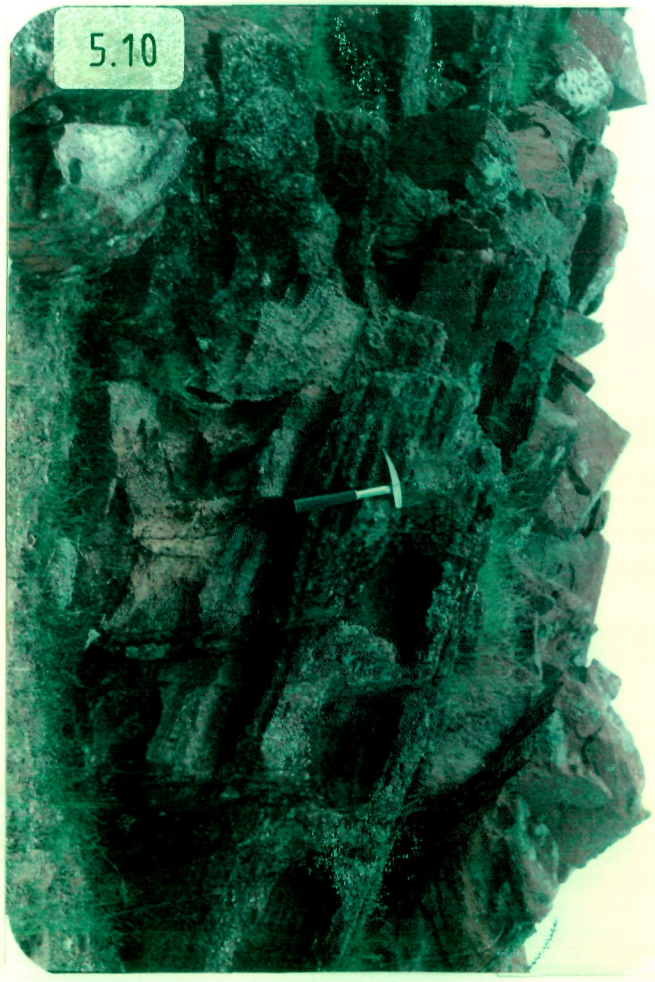
5.10

5.3.1.2 Conglomerate ,Stratified {Cg(h)}:

Massive conglomeratic beds are underlain by stratified conglomerate (Fig. 5.11). Average thickness of this facies is around 2 mt. It is dipping towards north with an average 30^{o} dip angle. Except clast : matrix ratio, which is around 90:10 or 80:20, other properties of this facies are almost similar to the massive conglomerate described above. This facies may be described as orthoconglomerate as it is stratified.

5.3.1.3 Conglomerate ,Graded bedded {Cg(g)}:

The stratified conglomerate merges into graded bedded conglomerates in stratigraphically "up" direction (Fig. 5.12). The average thickness of this facies is around 2 mt. The framework of this facies is comparatively more compact and clasts are tightly bounded. It exhibits the fining upward graded cycles. One cycle starts with coarser (~2 cm) clasts of vein quartz and ends up with a small size cluster. Their mean size of diameter (~2 cm) is rather smaller than the underlying massive and stratified conglomerate lithofacies. The upper layers have fine grained (1 cm to 0.5 cm in diameter) pebbles. This layer is again truncated with coarse grained quartzites thus completing one cycle of deposition. In this facies, the lower part exhibits clast supported framework with less amount of matrix whereas in the upper part gritty conglomerate with sandy matrix supported clasts are found which grades into quartzites. This set completes one cycle and hereafter, IInd cycle of graded sedimentation starts. Colour of this unit is blackish brown. Sometimes this facies directly overlies the massive or basal quartz pebble conglomerate.

Fig. 5.11 : This photograph shows the stratified nature of QPC (Cg(h)). It is about 2 mt. thick. This facies is supposed to be the result of deposition by water in a channel where discharge is more continuous. Location near Kalasapura.

Fig. 5.12 : Graded bedded facies of quartz pebble conglomerate (Cg(g)) shows the fining upward cycles. In this illustration cycle stants with coarser clarts which grades into finner one. This cycle truncates with coarser clasts of another cycle. Location near Marle.

Fig. 5.13 : Grity quartzite shows the development of medium scale trough cross stratification (Sg(t)). Locally cross stratified facies are suggestive of aggradation due to rapid deposition in localized channels at relatively low water stage. Location near Chickmagalur town.


5.11

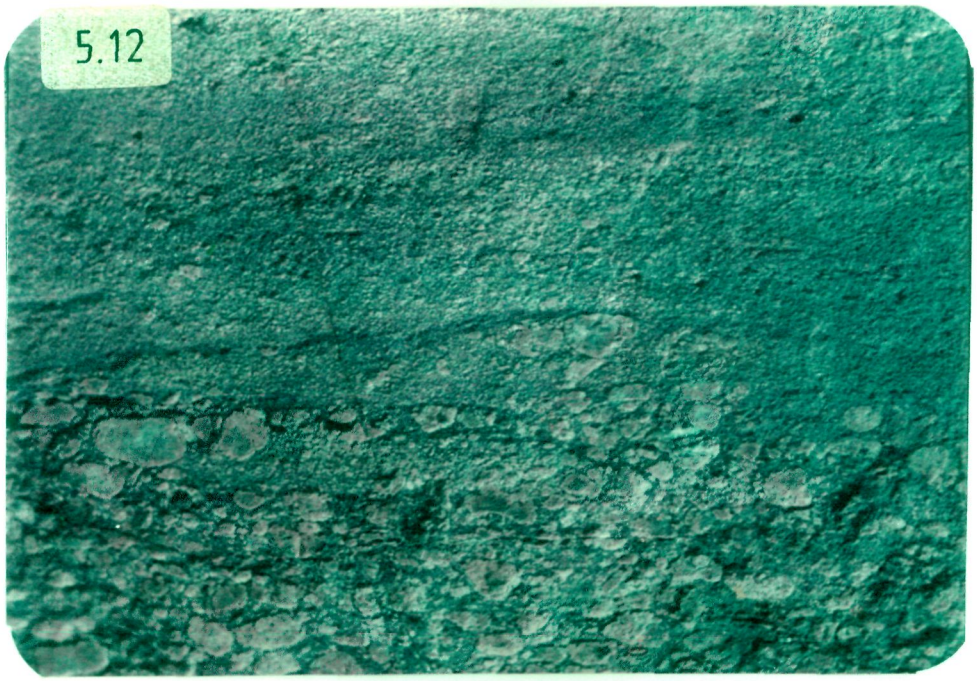
5.12

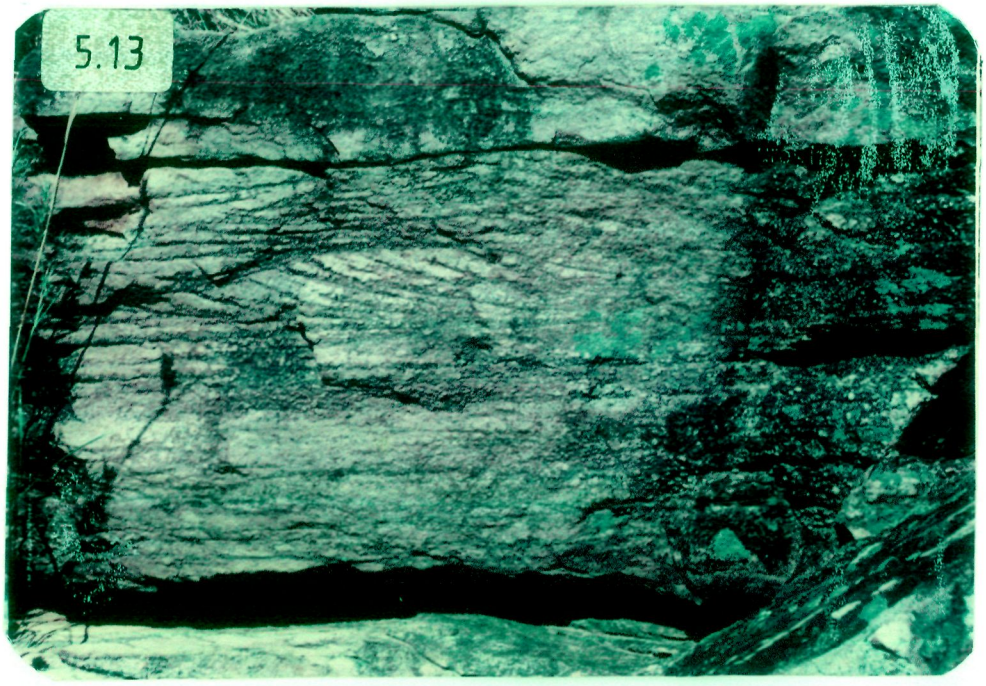
5.13

5.3.1.4 Grity quartzite ,Trough cross bedded {Sq(t)}:

This facies consists of small granules of quartz, embedded sporadically within the coarse grained quartzites. It contains bimodal or polymodal grain size of quartz. This facies is texturely immature but mineralogically mature indicating intense chemical disintegration of the granitoids in the source. As a whole, this facies is well stratified and individual beds are showing medium to large scale trough cross stratification (Fig. 5.13). Total thickness of this facies is not more than 2 mt. Beds are about 1-2.5 ft. thick with an uneven bedding surface. Set thickness of crossbedded strata reaches upto 25 cm, with foreset thickness being around 2-3 cm. at the maximum. Each trough cross strata is bounded by horizontally stratified beds.

5.3.1.5 Quartzites, Parallel bedded {S(h)}:

The well sorted and clast supported conglomerate passes upward into conglomeratic quartzitic facies, and ultimately grades into closely associated and often interstratified orthoquartzite or quartz arenite. This facies is generally mature both texturally and mineralogically. It shows well defined parallel bedding (Fig. 5.14). Total thickness of this facies is around 4-6 mts. and thickness of individual bed's ranges from 2 to 3 ft. This facies consists of medium size, well sorted, rounded to sub rounded grains of quartz which are compactly packed. They generally exhibit grey to brown colour, but locally it shows green color (fuchsite). It dips 25^{o} north with a strikewise persistence.

Fig. 5.14 : Field photograph showing the parallel beddings in quartzites, (S(h)), which are associated with QPC. Their thickness ranges from 4-6 mts. and individual beds are 2-3 ft. thick. Location near Devenahalli.

Fig. 5.15 : Photograph showing the development of medium to small scale planar cross stratification, (S(p)). Location near Devenahalli.

Fig. 5.16 : Photograph showing the development of medium scale trough cross stratification, (S(t)). Location near Chickmagalur town.


5.14


5.15

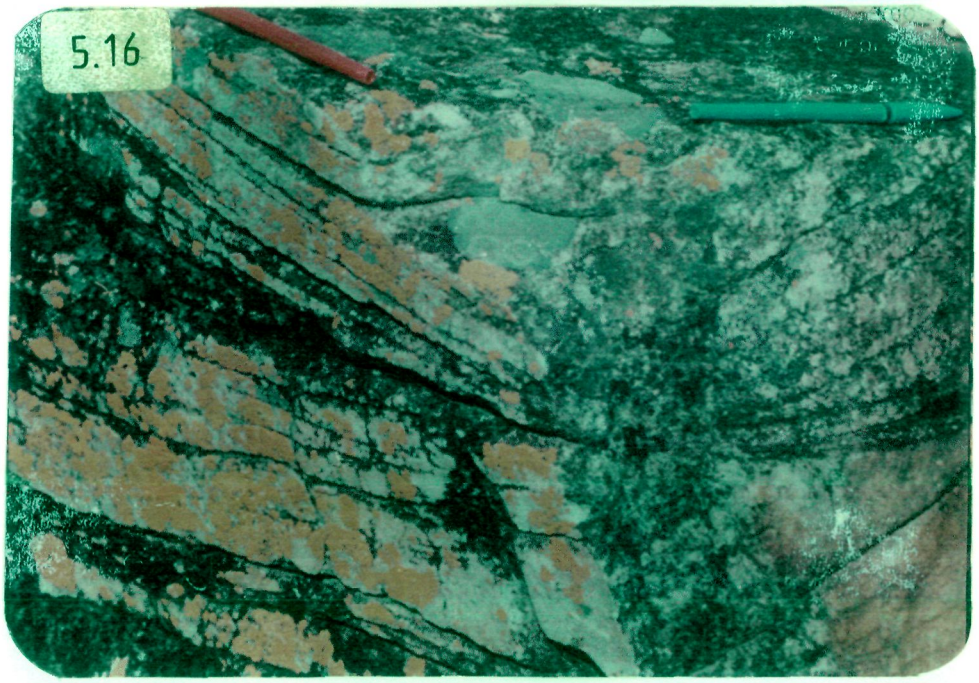
5.16

5.3.1.6 Quartzite,Cross bedded {S(p/t)}:

Parallel bedded quartzite is followed by cross bedded quartzite. This quartzite facies consists of medium size quartz grains cemented by a material which provides brownish to creamish colour. It shows development of medium to small scale cosets of planar (fig. 5.15) and trough (Fig. 5.16) cross stratification. Thickness of this facies ranges from 1-2 and 2-3 mts. respectively. Foreset thickness varies from 0.5 to 2 cm depending upon the grain size and set thickness. Ribbs and furraws structures also are present in this facies (Fig. 5.17).

Quartzite with herringbone cross bedding is also present and is represented as a separate lithofacies (Fig. 5.18). Its thickness is about 1-1.5 mts. and foreset thickness ranges hardly a few tens of mm. Rest of the characters of this lithofacies are similar to the above described quartzitic facies.

5.3.1.7 Quartzite,Ripple drift laminated/ripple bedded {S(rd/r)}:

Locally fine grained quartzite facies of brownish white colour, show ripple cross laminations, passing into ripple drift and climbing ripple laminations (Fig. 5.19). Occassionally, asymmetrical ripple marks are very neatly preserved on the upper surface of the bedding plane (Fig. 5.20). Ripple marks are of straight crest with a very nominal bifurcation, and of small scale with wave length of 4 to 8 cms. Their amplitude varies from 1 to 2 cms with a ripple index around 3 to 5.

Fig. 5.17 : Photograph showing ribbes and furrows as primary sedimentary surface structures, present in fine grained quartzites. Location near Lakya.

Fig. 5.18 : Herring bone cross bedded facies of quartzites is considered as a separate facies. Its thickness is about 1-1.5 mts. Location near Devenahalli.

Fig. 5.19 : Photograph illustrating ripple cross laminations, passing into ripple drift and climbing ripple laminations. Location Chickmagalur - Kadur road, near Chickmagalur town.

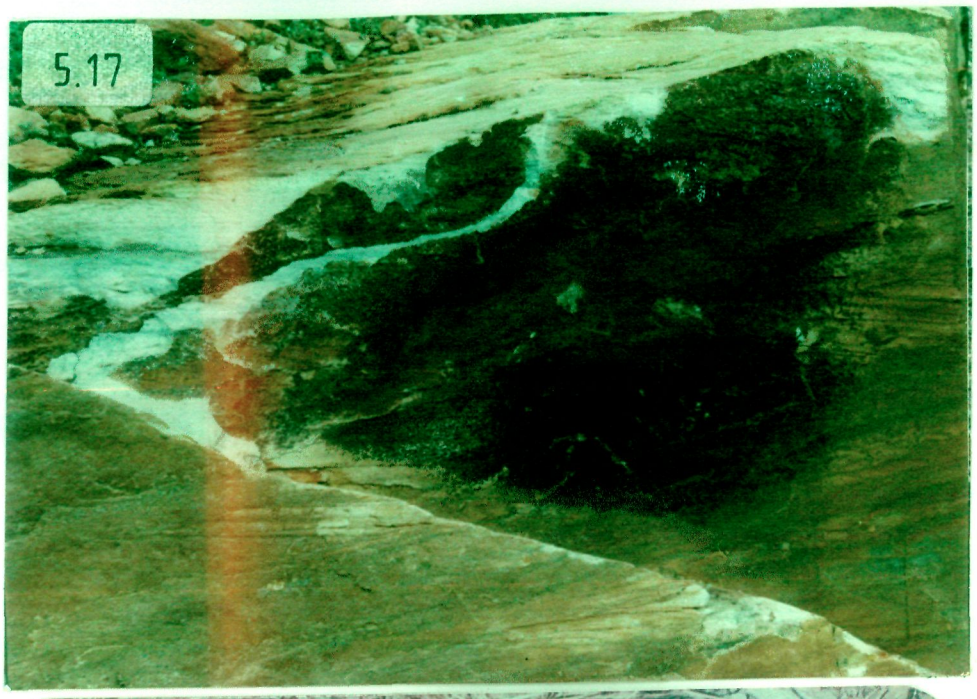
5.17

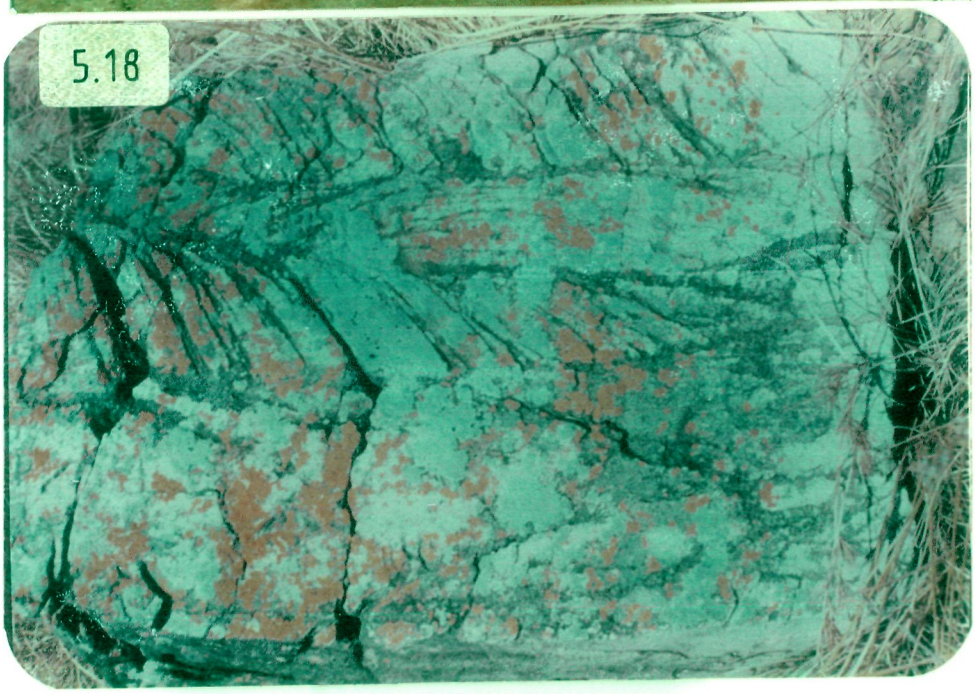
5.18


5.19

5.3.1.8 Quartzite, Mud cracks:

This facies is very thin, hardly 1/2 mt. or so. Constituent grains are fine grained and very well sorted. It is of white colour. Mud cracks are visible on top surface of the rock unit. (Fig. 5.21).

5.3.1.9 Phyllites, Paper thin laminated {F(l)}:

This facies is exposed on the top of the sedimentary piles of the Kalasapura Formation. Fine grained metaclastic unit, which is paper thinly laminated (Fig. 5.22), is commonly associated with quartzites of parallel bedding and metavolcanics. Generally in this formation chlorite-quartz phyllite is not as widespread as it is in younger formations. In this facies it is mainly of siliceous nature.

5.3.2 Mundre Formation:

The upper most formation of the Bababudan Group in this schist belt is the Mundre Formation, exposed in the northeastern part of the basin (Fig. 5.23). Prominent lithounit is the Kaldurga Polymictic Conglomerate, which has lateral transition into an association of interbedded phyllite and cross bedded locally fuchsitic quartzite. In all 3 types of lithofacies were recognised viz. conglomerate with graywacke matrix, quartzites and phyllites. Conglomerate which is polymictic in nature, has further been divided into three subdivisions (Fig. 5.24). Description of various lithofacies are given below.

Fig. 5.20 : Photograph showing assymetrical ripple marks. Ripple marks are of straight crest with a very nominal bifurcation. Location near Chickmagalur town.

Fig. 5.21 : Field photograph showing the presence of mud cracks in fine grained quartzites. Location as for fig. 20.

Fig. 5.22 : Photograph showing paper thin laminated fine clastics which is lying over the fine grained quartzites. Location near Chickmagalur town.

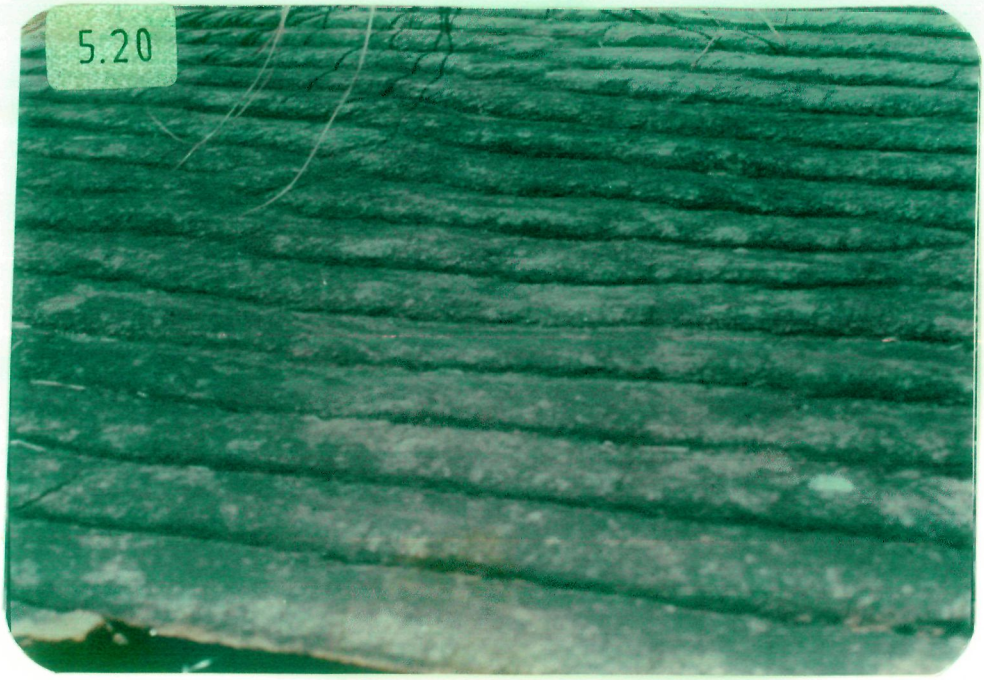
5.20

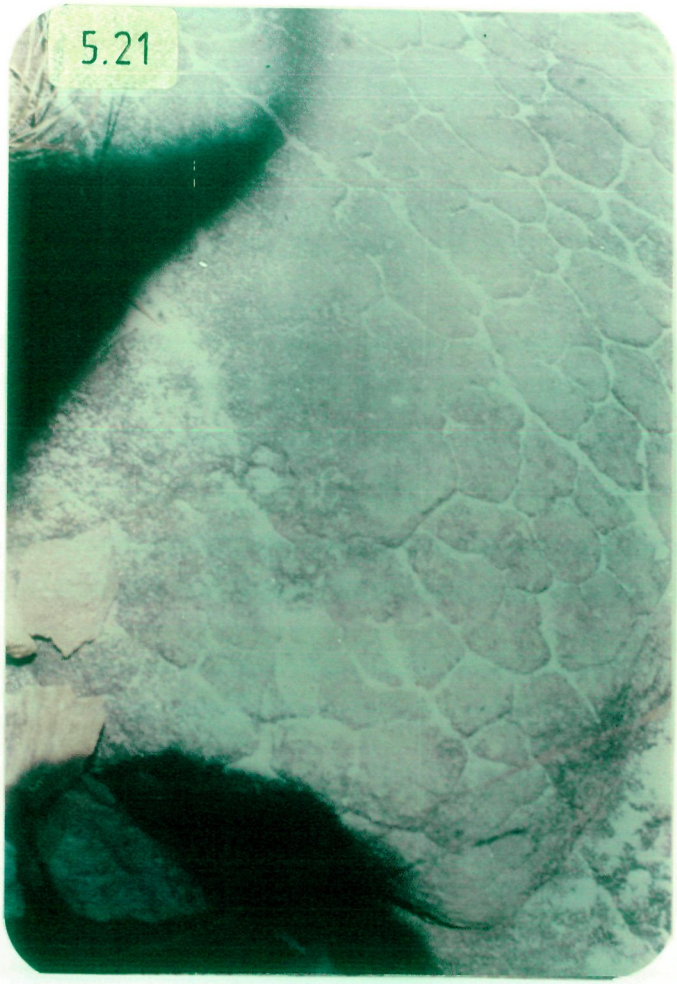
5.21


5.22

Fig. 5.23 : Geological map of the north eastern part of the Bababudan schist belt, showing the two fold division of the Kaldurga Conglomerate as proposed by Chadwick et al.,1985a. Superimposed are the palaeomud flow direction as analysed in this study.

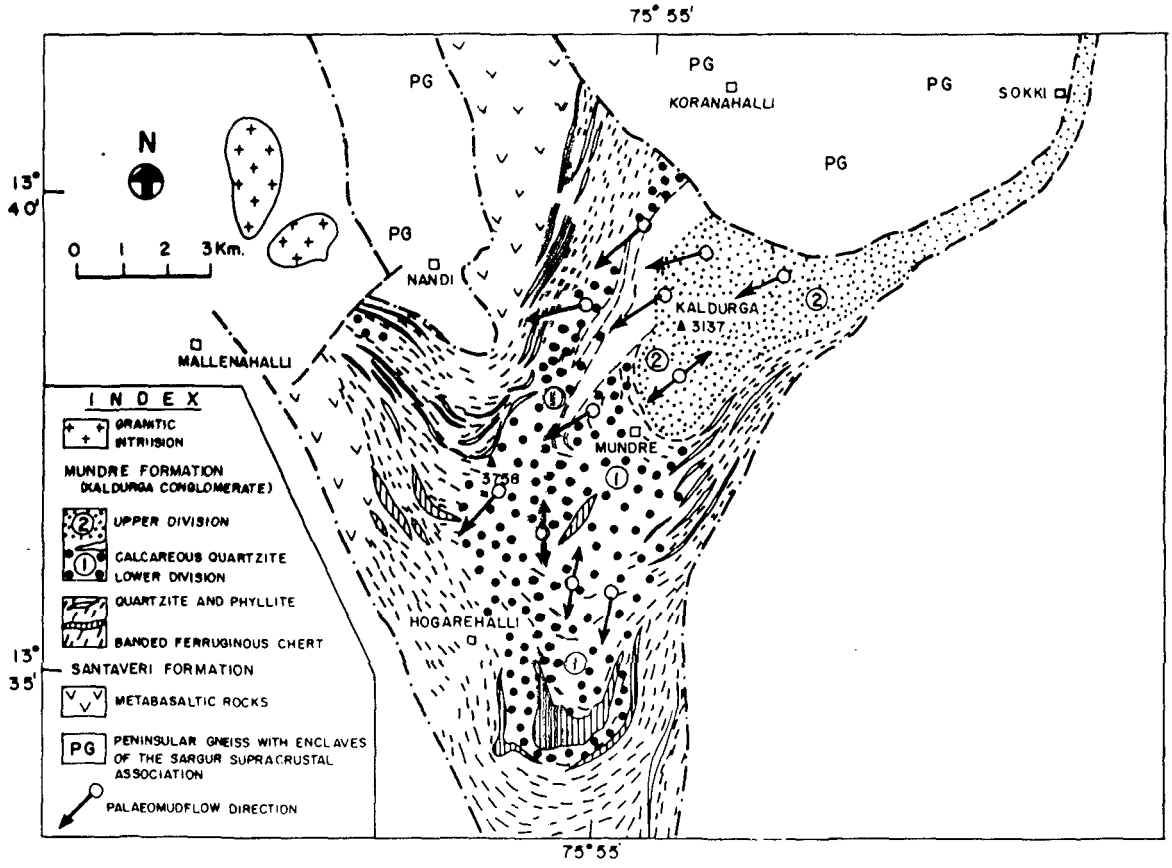
75° 55'
PG
KORANAHALLI
PG
SOKKI
PG
N
13° 40'
0 1 2 3Km.
PG
NANDI
KALDURGA
▲ 3137
MALLENAHALLI
MUNDRE
3758
HOGAREHALLI
13° 35'
INDEX
GRANITIC INTRUSION
MUNDRE FORMATION (KALDURGA CONGLOMERATE)
UPPER DIVISION
CALCAREOUS QUARTZITE
LOWER DIVISION
QUARTZITE AND PHYLLITE
BANDED FERRUGINOUS CHERT
SANTAVERI FORMATION
METABASALTIC ROCKS
PG
PENINSULAR GNEISS WITH ENCLAVES OF THE SARGUR SUPRACRUSTAL ASSOCIATION
PALAEOMUDFLOW DIRECTION
75° 55'

Fig. 5.24 : A generalized vertical sequence of the lithofacies assemblage in the outcrop of Mundre Formation.Facies codes are similar as given in table 5.1.

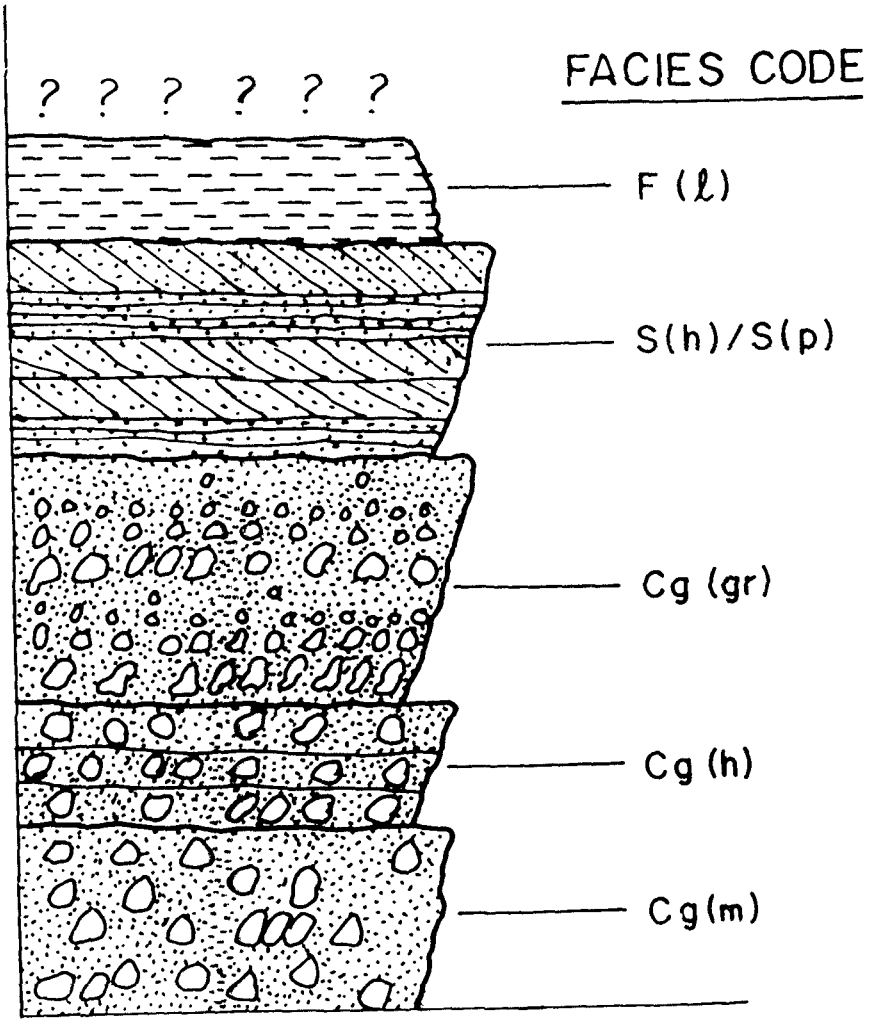
? ? ? ? ? ?
FACIES CODE
F (ℓ)
S(h)/S(p)
Cg (gr)
Cg (h)
Cg(m)

5.3.2.1 Conglomerate, Massive {Cg(m)}:

On the basis of dominant clast lithology, Chadwick et al. (1985a) divided the Kaldurga Conglomerate into two divisions, lower and upper (Fig. 5.23). Massive conglomerate facies; representing the lower division of the polymictic conglomerate (Fig. 5.25) mainly consists of clasts of quartzite, directionally embedded in an olive green matrix. Apart from quartzites, clasts of many other metasedimentary rocks like ferruginous chert, BIF marble and phyllite are also present. Clasts are poorly sorted, subrounded to subangular, and less spherical. Abundance of clast types is mainly dependent on their mechanical strength to bear the physical abrasion.

As a whole, the Kaldurga Conglomerate is matrix supported exhibiting disrupted framework. Cementing or binding material of different types of clast together is an olive green or dark green siliceous chloritic and/or amphibolitic schistose matrix. The matrix makes an important part of this facies, because most of the clasts are exhibiting floating framework, i.e. matrix:clasts ratio is fairly high. In this case also grade of metamorphism ranges from upper greenschist to lower amphibolite facies.

5.3.2.2 Conglomerate, Stratified {Cg(h)}:

This facies comprises of the lower part of upper division. The clast population present in facies is well stratified with varying thickness of an average thickness of about 12 cm. It includes a wide spectrum of clasts of varying rock types, viz. banded iron formation, quartzite, tonalite, trondhjemite, vein quartz, metavolcanics and granite etc. Clasts morphology is

Fig. 5.25 : Photograph showing the massive facies of the Kaldurga polymictic conglomerate. Location near Shivpura.

Fig. 5.26 : Photograph showing the clasts of various morphology and lithology. They are subangular, poorly sorted and crudely imbricated in the matrix of the Kaldurga Conglomerate. Location near Shivpura.

Fig. 5.27 : Photograph showing the secondary contact framework attained by the clasts of the Kaldurga Conlomerate. Location near Kudlur.

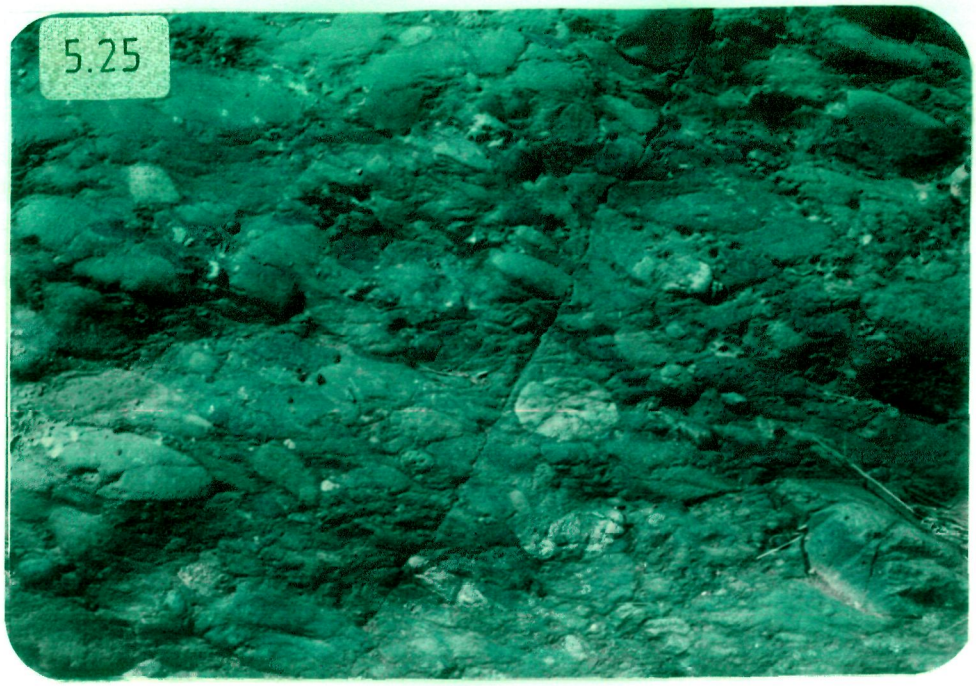
5.25

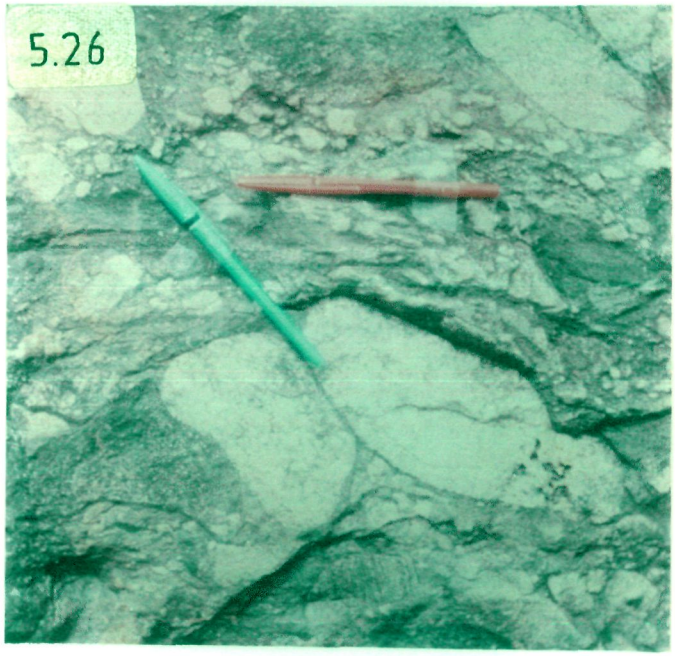
5.26

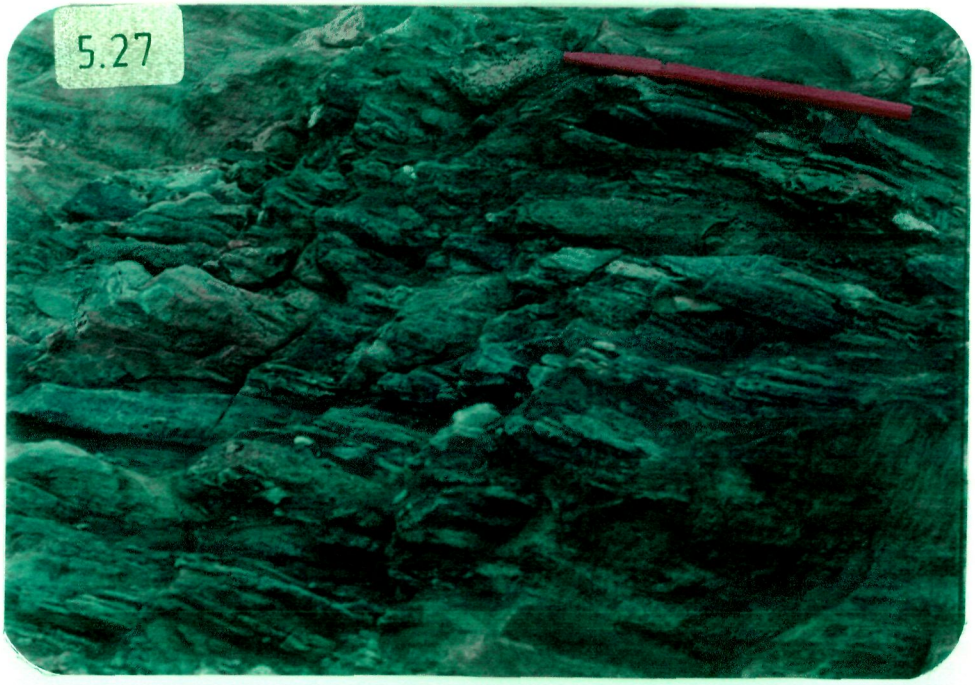
5.27

almost similar to the previous facies. Clasts are subangular, poorly sorted, rod shaped and crudely imbricated (Fig. 5.26). In general, clasts are showing floating type of packing. However, at places, probably due to deformation, some clasts have attained secondary contact framework (Fig. 5.27). In deformational fabric also clasts of varying lithologies are reflecting varying degree of strain. In general, clasts like ferruginous cherts, are apparently more stretched perpendicular to the direction of stress. At several places, even clasts of tonalite-trondhjemite gneiss are also stretched (FIg. 5.28).

5.3.2.3 Conglomerate, Graded bedded {Cg(g)}:

Stratified polymictic conglomerate gradually passes into graded bedded conglomerate. This facies is showing fining upward cycle i.e. a depositional cycle starts with comparatively bigger clasts and gradully it grades into finer layers having smaller pebbles. At the bottom, framework is clast supported or contact type, and on the top it changes into matrix supported or disrupted framework (Fig. 5.29). At the lower part of the graded cycle; where coarse clasts have been deposited, convincing geometry of imbrication is present (Fig. 5.26). The thickness of graded bedding sequences is highly variable and varies from 10 cm to 100 cms.

Presence of the clasts of the basement and not of the overlying cover, is the basic difference between this facies and the one described earlier. Common rock types present as a clast of varying size and shapes are tonalitic-trondhjemitic gneiss, granodiorites vein quartz, amphibolites and acid volcanics (listed

Fig. 5.28 : Photograph showing the intensity of subsequent episode of deformation, as indicated by stretched clast of TTG in the Kaldurga Conglomerate. Location near Kudlur.

Fig. 5.29 : Field photograph of the Kaldurga Conglomerate showing gradded bedding and the angularity of the amphibolite, TTG, vein quartz and other pebbles. Location near Mundre.

Fig. 5.30 : Photograph showing a big boulder of 30x30x15 cms.in size embedded in the matrix of the Kaldurga Conglomerate. Location near Mundre.

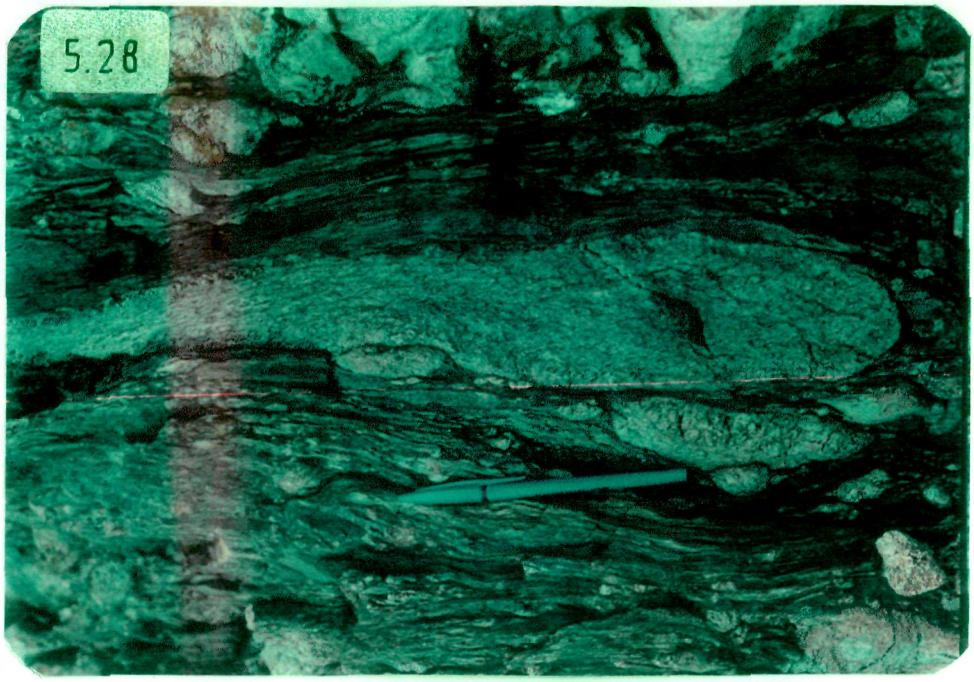
5.28

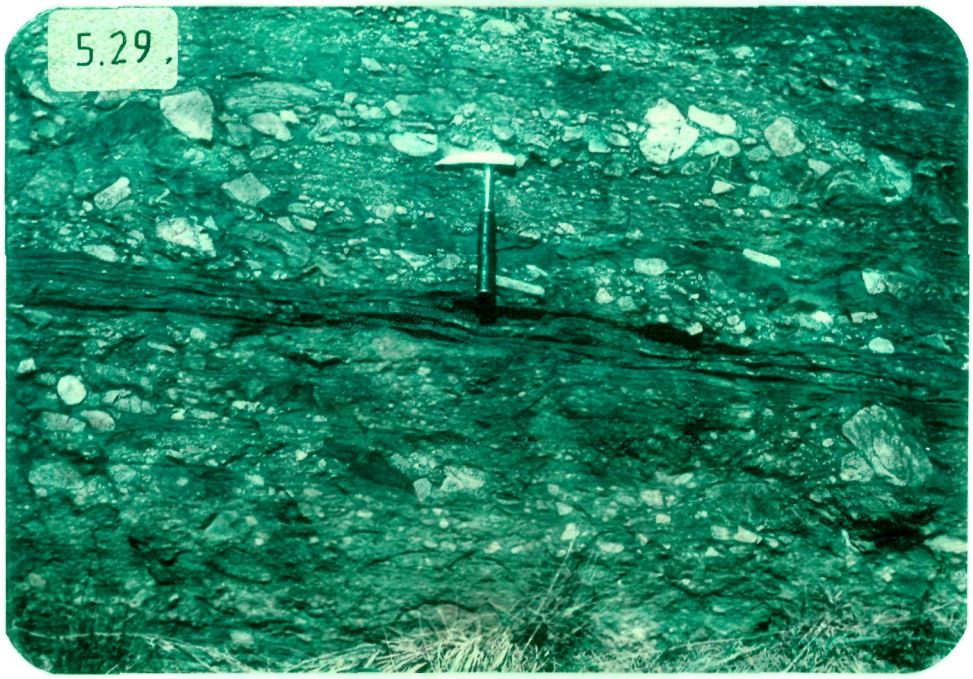
5.29

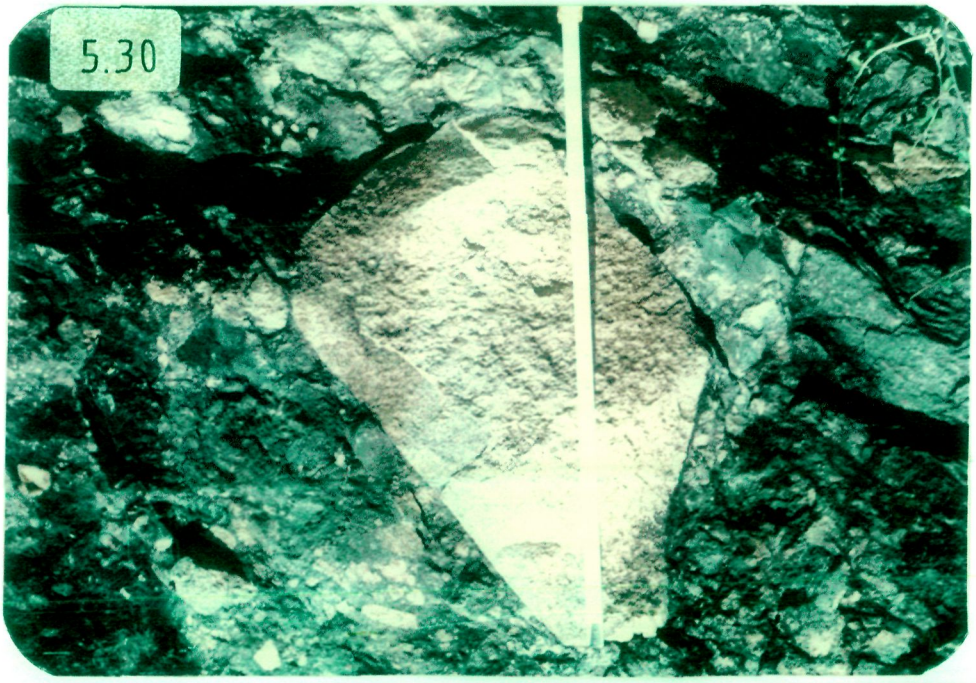
5.30

in decreasing order of abundance). TTG are most abundant type among embedded clasts. Tonalitic clasts of all shapes and sizes indicat very poor sorting, varying from granule to boulder size. The bottom portion of this facies is marked by big boulder of TTG, with the dimenion of 30x30x15 cm. (Fig. 5.30). Abundance of clasts of varying lithology is supposed to be a function of rheology of the clasts composition and the order of abrasion which they have undergone during transport. The characters of matrix of this facies are more or less similar to the earlier facies.

5.3.2.4 Quartzites, Cross bedded {S(p/t)}:

Various facies of the Kaldurga Polymictic Conglomerate with graywacke matrix laterally grade into stratified quartzite facies. Locally it is fuchsitic and cross bedded. This facies is fine grained, greyish otherwise greenish in colour. Estimation of true thickness is uncertain, but exposed and measured sections are about 12-15 mt. thick, showing small to medium scale planar cross bedding. They are present in cosets; set thickness is about 18 cm, while foreset thickness is ranging upto 1-1.5 cm. Individual coset thickness reaches upto 2.5 ft. It is underlained by fine clastics i.e. phyllites (Fig. 5.31). Across the strike in the stratigraphically up, these fine clastics are also found conformably resting on quartzites.

5.3.2.5 Phyllites (Fine clastics) {F(l)}:

Grades of metamorphism of fine clastics varies from lower greenschist to lower amphibolites than to phyllites and schists. It is brownish to green to olive green in colour and

Fig. 5.31 : Photograph showing the depositional contact between quartzite and phyllite, which are in association with the Kaldurga Conglomerate. Location near Mundre.

Fig. 5.32 : Photograph showing the splitted phyllites. It is due to close jointing and/or fractures cleavages. Location south of Mundre.


3.31


5.32

because of close jointing and fracture cleavage, it has been splitted into rods or needles (Fig. 5.32). Mainly it is chloritic-quartz schist but siliceous phyllites are also found. They are generally very intensely weathered and hence are not suitable for geochemical studies.

5.4 LITHOFACIES INTERPRETATION:

5.4.1 Quartz pebble conglomerate:

The conglomerate units which are massive or stratified are believed to be alluvial fan waterlaid deposits (Bull, 1972). Alluvial fan deposits may be found with various environmental association, depending on the topographical and climatic conditions (Reineck and Singh, 1980). Associated quartzites which have been considered as braided river deposits suggest that the most likely environment for the deposition of this association is the fluvial environment, where the alluvial fan deposits (conglomerate) are associated with braided river deposits. The massive conglomerate facies is interpreted here as a proximal unit of fluvial fan of McGowen and Groat (1971). The stratified and cross bedded conglomerate facies is considered as a mid fan facies of McGowen and Groat (1971). These basal conglomerate, generally considered orthoconglomerate (Chadwick et al., 1985a) are stratified also and typically show cross stratification. These are supposed to be the result of deposition by water in channel where discharge is more continuous (Davis, 1983) as a longitudinal braid bars (Boothryod and Ashleg, 1975). Locally cross stratified facies are suggestive of aggradation due to rapid deposition in

localized channels at relatively low water stage (Collinson and Thompson, 1982). Alluvial fan deposit, although not common, have been found in the Precambrian (Long, 1978). The clast supported and well rounded pebble conglomerate of an intercalated cross stratified quartzites of Moodies Group of Barberton Mountain Land, S. Africa also has been interpreted as proximal braided fluvial sequence (Eriksson, 1978;1980;1981).

5.4.2 Quartzites:

The parallel bedded, cross bedded and ripple drift laminated/ripple bedded arenaceous lithofacies showing upward fining cycles and nearly unimodal transport direction, are attributed to a fluvialtile/deltaic environments (Reading, 1986). The fluvial environments suggested above, are interpreted to be broad anastomosing braided fluvial plains, resulting the outcrop belts with strike length tens of kilometers long (Srinivasan and Ojakangas, 1986). The association of various lithofacies of quartzites with the proximal and mid fan facies, provides a logical ground to relate them with the distal fan facies. The distal fan is mainly a sandy area showing extensive bifurcation around lingoid bars (fine grained). Mainly planar cross bedding is produced, but units deposited during emergence contain small ripple bedding also (McGowen and Groat, 1971; Reineck and Singh, 1980). Alternatively, medium grained quartzite characterized by planar (Sp) and trough (St) cross stratified cosets may represent deposition by downstream accretion of the lithofacies of linguoid or transverse bars (Collinson, 1970; Smith,1978) and small scale sand dune (Collinson and Thompson, 1982) respectively, developed

in lower distal portion of braided fluvial plains. Hence, either the Saskatchewan type and platte type profile models for sandy braided stream deposits of Miall (1978) and Rust (1978), or distal fan facies model of McGowen and Groat (1971) with extensive bifurcation around lengoid bars, seem to be applicable to the Bababudan quartzites.

A rather limited occurrence of herringbone facies with juxtaposed cross beds and ripple bedded facies would mean that a tidally influenced environment should be prevailed at least locally. Nevertheless, they could be indicative of a transgressing marine environment (Srinivasan and Ojakangas, 1986). Furthermore, herringbone cross beds can form in fluvial environment where flow is reversed due to relationships of tributaries or where cross beds from adjacent bars are juxtaposed (Alam et al., 1985).

Fine grained quartzite showing ripple drift laminations assymetrical current ripple bedded facies of small scale i.e. ripple index varies from 3 to 5,might have been formed under relatively low velocities. Harms (1969) calls them low-energy ripples. In most of the cases ripple drift laminations or ripple lamines in drift are showing the preservation of only lee side, which is considered as a "type A" of Jopling and Walker (1968). Generally, they get preserved only when the supply of sediments is relatively higher and because of lower flow regime they are not able to get transported. Jopling and Walker (1968) have interpreted the formation of "type A" ripple drifted lamination. According to them (ibid) if the ratio of suspended load/bed load decrease, lesser sediments are available in suspension, then the

net result is that the stoss side of the ripples is eroded before they can be burried and preserved. So, as a consequence, only lee side could get preserved. The environment of periodically rapid accumulation of sediments is favourable for their deposition. Here, they are interpreted as levee deposits on the flood plains.

The presence of mud cracks as a surface structure on the very fine and well sorted quartzite is indicative of desiccation and compaction of water saturated muddy sediments i.e. wet conditions followed by a dry period. Such as, occurs in the intertidal zone or flood plains, abandoned river channels.

5.4.3 Fine Clastics:

Overlying fine clastics of paper thin laminated facies can also be interpreted as a unit deposited from suspension or surface cover in protected areas, for example in abandoned channels. Alternatively, they might have been deposited through suspension in a standing body of water similar to a flood plain or delta plain deposits (Gustavson, 1975).

5.4.4 The Kaldurga Polymictic Conglomerate:

This facies of conglomerate with disrupted framework, is characterized by subangular to angular clasts of quartzites, BIF, carbonates, metavolcanics, quartz veins, TTG and granites embedded into chloritic to amphibolitic matrix. Since it is impossible to deduce sedimentary environment directly from its sedimentary lithofacies, the first interpretation is attempted in terms of process (Walker and Pettijohn, 1971). The monatonous regular succession of massive to graded bedding conglomeratic strata

without any sedimentary features, indicative of agitated water, is therefore interpreted as having been deposited by highly viscous medium such as sedimentary gravity flow or debris flow (where fluid turbulance is important) in water too deep for regular disturbance by tidal, long shore or storm-suffered currents (Walker and Pettijohn, 1971; Walker, 1978). This mode of transportation was unable for reworking of the sedimentary debris load which is manifested by the poorly sorted matrix and angular clasts. Clasts imbrication in such a unsorted sedimentary rock,is the only depositional feature present in the lower part of the graded bedding facies of the Kaldurga Conglomerate. Although imbrication in debris flow deposition is rather uncommon (Reineck and Singh, 1980) but in more fluid debris flow deposits flat pebble can more or less be oriented in a prefered direction.

The most likely environment of deposition for the Kaldurga Conglomerate seems to be submarine valley, as a fanglomerate (Nocita and Lowe, 1990; Arora et al., 1991). The coarsest material, e.g. pebbles are deposited near the mouth of a submarine valley, in the upper part of the submarine fan (Hand and Emery, 1964; Stanley and Kelling, 1967). Walker (1976, 1978) has classified the sedimentary structures and facies within the submarine fan into three major settings, viz. upper, mid and lower fan sequence which commenc from mouth of the submarine Canyon to deep sea plains respectively (Fig. 5.33). Here, polymictic conglomerate is interpreted as the depository of the upper fan region of Walker (1978, 1984) in the upper fan channel, which usually shows a massive to graded bedded facies. It might be an equivalent of lower most portion of Bouma sequence (Bouma, 1962).

Fig.5.33 : Schematic model of submarine fan deposition (after Walker, 1978), the Kaldurga Conglomerate is interpreted as the depository of the upper fan region of Walker (1978;1984).

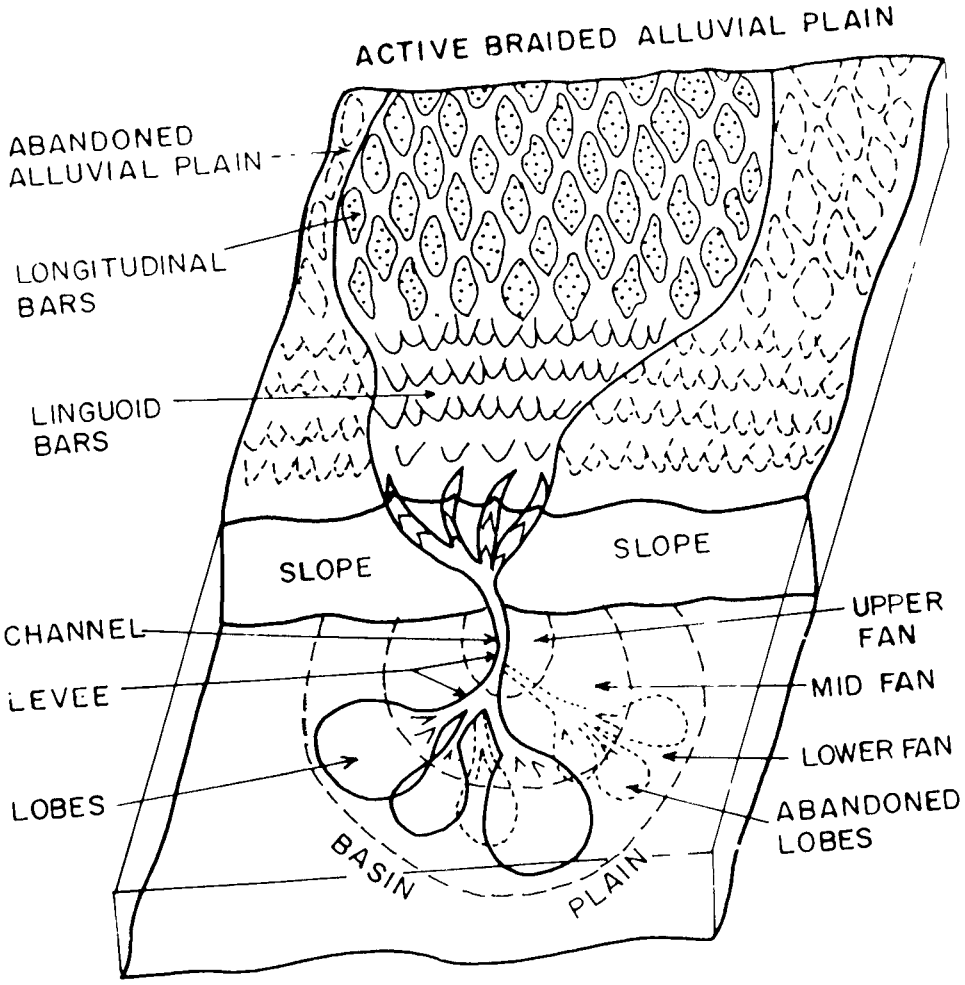
ACTIVE BRAIDED ALLUVIAL PLAIN
ABANDONED ALLUVIAL PLAIN
LONGITUDINAL BARS
LINGUOID BARS
SLOPE
SLOPE
CHANNEL
LEVEE
LOBES
UPPER FAN
MID FAN
LOWER FAN
ABANDONED LOBES
BASIN PLAIN

The associated fine grained quartzites which are locally small scale cross bedded and phyllite/schist can be considered as the lateral equivalent of upper fan deposit. i.e. conglomerate. These interbedded phyllites and quartzites are supposed to be natural levees and interchannel areas of the upper fan (Nelson et al., 1978). These facies may represent the upper portion of a Bouma sequence, with small scale cross stratified quartzite and overlying phyllite (mud).

5.5 PALAEOCURRENT ANALYSIS:

It has been recognised long ago that water-deposited primary directional structures can directly be related to the depositional current (Potter and Pettijohn, 1972) and may thus indicate the direction of source region. Linear fabrics viz. directional fabrics (sand grains), planar fabrics (oblate and prolate pebbles etc.) and cross bedding including other anisotropic structures have monoclinic symmetry. This concept has been successfully used in several Archaean terrains also, including the Dharwar craton (Henderson, 1975; Ojakangas, 1985, 1990; Srinivasan and Ojakangas, 1986; Gravenor and Wong, 1987; Arora et al., 1991). Various quartzites and the Kaldurga Conglomerate were studied for the palaeocurrent analysis.

5.5.1 Quartzites:

In southern part of the Bababudan schist belt there are various stratigraphic horizons of quartzites. Kalasapura quartzite (basal quartzite), which is closely associated with basal quartz pebble conglomerate, Lakya quartzite and Kaimara

quartzite are some of the horizons which have prolific development of various type of cross bedding and other primary sedimentary structures. Cross bedding of any scale has palaeocurrent value. Generally they are found in all kinds of sediments, but are most commonly present in sandsize rocks (Pettijohn, 1984). In Bababudan quartzites, mostly trough and planar cross bedding are present. As such herringbone corss bedding is also seen (see sec. 5.3). Assymmetrical ripple marks of small scale are also present, but palaeocurrent analysis of quartzites is mainly based on statistical study of cross bedded strata.

In all, down dip direction or cross beds azimuths and trough axes were measured at 15 localities in three stratigraphic horizons of quartzites (Fig.5.34). A total of 124 measurements were taken. Out of these 70 on the axes of troughs and rest 54 measurements were taken on planar/trough cross beds. Most of the data sets were collected from the vertical section (b.c. or ac plane), a few reading were taken from the crescentic trough at the bedding surface (ab plane).

The study carried out by Srinivasan and Ojakangas (1986), which is probably the first and the only detailed sedimentological study of Archaean sediments from India, has suggested that a correction for tilt was necessary, for the beds dip at angles as steep as 80^{o}, although most have dips of less than 45^{o}. Only a simple one tilt correction, rather than a two-tilt correction, was employed because of the plunge of the folds. The amount of plunge determined on the basis of bedding-cleavage intersections, were generally less than 20^{o} (Chadwick et al., 1985b). This amount of

Fig. 5.34 : Map showing the southern part of the Bababudan belt. Three horizons of quartzites are shown with palaeocurrent directions. Bipolar rose diagrams are the result of measurements on axis of trough cross beddings, while unipolarity is characteristic of planar cross beddings.
Bq= basal quartzite, associated with QPC.
Lq= Lakya quartzite
Kq= Kaimara quartzite.

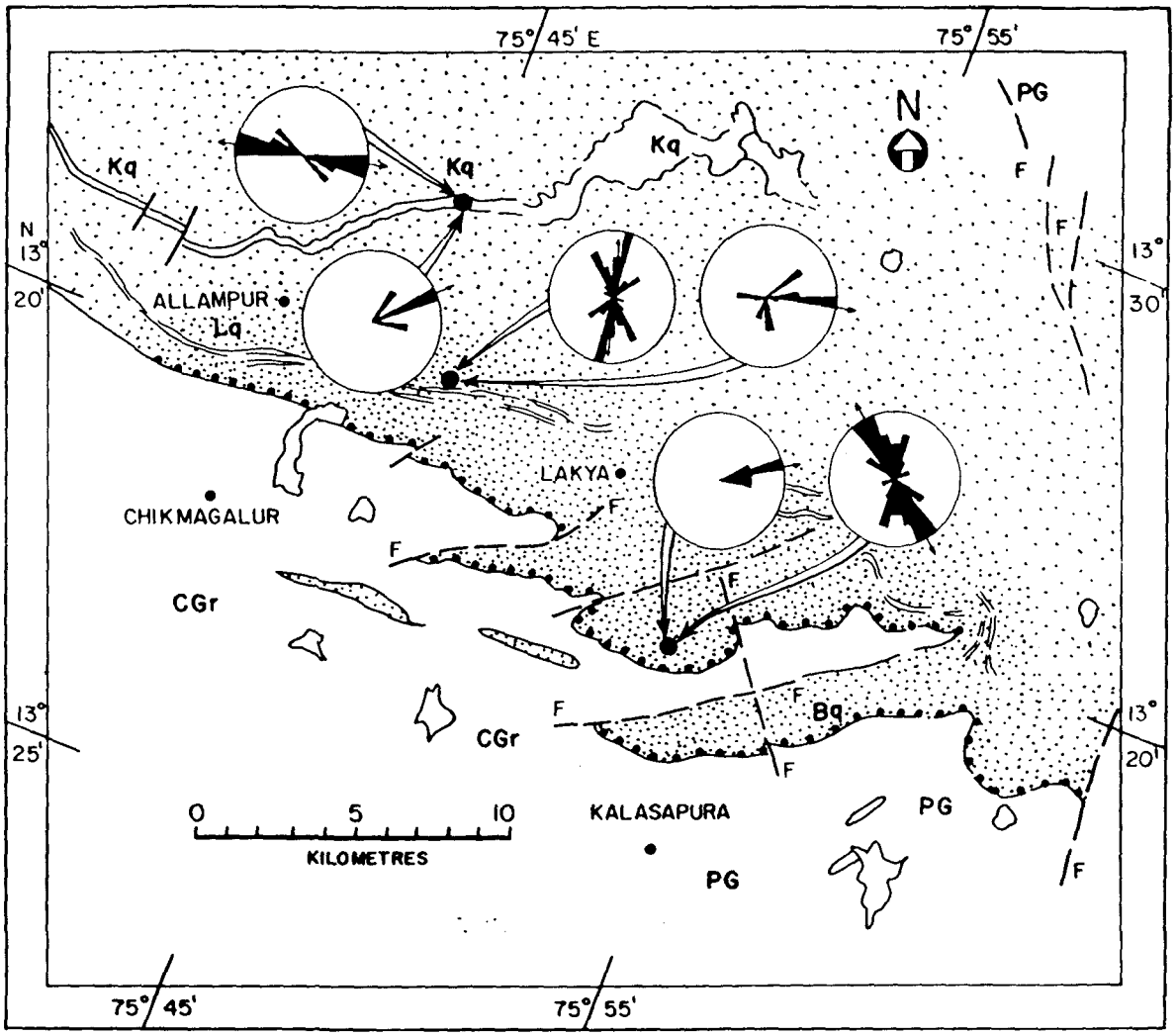
75° 45' E
75° 55'
N
PG
F
Kq
Kq
Kq
N 13° 20'
13° 30'
ALLAMPUR
Lq
LAKYA
CHIKMAGALUR
CGr
CGr
Bq
13° 25'
13° 20'
0 5 10
KILOMETRES
KALASAPURA
PG
PG
75° 45'
75° 55'

plunge with deformational dip of around 45^{o}, would result in an azimuthal correction of less than 10^{o} (Potter and Pettijohn, 1977).

After tilt corrections, the foreset and bedding plane data were treated statistically for vector mean (V), vector strength in percent (L%), and magnitude of the resultant vector (R) as shown in Table (5.2). Palaeocurrent plots of the three main quartzites horizons of the southern part of the Bababudan schist belt is shown in Fig. (5.34). In general, unidirectional data set is indicating the palaeocurrent trend to the eastern and southeastern direction, whereas bipolarity characterisation of cross beds indicate northwest- southeast or even north-south trend of palaeoflow.

5.5.2 The Kaldurga Conglomerate:

The Kaldugra Conglomerate shows the imbrication of various types of clast which are embedded into fine grained surrounding matrix. Imbrication is generally well preserved in the lower part of a graded bedding sequence whereas a fining upward cycle of gradation is starting with the pebbles and cobbles of clasts and framework is relatively clast supported.

The pebble fabric can be readily measured because of the coarseness and shape of the clasts. The largest, intermediate and shortest axes of a prolate clast are designated as "A", "B" and "C" respectively. The maximum projection plane is the "AB". In pebble fabrics, pebble units are commonly inclined in an up-current direction (Potter and Pettijohn, 1972; Davis, 1983; David and Lajoie,1989; Pettijohn, 1984). Most of data were

Table 5.2: Statistical parameters of palaeocurrent analysis.

Name of horizon	Kalaspura Quartzite		Lakya Quartziate		Kaimara Quartzite	
Name of structures.	S(p)	S(t)*	S(p)	S(t)*	S(p)	S(t)*
No. of outcrop	(7)		(5)		(3)	
N	25	34	4	6	25	30
θ_v	79°	154°-334°	65°	96°-276°	111°	6°-186°
R	4.92	23.15	3.73	4.14	11.96	26.31
L (%)	98.40	68.09	93.25	69.00	47.84	87.70

N = Number of total readings.
θv = Vector mean.
R = Vector magnitude.
L(%) = Consistancy ratio in %.
* = Mainly axes of trough cross bedding were measured.

collected on "ac" plane i.e. vertical exposure, because this plane can provide the azimuth of inclined "A" axis of the pebble, and angle of inclination with principal plane of deposition as well. Generally the principle plane of deposition is bedding plane only. However, when 'ac' plane is not well exposed, 'ab' planes were taken into consideration and only strike of the "A" axis was measured. In all 11 locations/outcrops were found suitable for paleocurent analysis and around 400 individual readings, both azimuth and strike of 'A' axis were recorded. Locations and synthesis of preferred palaoecurrent directions are shown in Fig. (5.23).

The possible paleocurrent analysis and inferred palaeodrainage pattern as shown in Fig. (5.23), indicates that, in general, the lower unit of the Kaldurga Conglomerate is characterized by SSW palaeocurrent direction. The upper unit, shows a slight deviation in palaeoflow direction towards the southwest. Because the strike of long axis of pebbles provides only a sense of flow rather than a preferred direction of flow, bipolar symbols are used. The average values of statistical attributes of palaeocurrent analysis, viz. L%, R, variance and standard deviation are 83^{o}, 14.40, 1322 and 36.35 respectively.

CHAPTER VI

PETROGRAPHY : TEXTURAL AND MINERALOGICAL STUDIES

6.1 INTRODUCTION :

The Petrography of a clastic sedimentary rocks is determined in large measure by provenance. The character of the immature sands, in particular, is controlled primarily by the nature of the source rocks (Pettijohn, 1984; Pettijohn, Potter and Siever, 1972). Although, a sedimentary rock retains its parental mineralogical characters, but at the same time the nature of the sedimentary processes within the depositional basin, and the kind of dispersal paths that links provenances to the basin, modify the mineralogical signatures (Dickinson and Suczek, 1979). Aforesaid modification can be visualized by the textural properties of the sedimentary rocks. Thus, utilizing mineralogy including heavy minerals, and texture, petrography is the first major step towards putting the parts of clastic sedimentary rocks together to form an integrated and meaningful description.

Original petrography of clastic metasedimentary rocks of the Bababudan schist belt has been partially obliterated because of the upper greenschist to lower amphibolite grade of regional metamorphism. Despite this difficulty some attempts have been made to decipher the nature of provenance and physical processes involved during sedimentation, e.g. Rama Rao et al. (1979), Naqvi et al.(1978 a), Aurora (1985), Srinivasan and Ojakangas (1986), Fareeduddin (1988), Arora et al. (1991).

This chapter includes (i) textural studies of quartz pebble conglomerate, quartzites and the Kaldurga Polymictic Conglomerate, (ii) Modal analysis of conglomerates quartzites and the matrix of the Kaldurga Conglomerate.

6.2 TEXTURES :

Textural characteristics are used for evaluation of sediment properties interpreting physical processes involved during transportation and environment of deposition of the Phenerozoic sediments. However, these studies have limitations for the Archaean sedimentary rocks, because of their obliteration due to varying grade of metamorphism and penecontemporaneous deformations (Spry, 1976). The obliteration in nature of original textures is due to low grade metamorphism, which produces a preferred orientation of minerals. However, textures involving large compositional differences or discontinuities (e.g. the Kaldurga Polymictic Conglomerate) may be preserved even in rocks which have been strongly deformed but delicate sedimentary structures are preserved in weakly deformed rocks (Spry, 1976; Srinivasan and Ojakangas, 1986; Naqvi et al., 1988). Although, the Bababudan schist belt has been metamorphosed from upper greenschist to lower amphibolites, but still this belt has retained its rather small and delicate sedimentary structures in clastic metasedimentary rocks. Thus, grain size analysis can be carried out for basal quartz pebble conglomerate and quartzites, however, a great precaution was taken while selecting the thin sections for the same purpose. In general, the sections in which i) original boundaries are well preserved, ii) the amount of original clayey

matrix is fairly good (3-5%) (as suggested by Srinivasan and Ojakangas, 1986) and iii) no serious interruption of mutual contact of grains due to deformed fabric; were selected for the petrography of basal quartz pebble conglomerates, quartzites and the Kaldurga Conglomerate.

6.2.1 Grain Size Analysis :

The grain size analysis of a detrital sedimentary rock is of considerable importance. The size and uniformity of size or sorting are measures of the competance and efficiency of the transporting agent. The several agents and modes of transport differ significantly in their sorting and transporting ability (Pettijohn, 1984; Folk, 1980).

With this objective and the reservations as discussed in earlier sections 15 samples of metasedimentary rocks were selected from Bababudan schist belt for the grain size and roundness analysis. Since disintegration method ordinarily used (Krumbein and Pettijohn, 1938) was not desirable, the grain size analysis was carried out from thin sections using petrological microscope. For this purpose, 5 samples/thin sections from each metasedimentary rock i.e. the matrix of basal quartz pebble conglomerate, associated/overlying quartzites and the matrix of the Kaldurga Polymictic Conglomerate, were chosen. These 15 samples showed comparatively less effect of metamorphism/ deformation. The apparent long diameter of grains were measured with the help of micrometer. Some 250-300 grains were counted per thin section as suggested by Friedman (1958) and considered to be satisfactory, as suggested by pioneers of this field

(Pettijohn et al., 1965; Friedman, 1958, 1962; Pettijohn, Potter and Siever, 1972; Pettijohn, 1984). We set our spacing in such a way that entire section was covered in each case. Grain less than 0.03 mm (>5 ϕ) in diameter were treated as clay or matrix (Spencer, 1963).

The recorded data were tabulated after following the $\sqrt{2}$ scale of Wentworth (1922) grade-scale . Since all these data were collected with the help of micrometer under microscope, the sieve equivalent diameters were obtained using Friedman's graph (1958). On the basis of present data, cumulative frequency curve was plotted for each rock sample to illustrate the grain size distribution of matrix of quartz pebble conglomerate, quartzites and matrix of the Kaldurga Polymictic Conglomerate (Fig. 6.1 A, B and C).

With the help of these cumulative curves, certain specific values of ϕ percentiles were determined, namely, ϕ_5, ϕ_{16}, ϕ_{25}, ϕ_{50}, ϕ_{75}, ϕ_{84} and ϕ_{95}. These values of ϕ are essential to compute the statistical attributes of grain size, such as inclusive graphic mean (M_Z), sorting coefficient (σ_I), skewness (SK_I) and Kurtosis (K_G) (all are computed according to the formulae, given by Folk, (1980).

6.2.1.1. Mean Size (M_Z):

The best graphic measure for measuring overall size is the inclusive graphic mean (M_Z),

$$M_Z = \frac{\phi_{16} + \phi_{50} + \phi_{84}}{3}$$

Fig. 6.1 : Illustration shows the cumulative frequency of size distribution curves for QPC(A), quartzites (B) and matrix of the Kaldurga Conglomerate (C). For the elaborative explanation of these curves please see the text and Table (6.1).

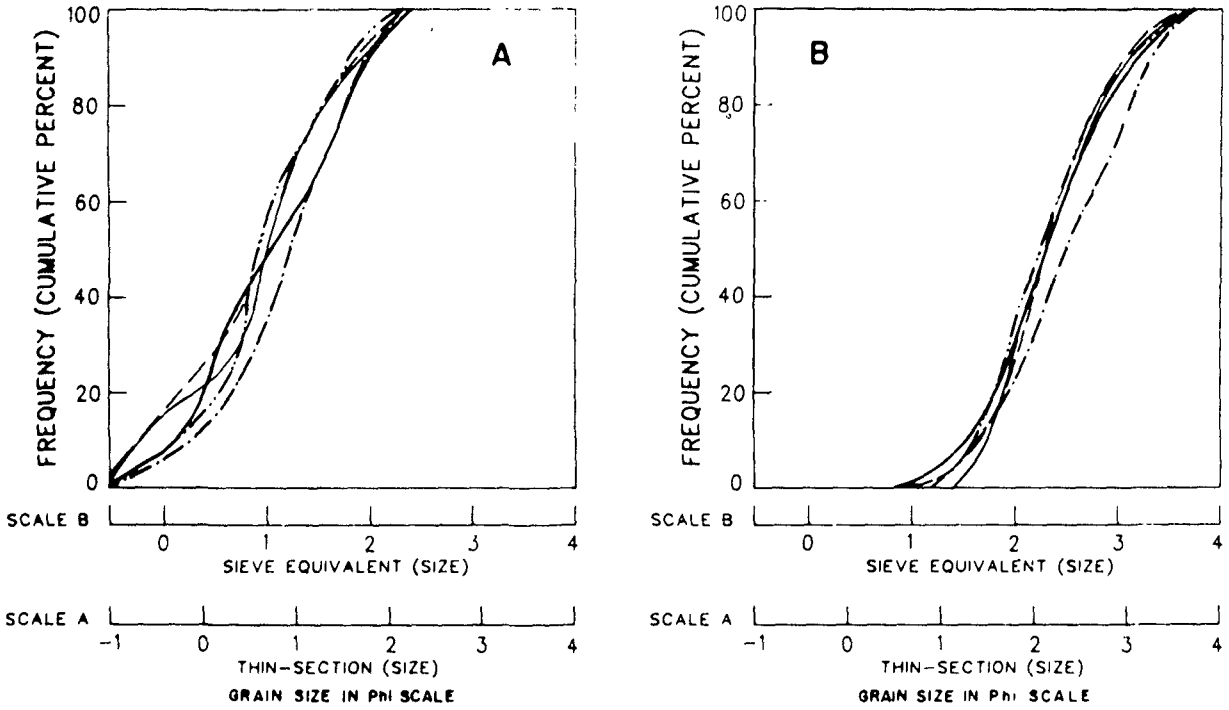
A
B
C
FREQUENCY (CUMULATIVE PERCENT)
100
80
60
40
20
0
SCALE B
0
1
2
3
4
SIEVE EQUIVALENT (SIZE)
SCALE A
-1
0
1
2
3
4
THIN-SECTION (SIZE)
GRAIN SIZE IN Phi SCALE

6.2.1.2 Coefficient of Sorting (σ_I):

The graphic standard deviation, σ_I, is a good measure of sorting and is computed as $\phi_{84} - \phi_{10/2}$. However, this takes only the central two thirds of the curve and a better measure is the inclusive graphic standard deviation, (σ_I).

$$\sigma_I = \frac{\phi_{84} - \phi_{16}}{4} + \frac{\phi_{95} - \phi_5}{6.6}$$

6.2.1.3. Skewness (SK_I):

Curves may be similar in average size and sorting but one may be symmetrical and other asymmetrical. Skewness measures the degree of symmetry as well as the "sign" i.e. whether a curve has an asymmetrical on left (-), or right (+), means whether grain size distribution is coarsely skewed or finely skewed. A better statistics for this, which includes about 90% of the curve, is the Inclusive Graphic Skewness (SK_I).

$$SK_I = \frac{\phi_{16} + \phi_{84} - 2\phi_{50}}{2(\phi_{84} - \phi_{16})} + \frac{\phi_5 + \phi_{95} - 2\phi_{50}}{2(\phi_{95} - \phi_5)}$$

6.2.1.4. Kurtosis (K_G):

Departure of a cumulative curve from a straight line, and the quantitative measure used to describe this departure from normality is called Kurtosis. It measures the ratio between the

sorting in the "tails" of the cruve and the sorting in the central portion. The Kurtosis measure used here is the Graphic Kurtosis, (K_G).

$$K_G = \frac{\phi_{95} - \phi_5}{2.44(\phi_{75} - \phi_{25})}$$

All these statistical parameters of the grain size distribution, so computed and tabulated in Table (6.1), may be described in terms of the verbal scale given by Folk (1980).

6.2.2 Roundness :

Roundness of the clastic grains of matrix of quartz pebble conglomerate, quartzites and matrix of the Kaldurga Conglomerate, were determined by comparing these with photographic chart for sand grains (Powers, 1953). To get the quantitative representation of roundness, it was transferred to ρ (rho) scale of roundness, as proposed by Folk (1980), in which the limits of very angular class are taken as 0-1, angular 1-2, subangular 2-3, subrounded 3-4, rounded 4-5 and well roundness taken as 5-6.

In all, 250-300 grains were measured from each thin section and the same 15 sections were studied, which were considered for other textural investigations. All these grains were grouped into different size intervals. In each grain size interval, grains were distributed in various vertical column of roundness accordingly. Then, the mean value of each roundness class in (rho) was multiplied by the number of grains lying in those

Table 6.1: Various statistical (textural) parameters of grain size of matrix of Quartz Pebble Conglomerate, quartzites and matrix of the Kaldurga Conglomerate.

		Mean size (M_Z)	Standard deviation (σ_I)	Skewness (SK_I)	Kurtosis (K_G)	Roundness (f)
	MK-55	0.08	0.72	-0.07	0.82	3.16
Q	MK-59	0.07	0.81	-0.20	1.33	3.41
P	MK-65	0.15	0.66	-0.05	0.96	3.01
C	MK-78	0.04	0.64	0.07	1.06	3.17
	MK-81	-0.17	0.83	-0.23	1.03	3.35
Q	MK-86	2.33	0.58	0.25	0.85	3.35
T	MK-91	2.34	0.70	0.06	0.99	2.93
Z	MK-92	2.51	0.70	0.01	0.85	3.35
S	MK-94	2.36	0.58	0.15	0.86	3.20
	MK-95	2.29	0.65	0.13	0.83	3.20
	MK-8	0.22	0.57	0.03	0.92	3.10
K	MK-17	-0.38	0.60	-0.09	0.73	2.98
C	MK-29	0.19	0.75	-0.18	1.08	3.17
M	MK-36	0.15	0.62	-0.15	0.89	3.00
	MK-39	-0.20	0.64	-0.10	0.91	2.99

classes. Afterwards, the multiplied numerical values were integrated and divided by the total no. of grains of that particular size class. Obtained value of ρ is the mean roundness of that size class. Average of ρ (rho) is the roundness of a given sample, and tabulated in Table (6.1).

6.2.3 Grain Size Characteristics:

6.2.3.1. Quartz pebble conglomerate:

In studying thin sections of matrix of quartz pebble conglomerate, maximum size of clastic grain varies from 3.92 mm (-1.95 ϕ) to 3.26 mm (-1.69 ϕ). The minimum size goes down around 0.28 mm (-1.82 ϕ). However, the mean size (M_z) varies from 0.90 (+0.15 ϕ) to 1.13 mm (-0.17 ϕ), with an average of 0.98 mm (+0.03 ϕ) i.e. on an average grains are very coarse. The value of inclusive graphic standard deviation (σ_I) for detrital grains varies from 0.64 ϕ to -0.83 ϕ , with an average value of 0.73 ϕ . The computed numerical values show that in general matrix of the conglomerate is moderately sorted.

An appreciable variation is observed in statistical value of inclusive graphic skewness of matrix of quartz pebble conglomerate. It ranges from -0.23 to +0.07 with an average of -0.10. Negative 'sign' indicates that in general, frequency distribution curve is asymmetrical and left skewed. It means that coarse grain detrital material is in excess in comparison to the finer one.

The value of inclusive graphic Kurtosis for the matrix of quartz pebble conglomerate ranges from 0.82 to 1.33 , with an

average of 1.04 . The value of K_G more than 2.00 shows the leptokurtic nature of size frequency distribution curves. It implies that the central part of size distribution is well sorted. Clastic grains of matrix of quartz pebble conglomerate are in general subrounded. Although they vary from angular to rounded one, but on the ρ (rho) scale of roundness, proposed by Felk (1980). the mean roundness varies from 3.01 to 3.41.

6.2.3.2. Quartzites:

In all, five thin sections of quartzites were found suitable for textural studies. The maximum grain size of quartzite varies from 0.53 mm (0.91 ϕ) to 0.46 mm (1.11 ϕ). The minimum grains size of quartzite varies from 0.53 mm (0.91 ϕ) to 0.46 mm (1.11 ϕ). The minimum size goes down upto 0.05 mm (4.28 ϕ). The graphic mean size (M_Z) of quartzites varies from 0.17 mm (2.53 ϕ) to 0.21 mm (2.23 ϕ). It indicates that studied horizons of quartzites are made up of fine grained clastic particles.

The value of inclusive graphic standard deviation (σ_I), which is ranging from 0.58 to 0.70 with an average value of 0.64, shows that grain size distribution is moderately well sorted. In comparison to matrix of quartz pebble conglomerate, quartzites are finer in size with relatively better sorting, which is an indication that quartzites components have undergone more regrous reworking and long transportation, than the QPC.

The statistical parameter of asymmetry of size distribution frequency curve i.e. inclusive graphic skewness (SK_I) of quartzites varies from 0.01 to 0.25 , with an average value of 0.12. The variation and mean value indicate that in general, size

distribution is fine skewed or right skewed, thus, finer fraction is more abundant than the coarser one.

Inclusive graphic kurtosis of quartzites shows a range between 0.83 to 0.99, with an average value of 0.88. These numerical values come under the platykuritic and mesokuritic verbal classes of Folk (1980). However, average kurtosis indicates that size distribution is platykuritic i.e. the centered portion of size distribution frequency curve is less sorted than the marginal part.

On the ρ (rho) scale of roundness, the clastic grains of quartzites varies from subangular (2.43) to subrounded (3.35). Although some of the individual grains are angular as well as well rounded also, but the average value of ρ (3.21) suggests that, in general, sediments are subrounded.

6.2.3.3. The Kaldurga Conglomerate:

The maximum size of grain in matrix of the Kaldurga Conglomerate ranges from 4.2 mm (-2.05 ϕ) to 2.8 mm (-1.47 ϕ). Minimum size varies from 0.28 mm to 0.34 mm (1.82 ϕ - 1.56 ϕ). The inclusive graphic mean size limits from 0.86 mm (0.22 ϕ) to 1.25 mm (-0.38 ϕ) with an average value of 1.03 mm (-0.05 ϕ). It indicates that by and large the matrix of the Kaldurga conglomerate is coarse grained with fairly wide range of size distribution. The same feature is further revealed by inclusive graphic standard deviation (σ_I), which varies from 0.57 to 0.83, with a mean value of 0.70. These numerical values show that, in general matrix is moderately sorted.

In general, roundness of the grains is subangular, although

angular to subrounded grains are also available in the matrix of the Kaldurga Conglomerate. Overall, textural characters and roundness show that the matrix of the Kaldurga Conglomerate is texturally immature to submature.

6.3 MINERAL COMPOSITION AND MODAL ANALYSIS:

This study of mineralogical characters of the metasedimentary lithounits of the Bababudan schist belt, includes the matrix of quartz pebble conglomerate, quartzites and the matrix of the Kaldurga polymictic conglomerate. This investigation is based on microscopic, EPMA and XRD examinations, but maximum information was obtained from thin and polished sections studied under ortholense-II Pal BK microscope. A some of 50 polished thin sections were prepared and studied from as many specimens of the matrix of quartz pebble conglomerate (10), quartzites (15) and the matrix of the Kaldurga Polymictic Conglomerate (25).

The mineralogy of the matrix of quartz pebble conglomerate was studied with two main objectives: i) to assess the mineralogical composition of the samples and, ii) to use this information for the interpretation of the chemical data. To understand the genetic relationship between various minerals, is a major point of interest for this study. No attempt was made to quantify mineral abundances (i.e. modal analysis). Though samples were collected from surface only as no borehole samples were available, but ore microscopy was mainly performed on these surface samples which were exceptionally fresh and there was no indication of alteration.

Modal analysis (by volume) of quartzites and the matrix of

Kaldurga Conglomerate was carried out for each thin sections using a "swift" electronic point counter. Six to ten traverses were made to cover the entire thin section of rock samples. Modal analysis was computed in terms of detrital framework constituents (size >0.03 mm), the groundmass material of matrix (<0.03 mm) or cement whatever present and, others as accessories. The number of traverses were dependent on the average grain size of detrital components, and the size of thin section. On an average each linear traverse was 5 mm and vertical spacing between two traverses was 1 mm.

Modal components of quartzites and matrix of the Kaldurga Conglomerate were recalculated as volumetric proportions of the following categories of grains (Graham et al., 1976) : (1) Stable quartzose grains (Q), including both mono and polycrystalline (Qm and Qp), (2) monocrystalline feldspar grains (F), consisting of K-feldspar (f) and plagioclase (p), (3) quartzitic and other labile rock fragments (L) and Matrix. Dolomite, micas, various heavy minerals were also calculated. Modal analysis of quartzites and matrix of the Kaldurga Conglomerate of the Bababudan schist belt is tabulated in Table (6.2) and (6.3) respectively.

The prime objectives for modal analysis of quartzites and the matrix of Kaldurga Conglomerate were to reconstruct the provenance, to classify them on the basis of their framework constituents, to assess the mineralogical composition of rock types and to understand the petrogenesis of quartzites and Kaldurga conglomerate. Modal analysis of quartzite and the matrix of the Kaldurga conglomerate has been proved very useful in order to interpret the chemical data.

Table - 6.2 Modal analysis of quartzites, the Bababudan schist belt.

Minerals	MK-86	MK-87	MK-88	MK-89	MK-90	MK-91	MK-92	MK-93
Quartz [Q_m]	69.40	82.20	77.80	59.00	77.60	77.40	67.60	72.60
Quartz [Q_p]	10.20	-	4.40	3.00	-	3.20	2.40	3.30
Plagioclase [p]	6.80	-	8.00	14.20	9.60	-	2.00	9.60
K-Feldspar [f]	6.00	-	4.40	3.60	6.80	-	1.60	6.00
Rock fragments (mainly quartz-ites) [$q+L_s$]	1.20	2.40	1.60	4.40	2.20	5.40	5.20	3.00
Miscellaneous (micaceous, heavy and opaque minerals)	2.80	6.80	-	2.60	-	2.60	6.80	0.30
Matrix [M]	3.60	8.60	3.80	13.00	3.80	10.80	14.20	5.00
$Q=Q_m+Q_p$	85.00	97.20	85.40	73.60	80.70	93.70	88.80	80.30
$F=p+f$	13.70	-	12.90	21.10	17.00	-	4.60	16.50
$L=L_s+q$	1.30	2.80	1.70	5.30	2.30	6.30	6.66	3.20
Q/F	6.20	-	6.62	3.49	4.75	-	19.30	4.87
C.M.I.	5.67	34.71	5.85	2.79	4.18	14.87	7.93	4.08

Minerals	MK-94	MK-95	MK-96	MK-97	MK-98	MK-99	MK-100
Quartz (Q_m)	67.40	78.00	79.40	75.00	62.20	62.00	71.20
Quartz (Q_p)	3.80	1.20	3.60	1.80	2.40	2.00	2.24
Plagioclase (p)	11.00	7.60	2.40	8.40	8.60	8.00	12.40
K-Feldspar (f)	3.60	2.80	1.80	1.80	4.60	2.00	2.00
Rock fragments (mainly quartzites) ($q+L_s$)	1.40	1.80	5.20	2.20	2.80	2.80	1.20
Miscellaneous (micaceous, heavy and opaque minerals)	2.00	1.00	2.00	2.20	3.40	6.80	2.00
Matrix (M)	10.80	7.60	5.60	8.60	15.40	14.00	9.00
$Q=Q_m+Q_p$	81.70	86.70	89.80	86.10	80.10	83.30	82.50
F=p+f	16.70	11.40	4.50	11.40	16.40	13.00	16.20
$L=L_s+q$	1.60	1.90	5.70	2.50	3.50	3.70	1.30
Q/F	4.89	7.61	19.96	7.55	4.88	6.41	5.09
C.M.I.	4.46	6.52	8.80	6.19	4.03	4.99	4.71

Table - 6.3 Modal analysis of the matrix [M_1] of the Kaldurga Polymictic Conglomerate, Bababudan schist belt, Karnataka nucleus, India.

Minerals	MK-8	MK-10	MK-13	MK-16	MK-17	MK-19	MK-20	MK-23
Quartz [Q_m]	19.60	30.80	19.60	17.80	10.50	17.40	10.60	11.50
Quartz [Q_p]	1.00	2.00	0.40	0.60	1.00	-	-	1.60
Plagioclase [p]	13.00	5.20	14.80	3.40	0.30	12.00	8.00	16.10
K-Feldspar [f]	9.20	12.00	11.80	-	-	13.60	4.60	19.50
Rock fragments (mainly quartz-ites) [$q+L_s$]	9.40	5.00	5.40	27.00	32.20	9.60	16.20	12.10
Dolomite/ Calcite	0.60	8.40	13.80	1.40	-	0.80	-	9.30
Miscellaneous (micaceous, heavy and opaque minerals)	2.10	9.40	-	0.60	2.00	2.40	3.00	2.50
Matrix [M_2]	45.10	27.20	24.20	49.00	50.60	44.20	57.60	20.10
$Q=Q_m+Q_p$	39.46	59.64	38.46	37.70	26.14	33.08	26.90	21.55
$F=p+f$	42.53	31.27	51.15	6.97	0.68	48.67	31.98	58.55
$L=L_s+q$	18.01	9.09	10.38	55.33	73.18	18.25	41.12	19.90
Q/F	0.93	1.91	0.75	5.41	38.44	0.68	0.84	0.37
Matrix [M_2]/ Clasts	0.82	0.37	0.32	0.96	1.02	0.79	1.36	0.25
C.M.I.	0.65	1.48	0.63	0.61	0.35	0.49	0.37	0.27

Minerals	MK-25	MK-27	MK-29	MK-30	MK-31	MK-33	MK-35	MK-38
Quartz [Q_m]	4.60	9.20	13.80	19.85	12.70	6.90	6.00	14.90
Quartz [Q_p]	3.00	1.80	0.40	2.20	1.00	1.00	1.20	-
Plagioclase [p]	16.00	13.40	11.20	3.20	0.40	3.00	2.50	1.80
K-Feldspar [f]	9.80	8.40	7.40	13.25	-	0.10	-	-
Rock fragments (mainly quartz-ites) [$q+L_s$]	11.40	7.60	8.20	4.75	4.60	8.10	4.50	4.50
Dolomite/ Calcite	8.00	-	4.00	-	-	2.50	-	1.80
Miscellaneous (micaceous, heavy and opaque minerals)	1.80	5.80	0.40	3.70	14.30	8.10	7.60	1.80
Matrix [M_2]	45.00	53.80	54.60	52.75	66.60	70.30	78.20	75.20
$Q=Q_m+Q_p$	16.96	27.23	34.63	50.98	73.26	41.36	50.70	70.28
$F=p+f$	57.59	53.96	45.37	38.04	2.14	16.23	17.61	8.49
$L=L_s+q$	25.45	18.81	20.00	10.98	24.60	42.41	31.69	21.23
Q/F	0.29	0.50	0.76	1.34	34.23	2.55	2.88	8.28
Matrix [M_2]/ Clasts	0.82	1.16	1.20	1.12	1.99	2.36	3.59	3.03
C.M.I.	0.20	0.37	0.53	1.04	2.74	0.71	1.03	2.36

Minerals	MK-40	MK-43	MK-44	MK-45	MK-46	MK-47	MK-48	MK-49	MK-50
Quartz (Q_m)	18.50	14.10	15.40	10.70	9.10	2.20	5.10	16.10	20.30
Quartz (Q_p)	2.20	2.10	2.40	3.70	0.80	-	-	1.90	2.20
Plagioclase (p)	8.90	4.50	12.30	10.80	5.00	11.60	2.80	17.70	19.30
K-Feldspar (f)	11.40	6.00	15.10	10.50	8.80	14.30	1.60	11.70	9.90
Rock fragments (mainly quartzites) ($q+L_s$)	9.00	7.70	14.10	11.90	2.70	3.30	4.10	17.70	5.70
Dolomite/ Calcite	11.60	-	-	2.90	-	2.10	11.50	-	10.10
Miscellaneous (micaceous, heavy and opaque minerals)	2.70	5.10	2.00	3.40	2.30	9.30	7.60	2.30	2.50
Matrix (M_2)	35.80	60.50	38.70	46.10	71.30	57.20	67.30	32.50	30.00
$Q=Q_m+Q_p$	41.40	47.10	30.02	30.25	37.50	7.01	37.50	27.65	39.20
$F=p+f$	40.60	30.52	46.20	44.75	52.27	82.48	32.35	45.16	50.87
$L=L_s+q$	18.00	22.28	23.78	25.00	10.23	10.51	30.15	27.19	9.93
Q/F	1.02	1.54	0.65	0.68	0.72	0.08	1.16	0.61	0.77
Matrix (M_2)/ Clasts	0.56	1.53	0.63	0.86	2.48	1.34	2.06	0.48	0.43
C.M.I.	0.70	0.89	0.43	0.43	0.60	0.08	0.60	0.38	0.64

6.3.1 Quartz Pebble Conglomerate:

The matrix of the quartz pebble conglomerate is of sand to clay size. Allogenic minerals include quartz, chert, feldspar (very rarely), pyrite, chalcopyrite, uraninite, fuchsite, quartzitic fragments and various heavy minerals e.g. rutile, zircon, etc. Authogenic matrix is comparatively rare and mainly indludes interstitially developed micas (for example serecite). At some palces recrystallized quartz is also present in the form of overgrowth. Their individual descriptions are as follows :

6.3.1.1. Quartz:

Quartz is the most abundant constituent of the matrix of QPC (Fig.6.2). Both mono and polycrystalline varieties of quartz are present, but former dominating over the later. Polycrystalline aggregate of quartz shows dusty inclusions and marginal granulation. Undulose extinction is very common. They are characterized by irregular grain boundaries. Monocrystalline quartz might have been derived from the quartz veins. Cherts grains are relatively rare amongst the matrix components.

6.3.1.2. Quartzite:

Amongst the other lithic fragments, present in the matrix of QPC,quartzites are predominant (Fig. 6.3). In this photomicrograph, rounded fragment of quartzite is surrounded by flakes of micas. Other rarely observed lithic fragments consist of sericitized feldspar and small quartz grains . These fragments appear to be derived from granitic/gneissic rocks. A few of the coarser quartzites show evidence of the presence of some original

Fig. 6.2 : Photomicrograph showing the presence of mono-crystalline quartz in matrix of quartz pebble conglomerate (x 90).

Fig. 6.3 : Photomicrographs showing rounded fragment of quartzite surrounded by flakes of micas in matrix of QPC. (x 90).

Fig. 6.4 : Photomicrograph (reflected light) showing the rounded grain of pyrite in matrix of QPC. Traces of abrasion (pits) and porous nature of grains with plenty of dusty inclusion may be noticed. (x 120).

Fig. 6.5 : Photomicrograph (UPL) showing a well rounded detrital grain of fuchsite in the matrix of QPC. (x 120).

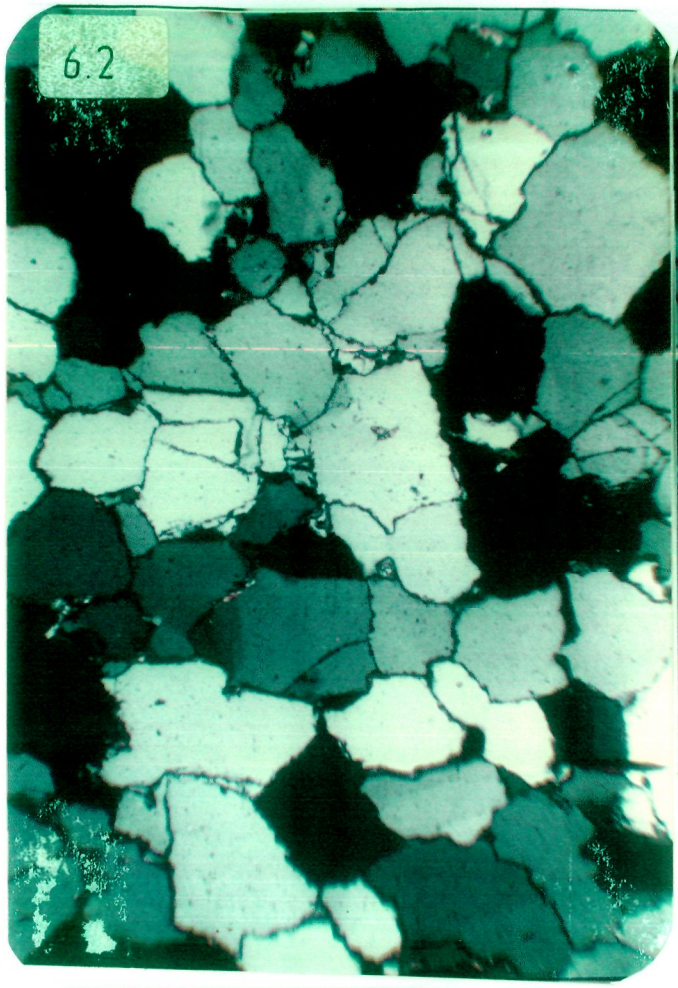
6.2

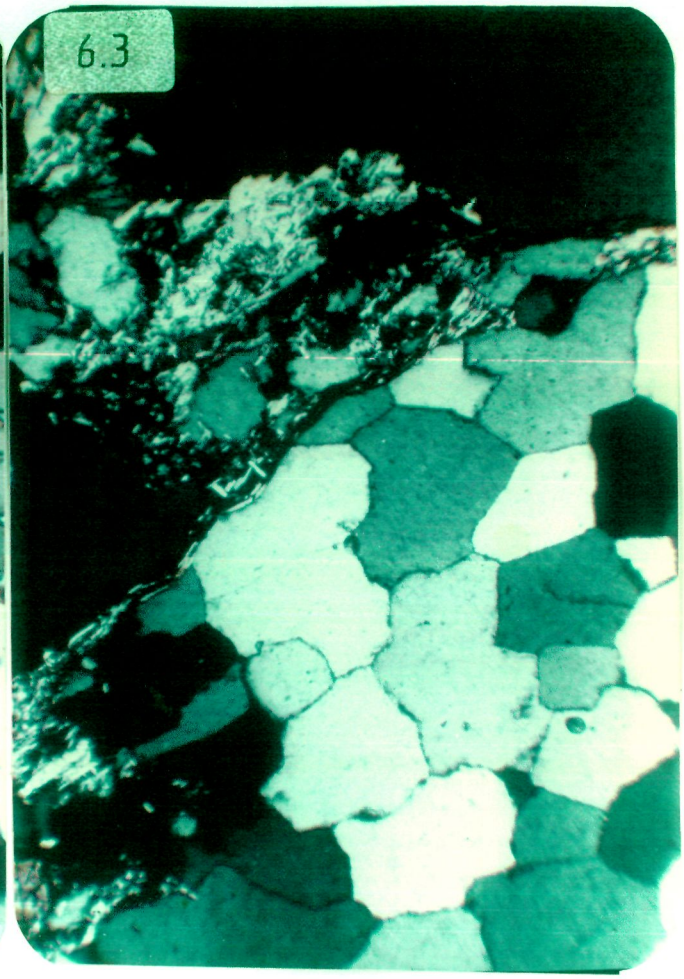
6.3

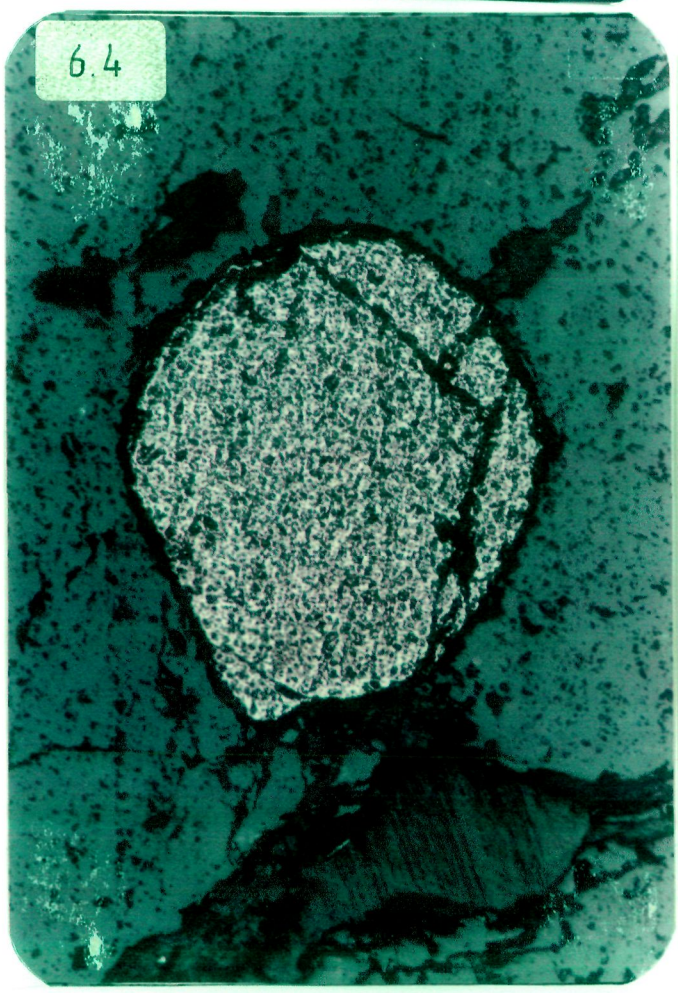
6.4


6.5

polycrystalline grains, although this is difficult to discern (Srinivasan and Ojakangas, 1986).

6.3.1.3. Pyrite:

Pyrite is the most characteristic mineral of the matrix of quartz pebble conglomerate of the Bababudan schist belt. Rounded to well rounded shape, traces of abrasion (pits), porous nature of grains with plenty of dusty inclusion (Fig. 6.4), are some ore-microscopic evidences which suggest the detrital nature of pyrite. Further more, their occurrences along the well defined bedding plane and $\delta^{34}S$ values extend the support to its detrital nature. The existence of detrital pyrite is a strong evidence in order to presume the anoxic and reducing environment during the deposition of quartz pebble conglomerate in the Bababudan schist belt.

6.3.1.4 Fuchsite:

Greenish tinge of the conglomerate is due to fuchsite flakes in the sand size matrix of quartz pebble conglomerate. Generally, fuchsite grows around an opaque mineral which is either a chromite or a metaultramafite (Fig. 6.5).

6.3.1.5 Uraninite:

Rare grains of uraninite occure in the conglomerate matrix . These are light grey with moderate reflectivity and dark-brown reflection pleochroism. The grains are highly porous and are studed with innumerable inclusions. Original abraded margins, indicating a detrital origin, are clearly preserved. The uraninite

from Kalasapura resembles very much the allogenic uraninite described by Aurora (1985), from Walkunji Conglomerate.

6.3.2 Quartzites:

Modal analysis of 15 samples of quartzites from different localities of the study areas, was carried out and is given in Table (6.2). Framework constituentes (> 0.03 mm) are important mineralogical assemblages of quartzites. The interstitial space between detrital framework minerals, are filled with matrix as a cementing material, however, its proportion is rather low.

As mentioned earlier, that all framework constitutes have been categarized into three main groups, i.e. quartz, feldspar and rock fragments. Most of the samples of quartzites are feldspathic quartz arenite, but 2 and 3 samples are quartz arenite and lithic quartz arenite respectively (Tab. 6.2 and Fig. 6.6).

Mono and polycrystalline quartz, plagioclase, microcline and orthoclase (very rare), rock fragments , are principle framwork constituents. Some heavy minerals like rutile, zircon, opaques and micas, are also present as miscellaneus components. Rounded to sub rounded grains, with well sorted nature and less amount of matrix, indicate that these quartzites are texturally sub mature to mature. The compositional maturity ($Q_m + Q_p$ / F + L) ranges from 2.79 to 34.71 with an average of 7.99, which indicates that these quartzites are texturally as well as compositionally mature and have been deposited under the influence of strong chemical weathering and prolonged hyderodynamic processes with thorough reworking.

Fig. 6.6 : Triangular diagrams exhibiting the ratio of quartz, Feldspar and rock fragments. Quartz, K. feldspar and Plagioclase exhibiting arenaceous character of quartzites.

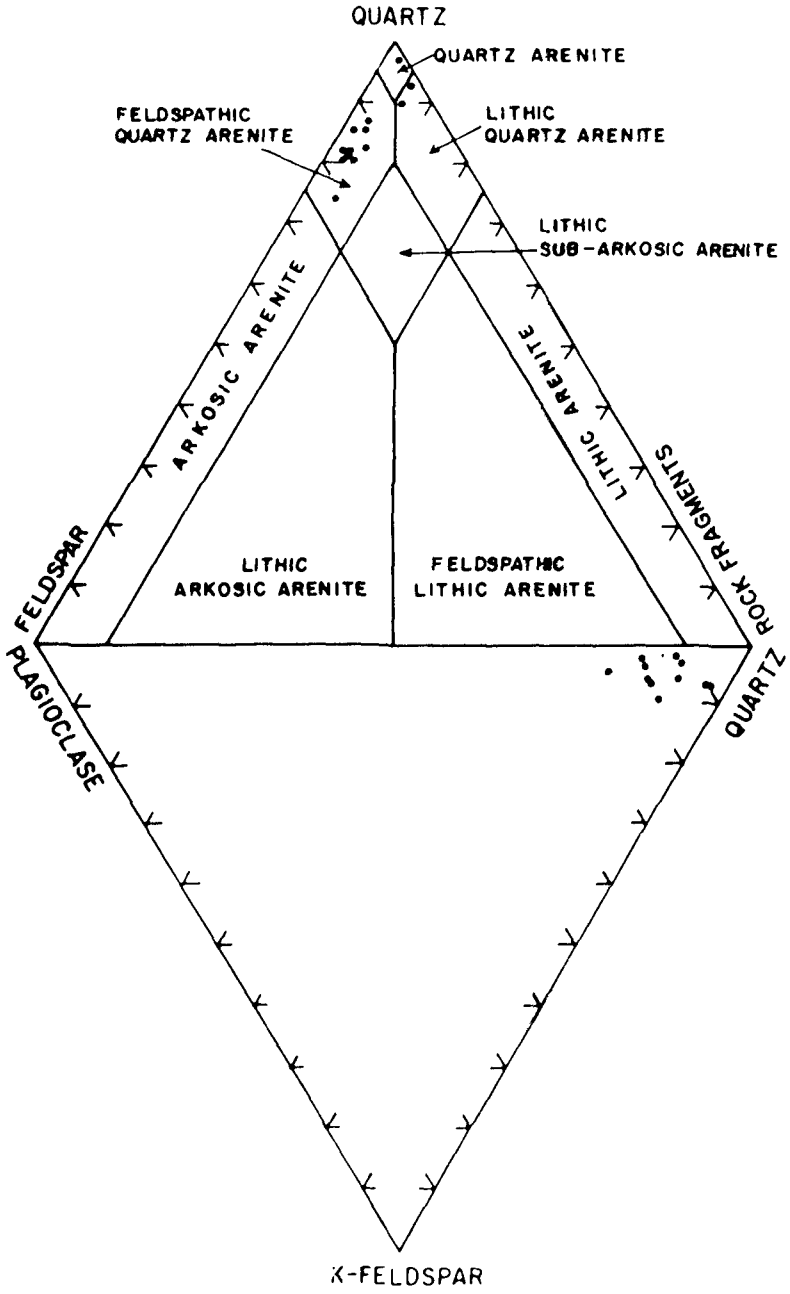
QUARTZ
QUARTZ ARENITE
FELDSPATHIC
QUARTZ ARENITE
LITHIC
QUARTZ ARENITE
LITHIC
SUB-ARKOSIC ARENITE
ARKOSIC ARENITE
LITHIC ARENITE
LITHIC
ARKOSIC ARENITE
FELDSPATHIC
LITHIC ARENITE
FELDSPAR
QUARTZ
ROCK FRAGMENTS
PLAGIOCLASE
K-FELDSPAR

6.3.2.1 Quartz:

Minerals of the quartz group are by far the most common detritals and consist mono and polycrystalline fragments. Monocrystalline, Q_m (Fig. 6.7) varies from 59 to 82 % of total volume of rock. In general, these are medium grained in size. Equidimentional grains show smooth to strongly undulose extinction; elongated grains commonly show undulose extinction. Generally, normal contact is seen between two individual grains, however , suture contacts are also present. Polycrystalline quartz as here recognised are similar to composite quartz of Pettijohn (1984), it occurs in small amount (1.20 to 10.20 %) than in monocrystalline quartz.

6.3.2.2 Feldspar:

Detrital feldspar is next to quartz in order of abundance, constituting about 4.60 to 21.10 % of total framework constituents. Among the species of feldspar - plagioclase, microcline and orthoclase are present.

Plagioclase content varies from 2.00 to 14.20 % of total volume of the rock. It is generally albite to oligeoclase in composition. Equant grains are common (Fig. 6.8) and sub-rounded grains boundaries are very minuetly corroded and show partial alteration to serecite.

Microcline and orthoclase together constitute about 1.80 to 6.80 % of total volume. Well rounded grains of microcline (Fig. 6.9) are present. The presence of microcline indicate that K-rich rocks were also present in source region. Most likely Chickmagalur granodiorite (~3.1 Ga) might have supplied K-feldspar to these

Fig. 6.7 : Photomicrograph showing the presence of mono-crystalline quartz in quartzite. Quartz grains are rounded to subrounded and display normal contact with each other. Moderate order of sorting can also be seen in this section. (x 90).

Fig. 6.8 : An equidimentional and subrounded grain of plagioclase in quartzites, showing effect of alteration especially along the plane of twinning. (x 90).

Fig. 6.9 : Photomicrograph showing well rounded grain of microcline in quartzite. (x 90).

Fig. 6.10 : A small fragment of gneiss in quartzite is traped between grains of quartz and plagioclase, (x 90).

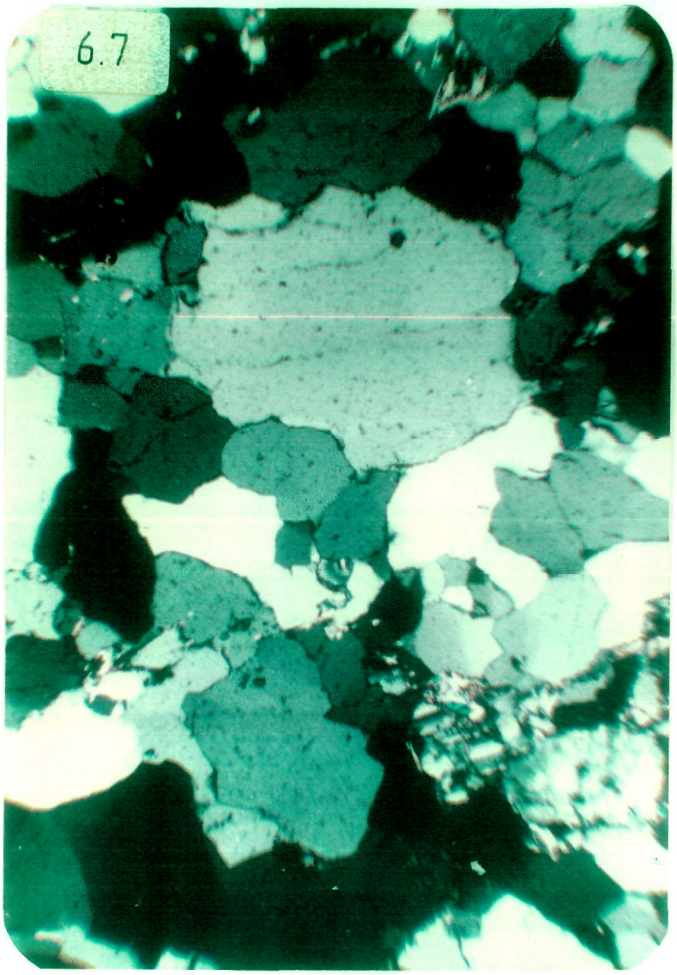
6.7

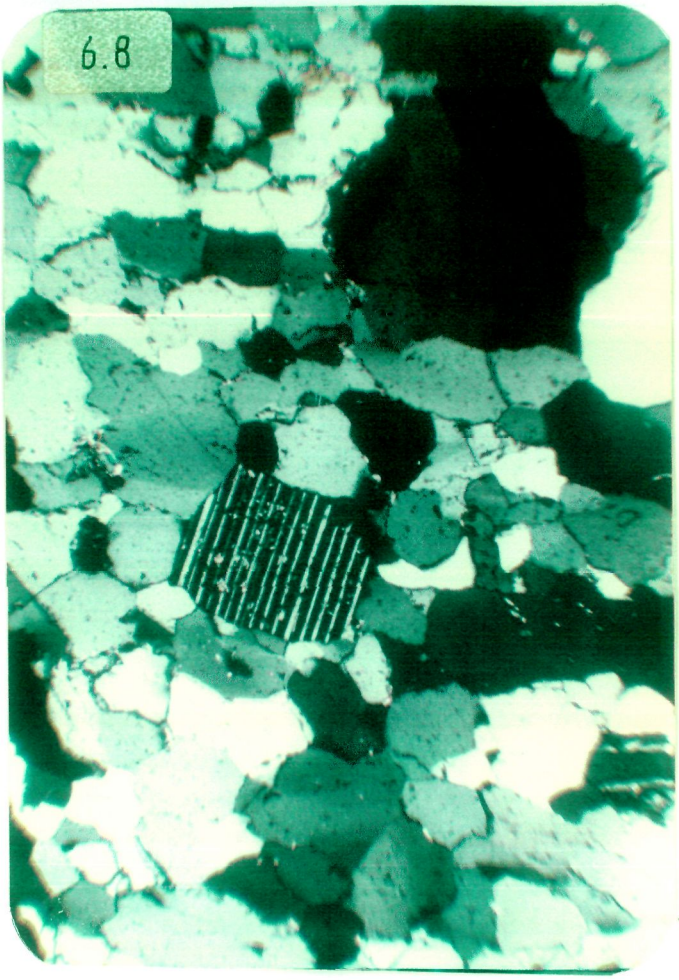
6.8

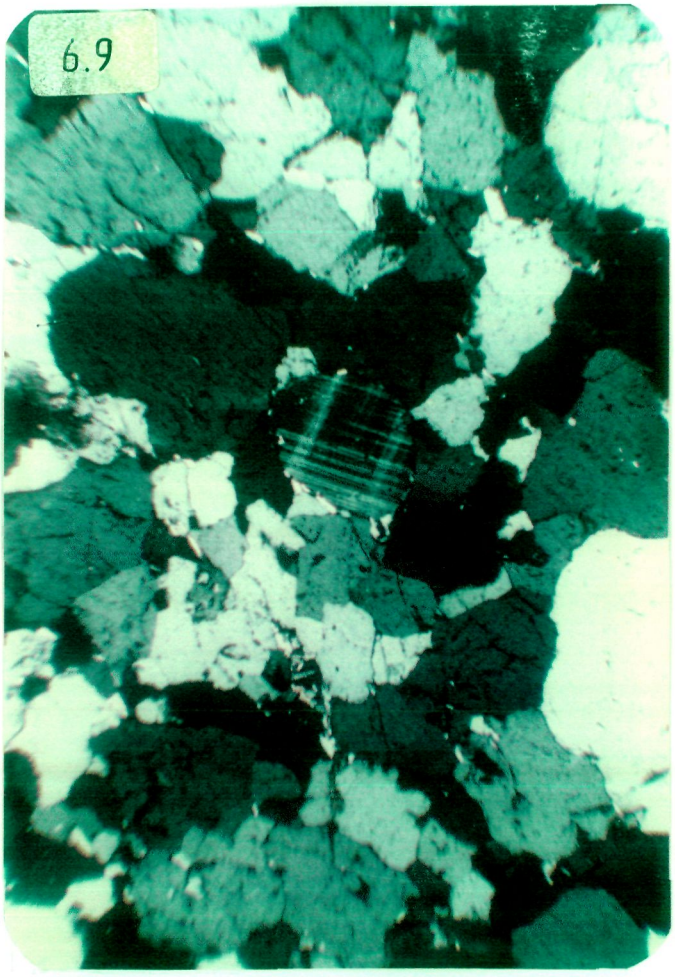
6.9

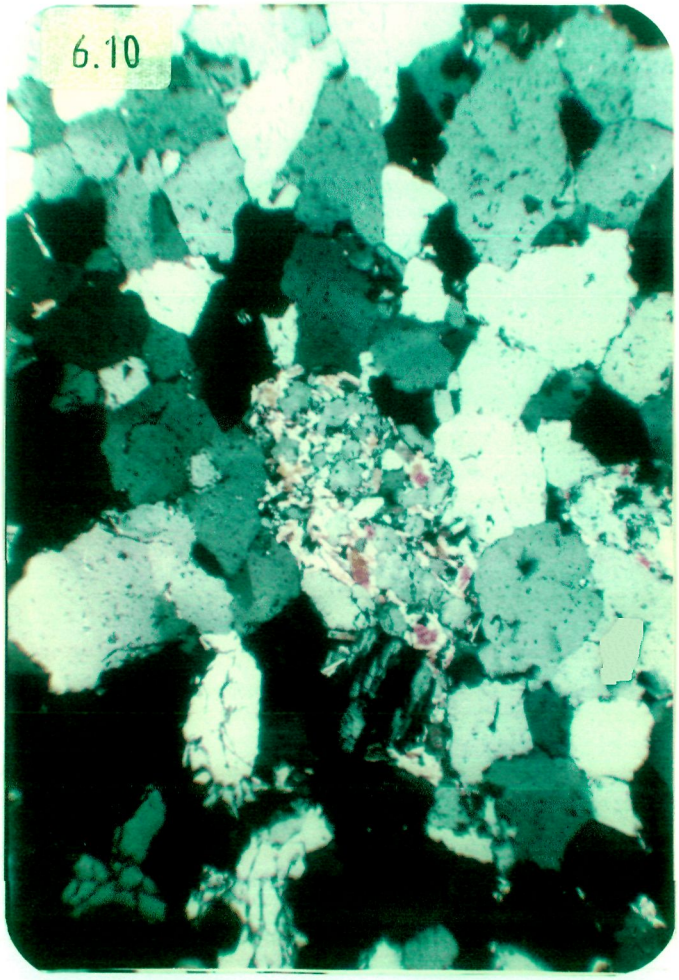
6.10

rocks. It is inconsistant with the model proposed by Taylor and McLennan (1985), that K-rich rocks are characteristic of the Proterozoic time and these rocks were almost absent in the Archaean.

6.3.2.3 Rock fragments:

The proportion of rock fragments varies from 1.20 to 4.40 % of total volume of the rock. As mentioned earlier that these quartzites are supposed to be deposited under strong hyderodynamic activities, thus only those rock fragments which were resistive enough,could servive, namely quartzites, gneisses etc. Fig. (6.10) shows a rounded fragment of gneiss.

6.3.2.4 Matrix:

Brownish to earthy coloured cementing material, which is mainly micaceous, is considered here as matrix. Its amount varies from 3.60 to 14.20 % (Tab. 6.2). Less amount of matrix give rise to contact framework, which is characteristic of arenites. Most of the matrix is primary in nature.

6.3.3 Matrix of the Kaldurga Conglomerate:

Modal analysis of the 25 representative samples of matrix (M_1) of the Kaldurga Conglomerate (KCM) from well preserved and unweathered exposures from different localities, was carried out and is given in Table (6.3). The matrix is made up of framework minerals and fine groundmass, which is designated here as matrix (M_2).

For the purpose of modal analysis of representative samples

of the matrix (M_1) of the Kaldurga conglomerate, the main emphasis was placed on the characters and proportions of detrital framework constituents of post Archaean sequences. Dickinson (1970) and Dickinson and Suczek (1979) suggested that the ratio of matrix (groundmass) to detrital fragments increases during diagenesis/metamorphism. This possibility is shown by the presence of two generations of quartz and feldspar in the matrix (M_2). However, sharp contacts of angular fragments of quartz and feldspar are present in some samples. A high proportion of schistose and amphibolitic framgnets appears to have gone into matrix (M_2) during transport, sedimentation, metamorphism and recrytallization, and hence the quantity of (M_2) appears to have increased in case of KCM (Arora et al., 1991). However, in graywackes from other schist belts, formation of the diagenetic matrix has been negligible (Naqvi et al., 1988).

In the case of the KCM, partial recrystallization of feldspar, schistose rock fragments and quartz appears to have taken place during various stages of developments including metamorphism. Differentiation of schistose rock fragments is not possible because of recyrstallization and gradation between the two. For this reason geochemical analysis is much more useful and reliable for provenance inferences. But geochemical parameters reflect the composition of the whole rock and cannot distinguished between SiO_2 present in Q, q, f or p. Therefore the use of both approaches is recommended to attain the objectives of this excercize (Bhatia and Crook, 1986; Naqvi et al., 1988). Important petrographic characteristics of the KCM are as follows:

(i) Most of the samples of the KCM have the mineralogical characteristics of the lithic arkosic wacke. Two samples were found to be lithic graywacke and two quartz-rich lithicwakce (Fig.6.11). Quartz, mono and polycrystalline types, feldspar including plagioclase and K-feldspar, and rock fragments; mainly quartzites, are the three dominant framework constituents. Such polygenetic quartz is common in Archaean turbidites (Henderson, 1972). In four samples, dolomite also constitutes a significant proportion (~10-13%) (Fig.6.12). Zircon, magnetite, rutile, kyanite and others make up about 3% of total volume and are grouped as miscellaneous. Sample No. MK-31 and 47, however, contain 9-14% of magnetite and other accessory minerals. Texturally and mineralogically the KCM is a immature rock. The compositional maturity index (Qm+Qp/F+L) ranges from 0.08 to 2.74. Quartz boundaries are, in general, corroded and fine grained micaceous flakes are present along the quartz boundaries (Fig.6.13). Both primary as well as recrystallized quartz i.e. first and second generation of quartz, are present. Among the first generation, two different varieties are found, as polycrystalline quartz, derived from the disintegration of plutonic rocks, the precursors of magmatic peninsular gneisses, b) monocrystalline quartz, indicating the presence of vein quartz in its source region. Second generation or recrystallized quartz is distinguishable on the basis of inclusions of different mineral species viz. zircon, kyanite, rutile and some micaceous minerals etc. Some of these

Fig. 6.11 : Triangular diagram illustrating quartz - K.Feldspar - Plagioclase and Quartz - Rock Fragments - Feldspar distribution in KCM characterizing it as Lithic - Arkosic wacke with a range upto Feldspathic Lithic and Lithic wacke.

Feldspar
Rock fragments
Quartz
Plagioclase
K-feldspar
Arkosic wacke
Lithic Arkosic wacke
Feldspathic Lithic wacke
Lithic wacke
Lithic sub
arkosic
wacke

Fig. 6.12 : Photomicrograph showing the presence of calcite/dolomite in matrix of the Kaldurga Conglomerate (KCM). Interstitial development of calcite/dolomite indicates that they are not of detrital in nature. (x 90).

Fig. 6.13 : Photomicrograph illustrates the corroded boundaries of quartz grains in the KCM - Mica flakes, present along the boundaries indicate their recrystallized nature. (x 90).

Fig. 6.14 : Photomicragraph showing recrystallized plagioclase, containing inclusion of zircon. This plagioclase itself is traped in recrystallized quartz. (x 120).

Fig. 6.15 : Photomicragraph showing microcline and plagioclase in the KCM. (x 90).

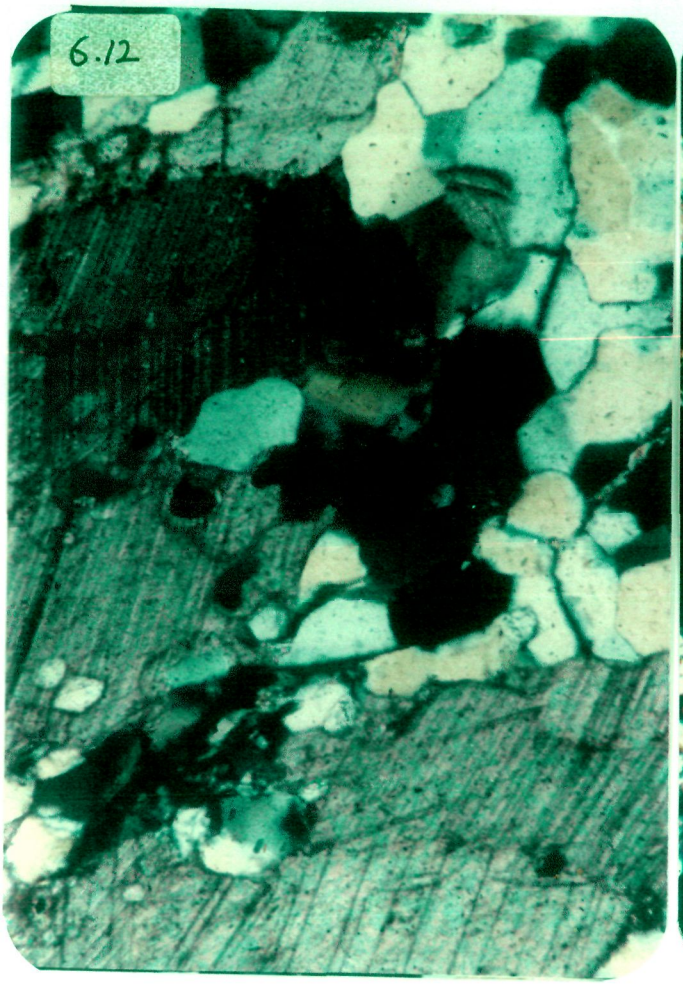
6.12


6.13

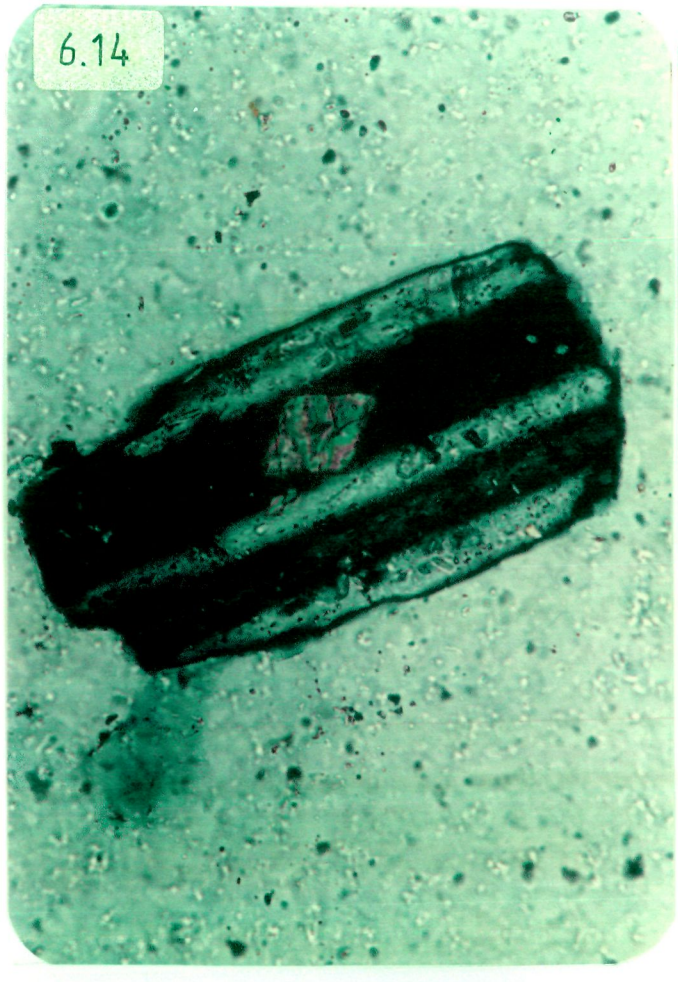
6.14

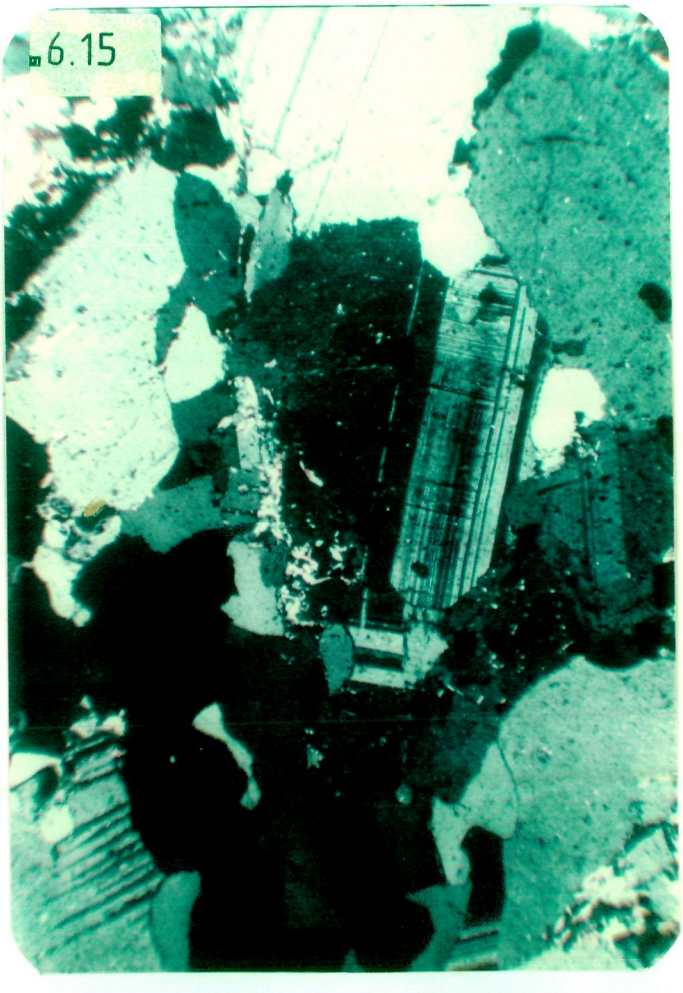
6.15

minerals are derived from older high grade metamorphic sequences, and get trapped within the grains of quartz and/or feldspar at the time of recrystallization. Fig. (6.14) shows an inclusion of zircon in plagioclase which itself is trapped within a quartz grain.

ii) Feldspar (F) content of the KCM includes plagioclase, orthoclase and microcline (Fig.6.15). Framework feldspars are angular and unsorted grains of medium size but coarser grains of plagioclase upto 5 mm in size are also present. Two generations of plagioclase and K-feldspar are found. The first generation is angular and free of inclusions, whereas the second generation formed by recrystallization of matrix, contains inclusions of kyanite and zircon (Fig.6.16). Kyanite is a characteristic mineral of the older schist belts metasedimentary sequences (Ramakrishnan et al., 1976). Presence of kyanite as a heavy mineral in the matrix is significant. The occurrence of kyanite as a heavy mineral inclusion in a recrystallized feldspar confirms the interpretation of Ramakrishnan et al., (1976) and Chadwick et al. (1985a) that a high grade metamorphic group of rocks which has been variously named as Sargur (Viswanath and Ramakrishnan, 1976), Holenarasipur (Naqvi, 1981) etc. exists below the Kalasapura unconformity. This group of high grade metamorphic rocks provided debris of the sediments for the Dharwar Supergroup.

Fig. 6.16 : Photomicrograph illustrates recrystallized K-feldspar (orthoclase) in the KCM containing inclusions of kyanite and quartz. (x 90).

Fig. 6.17 : Subrounded fragment of quartzite in the KCM. (X 90).

Fig. 6.18 : Photomicrograph showing the disintegration of originally schists, amphibolites and other volcanic rock fragments due to recrystallization during subsequent episoldes of metamorphism. They are considered as a recrystllized matrix (M_2) of matrix (M_1) of the Kaldurga Conglomerate. (x 90).

Fig. 6.19 : Photomicrograph shows the matrix (M_1) of the KCM, which is the dominant constituent of this rock type. Quartz, feldspar, rock fragments, micaceous minerals (biotite, muscosite, sericite) and amphiboles are present as a primary and secondary matrix. (x 90).

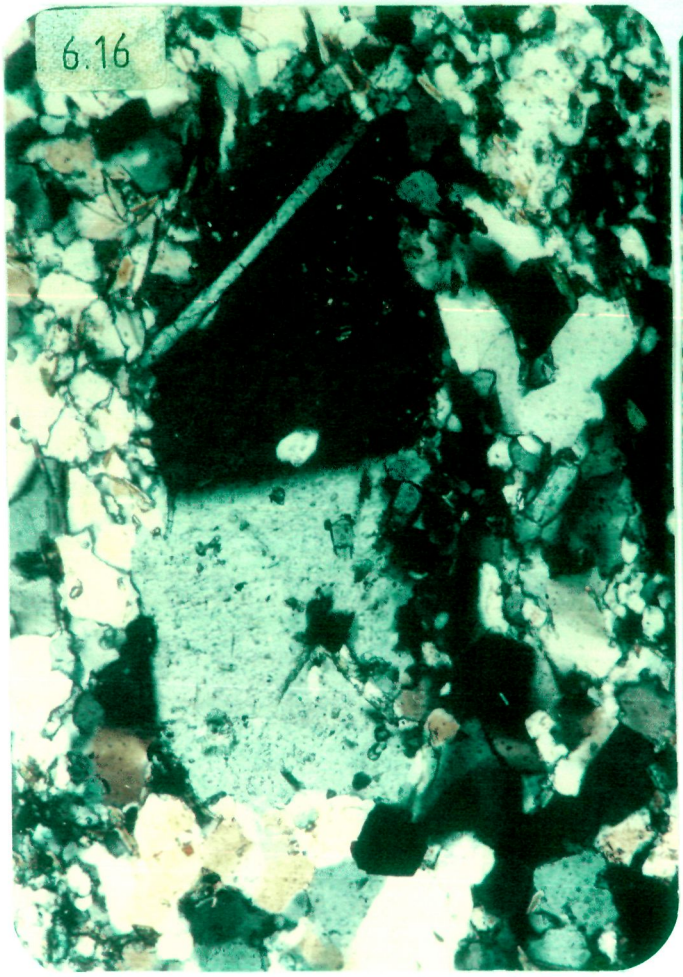
6.16

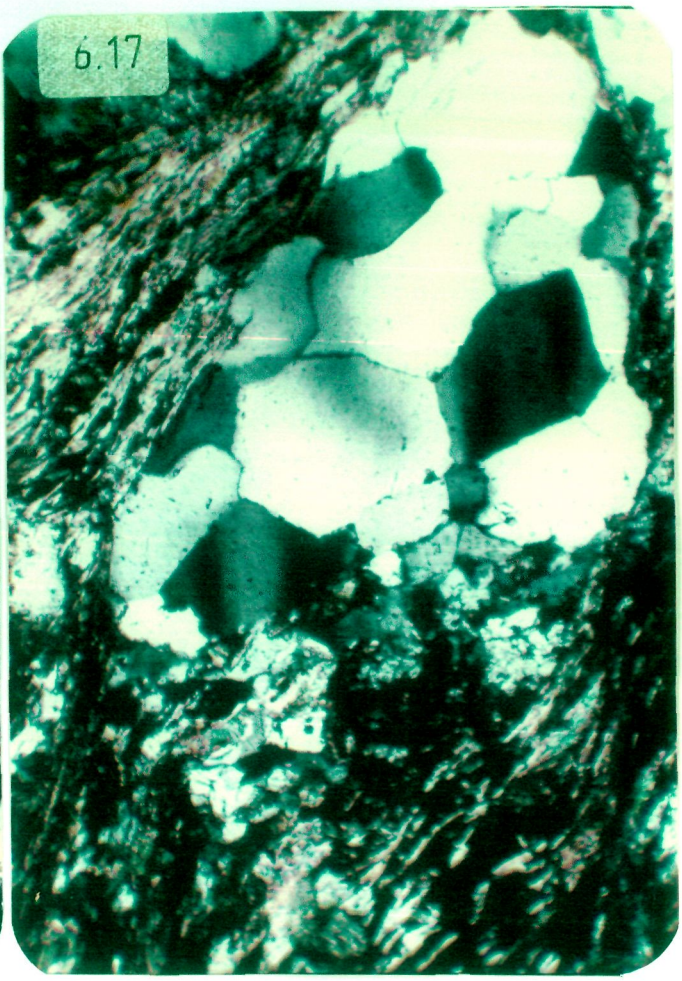
6.17

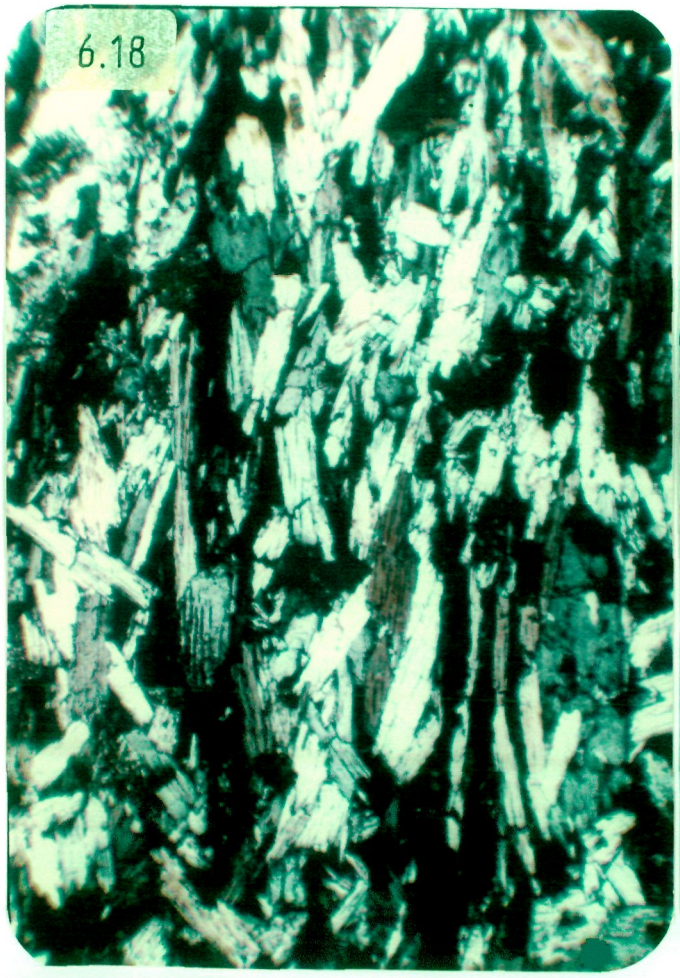
6.18

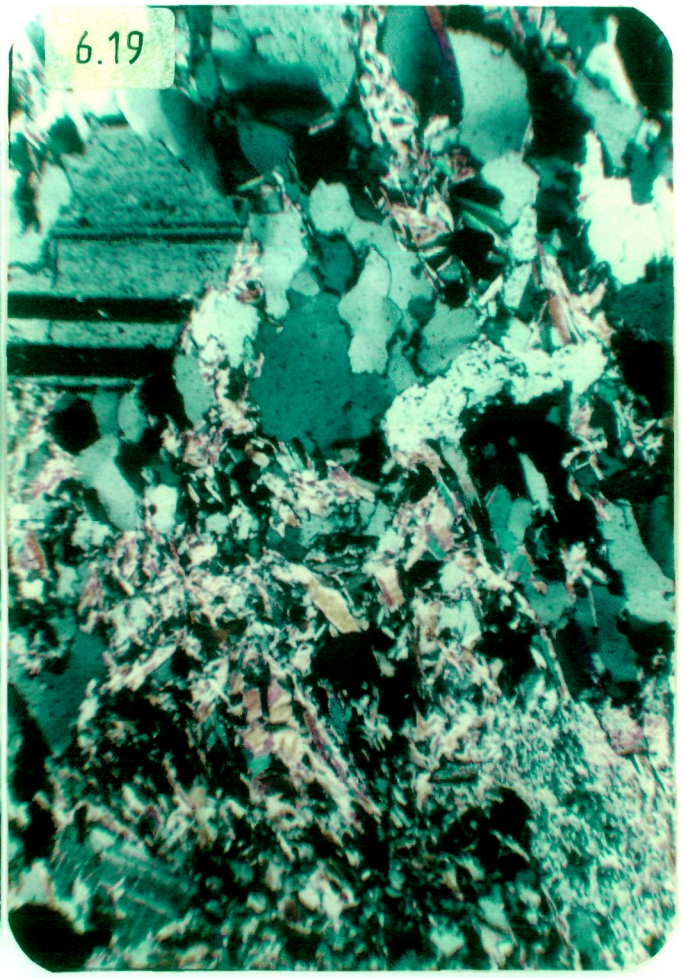
6.19

(iii) Lithic fragments in the KCM include quartzite, schistose amphibolites and volcanics. Quartzites fragments are easily identified; both cherts and quartzite fragments are grouped together (Fig.6.17). Schistose amphibolites and volcanic fragments have undergone partial to complete recrystallization and have contributed to the formation of matrix (M2) (Fig.6.18). Their identification as separate fragments from that of matrix (M2), is difficult. However, some volcanic rock fragments, amphibolites and other schistose rocks could survive in the form of pebbles of various sizes. The pebble composition of the Kaldurga Conglomerate shows the predominance of TTG, in the source area, whereas matrix composition exhibits predominance of mafic-ultramafic material.

(iv) Matrix (M2) is the dominant constituent of the KCM. It is composed of fine grained (<0.03 mm, Spencer, 1963) quartz, feldspar, rock fragments, micaceous minerals (biotite, muscovite, sericite) and amphiboles (Fig.6.19). Amphibole is the most abundant mineral present in the matrix (M2) (Fig.6.20). Chlorite is also present as a retrograde mineral. All these extremely fine grained minerals bind the framework minerals. The matrix/clasts ratio in (M2) is very high (Tab.6.3). Mostly floating type of framework is observed but contact framework is also present. Both primary and secondary matrix are present in (M2), primary matrix is represented by fine grained angular quartz and other granular detrital material like feldspar and rock fragments (Fig.6.21). Part of the primary matrix which was in the form

Fig. 6.20 : Photomicrograph showing the amphibolites (actinolite), which is most abundant recrystallized mineral in secondary matrix (M_2) of the KCM. (x 120).

Fig. 6.21 : Photomicrgraph showing fine grained detrital quartz, feldspar and rock fragments, which together form the primary matrix (M_2) of the KCM. (x 60).

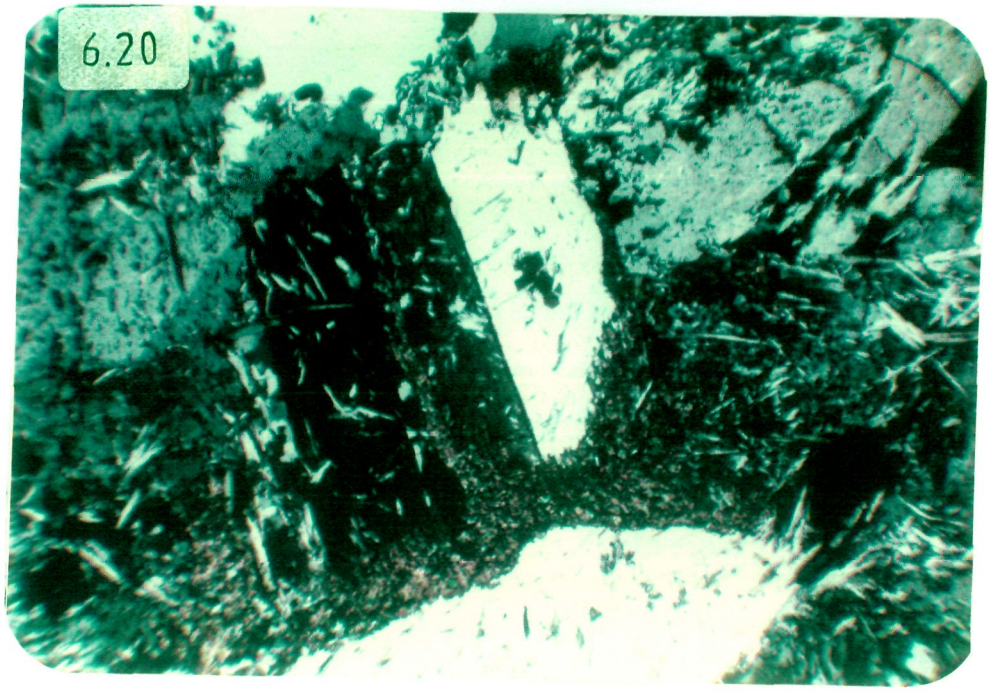
6.20

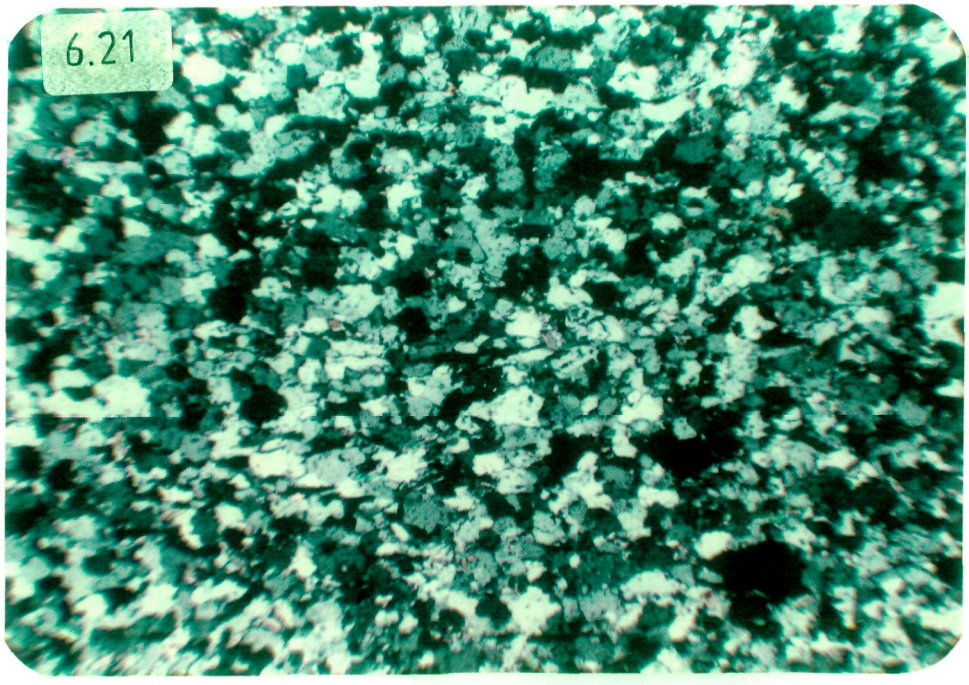
6.21

of clays, extremely fine grained feldspar, quartz and micas has been recrystallized to biotite, amphibole, quartz and feldspar. Most of the weathered mafic and ultramafic source material has contributed to the composition of the secondary matrix. Feldspars and unstable rock fragments also appear to have contributed to the secondary matrix.

CHAPTER VII

TECHNIQUES DEPLOYED FOR GEOCHEMICAL ANALYSIS

7.1 INTRODUCTION:

Major trace and REE of the sand size matrix of quartz pebble conglomerate, quartzite and the matarix of Kaldurga polymictic conglomerate, were determined by AAS, UV-visible spectrophotometer, XRF and ICP-MS at Geochemistry Division of National Geophysical Research Institute, Hyderabad, India. Mineral chemistry of a few feldspar minerals was also determined by EPMA at the same laboratory, whereas sulphur isotopes of pyrites separated from QPC, got analysed at Atomic Mineral Division, Atomic Energy Department, Hyderabad. The details of the analytical procedure, sampling techniques, accuracy and repeatability of the data, are discussed below.

7.2 SAMPLING:

In all 160 samples of quartz pebble conglomerate, quartzites and the matrix of the Kaldurga Conglomerate were collected from various localities. Extreme caution were taken to collect the fresh samples which have not been affected by alteration or metasomatism. A great difficulty was faced in order to collect the fresh samples from the horizon of quartz pebble conglomerate. The abundance of sulphide minerals, especially pyrite, in the matrix of quartz pebble conglomerate was the main cause for its susceptibility to chemical weathering. Hence, the subsurface fresh samples, were obtained after trenching. In the Kaldurga

Conglomerate, matrix rich samples were collected. For chemical analysis, 30 samples of quartz pebble conglomerate, 10 samples of quartzite and 49 samples of the matrix of the Kaldurga Conglomerate were selected on the basis of detailed petrographic study of thin sections. Quartzites samples were directly crushed to granules and then powdered to -200 mesh in a tungsten-carbide Herzog ring grinder. However, in case of quartz pebble conglomerate and the Kaldurga Conglomerate, fine clasts were removed by hand chipping and then the matrix was pulverized to -200 mesh in the same grinding machine. Pyrite was also separated from the matrix of quartz pebble conglomerate. For separation of pyrite the crushed matrix was sieved to -60 to -120 BSS mesh size and then washed and dried. Finally,monomineralic concentration i.e. pyrite was achieved by hand picking under a Leitz binocular microscope.

A few selected major elements of the matrix of quartz pebble conglomerate and quartzites were determined by UV-visible spectrophotometer and Atomic Absorption Spectrometer (AAS), whereas all the 10 major elements of the matrix of the Kaldurga Conglomerate were analysed by XRF. Trace and REEs including Th and U of all the samples, including pyrite samples (10) were analysed by ICP-MS. Sulphur isotopic ($\delta^{34}S$) data were generated by mass spectrometer.

7.3 SAMPLE PREPARATION FOR THE WET CHEMICAL ANALYSIS ON UVS, AAS AND ICP-MS:

7.3.1. Solution A:

The finely (-200) mesh powdered sample of weight 0.1 gm was fused with 15-20 pellets of sodium hydroxide in a nickel crucible. This was dissolved in 20 ml of 1:1 HCl and heated for about half an hour till a clear solution was obtained and then was made to one liter after complete cooling (Shapiro, 1975). It was used for the determination of Al_2O_3 in QPC and quartzites.

7.3.2 Solution B:

The 0.5 gm of the powdered sample was taken into teflon beaker of 100 ml capacity with 20-30 ml of Hydrofluoric acid (98%) and 5-6 drops of conc. H_2SO_4. The beaker was heated on steam bath till the sample was completely dried. Afterwards 10 ml of 1:1 HNO_3 acid was added and the contents were heated again till a clear solution was obtained. This was then made to 250 ml. This solution was used for the determination of K_2O, $Fe_2O_3^{(T)}$, MgO concentration in QPC and quartzite.

7.3.3 Solution for ICP-MS:

0.1 gm of sample was taken in a teflon beaker with 7 ml of HF (48%, EI grade) and 3 ml. of conc. HNO_3. This mixture was digested by keeping the beaker over hot plate. After complete, digestion, 10 ml of HNO_3 of 1:1 concentration was added and further kept on hot plate till a clear solution is obtained. When solution was cooled down volume was made to 100 ml with double distilled water after adding 100 ml of 1 ppm Indium solution as an internal standard and finally stored in a 100 ml. corning (Potts, 1987).

However, it was difficult to get the matrix of quartz pebble conglomerate and quartzite samples dissolved into the solution by the aforesaid method. The mere presence of rutile and zircon was making the sample resistent to go into solution completely. For such samples teflon bomb technique was used. In the method 0.1 gm of rock powder was transferred to a teflon bomb with 4 ml of HNO_3 (conc.), 1.0 ml of $HClO_4$ (60%) and 6 ml. of HF (48% EI grade). After sealing, the teflon bomb was kept in an oven for about 3 hours at 140°C. After the removal from oven, bomb was let to cool down at room temp. then unscrewed the bomb, and again kept on heating on hot plate at 140°C to get the complete dryness. Afterwards the same procedures were followed to make the volume as described in previous paragraph. This solution was used for all 18 trace elements (including Th and U) and REE concentration of the matrix of QPC, quartzite and the KCM.

7.4 UV-SPECTROPHOTOMETER (UVS):

A Shimadzu double beam spectrophotometer model UV-190 was used for Al_2O_3 and $Fe_2O_3^{(t)}$ determinations for the matrix of quartz pebble conglomerate and quartzite samples. The instrument comprises of tungsten lamp for radiation in visible range and a deuterium lamp for ultraviolet radiations. Both the lamps cover a complete range of wavelengths suitable for elements analysed. Absorbance/concentrations of standards and samples were measured under identical conditions (Potts, 1987).

7.5 ATOMIC ABSORPTION SPECTROPHOTOMETER (AAS):

A Varian-Techtron model AA6(D) atomic absorption

spectrophotometer was used for determining other major elements. It has a modulated hollow cathode lamp for obtaining radiation of suitable frequency which is characteristic of the element to be estimated, and a burner assembly where the sample solution is aspirated through a nebuliser resulting in atomization of the sample. The emergent flame in the burner assembly enters a monochromator where the isolation of the required spectral line is achieved. A photomultiplier is used to amplify and convert the signal to a digital readout of the absorbance. Absorbance is measured in a series of natural rock and synthetic standard solutions along with the unknown samples. The concentration of various major elements, in the form of their oxides in the unknown solutions is then measured in comparison with the standards. For detail procedure please refer to Naqvi et al. (1980) and Balaram et al. (1990).The precision and accuracy of different methods is better than $\pm$5% for most of the major elements.

7.6 INDUCTIVELY COUPLED PLASMA-MASS SPECTROMETER (ICP-MS):

The concentration of 18 trace elements and all 14 rare earth elements in the matrix of QPC, quartzite, pyrite (separated from QPC) and the KCM, were determined by an inductively coupled plasma mass spectrometer (VG Plasma Quad ICP-MS). The instrument mainly comprises the following three components:

i. A standard inductively coupled plasma torch (Fassel-type)

consists of nebuliser, spray chamber, work coil and associated power supply from 2.5 KW, 271.2 MHz, RF generator which is the same as that commonly used in optical spectrometers. This torch is mounted horizontally and linked with a water cooled glass spray chamber and a Meinhard concentric nebuliser.

ii. A quardrupole mass filter and associated data collection electronics which permits rapid scanning of selected mass range between 0-300 amu.

iii. An interface unit consisting of two water cooled nickel cones each containing a small orifice at the centre, which permits sampling of the plasma gases and transfer of the ions beam into the mass spectrometer. The ion detection and data acquisition system consists of a channeltron-type electron multiplier and multichannel analyser. An IEEE 488 data base allows the transfer of data to a central control computer. An outline IBM PC/XT microcomputer facilitates data acquisition, processing and storage.

After minimising the signal on ^{115}In in the single ion mode, the system is operated on a mass scanning mode in the mass range m/z 45-228 covering 18 trace elements (including Th and U) and all the 14 REE as well as the internal standard (Indium). Detection limit is calculated using the count rate obtained on the 0.1% solution of the standards.

Elemental concentration for the standard reference rocks such as SY-2, BCR-1 and MRG-1 using two standard curves, are in good

agreement. Precision is better than 5% RSD (relative standard deviation) for all the elements (Balaram et al.1990). Other details are as given in Balaram et al., (1990).

The operating parameters of the instrument are as detailed below :

1. Plasma :

Power = 1.35 KW

Nebulizer gas = 0.75 lit/min

Aux. flow rate = 0.5 lit/min

Coolant flow rate = 13 lit/min

Sample intake rate = 1 ml/min

2. MS conditions :

Vacuum stage 1 - <2.5 mbar

Vacuum stage 2 - $<10^{-4}$ mbar

Vacuum stage 3 - $<2.10^{-6}$ mbar

3. Scan conditions :

Mass range = 113-179 amu

Number of scan = 120

Dwell time/channel = 500 s

Number of channels used = 2048

7.7 X-RAY FLUORESCENCE: SAMPLE PREPARATION:

The -200 mesh sample powder of the matrix of Kaldurga Conglomerate was used to prepare pellets. For determining major elements, the rock sample powder was fused at ~1200^{o}C with lithium

tetraborate-metaborate flux with lithium carbonate added to bring down the melting point of the flux. The sample was fused in 5% gold-platinum crucibles using Herzog automatic fusing machine. Sample to flux ratio was kept at 1:10 with a total weight of 10 gms having 1.0 gm of sample weight, 7.5 gm of flux and 1.5 gm weight of Li_2CO_3. It has given pellets of 40 mm diameter.

7.7.1. X-Ray Fluorescence Spectrophotometer (XRF):

The Phillips PW-1400 microprocessor controlled, sequential XRF with 100 KVA. X-ray generator and 72 position automatic sample changer to load and unload, coupled to a Phillips P-851 online dedicated computer was used for calibration of regression analysis. Japanese, Canadian and East-German standards were used for calibration of curves. The procedure followed has an online computer programming for dead time correction, background line overlapping and matrix effect and gives output directly as concentrations in percent or ppm from calibration curves. A spinner was used to spin the sample inside the spectrometer while measuring the counts to remove sample heterogeneity, if any. A 33 mm primary beam aperture mark was used to restrict the X-ray beam only to the sample surface. Flow and scintillating detectors were used for couting the X-rays, pulse height discriminator and the fine collimator account for greater sensitivity of the data.

CT-1A, JGB-1, JB-2, BHVO-1, GSR-Z, DR-N international standards were used to calibrate the major elements data for the matrix of the Kaldurga Conglomerate. The precision and accuracy, reproducibility and the standard deviation from the above

mentioned is less than ± 5% (Govil, 1985).

7.8 ELECTRON PROBE MICRO ANALYSER (EPMA):

7.8.1. Slide Preparation:

Doubly polished sample thin sections of 0.03 mm thickness were got prepared on 46 mm long glass slides without the coverslip. A coating of carbon of about 150A^{o} units thickness was given by the carbon evaporation technique in a Hindivac Shadow Casting Unit at 10^{-6} Torr for obtaining uniform electrical conductivity.

7.8.2. Instrumentation:

To determine the species of plagioclase, present in the matrix of the Kaldurga Conglomerate, mineral composition was analysed by using a wavelength Dispersive Cameca make Camebax-Micro EPMA. The electronic microprobe consists of three fully focussed spectrometer (2 vertical and 1 inclined). The operating conditions were 15 KV accelerating voltage, 4.2 nA sample current, 20 seconds counting time with a beam diameter of 1-3 mm. ZAF corrections, suing the method of Bence and Albee (1968) were applied with the help of the PDP 11/03 computer. Analytical concentrations in the form of oxides wt. % were derived by applying intensity data of samples to a calibration curve established from intensity data of the standards. Precision was of the order of ±0.5-2.0% of the amount for major constituents. The following natural mineral standards were used, at wavelengths suitable for the corresponding element analysis:

Element	Standards	Wavelength	Crystal
Na_2O	Albite	46363	TAP
K_2O	Orthoclase	42765	PET

CHAPTER - VIII

GEOCHEMISTRY OF QUARTZ PEBBLE CONGLOMERATE, ASSOCIATED QUARTZITE AND PYRITE FROM QPC

8.1 INTRODUCTION:

The chemical composition of clastic sedimentary rocks is governed by many complex factors, including the average composition of source rocks, weathering processes, hydrodynamic processes during weathering-transportation and the environment of deposition (McLennan et al., 1980). The exact meaning of chemical composition of the sediments becomes further complicated in an area of metamorphic terrain. As a whole, if isochemical metamorphism has taken place (which is generally assumed), major elements are a good tool to decipher the nature of the source. They reveal the quality and quantity of the physico-chemical disintegration of the source rocks before deposition. Furthermore, the chemical composition of sedimentary rocks preserves an important record for the understanding of the evolution of continental crust through geological time (McLennan and Taylor, 1991). REE, Th, Sc and Co distributions in fine grained terrigenous sediments have been proposed as indicators of the composition of upper continental crust. These elements not only have low seawater/crust distribution coefficients and seawater residence time, but their ratios also are relatively insensitive to weathering, alteration and metamorphism (Taylor and McLennan, 1985).

This chapter deals with the geochemistry of the sand size matrix of Quartz Pebble Conglomerate (MQPC), and associated quartzites. The major trace and rare earth elements (REE) distribution patterns and their bearing on the composition of source rocks of QPC, and the nature of exogenic processes responsible for the generation of QPC are described and discussed. Since, detrital pyrite is an important and abundant component of the MQPC, and it has influenced the whole rock composition of QPC, it was separated from rest of the matrix and analyzed for its trace, REE and sulphur isotopic composition. The major, trace, REE data of 30 samples of the MQPC, 10 samples of quartzites and 10 samples of detrital pyrite, seperated from the matrix of QPC (Table 8.1, 8.2, and 8.3) are discussed below.

8.2 MAJOR ELEMENTS:

The quantity of sand size matrix of QPC, is very little and hardly reaches upto 5% of the total volume of the sample. The matrix was detached from the quartz pebbles and small detrital pyrite grains were separated. The sand size metrix of QPC (MQPC) containing pyrite and quartzites were analysed for their major, trace and REE contents. Pyrite was analysed for trace and REE and for sulphur isotopes. Among the major elements, only those elements were determined which are necessary for the interpretation of the trace and REE data. Since matrix of most of the samples, is made up of fine grained quartz, fuchsite, pyrite, uraninite and micas, like serecite, muscovite; estimation of K_2O, Na_2O, Fe_2O3, Feo, Al_2O_3, M_gO has been carried out. K_2O- Na_2O ratio, is very sensitive indicator of the abundance of the type

Table 8.1: Chemical composition of sand size matrix of quartz pebble conglomerate, the Bababudan schist belt.

Elements	MK-55	MK-56	MK-57	MK-58	MK-59	MK-60	MK-61	MK-62
Al_2O_3	6.51	7.04	6.59	5.84	6.81	5.67	6.71	6.51
FeO	7.23	8.14	4.78	6.07	2.22	4.85	1.85	4.49
MgO	0.27	0.30	0.36	0.48	0.30	0.32	0.48	0.29
CaO	0.65	0.58	0.50	0.54	0.50	0.58	0.52	0.60
Na_2O	0.81	0.68	0.52	0.46	0.70	0.66	0.82	0.98
K_2O	0.79	0.77	0.52	0.52	1.52	0.41	0.95	0.43
K_2O/Na_2O	0.98	1.32	1.00	1.13	2.17	0.62	1.16	0.44
Sc	4.04	4.60	3.13	3.82	6.68	3.02	6.23	2.98
V	28.56	37.02	25.20	32.16	51.91	21.12	46.85	19.31
Cr	403.42	642.53	353.06	462.62	609.58	375.19	596.38	338.17
Co	320.57	463.02	259.96	214.73	151.98	282.51	132.22	243.98
Ni	42.04	69.20	36.43	47.48	23.95	42.89	20.14	32.58
Cu	127.11	124.06	58.31	228.47	35.48	114.40	45.89	76.43
Zn	37.01	43.34	19.03	44.91	31.20	35.64	40.43	33.95
Ga	3.13	4.05	2.54	2.37	4.56	2.00	4.86	2.23
Rb	26.95	38.26	25.18	74.58	50.54	20.60	46.99	20.04
Sr	21.52	27.30	7.79	16.75	15.81	13.01	29.72	18.40
Y	10.92	31.19	11.11	22.00	20.16	17.71	18.40	22.05
Zr	152.94	293.84	108.61	186.27	419.56	138.92	392.01	312.28
Nb	5.10	12.99	4.31	7.07	3.84	6.02	3.47	5.23
Ba	74.26	58.77	32.59	37.53	65.64	37.09	74.15	36.84
Hf	7.58	12.27	6.00	10.51	17.85	6.12	19.32	15.36
Ta	0.91	2.00	1.30	0.53	0.18	0.59	0.05	0.32
Th	21.59	46.15	11.87	14.27	14.00	16.35	18.19	17.24
U	12.63	14.34	9.78	12.25	8.07	10.58	6.62	9.86
Rb/Sr	1.25	1.40	3.23	1.47	3.20	1.58	1.58	1.09
Cr/Ni	9.60	9.29	9.69	9.74	25.45	8.75	26.61	10.38
La	108.20	152.81	116.62	154.47	253.32	151.14	176.95	105.04
Ce	77.26	109.23	90.20	114.60	177.90	107.50	111.94	65.48
Pr	51.82	73.72	60.73	77.96	124.82	74.82	76.13	44.45
Nd	31.48	44.23	37.43	49.90	73.87	51.70	51.50	32.07
Sm	19.13	26.54	23.07	31.95	43.72	29.13	26.84	16.75
Eu	7.24	8.85	7.24	7.01	14.25	8.62	10.23	6.32
Gd	11.76	17.48	11.34	16.31	25.33	14.15	15.16	10.33
Tb	9.73	16.77	9.88	14.74	19.19	14.00	13.09	11.00
Dy	8.06	16.09	8.61	13.33	14.54	11.02	10.18	11.89
Ho	7.10	15.95	7.15	12.50	12.36	13.45	14.75	13.40
Er	6.27	15.82	5.94	11.73	10.52	9.56	9.04	10.52
Tm	5.90	17.42	7.58	16.85	11.52	11.24	16.67	14.04
Yb	10.08	23.19	9.35	19.60	18.35	12.70	14.76	18.06
Lu	7.87	20.73	6.30	14.70	14.70	10.76	12.34	13.91
ΣREE	361.90	554.83	401.44	555.65	814.39	519.79	553.58	373.26
LREE/HREE	4.31	2.81	4.96	3.58	5.32	4.28	4.43	2.58
Eu/Eu^*	0.48	0.41	0.45	0.31	0.43	0.42	0.51	0.48

Elements	MK-63	MK-64	MK-65	MK-66	MK-67	MK-68	MK-69	MK-70
Al_2O_3	6.71	4.95	5.54	4.12	5.32	6.21	3.22	5.69
FeO	6.11	2.99	5.49	3.71	5.79	3.92	4.55	4.71
MgO	0.38	0.67	0.50	0.32	0.77	0.52	0.65	0.59
CaO	0.52	0.65	0.50	0.63	0.63	0.52	0.56	0.56
Na_2O	0.84	0.81	0.92	0.91	0.99	0.66	0.55	0.54
K_2O	0.78	0.42	0.91	0.59	1.13	0.39	0.44	0.36
K_2O/Na_2O	0.93	0.52	0.99	0.65	1.14	0.59	0.80	0.67
Sc	4.86	3.30	5.06	3.17	5.98	2.84	3.11	3.24
V	38.38	27.18	40.61	18.99	52.93	22.09	28.83	27.20
Cr	663.07	465.03	537.68	335.13	699.14	313.73	451.89	424.99
Co	312.20	306.24	340.86	234.43	193.36	346.03	307.11	312.86
Ni	62.01	24.66	36.13	21.46	21.66	30.79	63.80	45.20
Cu	66.14	66.44	129.36	51.37	40.61	147.03	196.13	168.99
Zn	61.58	53.61	41.19	35.90	48.10	31.03	34.78	45.25
Ga	3.59	3.30	3.97	2.09	4.82	1.97	2.23	2.16
Rb	39.63	25.20	42.52	19.61	49.25	18.47	24.72	20.83
Sr	31.26	25.96	17.85	12.12	21.04	11.04	8.92	13.63
Y	18.13	17.76	23.51	16.87	30.38	14.85	17.48	16.99
Zr	221.80	214.89	297.40	202.87	395.78	137.91	162.45	229.22
Nb	7.55	5.30	4.20	5.72	7.77	6.81	5.70	4.12
Ba	54.64	68.46	55.79	35.41	69.63	29.41	30.97	34.52
Hf	9.32	9.60	12.62	9.88	16.17	6.52	6.74	9.29
Ta	0.32	0.02	0.20	0.16	0.12	1.31	0.44	0.23
Th	23.75	13.43	21.61	11.80	16.23	11.56	10.59	13.22
U	7.57	7.27	7.41	7.29	9.58	7.69	9.50	8.40
Rb/Sr	1.27	0.97	2.38	1.62	2.34	1.67	2.77	1.53
Cr/Ni	10.69	18.86	14.88	15.62	32.28	10.19	7.08	9.40
La	296.81	95.23	150.38	69.95	165.80	75.48	107.41	78.66
Ce	80.74	62.61	101.79	44.67	106.43	54.06	71.99	50.70
Pr	57.88	39.78	70.88	30.00	74.60	38.25	53.43	32.41
Nd	40.09	29.30	43.47	17.57	45.28	23.55	33.00	20.41
Sm	20.91	15.67	26.67	10.30	27.49	14.50	20.39	12.86
Eu	7.93	5.52	8.28	3.45	9.43	4.14	7.01	4.25
Gd	12.55	10.07	15.88	7.06	14.87	7.94	10.85	7.22
Tb	12.60	10.30	14.23	6.92	13.89	7.70	9.89	7.32
Dy	10.52	8.37	12.76	6.80	12.99	7.48	9.03	7.43
Ho	10.90	11.25	11.87	6.67	13.49	6.87	8.05	7.38
Er	9.08	8.43	11.04	6.55	14.02	6.31	7.19	7.35
Tm	10.96	10.96	14.89	9.55	16.85	8.43	9.27	8.43
Yb	13.02	14.40	15.77	13.95	19.88	11.90	11.65	13.15
Lu	11.27	12.34	13.91	11.02	16.27	10.24	9.71	9.71
ΣREE	595.26	334.23	511.85	244.46	551.29	276.85	368.46	267.18
LREE/HREE	5.46	2.82	3.56	2.52	3.43	3.08	3.78	2.87
Eu/Eu^*	0.49	0.44	0.40	0.40	0.47	0.39	0.47	0.44

Elements	MK-71	MK-72	MK-73	MK-74	MK-75	MK-76	MK-77	MK-78
Al_2O_3	5.16	5.32	7.76	5.39	3.89	5.92	6.60	6.21
FeO	5.50	2.64	4.64	4.64	2.42	5.28	2.85	4.85
MgO	0.59	0.76	0.34	0.29	0.40	0.56	0.38	0.22
CaO	0.61	0.75	0.46	0.37	0.28	0.46	0.39	0.41
Na_2O	0.89	0.30	0.63	0.23	0.25	0.40	0.78	0.54
K_2O	1.10	0.53	0.71	0.46	0.47	0.61	1.04	0.56
K_2O/Na_2O	1.24	1.77	1.23	2.00	1.88	1.53	1.33	1.04
Sc	3.78	3.33	4.55	2.94	2.93	3.80	6.09	3.96
V	34.43	28.98	31.41	26.06	28.21	33.99	45.89	26.84
Cr	518.12	396.61	910.33	363.45	266.36	435.08	640.70	829.58
Co	306.03	205.14	306.01	273.74	258.00	348.14	215.18	223.25
Ni	49.27	21.04	31.08	37.50	21.26	41.90	52.34	33.10
Cu	95.33	150.03	43.71	179.70	206.78	174.99	127.40	35.75
Zn	29.73	32.38	42.31	29.35	23.81	39.07	43.62	38.40
Ga	3.34	2.63	3.33	2.45	2.57	3.66	4.04	2.72
Rb	37.38	25.71	25.55	22.47	23.70	33.87	49.39	20.97
Sr	11.15	11.97	6.71	16.44	21.75	23.12	18.09	5.41
Y	16.66	37.20	26.79	17.35	12.66	19.65	30.89	26.41
Zr	247.87	180.51	579.21	120.34	98.14	186.11	392.94	571.08
Nb	4.21	6.29	11.32	4.87	5.96	8.17	6.09	10.37
Ba	34.80	33.12	38.90	38.57	43.76	66.62	59.75	43.42
Hf	8.40	6.58	23.42	4.73	3.70	8.30	15.94	25.24
Ta	0.47	0.62	1.54	0.47	0.25	0.64	0.77	1.20
Th	15.68	10.82	30.76	12.29	11.12	14.66	22.26	33.32
U	6.36	5.49	12.76	8.27	9.02	9.48	5.81	14.85
Rb/Sr	3.35	2.15	3.81	1.37	1.09	1.46	2.73	3.88
Cr/Ni	10.52	18.85	29.29	9.69	12.47	10.38	12.44	25.06
La	97.30	54.82	94.39	128.47	126.13	163.65	168.23	132.21
Ce	64.64	37.76	63.94	89.03	84.36	95.14	115.30	81.64
Pr	45.26	26.86	44.16	63.87	58.91	69.12	86.64	59.78
Nd	29.16	16.98	30.26	38.49	32.49	40.42	53.35	39.43
Sm	18.79	10.64	20.74	23.20	17.92	23.64	32.86	26.02
Eu	5.86	4.71	6.44	8.16	6.66	8.62	11.49	5.75
Gd	10.20	11.18	12.06	11.67	11.50	13.20	15.29	14.48
Tb	9.00	13.09	12.35	10.63	9.67	11.98	14.36	14.20
Dy	7.95	15.33	12.65	9.69	8.14	10.89	13.49	13.94
Ho	6.87	13.90	12.40	9.16	7.45	9.92	13.20	13.19
Er	5.94	12.61	12.17	8.67	6.83	9.04	12.93	12.49
Tm	9.27	15.45	14.89	9.27	5.90	13.20	14.89	18.26
Yb	9.64	16.90	20.97	11.25	8.51	13.71	20.12	23.79
Lu	7.61	13.91	17.06	9.19	7.61	12.34	15.75	19.16
ΣREE	327.49	270.71	374.48	430.75	392.08	494.87	587.90	474.34
LREE/HREE	3.84	1.31	2.21	4.31	4.87	4.16	3.80	2.62
Eu/Eu^*	0.42	0.43	0.41	0.50	0.46	0.49	0.51	0.30

Elements	MK-79	MK-80	MK-81	MK-83	MK-84	MK-85
Al_2O_3	6.82	5.93	5.71	5.92	5.29	5.39
FeO	3.21	6.21	3.35	3.28	4.14	1.64
MgO	0.56	0.46	0.40	0.56	0.52	0.50
CaO	0.35	0.35	0.33	0.37	0.61	0.31
Na_2O	0.67	0.42	0.66	0.60	0.49	0.40
K_2O	0.98	0.82	0.63	0.70	0.64	0.53
K_2O/Na_2O	1.46	1.95	0.95	1.17	1.31	1.33
Sc	6.18	4.74	3.73	3.64	3.24	3.06
V	46.87	41.15	30.04	31.30	29.78	26.08
Cr	681.30	699.08	684.99	429.80	408.91	470.25
Co	179.49	313.35	223.94	220.55	208.11	120.84
Ni	34.89	44.23	36.30	36.40	29.65	20.88
Cu	86.31	186.66	46.34	158.42	164.77	93.37
Zn	38.50	45.52	44.14	24.64	27.46	19.98
Ga	4.74	3.74	3.17	3.42	2.87	2.67
Rb	52.48	43.32	23.44	36.40	29.55	21.99
Sr	26.09	25.99	7.95	11.24	24.02	9.74
Y	18.80	26.44	31.62	18.64	12.60	17.45
Zr	302.64	347.19	553.04	177.06	157.22	340.58
Nb	6.57	9.79	9.24	3.94	3.94	4.89
Ba	72.00	54.95	43.12	46.33	47.78	43.09
Hf	12.62	13.64	22.12	7.16	7.60	13.06
Ta	0.95	0.92	0.69	0.37	1.45	0.10
Th	25.65	25.18	23.83	20.45	17.95	17.82
U	7.35	7.50	10.48	6.25	10.97	8.75
Rb/Sr	2.01	1.67	2.95	3.24	1.23	2.26
Cr/Ni	19.53	15.81	18.87	11.81	13.79	22.52
La	182.70	121.09	240.11	130.46	115.64	110.44
Ce	126.10	78.90	155.54	90.34	81.58	67.39
Pr	89.27	60.80	113.50	67.59	58.47	48.54
Nd	54.62	35.98	67.59	40.95	33.55	29.55
Sm	33.42	21.30	40.26	24.81	19.26	18.00
Eu	10.23	6.32	11.61	7.13	7.24	4.37
Gd	19.38	12.30	20.33	11.86	10.62	10.33
Tb	15.07	11.87	18.00	11.04	9.41	9.48
Dy	11.73	11.47	15.96	10.29	8.35	8.71
Ho	10.80	11.19	14.69	9.27	7.48	7.95
Er	9.96	10.92	13.53	8.31	6.71	7.27
Tm	11.52	15.73	17.98	9.27	8.71	9.83
Yb	13.10	19.56	22.30	11.90	9.03	11.41
Lu	10.24	16.01	18.37	9.19	7.61	9.45
ΣREE	598.14	433.44	469.77	442.41	383.66	452.72
LREE/HREE	4.78	2.92	4.37	4.36	4.54	5.02
Eu/Eu^*	0.40	0.39	0.41	0.42	0.51	0.32

1. All major elements are in wt. percent.
2. Trace and rare earth elements are in ppm.
3. All rare earth elements are normalized to chondrite.

Table 8.2: Chemical composition of quartzites, the Bababudan schist belt.

Elements	MK-86	MK-87	MK-88	MK-89	MK-90	MK-91	MK-92	MK-93	MK-94	MK-95
Al_2O_3	6.23	5.01	5.10	4.95	5.49	4.89	4.90	6.57	5.40	6.74
FeO	1.16	0.56	1.27	0.77	1.03	1.49	0.93	0.53	0.33	0.57
MgO	0.16	0.14	0.06	0.07	0.11	0.15	0.04	0.05	0.04	0.05
CaO	0.25	0.27	0.23	0.23	0.25	0.27	0.29	0.29	0.27	0.31
Na_2O	0.18	0.16	0.27	0.19	0.11	0.13	0.11	0.53	0.16	0.23
K_2O	2.05	0.35	0.08	0.12	1.16	0.10	0.22	1.97	0.69	2.53
K_2O/Na_2O	11.39	2.19	0.30	0.63	10.55	0.77	2.00	3.72	4.31	11.00
Sc	2.57	0.93	0.78	0.31	1.07	0.92	0.69	2.81	0.73	3.02
V	22.79	3.98	5.93	2.86	8.95	9.34	3.54	18.28	5.14	21.17
Cr	134.14	22.27	10.00	11.28	39.01	59.61	39.67	118.51	33.19	83.08
Co	176.92	140.72	219.65	166.72	207.91	180.21	226.38	180.72	149.60	108.92
Ni	2.76	2.12	5.46	2.53	8.51	9.54	2.01	1.94	3.34	2.22
Cu	72.85	27.29	16.28	75.27	83.10	16.42	4.42	3.81	2.34	2.82
Zn	3.54	4.65	ND	5.49	10.82	8.91	3.15	1.11	15.82	9.86
Ga	5.80	2.13	3.18	1.15	2.58	0.81	0.43	4.25	1.86	6.47
Rb	33.65	5.09	0.19	1.31	16.88	0.87	2.61	43.36	12.43	43.80
Sr	16.88	7.39	5.76	8.20	9.86	9.35	12.13	15.95	8.45	12.64
Y	3.44	3.05	2.91	0.48	5.31	5.60	3.14	15.26	4.37	7.55
Zr	220.19	5.53	3.54	1.13	103.12	98.96	38.36	323.78	69.82	119.60
Nb	2.50	0.65	0.67	0.63	0.99	2.20	1.28	3.54	1.32	1.62
Ba	77.52	8.81	2.78	4.32	46.65	6.83	5.23	34.59	25.30	126.27
Hf	4.57	0.22	0.24	0.06	1.58	2.06	0.77	5.25	1.11	1.82
Ta	1.14	0.22	0.26	0.46	0.58	0.89	0.79	1.31	0.52	0.83
Th	5.10	0.11	0.08	0.01	1.35	5.10	0.52	2.75	1.18	2.27
U	5.57	0.50	0.48	0.22	0.60	3.96	0.32	1.31	0.58	1.27
La	1.58	0.41	0.54	0.05	24.01	1.77	16.02	12.48	14.90	40.54
Ce	1.68	0.97	0.54	0.31	6.72	4.52	13.17	8.00	9.34	32.72
Pr	1.24	0.88	0.51	0.29	14.09	2.26	8.76	3.58	7.30	21.97
Nd	ND	ND	ND	ND	10.15	2.25	6.88	3.70	5.54	18.14
Sm	0.56	1.21	0.26	ND	2.86	0.69	2.16	2.38	2.16	6.71
Eu	0.69	0.50	ND	ND	3.56	0.23	1.03	1.38	1.49	4.14
Gd	0.26	0.64	0.75	0.16	2.06	1.41	1.24	3.27	2.39	5.00
Tb	0.86	1.21	1.03	0.86	3.97	4.48	2.24	4.83	1.72	3.79
Dy	1.15	0.58	1.13	0.18	2.13	2.81	1.21	5.14	1.99	2.76
Ho	1.06	0.71	1.06	ND	2.12	2.23	1.05	5.05	1.65	2.23
Er	1.45	1.37	0.68	0.36	1.89	2.25	1.08	6.22	1.33	2.93
Tm	2.45	1.40	1.12	ND	1.97	2.81	1.12	7.58	1.12	2.81
Yb	3.75	1.37	1.53	0.97	3.06	2.10	1.37	6.65	1.81	4.03
Lu	3.15	0.79	1.84	ND	1.84	2.36	1.08	6.82	1.31	2.36
ΣREE	19.88	11.82	10.45	3.18	80.43	32.17	57.59	75.91	54.05	150.13

1. All major elements are in wt. percent.
2. Trace and rare earth elements are in ppm.
3. All rare earth elements are normalized to chondrite.

Table 8.3: Trace, REE and $\delta^{34}S$ analysis of Pyrite, seperated from sand size matrix of quartz pebble conglomerate, the Bababudan schist belt.

Elements	MK-55	MK-58	MK-59	MK-60	MK-62	MK-66	MK-68	MK-71	MK-74	MK-83
Sc	0.73	1.20	0.70	0.70	0.76	0.66	0.42	0.54	0.42	0.44
V	ND	ND	ND	ND	ND	ND	ND	ND	ND	ND
Cr	67.20	58.00	27.45	34.47	23.22	41.86	35.11	39.36	25.35	66.54
Co	1388.4	1315.7	1286.0	1318.4	1317.3	1312.5	1056.4	1334.0	1485.3	1257.3
Ni	255.48	190.99	230.45	211.71	247.04	227.81	234.53	264.85	171.85	243.40
Cu	154.23	170.84	185.52	196.66	156.37	165.65	202.55	156.26	138.22	130.22
Zn	17.10	17.12	26.36	25.00	18.70	20.14	11.53	26.72	18.50	20.27
Ga	0.77	0.86	0.64	1.04	0.53	0.76	0.49	1.00	0.58	0.97
Rb	2.42	1.87	1.65	2.39	1.85	1.85	1.25	2.20	1.11	1.94
Sr	2.28	0.21	0.75	0.40	0.64	1.08	ND	1.13	0.72	3.59
Y	11.48	20.41	12.74	6.24	8.42	10.37	9.02	9.94	7.31	7.77
Zr	52.00	44.00	78.00	41.33	51.41	50.81	51.58	60.14	49.25	51.14
Nb	9.41	5.47	4.17	3.11	3.93	4.50	4.78	2.59	2.66	4.34
Ba	ND	ND	ND	ND	ND	ND	ND	ND	ND	ND
Hf	1.56	4.00	11.08	0.42	0.45	0.58	0.83	0.77	0.37	0.61
Ta	0.48	0.28	0.35	0.22	0.20	0.23	0.19	0.10	0.14	0.18
Th	4.25	2.32	1.70	1.56	1.30	2.06	1.46	1.88	1.22	2.83
U	2.31	2.09	2.10	1.18	0.80	1.35	0.86	0.72	1.26	0.85
La	15.99	13.27	14.88	10.47	3.81	11.12	7.30	13.51	6.95	13.90
Ce	14.51	14.83	12.43	11.80	5.85	11.32	7.89	12.69	10.07	11.85
Pr	11.24	10.44	10.00	7.45	4.01	7.78	5.18	8.32	4.16	9.20
Nd	7.94	7.80	7.01	6.05	2.20	5.19	4.81	6.50	5.22	6.99
Sm	4.24	3.85	3.38	3.29	0.87	3.17	3.03	3.77	2.64	3.42
Eu	1.16	1.49	0.57	0.11	0.12	0.61	0.14	0.57	0.34	0.92
Gd	3.20	3.17	2.65	1.05	1.08	1.92	1.11	1.80	0.85	2.35
Tb	2.49	2.74	2.16	1.19	1.28	1.72	1.20	1.64	0.91	1.83
Dy	1.94	2.36	1.76	1.36	1.52	1.57	1.29	1.50	0.97	1.42
Ho	2.05	3.26	1.99	1.36	1.28	1.64	1.35	1.34	0.86	1.28
Er	2.17	4.50	2.25	1.37	1.08	1.77	1.41	1.20	0.76	1.16
Tm	1.97	7.30	3.37	0.56	0.56	2.09	1.12	1.97	0.56	1.40
Yb	3.19	6.94	4.48	1.29	0.77	2.46	2.02	1.37	1.29	0.76
Lu	3.41	7.35	6.56	1.57	2.36	2.89	1.31	1.31	1.05	1.05
ΣREE	75.60	89.30	73.49	48.92	26.79	52.25	39.16	57.49	36.63	57.53
$\delta^{34}S$	+3.3	+2.9	+2.8	+2.1	+2.4	+2.4	+2.4	+2.4	+2.1	+2.3

1. Trace and rare earth elements are in ppm.
2. All rare earth elements are normalized to chondrite.
3. $\delta^{34}S$ are in $^{0}/_{00}$.

of feldspar in the source area. It is also considered to be changing its character around the Archaean-Proterozoic boundary (Fig. 8.1A). Around 2.5 Ga ago K_2O/Na_2O ratio suddenly increases and becomes more than one in all types of sediments whereas before 2.5 Ga it remains below one. Similarly $^{86}Sr/^{87}Sr$ ratio also increases after 2.5 Ga (Engel et al., 1974; Veizer, 1976). This ratio for the matrix of QPC and quartzites is given in (Fig.8.2B). It varies from 1:2 to more than 2:1, indicating that the source rocks had K feldspar, plagioclase and mica in it and thus a greater scatter in K_2O/Na_2O ratio has been produced (Fig. 8.2B). K_2O-Na_2O ratio of most of the samples of the MQPC and the quartzites, is > 1, which is significantly different from those of the KCM (<1). It may be noted that there is a great difference in fuchsite content of the MQPC and quartzites. The total feldspar contents of the quartzite varies from 3.30% to ~ 18.00% and the same is reflected in the major element composition of quartzites especially in the abundances of K_2O. Therefore K_2O/Na_2O ratios of most of samples of the MQPC are lower than those of quartzites (Fig. 8.2B). It may be noticed that the petrological and geochemical characteristics of the two conglomerates namely QPC and the Kaldurga Conglomerate are distinct from each other, and this distinction is probably because of their mode and environment of weathering, deposition and tectonic setting. The source area has K-rich rocks and the hydrodynamic processes have resulted in the removal of the mobile elements, present in feldspar and other mineral constituents of the source rocks, other than micas. Inspite of the low density of mica, part of the mica from the source area has been retained in

Fig. 8.1 (A) Diagram illustrating: (top)-secular evolution of K_2O/Na_2O ratios in sediments and igneous rocks, according to Engel et al. (1974); (bottom) $^{87}Sr/^{86}Sr$ in seawater according to Veizer (1976).

(B) K_2O/Na_2O distribution pattern in QPC and quartzite showing a large scatter in the K_2O/Na_2O ratio. Correlation coefficient values for QPC and quartzites are given as r_1 and r_2 respectively. Solid dots represent QPC, crosses indicate quartzites. In all subsequent illustrations these symbols are followed, and r_1 and r_2 will stand for the correlation coefficient of QPC and quartzites respectively.

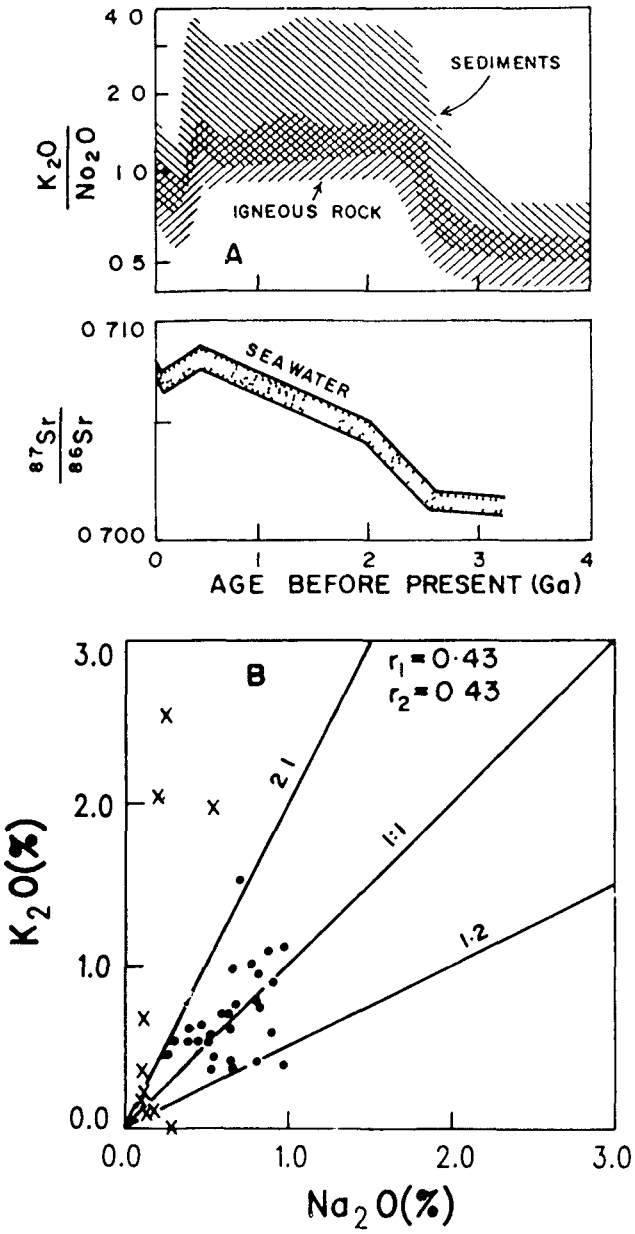
4 0
2 0
1 0
0 5
$\frac{K_2O}{Na_2O}$
SEDIMENTS
IGNEOUS ROCK
A
0 710
0 700
$\frac{^{87}Sr}{^{86}Sr}$
SEA WATER
0
1
2
3
4
AGE BEFORE PRESENT (Ga)
3.0
2.0
1.0
0.0
B
$r_1 = 0{\cdot}43$
$r_2 = 0\ 43$
2:1
1:1
1:2
$K_2O(\%)$
$Na_2O(\%)$

the MQPC and quartzites, therefore, most of the samples of the MQPC and quartzites exhibit K_2O/Na_2O ratio more than 1. Most of the mica, present in the MQPC is in the form of fuchsite. This aspect is very clearly reflected in the +ve correlation (r =0.52) between K_2O and Cr. On K_2O vs Cr binary plot, though two different populations, one of quartzites and the other of the MQPC are seen, this difference is mainly due to the enrichment of Cr in the fuchsite present in the MQPC (Fig. 8.2A). Similarly, there is high order positive correlation (r = 0.96) between Al_2O_3 and Cr in the samples of quartzites, but the positive correlation between Cr and Al_2O_3 for the MQPC is not of that high order (r = 0.51). Here also quartzites and MQPC form two separate populations (Fig. 8.2B). A strong +ve correlation between Na_2O and K_2O is seen. A general scatter with weak positive correlation between Al_2O_3 and K_2O is seen in Fig. (8.2C). Quartzites samples define linear relationship, expect two samples, but the MQPC samples exhibit a great variation in Al_2O_3 content at 0.5 to 1.0% K_2O level, idicating that some Al_2O_3 rich components like clays are present in the MQPC. These data along with the presence of detrital pyrite indicate that intense chemical leaching of the source area has occurred under anoxic environment. Scatter between the Na/Al and K/Al ratios (Fig. 8.2D) substantiate the inferance that except micas, high Al_2O_3 componant including fuchsite, mobile elements of other minerals have been leached under intense chemical weathering. Detrital rounded grains of fuchsite quartzite in the MQPC have contributed most of Al_2O_3, K_2O and Cr. However presence of K_2O and Al_2O_3 in the form of illite or some clay can not be ruled out in view of

Fig. 8.2 (A) $Cr-K_2O$ binary plot showing the enrichment in Cr in QPC due to presence of fuchsite.

(B) $Cr-Al_2O_3$ binary plot showing moderate positive correlation coefficient.

(C) $Al_2O_3-K_2O$ binary plot illustrating the micaceous composition of matrix of QPC and quartzites.

(D) Na/Al and K/Al binary plot reflecting the K-enrichment in most of the samples of QPC and quartzites due to K-enriched micas.

(E) K_2O-MgO plot showing random scatter in QPC and quartzites.

(F) Na/K and Mg/K plot showing depletion in Mg as compared to Na.

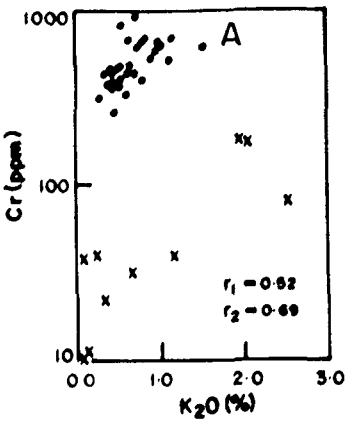
A
1000
100
10
Cr (ppm)
$r_1 = 0.62$
$r_2 = 0.69$
0·0
1·0
2·0
3·0
K_2O (%)

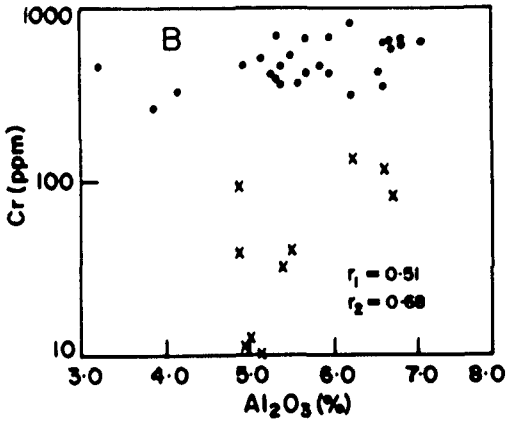
B
1000
100
10
Cr (ppm)
$r_1 = 0.51$
$r_2 = 0.68$
3·0
4·0
5·0
6·0
7·0
8·0
Al_2O_3 (%)

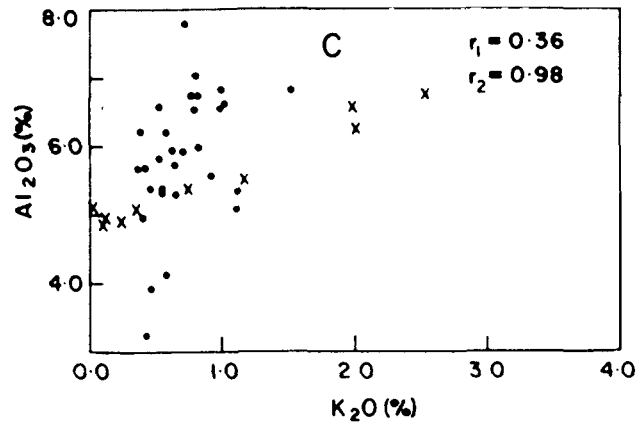
C
$r_1 = 0.36$
$r_2 = 0.98$
8·0
6·0
4·0
Al_2O_3 (%)
0·0
1·0
2·0
3·0
4·0
K_2O (%)

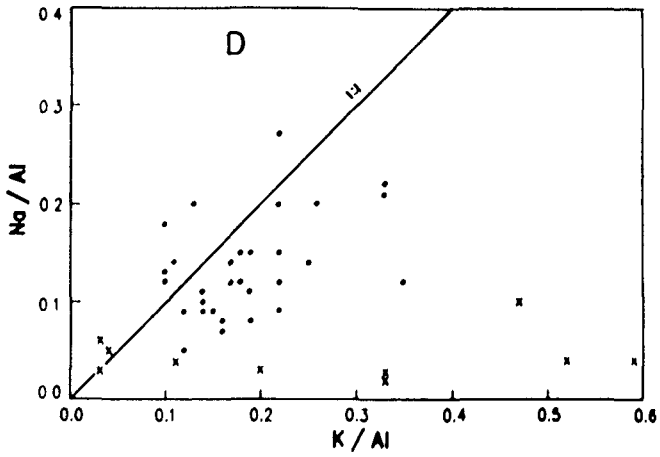
D
0·4
0·3
0·2
0·1
0·0
Na / Al
1:1
0.0
0.1
0.2
0.3
0.4
0.5
0.6
K / Al

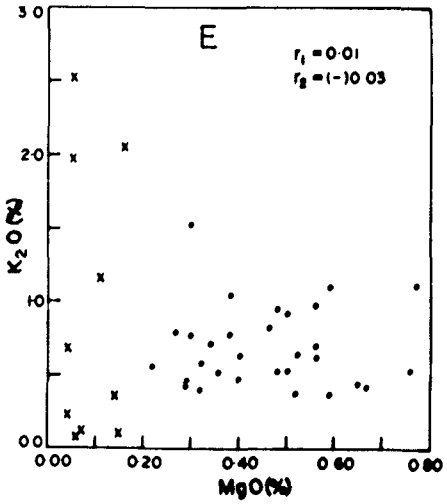
E
$r_1 = 0.01$
$r_2 = (-)0.03$
3·0
2·0
1·0
0·0
K_2O (%)
0·00
0·20
0·40
0·60
0·80
MgO (%)

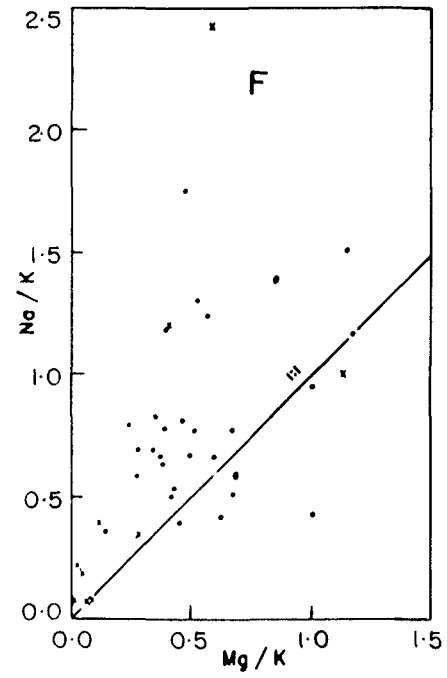
F
2·5
2·0
1·5
1·0
0·5
0·0
Na / K
1:1
0·0
0·5
1·0
1·5
Mg / K

Al_2O_3 and K_2O distribution (Fig. 8.2C). Complete or extreme depletion in Na_2O suggests that the plagioclase has been mostly removed from the MQPC and quartzites. It indicates strong chemical weathering and hydrodynamic action. This is further substantiated by low concentration of M_gO and C_aO (Table 8.1 and 8.2). MgO content of the KCM reaches up to 26% (Chapter XI). The KCM is a highly immature sedimentary rock, both mineralogically and texurally. Intensive chemical leaching has not occurred at the time of generation of debris for the KCM. In fact KCM is a product of intense mechanical weathering thus the mobile elements are not taken away from the debris. Since the MQPC is a product of intense chemical weathering and strong hydrodynamic activity mobile elements have been leached away. This is further evidenced by K_2O and MgO relationship, and over all depletion in MgO (Fig. 8.2E). The presence of rocks of enriched Mg, Cr, Ni and Co in the source area can not be denied in view of the composition of the KCM and the presence of Komatiite in older schist belts. Inspite of these facts, the end product in the form of MQPC is depleted in MgO, Co and other constituents and resulted in a rock suite, which exhibits scatters in the low quantities of MgO and Mg/K - Na/K ratios (Fig. 8.2F). K_2O-Cr binary relationship (Fig. 8.2A) has shown that Cr is present in fuchsite. MgO-vs Cr relationship shows that Cr content of these rocks is independent of MgO (Fig.8.3A). Since almost all K_2O content is present in micas and Rb goes with K_2O, there is a very strong positive correlation between K_2O and Rb content of the sample studied (Fig. 8.3B). Similarly Ba is also positively correlated with K_2O as Ba substitutes for K in feldspars and micas (Fig.8.3C). The major and

Fig. 8.3 (A) Binary plot of Cr and MgO showing that Cr concentration of QPC and quartzites is independent of MgO.

(B) Plot of Rb versus K showing covariance of the elements in quartzites and QPC.

(C) A binary plot of Ba and K showing mutual relationship in quartzites and QPC.

(D) Plot of Cr versus Ni illustrating that the con centration in QPC, quartzites and pyrites are distinct from each other. Three distinct groups are visible.

(E) Distribution in QPC, pyrites and quartzites. In this diagram also the distinct grouping is visible.

(F) Co and Cr distribution in QPC, pyrites and quartzites showing separate grouping of the rock types.

Fig. 8.3 (D), (E) and (F) indicate differences in the ferromagnesian trace element content of these rock suites.

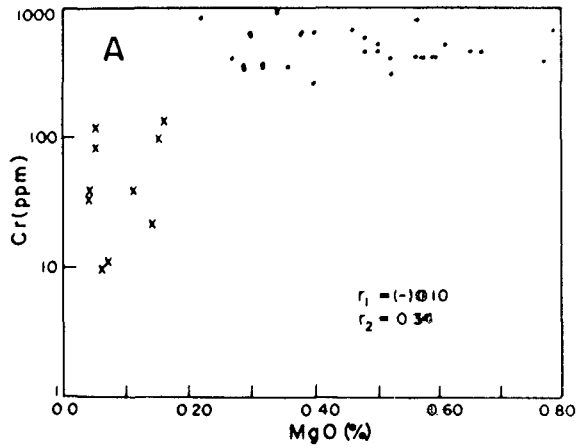
A
Cr(ppm)
MgO (%)
r_1 =(-)0 10
r_2 = 0 36

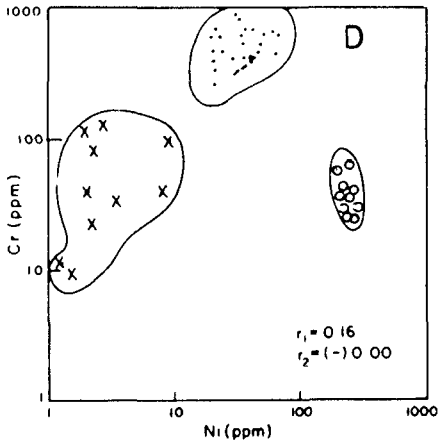
D
Cr (ppm)
Ni(ppm)
r_1 = 0 16
r_2 =(-) 0 00

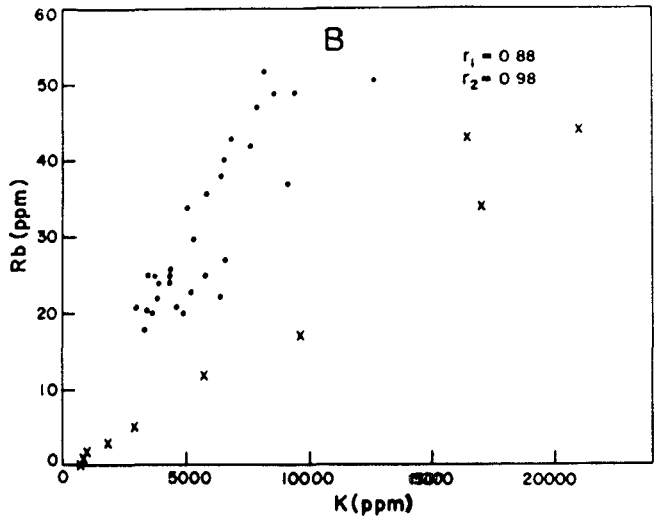
B
Rb (ppm)
K(ppm)
r_1 = 0 88
r_2 = 0 98

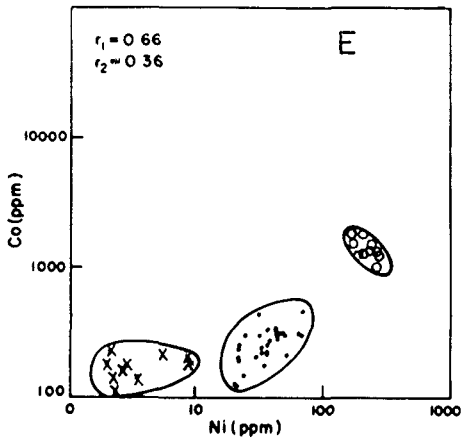
E
Co(ppm)
Ni(ppm)
r_1 = 0 66
r_2 = 0 36

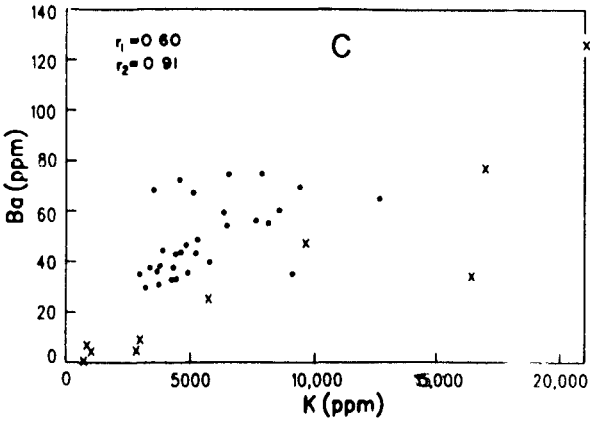
C
Ba (ppm)
K (ppm)
r_1 =0 60
r_2 = 0 91

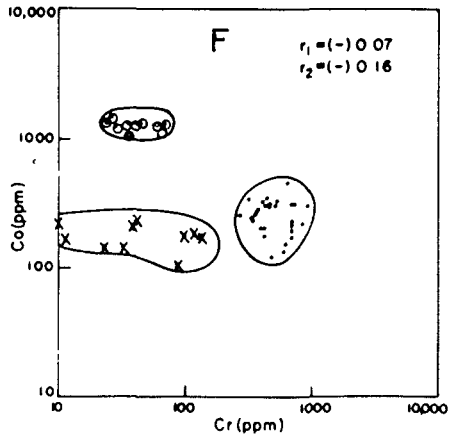
F
Co(ppm)
Cr(ppm)
r_1 =(-) 0 07
r_2 =(-) 0 16

trace element chemical characteristics of the MQPC and quartzites, presented above strongly suggest that the unstable minerals of source rocks were very intensely weathered and leached. During transportation the debris appears to have suffered strong chemical fractionation. Hence, only restites could be deposited on the shelf.

8.3 TRACE ELEMENTS:

Trace elements data of the MQPC and quartzites are given in Table (8.1 and 8.2). MQPC is enriched in Co, Cr, Ni, and Cu. A few samples, are enriched in Zr also. The Cr enrichment is caused by fuchsite of matrix, as evidenced by a strong positive correlation between K_2O and Cr ($r = +0.52$) (Fig. 8.2A). Distinct abundance level differences, between ferromagnesian trace element content of MQPC and quartzite are found. In MQPC, Cr and Ni concentrations are higher than those found in quartzites (Fig. 8.3D). However, co content of many samples of the quartzite is similar to that of some samples of MQPC. (Fig. 8.3E). The correlation coefficient (r) calculated for Cr-Co, Cr-Ni and Co-Ni are of very low order, indicating that the concentration of these elements in MQPC and quartzites are independent of each other. Their abundance level in the two horizons is dependent on the relative abundance of fuchsite and pyrite, as these minerals containing Cr, Co, and Ni are not extensively present in quartzites. When the total population of samples of the MQPC and quartzites are considered together, inspite of two different population clusters, representing two rock types, a low order positive correlation coefficient is seen on Cr-Ni plot (Fig.

8.3D), but such positive correlation coefficient is not visible on Ni-Co and Co-Cr plot (Fig. 8.3E and 8.3F). Co is situated as its sulphide inclusions in detrital pyrite. The pyrite analysis (Table 8.3), shows Co concentration ranging upto 1485 ppm (Fig. 8.3E, 8.3F). Co concentration of the quartzites also reached upto 220 ppm (Fig. 8.3E, 8.3F), especially in those samples, in which cementing material is more. The alteration of the matrix has given brownish colour, indicating that there was some pyrite present in the quartzites also, which contained some Co bearing sulphides. However, the Ni concentration of quartzites remains between 2 to 9 ppm (Fig. 8.3D, 8.3E), whereas in MQPC, Ni concentration varies from 20 to 70 ppm (Fig. 8.3D, 8.3E). The detrital pyrite of the MQPC contains Ni concentration from 171 to 255 ppm (Fig. 8.3E, 8.3D). Pyrite contains Cr between 23 to 67 ppm, this shows that most of the Cr in MQPC is from fuchsite and Ni and Co are situated in pyrite. The concentration of Cr in quartzite reaches from 10 to 140 ppm. This indicates that fuchsitic mica is present in quartzite also. The concentrations of Cu and Zn are more in MQPC than in the quartzite, and as indicated by the composition of pyrite (Table 8.3), Cu is present in pyrite of MQPC with an abundance level between 130-202 ppm. Zn concentration of pyrite is lower than its concentration in MQPC, indicating that Zn is present in other sulfide minerals in addition to pyrite in MQPC. Zn concentration of the quartzite varies between 1 - 16 ppm, where as Cu reaches upto 83 (Fig. 8.4A). This substantiates the above inferance that not only in MQPC, but also in quartzites sulphides are present in detrital form, or in the form of cement.

Zr, Hf, Rb, Sr, V, Sc, Nb, Ta and Y show a great variation

Fig. 8.4 (A) Distribution and mutual relationship of Cu and Zn. illustrating Cu enrichment in pyrite, and Zn enrichment in QPC. The latter appears to be due to the presence of traces of zinc sulphide as a separate mineral.

(B) Illustrates mutual relationship and simultaneous increase of Cr and Zr. Plot of Cr versus Zr showing co-variance.

(C) Illustrates linear covariance between Hf and Zr. The plot of Hf versus Zr illustrating covariance.

(D) Shows random scatter of Zr against MgO. The plot of Zr against MgO showing random scatter.

(E) Shows binary relationship between Rb and Sr. Distribution Rb and Sr showing minor positive correlation.

(F) Illustrates high order positive covariance between V and Sc.

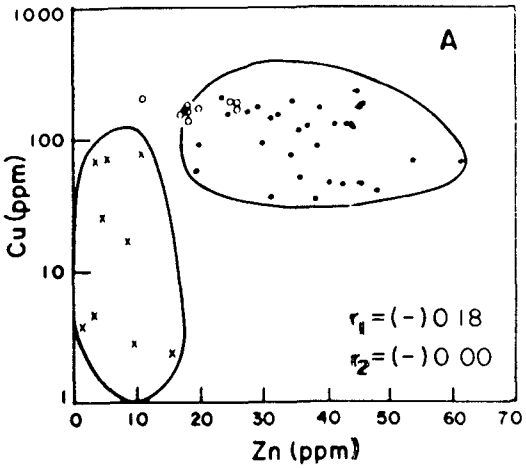
A
Cu (ppm)
Zn (ppm)
$r_1 = (-)0.18$
$r_2 = (-)0.00$

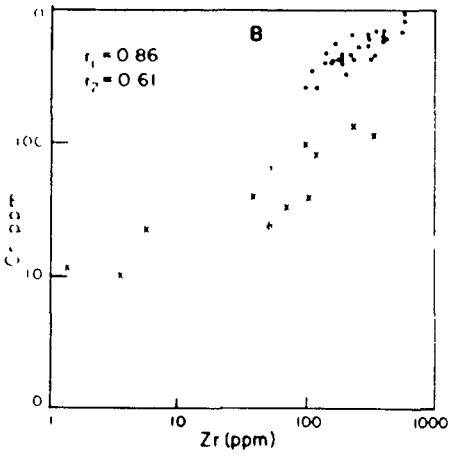
B
$r_1 = 0.86$
$r_2 = 0.61$
Zr (ppm)

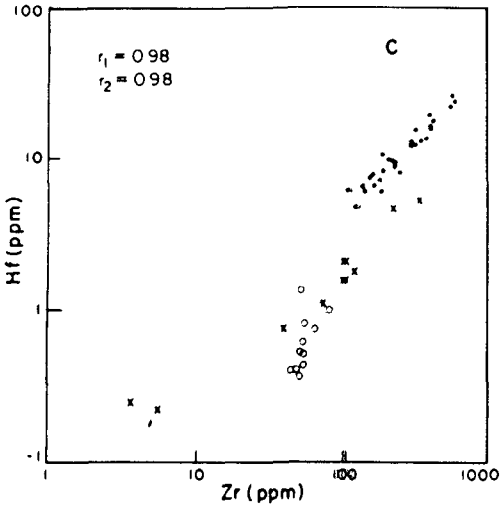
C
$r_1 = 0.98$
$r_2 = 0.98$
Hf (ppm)
Zr (ppm)

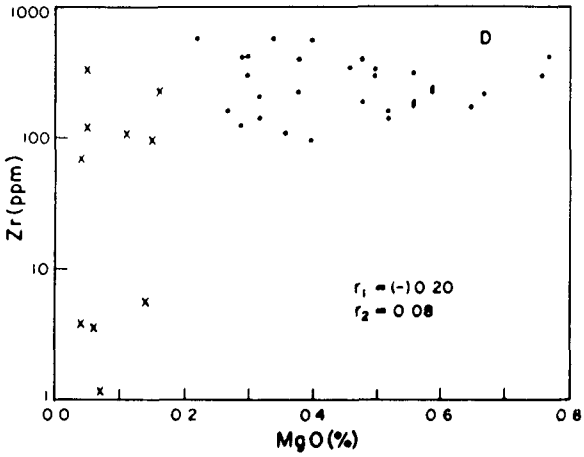
D
$r_1 = (-)0.20$
$r_2 = 0.08$
Zr (ppm)
MgO (%)

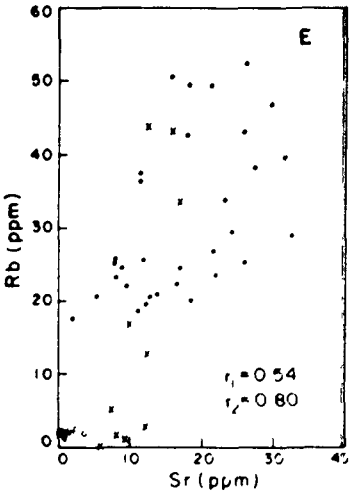
E
$r_1 = 0.54$
$r_2 = 0.80$
Rb (ppm)
Sr (ppm)

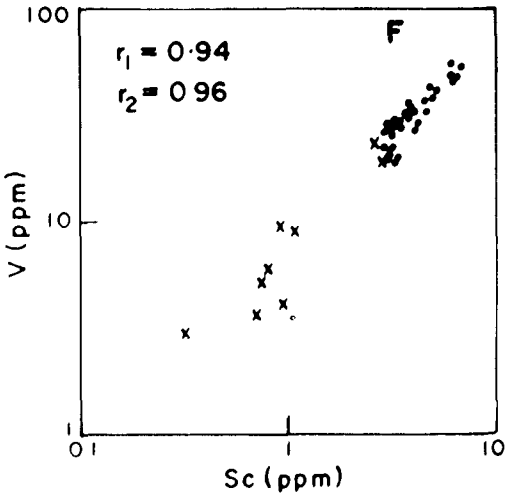
F
$r_1 = 0.94$
$r_2 = 0.96$
V (ppm)
Sc (ppm)

and scatter in both the MQPC and quartzites (Table 8.1 & 8.2). Zr varies from 1 - 323 ppm in quartzite and from 98 to 579 ppm in MQPC. In mature sediments the resistive minerals like Zircon tend to concentrate. Cr and Zr plot (Fig. 8.4B) shows high order correlation between Cr and Zr of quartzite and MQPC both. Coefficient of correlation (r) between Cr and Zr of MQPC is + 0.86 and in quartzite it is + 0.88. The high order correlation coefficient between Cr and Zr is very significant and indicates that both Cr and Zr are derived from a silicic source (Zircon and fuchsite). It may be noted that, in general, a strong - negative correlation coefficient is found between Cr and Zr, as they are characteristic and diagnostic trace elements of divergent rock types. The mafic - ultramafic rocks are enriched in Cr whereas, acid plutonic rocks are enriched in Zr. In unsorted sediments derived from a mixed provenance, for example, the KCM, a negative correlation coefficient between Cr and Zr is found (Chapter XI). The Cr and Zr abundances and the positive correlation coefficient between the two element in MQPC and quartzite, indicates that the intense chemical weathering and hydrodynamic processes have removed the mafic-ultramafic component of the source and only restites could be deposited at the base and the shelf margin of the basin. Very weak relationship between MgO and Cr (Fig. 8.3A) with strong depletion in MgO in MQPC and quartzite, at one hand and enrichment of these components in the KCM, is self explanatory of this process. It is proposed that the exogenic processes were intensely active at the time of initiation of sedimentation in the Bababudan basin. During this period very intense chemical and physical weathering was taking

place in the source region.

These inferences are further substantiated from Hf-Zr binary relationship as illustrated in Fig. (8.4C). MQPC exhibits an excellent strong positive correlation coefficient of the order of + 0.97. Similarly in quartzite the correlation coefficient between Zr and Hf is of the order of + 0.90. This is an extremely significant feature, demonstrating that only restites and sulfides could survive the intense chemical weathering and hydrodynamic processes in an anoxic atmosphere, and the mafic-ultramafic constituents of the source area were completely removed. These conditions of intense chemical weathering and high energy hydrodynamic processes changed to intense physical weathering and to the hydrodynamic processes which generated slurry for the deposition of the KCM (Chapter XI). Tectonic conditions in provenance and depository also appear to have changed from the time of deposition of QPC - quartzites to the KCM. The change in tectonic setting resulted in upheaval in the source area and sudden subsidence of the basin, causing high angle slope for the deposition of boulders of the size of 3x2x1 ft. along with the sand size material of less than 2 mm in the Kalduga Conglomerate. Zr and MgO are diagnostic constituents of silicic and basic-ultrabasic rocks respectively, and the higher abundances of any of the two in the sediments are indicative of their derivation from either silicic source or basic-ultrabasic rocks. A difference in concentration of Mg and Zr between the MQPC and quartzites is visible (Fig. 8.4D). The maximum concentration of Zr in the MQPC is 579 ppm and in quartzites it reaches upto 323 ppm. Maximum concentration of MgO in the QPC and quartzites are 0.67% and 0.16%

respectively. Since there has been relatively more space between the pebbles of QPC, retention of restites (e.g., fuchsite, zircon and pyrite) in QPC became much more possible than in the quartzites.

Rb-Sr concentrations of the MQPC and quartzites show an extremely random scatter (Fig. 8.4E), which is understandable *because of the mobility of Rb and Sr during weathering, diagenesis* and metamorphism (McLennan et al., 1980, Taylor and McLennan, 1985; McLennan and Taylor, 1991). Since the Rb content in these rocks is expected to be situated in the micaceous constituents, fuchsite bearing MQPC and three samples of quartzites, show higher abundance of Rb, reaching upto 52 ppm level and the Sr content reaches upto 31 ppm. Rb and Sr contents of Pyrite are extremely low, they range between 1-2 ppm and 0.2 to 2.2 ppm respectively. A scatter between Rb and Sr data, further substantiate the inference that the MQPC and quartzites are products of intense chemical weathering of source area and hydrodynamic process on land and at the margin of the basin.

The fact that trace elements of most of the samples of quartzite and the MQPC are distinct from each other, is excellently demonstrated by V-Sc plot (Fig. 8.4F). Three samples of the quartzites fall at the lower level of concentration of V-Sc of the MQPC. The correlation coefficient between V-Sc is +0.94 for the MQPC and +0.96 for quartzites. This positive correlation between the two elements, clearly demonstrate that the unstable minerals present in the source area were largely removed to the *deeper part of the basin by intense chemical weathering and* hydrodynamic processes. Some of these components must have been

deposited in argillites, which are very intensevely weathered and thus became unsuitable for any geochemical work. The point which is asserted from these data, is that, there was drastic change in the style of weathering and hydrodynamic processes, from the time of initiation of sedimentation in the Bababudan basin to the time of deposition of the Kaldurga Conglomerate.

Nb-Ta become more concentrated in those rock types, which are formed at the very last stage of magmatic fractionation. Actually Nb-Ta minerals are found to be concentrated in pegmatites. On the other hand, rocks of mafic-ultramafic composition and chemical precipitation from mantle derived hydrothermal solutions are extremely depleted in Nb and Ta. Similarly, Nb-Ta are unable to find their place in the crystal structure of quartz, thus sedimentary rocks which are extremely rich in quartz, show a very low concentration of Nb-Ta (Fig. 8.5A). The Nb concentration of the MQPC is comparatively higher than that of quartzites. The low concentration of Nb and Ta indicates that minerals like Neutolites were not concentrated in these sediments and probably were not present in pegmatites or quartz veins, which had supplied pebbles to QPC. Quaratzites and MQPC form two separate populations as far as Nb-Ta distribution is concerned (Fig.8.5A). These two populations have been noticed in the case of other elements also. Nb-Ta content of the pyrite is somewhat similar to that of MQPC.

V and Y binary plot (Fig. 8.5B) shows that these two elements are depleted in quartzites in comparison to those of the MQPC. It may be noticed that in all the samples of pyrite. V is invariably below detection limit (Table 8.3). This suggests that V, in the MQPC, may lie in fuchsite and/or some other micaceous

Fig. 8.5 (A) Shows Nb and Ta distribution pattern.

(B) Illustrates V-Y behaviour.

(C) Shows U/Th concentration and their mutual relationship.

(D) Illustrates Th/Sc ratio vs. Sc. The area shown by oblique lines indicate the field of Archaean active plate margin turbidites.

(E) Shows Th/U ratios vs. Th concentration.

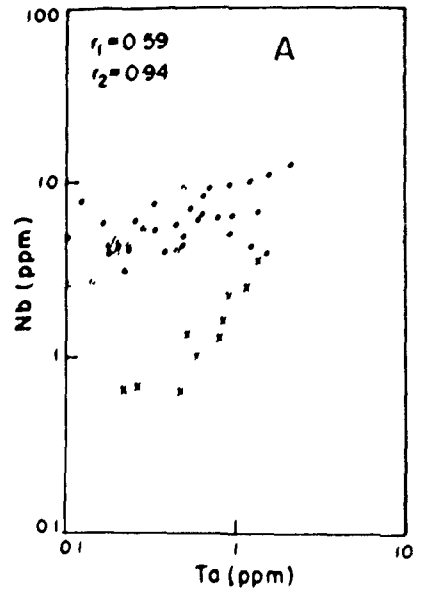
A
r_1=0.59
r_2=0.94
Nb (ppm)
Ta (ppm)

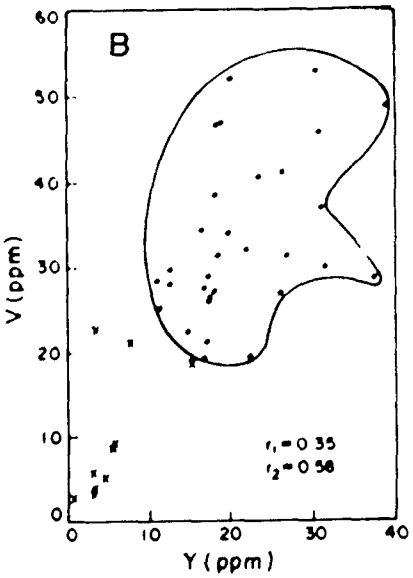
B
r_1=0.35
r_2=0.58
V (ppm)
Y (ppm)

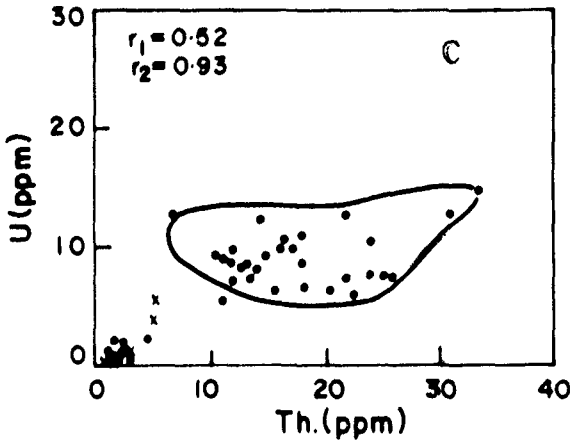
C
r_1=0.52
r_2=0.93
U (ppm)
Th. (ppm)

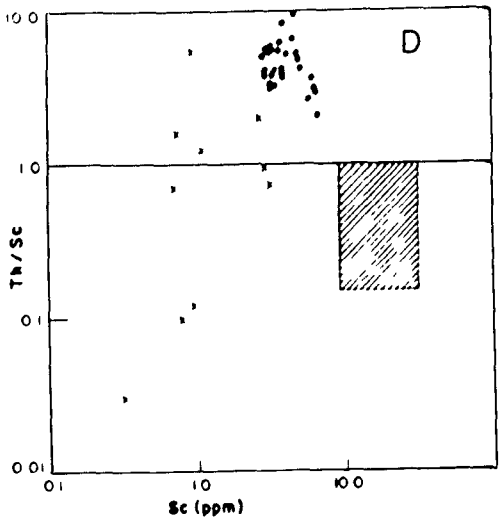
D
Th/Sc
Sc (ppm)

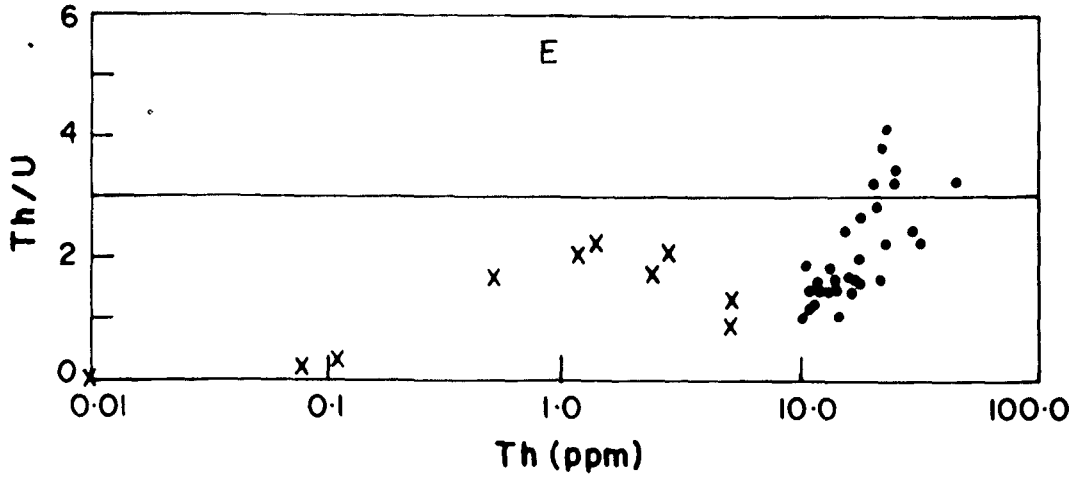
E
Th/U
Th (ppm)

mineral. These two elements i.e. V and Y, show positive correlation coefficient for quartzites, but a higher order random scatter with very low positive correlation coefficient for MQPC.

Similar divergent characteristics of QPC and quartzite are found in the U-Th distributions (Fig. 8.5C). In MQPC, the maximum concentrations of U and Th has reached upto 15 ppm and 36 ppm respectively. In quartzites maximum concentration of U and Th is found at 5.5 ppm and 5.1 ppm respectively. Despite their low abundance in quartzites, these radioactive elements show a very strong positive correlation coefficient of the order of 0.93, whereas in the MQPC, a rather insignificant correlation ($r = 0.52$) and scatter is seen. At several places, the QPC in this belt is found to contain uranium in the form of uraninite. Since U is a strategic mineral, we have not sampled the locations which are rich in uraninite. U/Th ratios of the samples studied are always less than 1. The concentration of U and Th in pyrite is varying upto 2.3 ppm and 4.2 ppm respectively, indicating that maximum part of U and Th, in sand size matrix of QPC, is situated in uraninite.

Most of the Archaean graywackes and shales have Th/Sc ratio less than one and more than 0.1 (McLennan and Taylor, 1991). This ratio probably best reflects the overall composition of provenance (Taylor and McLennan, 1985). Th/Sc values > 1.0 can be found in most tectonic settinsg where stable crust or recycled sediments are exposed. This ratio in the MQPC and quartzites shows a great scatter when plotted against Sc (Fig. 8.5D). It varies from 0.05 to 10.00, which probably indicates a high order of reworking of

generally vary between 3.0 to 6.0 (McLennan and Taylor, 1991). This ratio in MQPC and quartzites varies from less than one to slightly more than four (Fig. 8.5A). It probably indicates the derivation of these sediments from the reworking of the crust and also the enrichment in U and depletion in Th, due to the presence of detrital uraninite.

8.4 RARE EARTH ELEMENTS AND Eu ANOMALIES:

REE data of the MQPC was determined in all 30 samples (Table 8.1) and almost all samples show a monotonous pattern with a slight variation in the abundance of ΣREE. Since these samples overlap each other, they have been plotted in six separate figures to maintain the clarity of each pattern (Fig. 8.6A-D). REE patterns of eight quartzite samples are plotted in Fig. 8.7A and B. Three quartzite samples show different patterns than those of MQPC (Fig. 8.7A). Two of them have negative Eu anomalies whereas one exhibit positive Eu anomaly. They also show positive Ce anomalies, which indicates that Ce^{+3} has not been oxidized to Ce^{+4} and thus further supports the reducing environment which is otherwise evidenced from the preservation of detrital pyrite itself. Four samples of the quartzite have REE patterns similar to those of MQPC. Four of them show negative Eu anomaly whereas one of them exhibits positive Eu anomaly (Fig. 8.7A and B). Most of the samples of quartzite also show -ve Eu anomalies and a very large variance in their ΣREE concentrations, from 3.18 - 150 ppm (Table 8.2). Since most of these samples of quartzite, contain 80-90% of quartz, and in addition some of them contain feldspars, the variation of the shape of REE patterns, nature of Eu anomalies

Fig. 8.6 Shows the rare earth patterns of the QPC samples. All the samples have similar REE pattern shape, negative Eu anomalies. For the sake of clarity have been plotted in different diagrams.

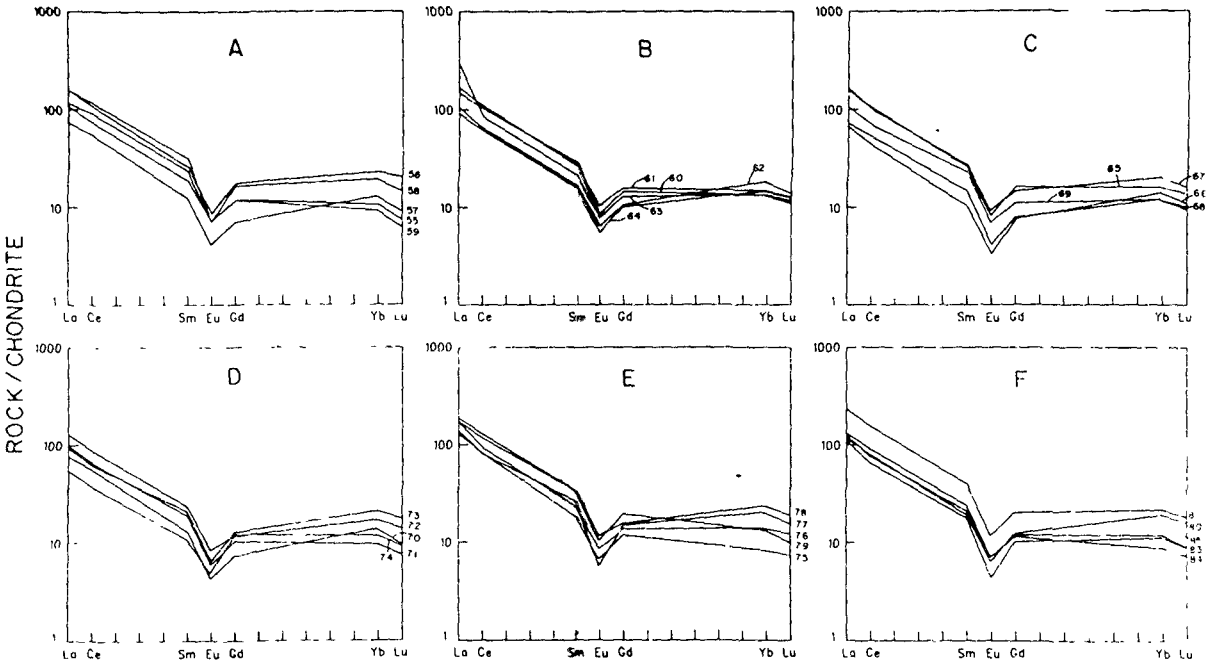
ROCK / CHONDRITE
1000
100
10
1
A
B
C
D
E
F
La Ce
Sm Eu Gd
Yb Lu

Fig. 8.7 (A&B) Show REE distribution patterns in quartzites.

(C) Maximum and minimum REE concentration of QPC and quartzites are compared with NASC (North American Shale Composite), AAS (Average Archaean Shale) and ASLMR (Average Suspended Load in Modern Rivers).

(D) Shows REE pattern in pyrite samples; for comparison REE pattern of sulphide facies BIF from Chitradurga is shown. Differences of the two may be noticed.

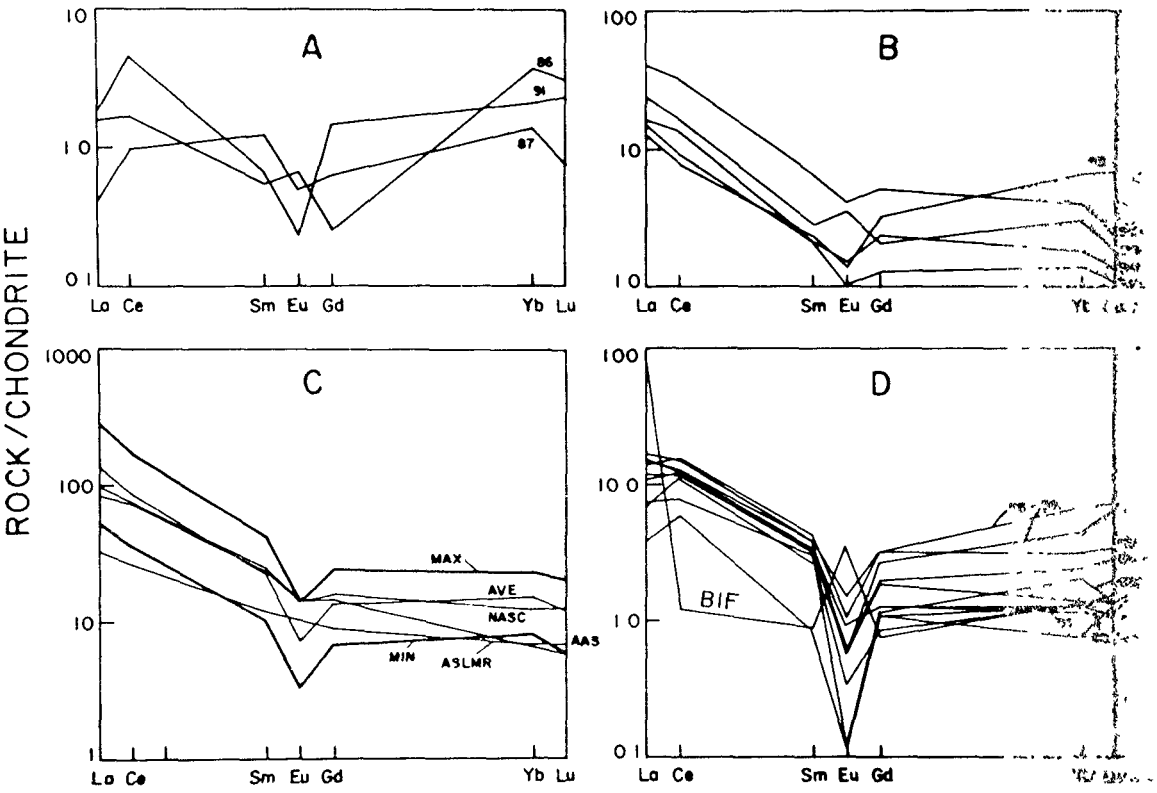
ROCK/CHONDRITE
A
B
C
D
10
1 0
0 1
100
10
1 0
1000
100
10
1
100
10 0
1 0
0 1
La Ce
Sm Eu Gd
Yb Lu
86
91
87
MAX
AVE
NASC
MIN
ASLMR
AAS
BIF

and the LREE/HREE ratios are expected to be explained by the presence or absence of plagioclase and heavy minerals. Sample No. MK-90, which contains about 10% plagioclase, is having a moderate +ve Eu anomaly. However, sample (MK-93) containing about 10% plagioclase shows -ve Eu anomaly. Vice versa, Sample No. MK-91 shows a very strong -ve Eu anomaly, though it does not contain any K-feldspar (Table 6.2). However, in this sample about 11% cementing and micaceous constituents are present and the Eu anomaly may be attributed to this micaceous constituent. At high level of abundance of quartz, REE are expected to be depleted in ΣREE. Since cementing material, plagioclase, mica and heavy minerals are found in different proportions in these quartzites, they exhibit inconsistent REE patterns and abundances.

An average of 30 samples of MQPC has been taken for comparison with the other sediments like NASC and AAS and also with average ΣREE of the suspended load in the modern rivers (Fig. 8.7C). It may be seen that the MQPC has quite high average ΣREE content which ranges from 244-814 ppm. All samples show LREE enrichment with sloping pattern from La to Sm, a strong -ve Eu anomaly and mostly flat HREE pattern (Fig. 8.6A-D). La/Lu and LREE/HREE ratios are more than one (Table 8.1 and 8.2). Though there is some difference in the magnitude of Eu anomalies (Eu/Eu^* = 0.30 to 0.51), they largely resemble to NASC, and the average suspended load in modern rivers (Fig. 8.7C). As compared to AAS, they have pronounced differences in LREE enrichment and -ve Eu anomalies and moderately fractionated LREE.

Pyrite of MQPC, shows moderate abundance of ΣREE, varying from 26 ppm to 89 ppm (Table 8.3, Fig. 8.7D). Pronounced -ve Eu anomalies, slopy pattern from Ce to Sm with flat pattern from Gd to Yb or Lu, are characterstic of the detrital pyrite (Table 8.3, Fig. 8.7D). Pyrite of the sulphide facies of BIF of Chitradurga schist belt and other regions, generally exhibits La enrichment, +ve Eu anomalies and extreme ΣREE depletion (Fig. 8.7D) (Barrett et al, 1988; Gnaneswar Rao, 1991). The pronounced REE difference in pyrite of MQPC and pyrite from sulphide facies BIF, suggests that the origin of these two types of pyrite is different. Rare Earth Elements data from the Archaean BIF indicate that the mantle derived hydrothermal solutions have played an important role for the formation of BIF (Derry and Jacobsen, 1990). The εNd = $^{143}Nd/^{144}Nd$ isotopic data which is around +4 along with the +ve Eu anomalies of all facies of BIF also indicate that hydrothermal solutions from depleted mantle provided Fe and REE of BIF (Jacobsen and Piemental-Klose, 1988). Therefore, the REE patterns of pyrite from MQPC do not indicate that this pyrite was derived from some older sulphide facies BIF or from mantle derived hydrothermal activity. It is possible that this pyrite, formed during the formation of TTG and was present as veins or porphory in TTG. Since detrital uraninite is also associated with this pyrite, it seems appropriate to suggest that it has come from a vein type sulfide deposit. It is further substantiated with sulphur isotopic ($\delta^{34}S$) data, which ranges from +2.1 to +3.3 (Table 8.3), excluding the isotopic fractionation through biogenic mediation.

LREE/HREE ratios in MQPC vary from 1.31 to 5.32. LREE enrichment and relative HREE depletion in all samples of MQPC is clearly visible in (Fig. 8.8A). Between 65 ppm to 143 ppm concentration of HREE, a scatter between 147 ppm and 673 ppm LREE is found in the samples of MQPC (Fig. 8.8A). Low order +ve correlation coefficient exists between LREE and HREE (r = 0.58), which may be explained due to variable concentration of pyrite, fuchsite and zircon. Simultaneous linear increase in LREE and HREE is not observed in MQPC (Table 8.1). Both LREE and HREE are depleted in quartzite compared to MQPC. However a +ve low order correlation coefficient (r = 0.38) between LREE and HREE is observed in quartzites (Fig. 8.8A). In six samples of the quartzite, HREE are generally more than LREE, and in four samples LREE are enriched compared to HREE (Fig. 8.8A) and LREE/HREE ratios vary from 0.14 to 4.63. The differences in abundances of LREE and HREE of MQPC are the result of the presence of variable matrix constituents, like pyrite and fuchsite. Similarly La/Lu ratio of the MQPC shows a great range from 3.92 to 26.94. In quartzite this ratio varies from 17.18 to 0.29 (Table 8.2) showing a scatter with weak positive correlation coefficient (Fig. 8.8B). In four samples of quartzite La/Lu ratios are nearly one (Fig. 8.8B). It may be noticed that in MQPC La concentrations as high as 300 ppm are found whereas maximum concentration of Lu is only 20 ppm. LREE enrichment, a characteristic of MQPC and upto certain extent quartzite also, coupled with the variation in the concentration of La, indicates that the silicic restites and terrigenous clays have been retained in these rocks and the heavy minerals like zircon and garnet are not present in high percentage

Fig. 8.8 (A) Illustrates simultaneous increase of LREE and HREE. The ratio of LREE/HREE between the two is more than one in all samples except six samples of quartzites.

(B) Shows simultaneous increase of La and Lu, La/Lu ratio is more than one in all samples except three samples of quartzites.

(C) Illustrates simultaneous increase of Zr and ΣREE.

(D) Illustrates simultaneous increase of Zr and HREE.

(E) Shows that both Rb and ΣREE increase in QPC whereas pyrite samples are depleted in Rb and ΣREE.

(F) Illustrates that except two, all samples including pyrite exhibit negative Eu anomalies as they fall below the line showing 1:1 ratio of Eu and Eu*.

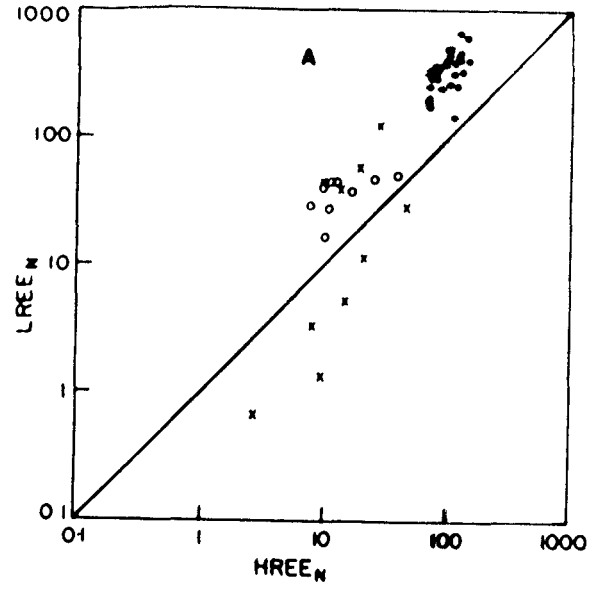
A
1000
100
10
1
0.1
0.1
1
10
100
1000
LREE$_N$
HREE$_N$

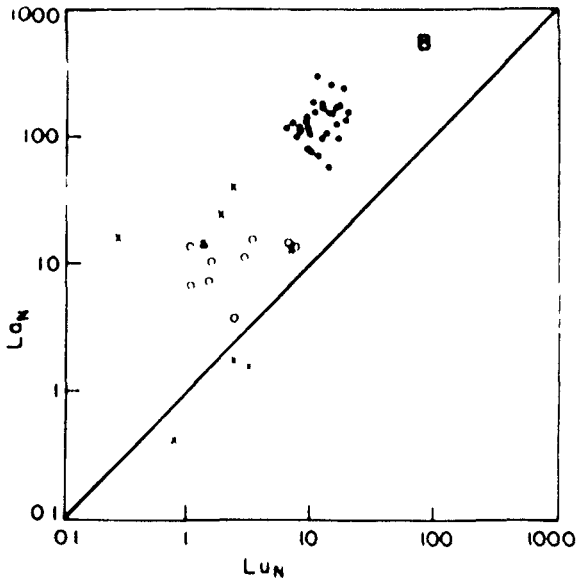
B
1000
100
10
1
0.1
0.1
1
10
100
1000
La$_N$
Lu$_N$

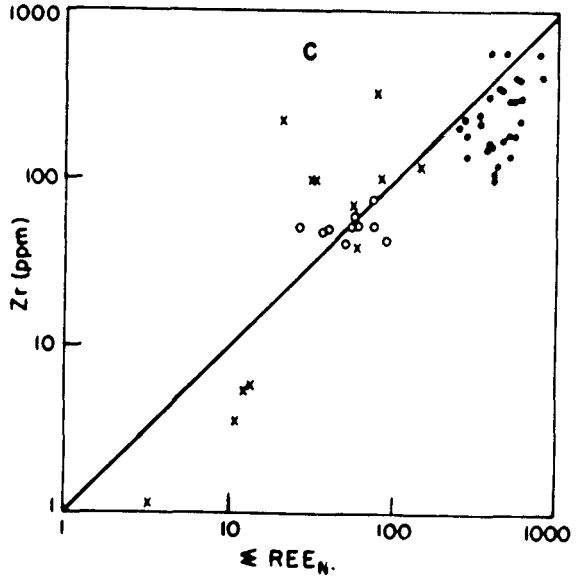
C
1000
100
10
1
1
10
100
1000
Zr (ppm)
Σ REE$_N$.

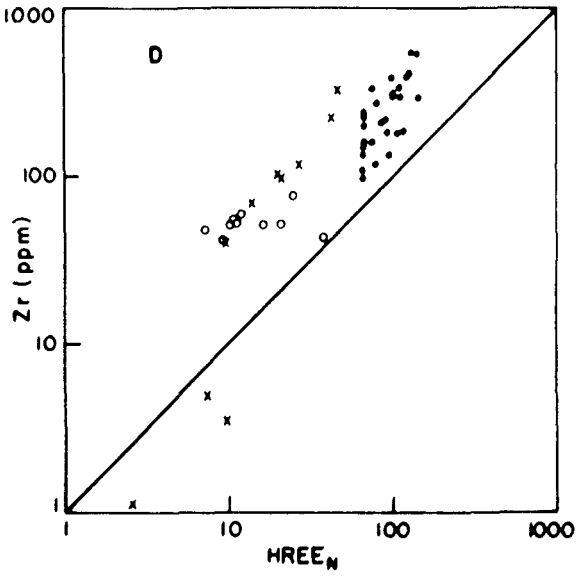
D
1000
100
10
1
1
10
100
1000
Zr (ppm)
HREE$_N$

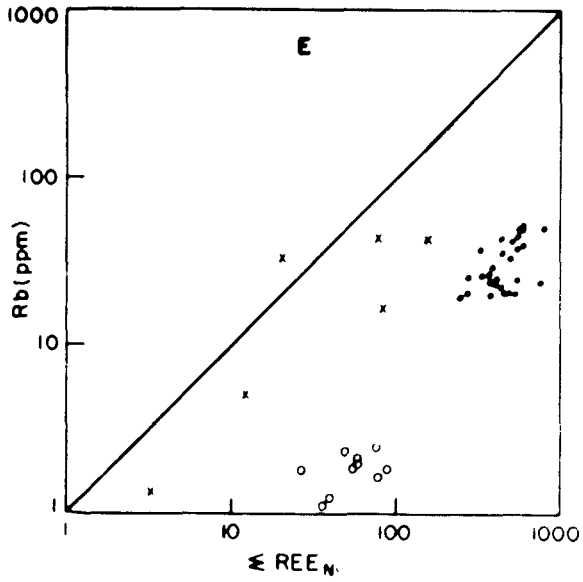
E
1000
100
10
1
1
10
100
1000
Rb(ppm)
Σ REE$_N$.

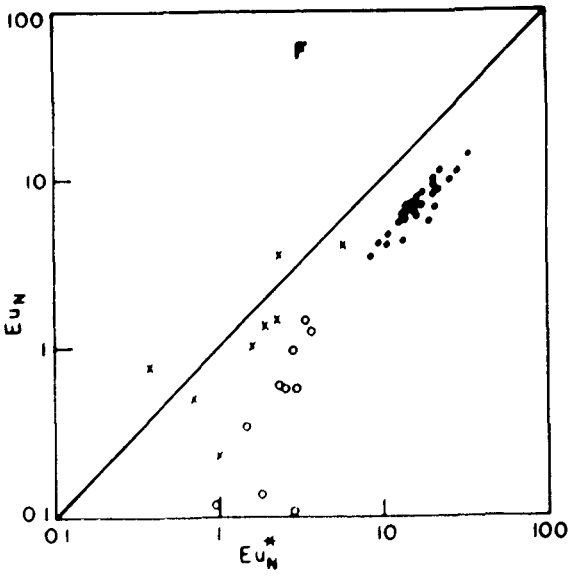
F
100
10
1
0.1
0.1
1
10
100
Eu$_N$
Eu$^*_N$

in the matrix in appreciable quantities. If zircon and garnet would have been present in appreciable quantity, HREE would have increased and Lu content would also have gone up. Maximum Zr concentration of MQPC is found around 580 ppm, with minimum value of 98 ppm. In quartzites, Zr varies between 11 ppm to 335 ppm. The ΣREE content of MQPC shows a scatter against Zr (Fig. 8.8C). No significant +ve correlation between Zr and REE is noticed. When Zr concentration is plotted against HREE content of these samples, a positive correlation coefficient (r = 0.71) is visible (Fig. 8.8D). It shows that Zr concentration has definitely contributed *towards the HREE concentration of MQPC and quartzites. However,* this effect is diluted by the presence of considerable amount of pyrite (Fig. 8.8D). When 10 samples of quartzite are considered, a very strong +ve correlation (r = 0.86) between Zr and HREE is observed (Fig. 8.8D). This shows that the abundance of heavy mineral in these quartzite and conglomerates is randomly distributed and though it has effectively contributed to the REE concentrations and patterns, interferance from other phases like pyrite has obliterated the effect of Zr abundance of HREE. It can be seen that Zr and HREE or ΣREE do not show any interdependence *in the pyrite samples (Fig. 8.8B, 8.8C, 8.8D). As such there is* no relationship between Zr and HREE of pyrite of MQPC. But its abundance level appears to have interfered with the relationship between the two.

As observed in Rb-Sr plot (Fig. 8.4E) the Rb concentration of MQPC and quartzite, is not distinct for the two suites. However, a binary plot between REE and Rb has separated these two populations and the pyrite also (Fig. 8.8E). It shows a low order correlation

(r=0.55 and 0.68) between ΣREE and Rb. The relationship between Rb and K, Rb and ΣREE and Al_2O_3-ΣREE (Table 8.1 and 8.2) clearly demonstrates that the enrichment in ΣREE_N is dependent on the amount of micaceous minerals present in the matrix. The pure chert and quartzites are found to be extremely depleted in ΣREE (Taylor and McLennan, 1985).

A perfect linear relationship between Eu and Eu^* is illustrated by MQPC and quartzites (Fig. 8.8F). With the exception of two samples of quartzite, all samples of quartzites and MQPC are having -ve Eu anomalies of variable magnitude. The order of -ve Eu anomalies in MQPC is high (Eu/Eu^*=0.51 to 0.30) compared to quartzites (Eu/Eu^*= 0.23 to 1.82). All samples fall below 1:1 line. Simultaneous increase in Eu and Eu^* is visible. This indicates that with the increase in ΣREE which is reflected by Eu concentrations, the magnitude of -ve Eu anomalies is also increased (Fig. 8.8E). It has already been demonstrated that the ΣREE abundances are dependent on Al_2O_3 and K_2O, thus on micaceous minerals. Therefore, the magnitude of -ve Eu anomalies is an after effect of the quantity of micaceous minerals present in the matrix and cement. This phenomenon reflects the compositional characteristic of the stable minerals present in the source area, which have been left in these sediments.

Presence of detrital pyrite indicates anoxic environment of weathering and reducing environment of deposition. This is further substantiated by the presence of positive Ce anomalies in some samples of quartzites. Inspite of such environment over source area and within the basin, rocks with strong -ve anomalies are formed. This reflects that the nature of the Eu anomalies are

mainly dependent on the nature of the minerals present in the source area and not on the oxygen fugacity of the weathering or depositional environment. Cr is present in fuchsitic mica, which is more abundant in MQPC, therefore both Cr and REE simultaneously increase (Fig. 8.9A). Geochemical characteristics of REE and Cr are distinctly divergent. Cr is found abundant in ultramafic rocks which are extremely depleted in REE, but the common factors between the two are K_2O and Al_2O_3 of fuchsite and thus both increase together in MQPC. It must be noted that REE patterns and their relationship with different elements in the overlying BIF and the KCM are entirely different from MQPC and quartzites (Chapter X and XI).

At several places QPC and associated quartzite are found enriched in U and Th (B.V. Rama Rao, 1974). In our samples, significant relationship between La (representing REE), and U + Th is found (Fig. 8.9B). Generally it is expected that in a rock suite, LREE and U-Th go together (Taylor and McLennan, 1985). Our data indicate that MQPC which contain higher U+Th also contain elevated concentration of La which represents LREE. Interference from pyrite in our samples has obliterated this relationship to some extent.

Archaean graywackes (active margin turbidites) and shales show a very large scale scatter when their Eu/Eu^* and Gd/Yb ratios are plotted (McLennan and Taylor, 1991). Most of the samples of Archaean active margin turbidites occupy thus a place in the quarter of $Eu/Eu^* = 0.85$ and $Gd/Yb = 2.0$ (Fig. 8.9C) far away from the place of active margin turbidites. Our data, since it belongs to mature sediments fall between $Eu/Eu^* = 0.7$ and $Gd/Yb = 1.5$.

Fig. 8.9 (A) Illustrates simultaneous increase of Cr and ΣREE.

(B) Demonstrates the enrichment of La and U, Th in QPC.

(C) Plot of Eu/Eu^{*} and Gd/Yb. This illustration demonstrates the stable platformal tectonic setting of deposition for QPC.

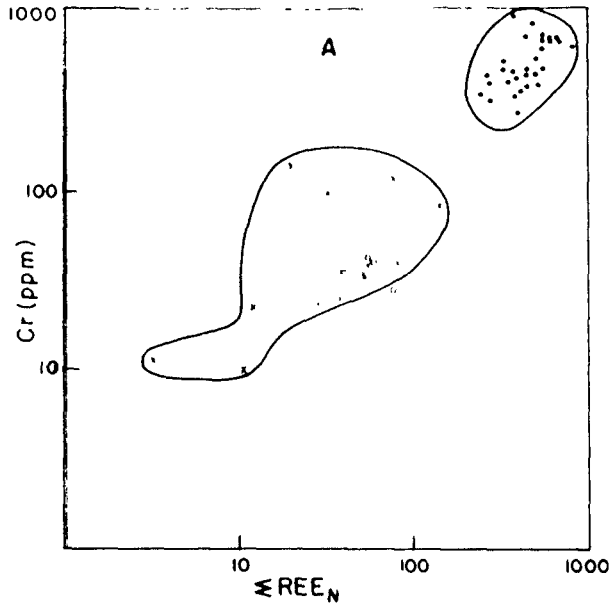
A
1000
100
10
Cr (ppm)
10
100
1000
ΣREE$_N$

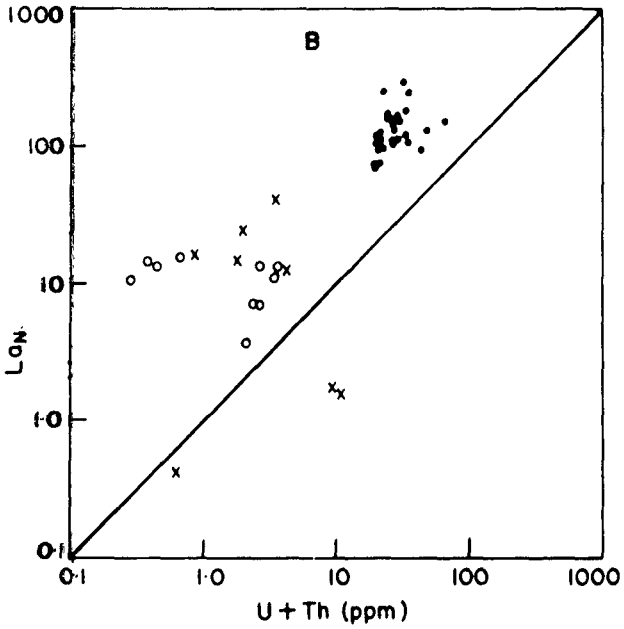
B
1000
100
10
1·0
0·1
La$_N$
0·1
1·0
10
100
1000
U + Th (ppm)

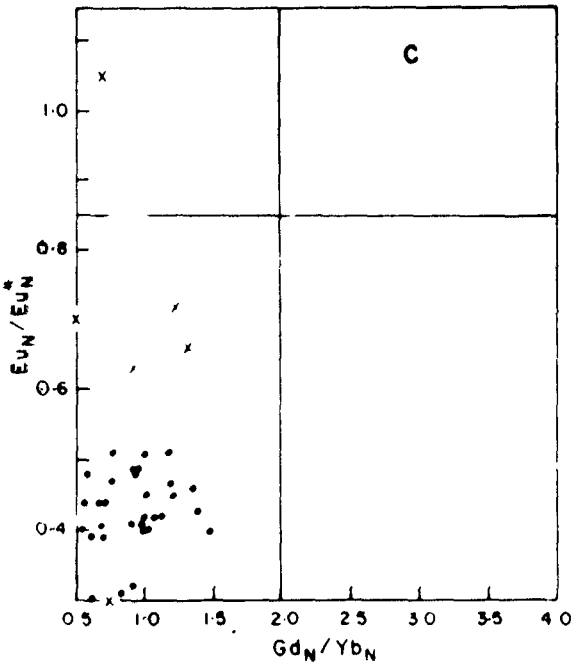
C
1·0
0·8
0·6
0·4
Eu$_N$/Eu$^*_N$
0·5
1·0
1·5
2·0
2·5
3·0
3·5
4·0
Gd$_N$/Yb$_N$

This is a very clear indication that mobile elements have been leached away and restites supplied from the continental crust are controlling these ratios due to environment of weathering and deposition.

The data presented above indicate that QPC and quartzite have been produced by intense chemical weathering and strong high energy hydrodynamic processes. They have been deposited in a reducing environment above wave base and photic zone. Presence of detrital pyrite and uraninite is a very strong evidence to suggest that the atmosphere in the zone of weathering was anoxic and at the site of deposition, it was highly reducing. However, within a distance of a few kilometres and stratigraphically a few hundred meters above, this environment became rhythmically oxidizing and produced one of the most widespread and thickest oxide facies of BIF. Geochemistry of BIF and interbedded sequences of volcanic rocks of the Bababudan schist belt is described in Chapters IX and X.

The changes in the weathering environment and style, and also in the tectonic setting and depositional environment as envisaged from these data along with the data on volcanic rocks BIF and KCM are discussed in Chapters XIII and XIV.

CHAPTER IX

GEOCHEMISTRY OF ASSOCIATED VOLCANIC ROCKS

9.1 INTRODUCTION:

Volcanism plays a vital role in all the stages of lithospheric evoluation. Advent of Plate Tectonics has revolutionised the approach to many of the problems, related to the crustal evoluation. Burke and Kidd (1980) have reviewed the various types of volcanic rocks and their probable tectonic environments. They suggest that basalt forms at divergent plate boundaries; tholeiitic and calc-alkaline rocks, most characteristically andesite dominate where arcs form above subduction zones; highly potassic volcanics are associated with active continental collision. Burke and Kidd (1980) believe that these processes along with the intraplate volcanism, appear to have operated at plate margins throughout most of the earth's history.

Like other greenstone belts, the Bababudan schist belt, has also been constituted of basic volcanics, thus for better understanding of the tectonic setting of this belt throughout its development, the geochemical inputs from volcanic rocks and BIF are necessary. Again, for proposing a more realistic model to reconstruct the evolutionary stages of the basin, the incorporations of these studies with the main subject of work, is very significant. The validity and relevance for the proposed model for basin evolution, depends upon its capabilities to explain the mode of genesis of each and every rock type, present

within the basin, and it should be in accordance with the global scenario and understanding of similar sequences exposed elsewhere. With this objective, the geochemical characteristics of volcanic rocks and BIF of Bababudan belt are included in this chapter and chapter-X respectively.

The database (Table 9.1) used in this chapter is borrowed from the earlier published work (Bhaskar Rao, 1980; Bhaskar Rao and Drury, 1982; Drury, 1983), in this table major elements are in wt. percent and trace & REE are in ppm. Main emphasis is given to their (volcanic rocks) compositional variation, and geochemical data were mainly used to understand the petrogenesis of these volcanics with a view to understand their possible tectonic setting.

9.2 GENERAL GEOCHEMICAL CHARACTERS:

Compositionally, the metavolcanics of the Bababudan schist belt are of unimodal (basalt-basaltic andesite) association (Pichamuthu, 1946; Sreenivas and Srinivasan, 1974). However, Santaveri volcanic suite includes a small but significant proportion of siliceous volcanics (rhyodacite - soda rhyolites) and is thus bimodal (Bhaskar Rao and Naqvi, 1978). Bhaskar Rao (1980) has carried out detailed geochemical studies of these volcanic rocks, he suggests that all suites display distinct tholeiitic affinity and are characterized by moderate $Al_2O_3^{(t)}$ and low TiO_2, K_2O abundances. A decrease in iron enrichment in basaltic andesites in the order of basal to upper parts, suggests a progressive increase in the calc-alkalic affinity from "low" to "high" stratigraphic levels. The volcanic suites associated with

Table 9.1

Average chemical composition of Volcanic rocks of the Bababudan schist belt (Sources Bhaskar Rao, 1980; Bhaskar Rao and Drury 1982; Drury 1983).

Elements	MAX.	MIN.	AVE.	NO.OF SAMPLE
SiO_2	74.70	42.20	60.26	22
Fe_2O_3	15.30	7.40	11.65	22
TiO_2	1.99	0.49	1.09	22
Al_2O_3	14.70	3.70	11.88	22
MnO	0.32	0.05	0.18	22
MgO	29.80	0.17	5.70	22
CaO	11.43	0.79	5.66	22
Na_2O	6.90	1.30	3.24	21
K_2O	2.10	0.08	1.04	21
P_2O_5	0.24	0.05	0.13	21
Sc	39.00	6.28	22.26	16
V	434.00	4.00	248.20	5
Cr	2908.00	3.00	334.29	21
Co	147.00	27.00	69.59	22
Ni	2305.00	1.20	250.58	21
Rb	73.00	1.00	25.07	20
Sr	400.00	38.00	20.27	20
Y	65.00	10.00	33.64	22
Zr	334.00	10.00	163.05	21
Nb	19.00	2.10	10.61	21
Ba	563.00	36.00	233.58	19
Hf	8.92	0.10	0.45	16
Ta	1.53	0.39	0.89	15
La	61.90	7.10	25.70	16
Ce	136.50	12.40	51.69	16
Nd	66.50	5.40	26.70	16
Sm	13.80	0.80	5.93	16
Eu	2.85	0.30	1.61	16
Gd	11.40	0.90	5.90	16
Tb	1.72	0.20	0.51	16
Tm	1.06	0.10	0.52	16
Yb	6.05	0.40	3.01	16
Lu	0.84	0.10	0.48	15

the BIF are probably calc-alkalic. (Bhaskar Rao, 1980). Bhaskar Rao and Drury (1982) studied the incompatible elements of these volcanics. Mainly Ti, Rb, Sr, Ba, Zr, Nb, Y and REE, Sc, Hf, Ta and Th were described and interpreted. They suggest that these volcanic suites are genetically related and show general calc-alkaline affinities. The parent magma is proposed to have been formed by about 15% partial melting of mantle at shallow depth (Bhaskar Rao and Drury, 1982). Drury (1983) studied volcanic rocks of the Bababudan belt, alongwith other four Archaean volcano-sedimentary assemblages, and suggested that volcanism in each belt was petrogenetically similar and form a single geochemical population, which may indicate that either a single major cycle of magmatic activity is represented by variably deformed and metamorphosed volcano-sedimentary belts, or several cycles involving similar sources and petrogenetic processes.

The source mantle for the volcanic rocks of the Bababudan schist belt, is shown to have been enriched in LREE and Zr relative to primitive fractionation of first olivine and pyroxene to produce compatible elements enriched and Cr, Ni and Co depleted tholeiites, which were then accompanied by plagioclase feldspar and possibly magnetite to generate the andesites and rhyodacites (Bhaskar Rao and Drury, 1982). However, there is a wide range of variation in the trace elements concentration of volcanic rocks of the Bababudan belt. Tholeiites of Kalasapura Formation show an enrichment in Cr, Ni and Co comparable to most of the Archaean tholeiites from other cratons and Chitradurga volcanics, within the same craton (Naqvi, 1972, Naqvi and Hussain, 1973 a and b). Whereas Santaveri volcanics show characteristically lower Cr, Ni

and Co and has no analogue either in the Archaean or in the Phanerozoic (Bhaskar Rao, 1980). In contrast to the basalts and basaltic andesites, the siliceous volcanics in the same stratigraphic horizon, have abnormally high Cr and Ni abundances and these basalts and basaltic andesites are characterized by LREE enriched REE patterns, having higher Zr, Y, Zr/Y, Y/Ni, Ti/Y ratios and depleted Ti (Bhaskar Rao and Drury, 1982, Drury 1983).

9.3 TRACE ELEMENTS GEOCHEMISTRY AND TECTONIC SETTING:

During the last two decades, a number of trace element studies have been made on volcanic rocks of different places and time, with the aim of identifying their eruptive environment (Pearce, 1973; Bickle and Nisbet, 1972; Pearce, 1975; Sevigny and Brown, 1989). Burke and Kidd (1980) have given an excellent summary on this aspect. Bhaskar Rao and Drury (1982) in their studies on Bababudan volcanics, concluded that standard tectonic characterization parameter do not give consistant results for this suite and until more is known about overall structure, stratigraphy and relative ages within the south India Archaean Craton, a precise setting can not be described. However, for volcanic rocks of five greenstone belts of south India, Drury (1983) believes that the favoured tectonic setting for the magmatism is that suggested by Weaver and Tarney (1979), namely diapirism above a shallow angled subduction zone, and magma emplacement through older crust into multiple back-arc basins. Drury (1978) explained that the paralle "Swarm" of Indian volcano-sedimentary belts is a consequence of the "controlling subduction zone". This zone was shallow angled, involving thin

and hard lithosphere so that diapirs were triggered over a wide area from similar depths. In our view, this probable proposed tectonic settings do not explain the existence of juxtaposed underlying quartzites and overlying Banded Iron Formation; since for the deposition of BIF, hydrothermal input sites (Vents) are needed, which are usually associated with mid-oceanic ridges. For this reason, an attempt is made to reconstruct the eruptive environment of Bababudan volcanics and integrate it with the conclusions drawn from the field, petrography and geochemistry of QPC, quartzites, BIF and the KCM.

Because of the problem of element mobility during alteration, this work concentrates on elements (Cann, 1970; Humphris and Thompson, 1978) of high ionic potential which are considered to be immobile in basalts during weathering and metamorphism upto greenschist facies.

The discriminative diagrams presented below have been devised from a data bank containing some 3000 immobile element analyses of some of the most suitable elements for separating normal mid-ocean ridge basalt (MORB), island arc tholeiite (IAT) and within plate basalt (WPB) magma types (Pearce, 1980). However, while descriminating magma types after using these diagrams, their possible and probable transitional tectonic setting should also be taken into account. For example, MORB/IAT types can be found in some marginal basin setting (Reay et al. 1974): MORB/WPB types can be found in diffuse spreading centers; WPB/IAT types may be formed above subduction zones in areas where continental back arc rifting is also taking place or close to trench - transform fault intersections (De Long et al., 1976).

9.3.1 Ti-Zr Diagram:

Volcanic suites of the Bababudan Schist Belt are plotted in Ti-Zr binary diagram (Fig. 9.1 A). In these suites TiO_2 varies from 0.49 to 1.99%, whereas Zr ranges from 10-334 ppm (Table 9.1). This diagram provides a means of filtering off and classifying intermediate and acid rocks from the basalts. Compositionally volcanic rocks of Bababudan greenstone belt vary from basalt to rhyodacite through basaltic andesite and andesite, which is reflected in a wide scatter of data points (Fig. 9.1 A). Nevertheless, a sizeable number of data point fall into the field of within plate type and one sample occupies its place in the field of MORB and three samples fall within the Island Arc tholeiite field.

9.3.2 Geochemical Patterns:

For the purpose of comparison, the incompatible element pattern for basalts normalized to an average MORB composition is a useful guide to magma type (Pearce, 1983). In Fig. (9.1 B) some patterns from Bababudan volcanics are plotted. All the incompatible elements (e.g., Sr, K, Rb, Ba, Ta, Nb, Ce, kP, Zr, Hg, Sm, Ti, Y, Yb, Sc and Cr) have been normalized to average MORB concentration, analysed by Pearce (1980). Pearce (1980) found that these patterns show that the distinguishing features of WPB relative to MORB are the higher content of all elements except those (Y, Yb, Sc and Cr) compatible with a garnet lherzolite. Similarly the distinguishing feature of IAT relative to MORB is the lower content of all immobile elements. Six, out of total 21 samples, show a variable behaviour of different elements with

Fig. 9.1 : (A) Ti-Zr diagram for metavolcanic rocks of the Bababudan schist belt. Ten samples are falling into the field of Island Arc Tholeiite (IAT), one sample shows the characteristics of Mid Oceanic Ridge Basalt (MORB) type. Four samples are not falling in either zone, having more or less same level of TiO_2 but with a greater variation in their Zr contents.

(B) Geochemical patterns (spider diagrams) for some incompatible elements of the volcanic rocks from the study area, which are normalized to a typical MORB analysis (Sr = 120 ppm; K_2O = 0.15%; Rb = 2.0 ppm; Ba = 20 ppm; Ta = 0.18 ppm; Nb = 4 ppm; Ce = 10.0 ppm; P_2O_5 = 0.12%; Zr = 90 ppm; Hf = 2.4 ppm; Sm - 3.3 ppm; TiO_2 = 1.5%; Y = 30 ppm; Yb = 3.4 ppm; Sc = 40 ppm; and Cr = 250 ppm). It is clear from this diagram that Bababudan volcanics, are calc-alkaline.

(C) Plot of Cr against Y to discriminate volcanic rocks of different tectonic settings. It shows the field of Within Plate Basalt (WPB) occupied by the Bababudan volcanics. However, 2 samples are falling into the field of MORB, but MORB/WPB types can be found in diffuse spreading centres such as Iceland and Afar.

(D) Plot of Zr/Y against Zr showing that most of the samples of Bababudan volcanics represent the characteristics of WPB type. (Fields after Pearce, 1980).

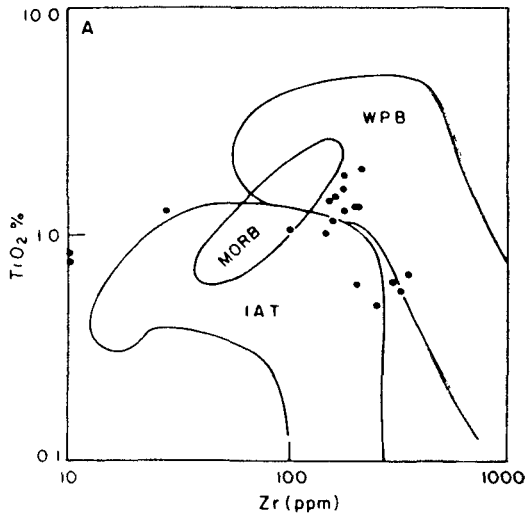
A
10 0
1 0
0 1
TiO_2 %
10
100
1000
Zr (ppm)
WPB
MORB
IAT

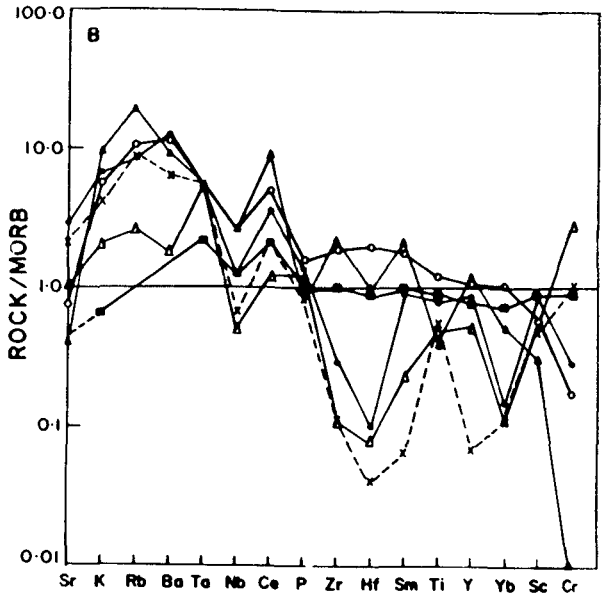
B
100·0
10·0
1·0
0·1
0·01
ROCK/MORB
Sr K Rb Ba Ta Nb Ce P Zr Hf Sm Ti Y Yb Sc Cr

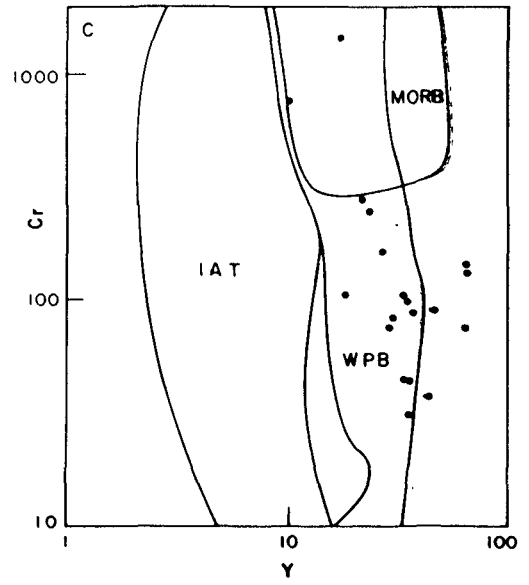
C
1000
100
10
Cr
1
10
100
Y
MORB
IAT
WPB

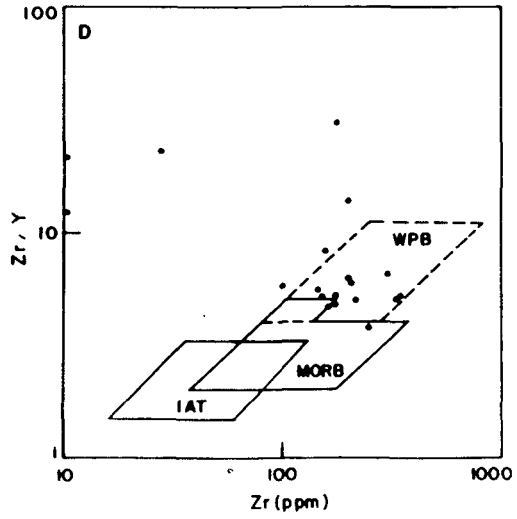
D
100
10
1
Zr, Y
10
100
1000
Zr (ppm)
WPB
MORB
IAT

respect to MORB. In general, Sr, K, Rb, Ba, Ta, Nb, Ce and P show comparatively higher concentration than the MORB average concentrations. Except 2 to 3 samples, they show a pattern similar to WPB type volcanics. Exceptionally low concentrations of Zr, Hg and Sm, which are supposed to be characteristic elements, concentrated in WPB along with comparatively higher TiO_2, have partially obliterated elemental pattern of typical WPB. It is also noticed that these patterns show very high concentrations of K, Rb and Ba, indicative of high content of alkalines. The CaO contents in these samples range upto 9.63% (Table 9.1), and show the calc-alkaline nature of volcanic rocks. Pearce (1980) in his original work has not considered the calc-alkali basalts from WPB setting. These patterns obviously vary as a result of fractional crystallization, especially the Sr, Cr and Sc components. Therefore, these observed patterns might be representative of this particular variety. Similar type of volcanics have also been reported from Tibesti (Burke and Kidd, 1980).

9.3.3 Y-Cr diagram:

Generally WPB consists comparatively higher concentration of immobile trace elements, in comparison to MORB and IAT for lavas that had undergone approximately equal degrees of fractional crystallization (Pearce and Cann, 1973; Condie and Crow, 1990). Thus a diagram of such element (Y) against a fractionation index (Cr), should separate the IAT group from rest of WPB and MORB (Pearce, 1980). As shown in Fig. (9.1 C), it is clear that within a short limit of Y (10-65 ppm), there is a wide variation in the

concentration of Cr from 30 to 1400 ppm (Table 9.1). It must be noted from Fig. (9.1 C) that although volcanic rocks of the Bababudan belt show a large variation in their degrees of crystal fractionation, their Y content ramains limited and they fall in the field of WPB. However, with the same range of concentration of Y, but with the extremely high degree of crystal fractionation, it is impossible to distinguigh beteeen WPB and MORB.

9.3.4 Zr/Y-Zr Diagram:

As suggested by Pearce (1980), the distinguishing immobile element feature between WPB and MORB is the high content of elements like Nb, Ce and Zr relative to Y and Nb. Although in our samples Nb and Ce show relatively high contents, but Zr is not that well distinguishable, because in four samples it is comparatively higher whereas in rest two samples it is relatively lower than the corresponding value of Y. A ratio such as Zr/Y should therefore be most effective in distinguishing these two magma types. The ratio Zr/Y varies from 3.8 to 30.56 (Table 9.1) and plotted against Zr in Fig. (9.1 D). It may be noted from Fig. (9.1 D) that about 11 points fall into the field of WPB and except one which is well within MORB field, rest of points are showing higher Zr/Y ratio, therefore fall outside the devised field.

On the basis of the data presented above it may be seen that the Bababudan volcanic rocks represents a product of transitional tectonic setting of WPB and MORB. In the initial stages probably on the rift developed in the Intracratonic Shallow water basin WPB were emplaced and as the spreading took place MORB were emplaced and by the time the tensional regime gave way to compressional regime, volcanic rocks of active continental margin were erupted.

CHAPTER X

GEOCHEMISTRY OF BANDED IRON FORMATION

10.1 INTRODUCTION:

Banded iron formations form an important component of the Archaean schist belts all over the world and occupy a unique position in the Archaean Sedimentation history as they have no modern analogue. In Indian Archaean greenstone belts, oxide facies BIFs have attained a thickest sequence in the Bababudan schist belt, which is not exposed anywhere else in rest of the world (Radhakrishna et al., 1986).

One of the major gaps in our knowledge about the evolution of the Archaean greenstone belts of Dhrawar Craton is the lack of understanding of geochemical characteristics of BIF. As Radhakrishna et al. (1986) have pointed out that no systematic comparative geochemical investigation of the different facies of BIF of India has been attempted so far. Due to the lack of relevant data, like trace elements, REEs and isotopic genetic interpretation of BIF has not been attempted. Consequently the constraints from BIF geochemistry for the evoution of the Archaean greenstone belts were not applied.

BIF of Bababudan schist belt proper are being studied by Govil and Naqvi (personal communication). BIFs equivalent to the horizon exposed in Bababudan schist belt are found in Kudremukh, Sandur and Chitradurga belts which have been studied in great detail by Khan et al. (1991, Kudremukh schist belt), Manikyamba et al. (1991, Sandar schist belt) and Gnaneswar Rao (1991,

Chitradurga schist belt). As discussed in previous chapters, the prime objective of the present work is to reconstruct the depositional, tectonic environment and and the evolution of the Bababudan schist belt. This model should be able to explain the mode of genesis of each and every lithology present in the basin. Constraints provided by the BIF of the basin are essential for suggesting a model for the evolution of the basin and the middle late Archaean crustal development.

Since Kudremukh oxide facies BIF is equivalent to the BIF of Bababudan schist belt (Swami Nath and Ramakrishnan,1981), the major (wt. per.) trace and REE (in ppm) data of BIF of Kudremukh Schist belt are borrowed (Table 10.1) from Khan et al. (1991) and the possible interpretation proposed by these (ibid) authors.

10.2 GEOCHEMICAL CHARACTERISTICS OF BIF:

10.2.1 Major and Trace Elements:

Table (10.1) shows that there is a significant variation in almost all the major elements especially SiO_2, Al_2O_3, Fe_2O_3, TiO_2, and K_2O The variation in $SiO_2/Fe_2O_3{}^{(t)}$ depends upon the thickness of the meso and micro bands present in the sample. On the basis of Al_2O_3 and TiO_2, BIF have been divided into cherty BIF (CBIF) and shaly BIF (SBIF). It may be noted from Fig.(10.1A), that SBIF are enriched in both Al_2O_3 and TiO_2 whereas CBIF contain comparatively low concentration of these two oxides, even most of the samples are containing only 0.01% of TiO_2 with less than 1% Al_2O_3. SBIF are further characterized by relatively high concentration of K_2O, Na_2O, Rb and Sc (Table 10.1). These data

Table 10.1: Average chemical composition of CBIF and SBIF from Kudremukh schist belt (Source Khan et al., 1991).

Elements	CBIF				SBIF			
	MAX.	MIN.	AVE.	NO.OF SAMPLE	MAX.	MIN.	AVE.	NO.OF SAMPLE
SiO_2	68.16	60.32	69.58	32	61.43	31.12	45.60	9
Fe_2O_3	0.38	0.87	0.46	32	51.86	4.32	32.10	9
TiO_2	15.39	15.78	12.61	29	4.58	0.01	1.54	9
Al_2O_3	3.78	7.86	4.48	29	14.40	3.11	7.10	9
MnO	0.05	0.10	0.07	32	0.54	0.01	0.15	8
MgO	2.09	4.63	2.55	32	13.64	0.56	3.61	9
CaO	0.38	0.67	0.86	30	5.23	0.14	2.00	7
Na_2O	4.05	2.89	2.96	31	1.69	0.12	0.62	9
K_2O	2.15	3.20	2.80	32	4.65	0.76	2.68	9
P_2O_5	0.15	0.16	0.10	31	0.12	0.01	0.06	4
Sc	5.49	0.21	2.04	32	37.89	1.55	13.00	9
V	133.00	1.11	39.18	30	349.35	4.95	101.11	9
Cr	94.01	1.82	19.39	32	1709.65	10.09	275.43	8
Co	148.05	8.92	42.85	32	86.24	12.38	38.40	9
Ni	33.17	0.21	9.09	32	687.30	3.65	108.87	9
Cu	84.90	0.44	17.35	32	364.36	2.19	67.25	9
Zn	175.18	9.16	35.03	32	324.50	42.55	104.87	9
Ga	5.74	0.37	1.96	32	19.98	2.65	10.42	9
Rb	140.72	0.22	24.72	32	953.37	151.38	451.82	9
Sr	110.11	1.91	43.52	32	287.80	5.05	83.93	9
Y	9.54	1.47	5.27	32	26.05	1.00	12.20	9
Zr	24.88	0.55	8.58	32	412.38	3.40	109.39	9
Nb	1.13	0.03	0.38	32	20.03	0.70	6.69	9
Ba	479.10	1.16	93.28	32	996.24	124.63	497.85	9
Hf	0.57	0.02	0.26	28	7.96	0.02	2.21	9
Ta	1.09	0.09	0.80	32	3.54	0.12	1.08	9
La	10.43	0.35	4.34	32	106.30	1.19	23.58	9
Ce	21.15	0.74	5.44	32	308.68	3.15	66.62	9
Pr	2.17	0.08	0.56	32	38.28	0.44	7.61	9
Nd	9.00	0.23	3.78	32	128.42	1.99	28.14	9
Sm	2.97	0.03	0.75	32	24.03	0.39	4.96	9
Eu	2.18	0.02	0.48	32	3.42	0.05	1.03	9
Gd	2.73	0.06	0.79	32	18.95	0.43	4.53	9
Tb	0.46	0.01	0.13	32	2.23	0.07	0.61	9
Dy	2.85	0.10	0.79	32	9.06	0.36	3.09	9
Ho	0.56	0.03	0.15	32	1.52	0.07	0.60	9
Er	1.55	0.07	0.41	32	3.38	0.18	1.49	9
Tm	0.23	0.02	0.06	32	0.46	0.02	0.20	9
Yb	1.26	0.05	0.38	32	2.77	0.12	1.22	9
Lu	0.20	0.01	0.07	32	0.40	0.01	0.18	9

Fig. 10.1 : (A) Al_2O_3 vs. TIO_2 plot shows enrichment of Al_2O_3 and TiO_2 in SBIF and depletion in most of the CBIF indicating mixing of continental debris along with the chemical precipitation of iron and silica, especially in SBIF. Solid circle = Cherty BIF (CBIf); Open circle = Amphibolite layer within CBIF; Open square = Shaly BIF (SBIF ; Amphibole bearing). Same symbols are used in Fig. 10.1 (B) also.

(B) Variation of Cr and MgO shows that a sample of SBIF is extremely enriched in Cr and MgO, it is a volcaniclastic material deposited along with chemical precipitates and a sample of CBIF is extremely depleted in MgO and have low Cr concentration as it is made up of chert/quartz and magnetite only.

(C) REE pattern of four samples of SBIF including a sample (X) from amphibolite layer within the CBIF. These patterns show enrichment in ΣREE with strong negative Eu anomalies. These plots suggest mixing of hydrothermal solution with ambient Sea water and clastic input to the basin.

(D) REE pattern of 6 samples of CBIF showing depleted ΣREE, moderate to strong positive Eu anomalies with high La enrichment indicating mixing of hydrothermal solution with ambient Sea water.

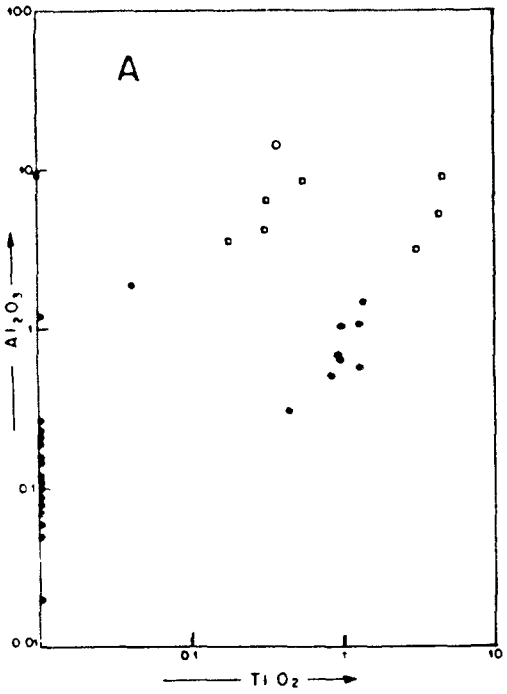
A
100
10
1
0·1
0·01
0·1
1
10
— Al2O3 —
— TiO2 —

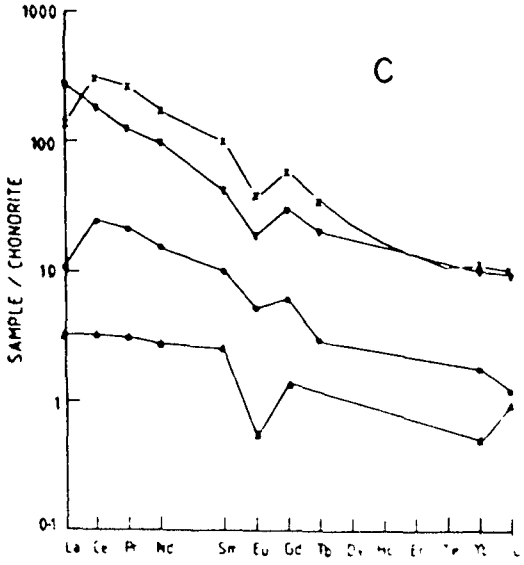
C
1000
100
10
1
0·1
SAMPLE / CHONDRITE
La Ce Pr Nd Sm Eu Gd Tb Dy Ho Er Tm Yb Lu

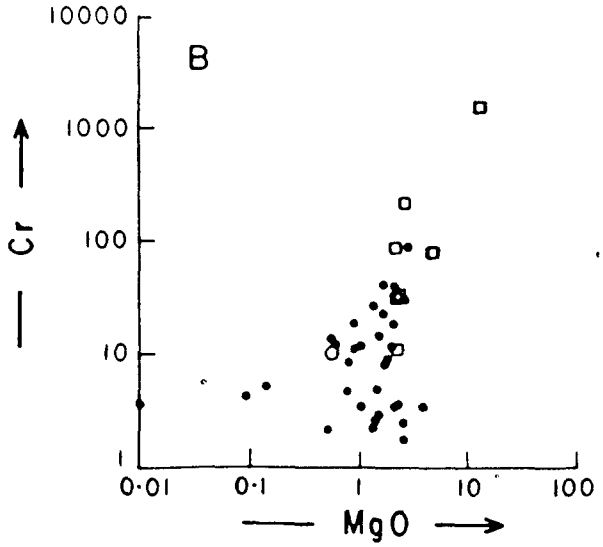
B
10000
1000
100
10
1
0·01
0·1
1
10
100
— Cr —
— MgO —

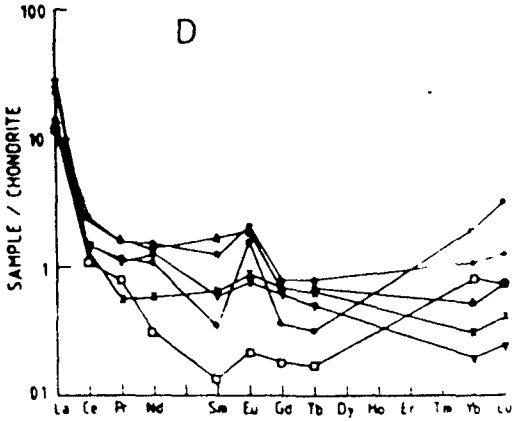
D
100
10
1
0·1
SAMPLE / CHONDRITE
La Ce Pr Nd Sm Eu Gd Tb Dy Ho Er Tm Yb Lu

very clearly show that terrigenous component has been a very significant source of contamination (SBIF) in these otherwise chemical sediments (CBIF). The trace element contents of the CBIF and SBIF, though show a gradation, are distinct for the two groups, as the CBIF is depleted in all elements except Fe and Si, and SBIF is relatively enriched in Rb, Sc, Zr, Y, Cr, Ni, Mg, V and rare earth elements (Table 10.1). Mutual relationship between Zr-Hf, Y-Sc and their dependence upon Al_2O_3, K_2O, TiO_2 do not leave any doubt that SBIF is enriched in these elements which are diagnostic of the terrigenous input.

Cr content of SBIF and CBIF shows a great scatter with a weak but sympathetic relationship between Cr and MgO (Fig. 10.1B). Samples which are enriched in MgO (13%) and $Fe_2O_3^{(t)}$ (19%) are also enriched in Cr (~ 1700 ppm). Similar correlation is found between Cr and Ni. It indicates that volcaniclastic material has also been accumulated along with terrigenous input and chemical precipitation. The large scatter in the abundances of Cr, Ni and MgO, is attributed to quantitative or qualitative inconsistency of volcaniclastic contribution. Nevertheless, it is quite clear that these elements are fairly high in case of SBIF than the CBIF. Further more, the next line of evidence in order to strengthen the conclusion, is found in the relationship between Zr and (Cr+Co+Ni), which clearly indicates that SBIF are enriched in both Zr as well as (Cr+Co+Ni) in comparison to CBIF. Zr, which is a diagnostic element for the terrigenous input and Cr+Co+Ni and used as an index of volcaniclastic contribution, show that these two sources have contributed for the deposition of SBIF. Incomplete mixing for the shaly precursors of the SBIF is well documented.

Similar behaviour has been noticed in Cr-Zr relationship (Table 10.1).

10.2.2 REE Geochemistry:

CBIF, which is mainly made up of silica and iron was deposited from Archaean ocean water, in which Fe, SiO_2 and REE were added by hydrothermal solutions, brought from the mantle at the vent sites on MOR (Derry and Jacobsen, 1990; Jacobsen and Pimentel-Klose, 1988; Khan et al., 1991). High contents of SiO_2 and $Fe_2O_3^{(t)}$, extreme depletion in REE, anomalous behaviour of Ce and consistent moderate to strong +ve Eu anomalies coupled with La spiking (Table 10.1) indicate that hydrothermal solution had supplied the material for the precipitation of cherty BIF. Few representative REE patterns of the BIF of Bababudan Group are shown in Fig. (10.1 C&D).

CBIF are characterized by depleted to moderate ΣREE (including La), LREE/HREE ~ 1, Nd/Yb ~ 1, weak to strong positive Eu anomalies (Fig. 10.1D). All major trace and REE data suggest that there is a total range of pure shale to pure chert with intermediate SBIF to CBIF.

Hydrothermal solutions are extremely depleted in ΣREE but have a strong positive Eu anomaly (Fig. 10.2A). Away from the MOR vent sites, this positive Eu anomaly vanishes both vertically and horizontally. The metalliferous deposits just at the vent site also show depleted ΣREE, positive Eu anomalies and La enrichment (Ruhlin and Owen, 1986). Barrett et al. (1988) have found the similar REE characters for the Red Sea hydrothermal solutions and metalliferous sediments. Present day ocean water has an extremely

Fig. 10.2 : (A) NASC normalized REE pattern of three samples of hydrothermal water at East Pacific Ridge (EPR) 21^{o} N NGS vent, showing strong positive Eu anomalies and extremely depleted in ΣREE. (After Piepgras and Wasserburg, 1985).

(B) (Cu + Co + Ni) vs. ΣREE plot shows most of the samples falling within well defined field of hydrothermal deposits. Some samples lie outside this field indicating mixing of continental debris and volcaniclastic material with hydrothermal solutions. (Fields after Klein and Beukes, 1989).

(C) NASC normalized REE plot of EPR hydrothermal fluid indicates that mixing of these solution with sea water in 1:100 proportion explains the observed REE pattern of BIF. (After Klein and Beukes, 1989).

(D) Model for BIF deposition. Deep water enriched in Fe^{2+} from hydrothermal sources, moves up onto a shallow shelf and precipitates Fe and Si as a result of oxidation and evaporation. Lake Superior - type BIFs are deposited on Atlantic-type Continental shelves while Algoma-type BIFs are deposited in shallow waters surrounding island arcs. (After Jacobsen and Pimental-Klose, 1988).

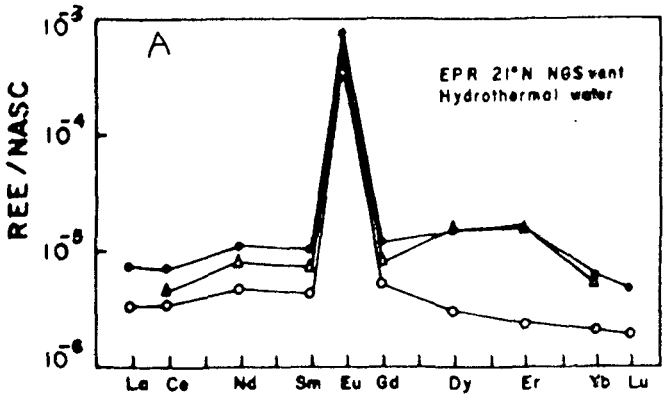
A
EPR 21°N NGS vent
Hydrothermal water
REE/NASC
La Ce Nd Sm Eu Gd Dy Er Yb Lu

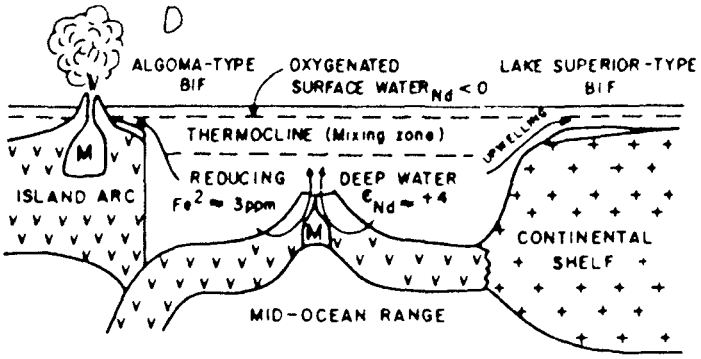
D
ALGOMA-TYPE BIF
OXYGENATED SURFACE WATER
LAKE SUPERIOR-TYPE BIF
THERMOCLINE (Mixing zone)
UPWELLING
REDUCING DEEP WATER
ISLAND ARC
CONTINENTAL SHELF
MID-OCEAN RANGE

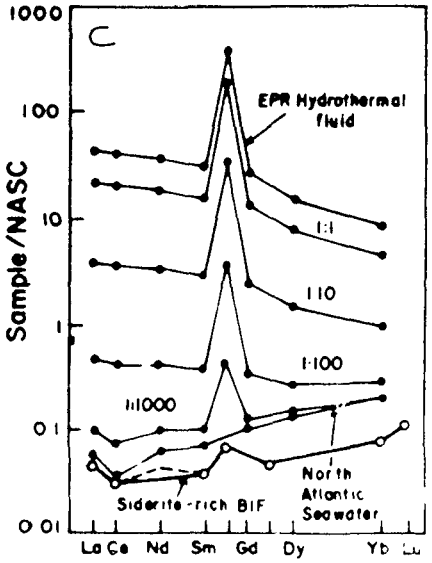
C
EPR Hydrothermal fluid
1:1
1:10
1:100
1:1000
North Atlantic Seawater
Siderite-rich BIF
Sample/NASC
La Ce Nd Sm Gd Dy Yb

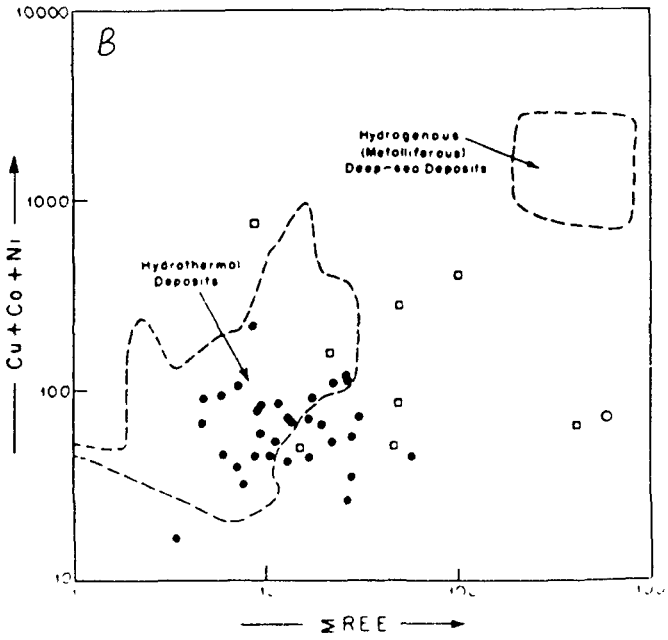
B
Hydrogenous (Metalliferous) Deep-sea Deposits
Hydrothermal Deposits
Cu+Co+Ni
ΣREE

depleted pattern of ΣREE with no Eu enrichment and most of the ocean water REE flux is provided as the dissolved load to the oceans (Goldstein and Jacobsen, 1988). In Fig. (10.2B) the Cu+Co+Ni concentration of BIF is plotted against ΣREE. In this illustration most of the samples occupying the field of hydrothermal solutions indicating that elemental constituents of BIF are provided by hydrothermal solutions. These studies very clearly suggest that silica, iron and REE for CBIF were provided through mantle derived hydrothermal or fumarolic activity (Dymek and Klein, 1988; Klein and Beukes, 1989; Michard, 1989; Derry and Jacobson, 1990). Mixing of hydrothermal solutions with ocean water in 1:100 proportion explains the observed REE patterns of BIF (Fig. 10.2C). ε Nd values of the Archaean BIF are ≈ 0.4 which are close to the mantle values. Therefore ε Nd data shows that the hydrothermal solutions are derived from mantle. Based on these data Jacobsen and Pimentel-Klose (1988) have suggested a model of deposition of BIF. The essential point of this model is that the Fe, Si and REE rich solutions are added from MOR vents (Fig. 10.2.D).

10.3 DEPOSITIONAL ENVIRONMENT OF BIF:

The oxide facies of BIF of Kudremukh Schist Belt and also of the Bababudan Group of the Sandur and Chitradurga Schist belts, show extremely depleted ΣREE with La enrichment and positive Eu anomalies. Although at Kudremukh they do not show negative Ce anomaly, it is very common in Sandur and Chitradurga schist belts, where BIFs are overlying stromatolites. All these chemical constraints, coupled with ε Nd data (ε Nd = $^{143}Nd/^{144}Nd$), which

varies around +4, clearly demonstrate that the source of silica and iron was mantle derived hydrothermal solutions. These hydrothermal solutions, which are depleted in ΣREE, were added into the Archaean Proto oceans from the vent sites through hydrothermal activity at Archean mid oceanic ridges (Klinkhammer et al., 1983; Bowers et al., 1985; Goldstein and Jacobson, 1988). These BIF have been deposited below wave base and photic zone of the shallow shelf regions. Since hydrothermal solutions would have brought iron in ferrous state and it was precipitated in ferric state, thus it could have been possible only if the ambient ocean had an intermittent oxygenated atmosphere at the deeper part of the shelf.

Geochemical investigations presented earlier in this work suggest that at the time of deposition of basal quartz pebble conglomerate with associated quartzites, atmosphere at the site of weathering was anoxic, and at the site of deposition it was reducing, but overlying oxide facies BIF indicate a rythemically aerobic environment below wave base. The reason behind change of the anaerobic to aerobic atmosphere is still speculative. Many models have been proposed so far (Cloud, 1983; Towe, 1990). Recently, Naqvi and his group (Khan et al., 1991; Gnaneswar Rao, 1991; Manikyamba et al., 1991) have suggested that oxygen was produced at the shallow part of the basin by photoautotrophy, i.e., by the photosynthesis of bacteria developing stromatolites and other microbiotas. Although in Kudremukh and Bababudan schist belts, discoveries of stromatolites and microbiota are yet to be made, but in the Sandur, Chitradurga and the Shimoga schist belt they have already been discovered in abundance (Naqvi et al.,

1987; Srinivasan et al., 1988; Vasudeva et al., 1989; Srinivasan and Naqvi, 1990). According to Manikyamba et al. (1991), the silica and iron, added at vent site near MOR, from deeper part of the basin, were brought to the shallow region due to chemical and thermal potential differences. Since at shallow shelf region oxygen was available, they got precipitated as CBIF, and also were contaminated through terrigenous and volcaniclastic input. Although it has remained an extremely attractive and provocative hypothesis to suggest that biologically produced oxygen had played a major role in the precipitation of BIFs, because these biological records are present, in associated rocks and not in BIF itself.

Nevertheless, whatsoever the reasons behind the evolution of aerobic atmosphere during the time of deposition of BIF, what is important to note here is the drastic change from reducing environment at the time of QPC deposition; as evident by detrital pyrite; to oxidizing environment evidenced by BIF. Not only atmospheric change is indicated, but geochemical studies also show that before the deposition of BIF, mid oceanic ridges had been developed and basin opening was in its advance stage. Hargraves (1986) computed that ridge length during Archaean was at least 27 times more than present. Therefore the distance between site of addition of Fe, si rich hydrothermal solutions and site of deposition was not more than a few hundred kms. These inferences form BIF put a great constraint on the basin evolution model and to a greater extent explain the juxtaposed existence of rock suites formed in stable shelf trailing edge - MOR and subduction zone (active margins) tectonic settings.

CHAPTER XI

GEOCHEMISTRY OF THE KALDURGA POLYMICITIC CONGLOMERATE

11.1 INTRODUCTION:

Geochemical studies of clastic-sedimentary rocks have been very successful for the understanding and estimation of the composition of continental crust explosed at various times (Naqvi et al., 1988; Feng and Kerrich, 1990; MeLennan and Taylor, 1991). Particularly the best candidates for such studies are polymictic conglomerates in which clasts from the older sequence are found. The matrix and clasts of these conglomerates are expected to have sampled the near average composition of the older crust exposed in the source area (Taylor and McLennan, 1985). Clasts compositions of the Kaldurga Conglomerate were studied by Naqvi et al. (1978a). Geochemical analysis of pebbles from 2.6 Ga old conglomerates by these authors, indicates that their source areas were made up of basic-ultrabasic volcanics, TTG and other metasediments. Moreover an average composition is difficult to obtain from clasts composition because all the rock types present in the source area, due to rheological differences, are not present as clasts. Therefore the matrix appears to be more representative than the clasts. With this objective the geochemical characteristics of the matrix of the Kaldurga Conglomerate (KCM) of Bababudan schist Belt was studied and its major, trace and REE are discussed in this chapter.

11.2 MAJOR ELEMENTS:

Two main populations are identified on the basis of MgO - $Fe_2O_3^{(t)}$ abundances; a high mafic population with MgO > 12% and Fe_2O_3 > 10% and relatively low mafic population with MgO < 12% and Fe_2O_3 < 10% (Table 11.1). However, a gradation between mafic enriched and depleted samples is seen in almost all elements except in five samples which contain more than 25% MgO and occupy a distinct place in MgO vs SiO_2 plot (Fig. 11.1A). It is evident that in spite of being highly immature and unsorted sediments, still there is a low order effect of dilution by SiO_2 on some major and trace elements; a characteristics of sediments which undergo rapid weathering, short transport and less sedimentary fractionation. For example, SiO_2 concentration varies from 42 to 71% and within this range MgO, Fe_2O_3. K_2O, Al_2O_3 and TiO_2 are showing a scatter with less effect of dilution reflected in overall depletion in concentration of these oxides with respect to increase in SiO_2 abundances (Fig. 11.1). Minor constituents like P_2O_5 and MnO show random scatter (Fig. 11.1 G&H). SiO_2/Al_2O_3, ratio is an agreed index of maturity. Since, the removal of feldspar has not been very effective, a scatter in SiO_2/Al_2O_3 ratio is exhibited (Fig. 11.1C). Not only by SiO_2/Al_2O_3 but also by SiO_2/Na_2O scatter (Fig.11.1D) it is evident that plagioclase has not been effectively weathered. This is confirmed by petrographic data (Table 6.3). The An content of the plagioclase in these samples is extremely vaiable as both highly calcic and sodic plagioclase are found. Simultaneous increrase in Na_2O and SiO_2 (Fig.11.1D) reflects that both quartz and plagioclase have accumulated in the debris and were derived from the TTG. A faint

Table 11.1: Chemical composition of the matrix (M_1) of the Kaldurga Polymictic Conglomerate, the Bababudan schist belt.

Elements	MK-1	MK-2	MK-3	MK-4	MK-5	MK-6	MK-7	MK-8
SiO_2	68.16	60.32	69.58	58.17	65.34	70.34	53.55	50.76
TiO_2	0.38	0.87	0.46	0.59	0.56	0.34	0.89	0.77
Al_2O_3	15.39	15.78	12.61	11.25	13.34	14.63	15.64	16.60
$Fe_2O_3(T)$	3.78	7.86	4.48	12.45	8.39	4.00	11.93	12.44
MnO	0.05	0.10	0.07	0.13	0.10	0.06	0.13	0.13
MgO	2.09	4.63	2.55	8.12	4.29	2.14	8.24	10.07
CaO	0.38	0.67	0.86	6.76	1.65	0.80	1.12	0.65
Na_2O	4.05	2.89	2.96	0.95	2.22	4.54	2.89	2.41
K_2O	2.15	3.20	2.80	0.88	1.44	2.09	2.13	2.80
P_2O_5	0.15	0.16	0.10	0.14	0.15	0.15	0.14	0.20
Total	96.58	96.48	96.47	99.44	97.48	99.09	96.66	96.83
C.I.A	70.05	70.00	65.57	56.70	71.53	66.92	71.81	73.90
K_2O/MgO	1.03	0.69	1.10	0.11	0.34	0.98	0.26	0.28
K_2O/Na_2O	0.53	1.11	0.94	0.93	0.65	0.46	0.74	1.16
SiO_2/Al_2O_3	4.42	3.82	5.52	5.17	4.90	4.81	3.42	3.06
Sc	6.54	12.52	7.15	18.48	12.58	6.40	16.60	22.34
V	70.18	117.58	81.33	138.41	136.81	63.23	182.67	236.06
Cr	43.63	88.89	90.91	282.13	295.26	50.58	185.72	157.60
Co	61.24	40.46	56.21	54.32	55.46	43.63	53.40	50.47
Ni	27.61	55.81	29.88	134.48	95.75	32.09	151.51	93.55
Cu	10.40	44.38	23.90	5.29	6.37	25.30	32.74	60.81
Zn	27.26	74.41	39.49	35.98	69.28	26.17	68.88	76.36
Ga	15.78	17.46	13.08	10.73	14.10	13.52	16.26	19.13
Rb	61.95	100.02	70.79	22.73	38.16	56.91	49.35	75.12
Sr	203.47	126.01	95.47	69.35	68.86	161.50	62.01	45.41
Y	18.32	24.83	15.81	9.94	5.92	8.69	8.68	25.98
Zr	76.52	60.12	64.70	66.03	74.35	69.46	108.76	97.57
Nb	3.79	6.01	3.73	1.93	1.73	2.33	6.11	6.82
Ba	204.26	220.08	207.74	52.17	67.93	150.46	72.61	141.84
Hf	1.84	1.69	1.83	1.69	1.00	1.46	1.17	1.20
Ta	0.61	0.53	0.47	0.26	0.10	0.39	0.16	0.30
Th	12.18	17.10	4.19	2.50	1.61	4.19	1.34	2.08
U	1.21	8.90	0.87	0.45	0.43	0.71	0.37	0.26
K/Rb	288.12	265.61	328.37	321.38	313.26	304.88	358.32	309.44
Rb/Sr	0.30	0.79	0.74	0.33	0.55	0.35	0.80	1.65
Cr/Ni	1.58	1.59	3.04	2.10	3.08	1.58	1.23	1.68
La	44.52	67.17	41.74	22.13	15.20	26.73	9.24	23.38
Ce	35.79	46.45	32.36	21.52	12.16	23.99	9.71	23.78
Pr	27.30	39.85	23.36	17.96	10.95	17.88	9.27	19.34
Nd	19.30	30.10	17.03	13.57	6.96	11.60	7.14	13.04
Sm	13.64	22.73	12.42	10.26	4.42	7.53	5.50	8.79
Eu	8.62	14.94	6.78	5.63	2.30	5.40	1.61	6.90
Gd	10.29	22.65	7.97	8.46	3.76	6.24	3.56	6.76
Tb	9.50	23.83	6.87	5.85	2.13	4.38	2.16	5.76
Dy	8.77	25.07	5.93	4.04	1.21	3.07	1.31	4.91
Ho	7.39	25.02	5.28	4.00	0.98	3.33	1.25	4.51
Er	6.22	24.98	4.70	3.98	0.80	3.61	1.20	4.14
Tm	8.43	26.12	6.46	5.62	0.56	2.53	1.69	3.37
Yb	6.45	22.46	4.35	4.40	1.37	3.02	1.49	3.51
Lu	5.77	18.37	4.72	5.51	1.84	3.15	2.36	2.62
ΣREE	211.99	409.74	175.25	132.93	64.64	122.46	57.49	130.81
LREE/HREE	2.24	1.09	3.05	2.04	3.93	2.99	2.72	2.48
Eu/Eu^*	0.73	0.66	0.68	0.60	0.56	0.79	0.36	0.90

Elements	MK-9	MK-10	MK-11	MK-12	MK-13	MK-14	MK-15	MK-16
SiO_2	58.91	69.32	60.77	71.39	55.24	61.49	42.82	51.28
TiO_2	0.77	0.43	1.23	0.43	0.60	0.68	0.38	0.63
Al_2O_3	13.97	8.50	13.30	7.38	16.92	14.70	3.50	8.61
$Fe_2O_3(T)$	9.95	9.64	7.85	8.71	10.62	7.40	9.97	12.49
MnO	0.11	0.10	0.09	0.08	0.14	0.10	0.25	0.17
MgO	6.27	4.56	4.70	4.21	7.82	3.97	28.72	13.09
CaO	1.01	1.92	0.55	1.59	3.94	0.41	9.99	8.77
Na_2O	3.69	0.70	5.94	2.35	2.29	4.72	0.64	1.25
K_2O	1.83	1.20	2.07	1.15	1.78	3.29	0.01	0.08
P_2O_5	0.28	0.12	0.23	0.22	0.18	0.22	0.22	0.18
Total	96.79	96.49	96.73	97.51	99.53	96.98	96.50	96.55
C.I.A	68.15	68.99	60.84	59.18	69.54	63.58	24.75	46.02
K_2O/MgO	0.29	0.26	0.44	0.27	0.23	0.83	-	-
K_2O/Na_2O	0.50	1.72	0.35	0.49	0.78	0.70	-	-
SiO_2/Al_2O_3	4.22	8.16	4.57	9.67	3.26	4.18	12.13	5.96
Sc	13.87	10.39	10.10	10.41	16.29	10.39	17.31	32.19
V	154.95	108.33	87.77	106.67	192.50	99.63	103.28	221.92
Cr	140.89	189.75	32.83	146.38	149.02	101.04	1975.22	1353.66
Co	48.76	70.79	40.03	75.01	36.30	37.70	94.08	63.00
Ni	75.76	72.94	38.04	85.07	82.20	48.53	1010.73	300.00
Cu	88.90	118.39	93.62	70.85	4.26	59.71	95.23	50.31
Zn	44.84	21.48	51.54	24.19	49.42	56.51	52.09	58.78
Ga	15.20	8.17	12.87	7.98	16.37	14.73	4.30	10.36
Rb	45.47	24.04	75.26	22.28	38.04	76.91	0.44	1.06
Sr	63.57	25.24	104.04	33.14	91.84	114.25	116.63	81.40
Y	29.61	6.73	14.44	7.36	10.12	23.23	5.68	17.29
Zr	124.00	50.40	67.77	43.03	100.65	65.87	5.77	9.10
Nb	7.50	1.48	3.30	1.65	3.32	5.27	1.59	1.69
Ba	60.73	85.85	32.44	59.24	63.18	195.96	-	2.68
Hf	1.62	1.36	0.96	1.04	1.82	1.84	0.04	0.21
Ta	0.27	0.36	0.15	0.40	0.14	0.38	0.04	0.13
Th	1.05	1.80	0.67	1.31	1.58	3.06	-	0.57
U	0.42	0.34	0.42	0.38	0.23	1.26	-	0.13
K/Rb	334.11	414.39	228.34	428.50	388.46	355.13	188.64	624.42
Rb/Sr	0.72	0.95	0.72	0.67	0.41	0.67	-	0.01
Cr/Ni	1.86	2.60	0.86	1.72	1.81	2.08	1.95	4.51
La	38.61	19.59	15.45	16.40	14.66	32.18	1.50	2.81
Ce	29.64	17.52	14.67	13.19	16.31	31.13	1.44	5.58
Pr	21.46	13.28	10.07	9.12	12.34	21.90	1.61	4.96
Nd	16.83	10.88	7.87	8.26	9.86	16.32	1.42	5.22
Sm	13.20	8.92	6.15	7.49	7.88	12.16	1.26	5.50
Eu	3.91	4.37	2.76	3.91	2.76	7.24	0.23	4.37
Gd	5.52	4.51	4.90	3.73	3.86	9.12	0.85	3.82
Tb	5.76	3.62	3.69	3.58	3.37	9.01	0.98	4.60
Dy	6.01	2.91	2.78	3.44	2.94	8.90	1.13	5.54
Ho	4.50	2.35	2.24	2.58	2.00	8.50	0.95	4.84
Er	3.37	1.89	1.81	1.93	1.37	8.11	0.80	4.22
Tm	5.90	3.37	2.53	1.97	1.97	10.39	0.28	6.18
Yb	12.30	3.23	2.62	3.02	2.21	7.78	1.17	5.28
Lu	3.94	2.89	2.10	3.67	3.36	7.35	1.05	4.20
ΣREE	170.95	99.33	79.64	82.29	84.89	190.11	13.17	67.12
LREE/HREE	2.53	2.83	2.39	2.28	2.90	1.64	0.79	0.62
Eu/Eu^*	0.46	0.69	0.50	0.74	0.50	0.69	0.22	0.95

Elements	MK-17	MK-18	MK-19	MK-20	MK-21	MK-22	MK-23	MK-24
SiO_2	61.23	54.63	54.09	51.92	49.27	57.71	61.22	58.22
TiO_2	0.40	0.86	1.32	0.45	0.52	0.77	0.46	0.79
Al_2O_3	7.73	12.18	12.97	8.65	14.87	13.65	12.68	14.39
$Fe_2O_3(T)$	5.47	13.27	12.66	13.82	14.41	10.88	4.80	10.42
MnO	0.21	0.19	0.12	0.20	0.16	0.14	0.04	0.10
MgO	17.79	11.10	10.27	11.34	13.06	8.71	5.35	7.92
CaO	7.93	0.78	0.81	6.59	0.43	0.90	4.42	0.27
Na_2O	-	1.31	2.41	2.41	1.80	1.37	3.96	1.98
K_2O	0.01	2.02	1.64	0.08	1.76	2.21	2.87	2.26
P_2O_5	0.08	0.16	0.20	0.23	0.22	0.16	-	0.15
Total	101.85	96.50	96.49	95.69	96.50	96.50	95.80	96.50
C.I.A	49.33	74.77	72.74	48.79	78.84	75.29	52.99	76.14
K_2O/MgO	-	0.18	0.16	-	0.13	0.25	0.54	0.29
K_2O/Na_2O	-	1.54	0.68	0.03	0.98	1.61	0.72	1.34
SiO_2/Al_2O_3	7.92	4.49	4.17	6.00	3.31	4.23	4.83	4.05
Sc	8.50	20.98	20.86	35.69	19.93	18.79	0.12	15.44
V	64.60	158.88	181.85	260.27	135.58	160.97	8.46	153.92
Cr	943.87	527.79	282.48	951.19	187.48	246.26	1.03	154.29
Co	41.09	56.71	62.51	73.05	42.47	42.69	5.66	48.04
Ni	515.06	161.64	151.27	268.16	114.70	113.42	-	85.33
Cu	1.62	68.66	79.11	356.11	27.40	45.09	-	19.03
Zn	99.19	77.25	77.38	68.78	51.09	58.57	1.23	55.37
Ga	10.93	13.22	13.43	9.69	12.17	12.52	1.55	14.83
Rb	0.43	54.24	45.60	0.92	45.17	55.33	8.52	55.83
Sr	125.81	45.07	71.28	48.63	25.65	73.05	9.82	34.10
Y	5.28	15.91	19.54	14.64	12.00	6.79	1.48	6.12
Zr	36.01	57.01	59.27	44.39	104.59	83.48	9.91	71.73
Nb	2.11	4.49	8.13	3.68	3.72	2.65	0.29	3.67
Ba	0.67	89.40	72.48	1.26	49.46	107.68	268.76	139.48
Hf	1.20	1.45	1.20	1.00	2.43	1.73	2.37	1.43
Ta	0.23	0.40	0.64	0.26	0.26	0.24	0.56	0.29
Th	2.20	2.56	1.80	0.77	1.24	2.26	4.15	1.62
U	0.14	0.43	0.51	0.10	0.69	0.39	1.33	0.37
K/Rb	193.02	309.18	298.57	721.74	223.47	331.59	2796.48	336.06
Rb/Sr	-	1.20	0.64	0.02	1.76	0.76	0.87	1.64
Cr/Ni	1.83	3.27	1.87	3.55	1.63	2.17	-	1.81
La	37.22	11.63	20.35	4.14	12.59	18.23	57.49	22.04
Ce	24.57	13.27	17.02	7.48	16.88	17.08	36.79	22.36
Pr	19.85	10.44	14.53	7.00	10.95	13.21	27.30	18.76
Nd	17.59	9.62	12.23	6.37	9.06	10.31	21.03	13.87
Sm	10.52	8.87	10.30	5.80	7.49	8.05	15.11	10.26
Eu	6.67	4.82	8.05	3.22	4.25	5.29	10.00	5.86
Gd	6.90	6.57	6.50	4.61	4.80	5.33	10.59	6.76
Tb	4.31	6.63	6.18	4.19	5.00	3.63	7.93	4.21
Dy	3.10	6.69	5.88	3.81	5.22	2.47	11.34	2.62
Ho	1.88	5.80	5.48	4.20	3.99	2.07	8.81	2.18
Er	1.81	5.02	5.10	4.62	3.05	1.73	6.10	1.81
Tm	2.53	5.90	7.02	5.34	3.93	2.25	6.46	1.97
Yb	1.90	5.24	5.73	4.72	6.37	2.18	4.80	1.98
Lu	1.84	4.72	4.25	4.20	3.94	2.10	4.99	2.36
ΣREE	140.69	105.22	129.62	69.70	97.52	93.93	228.74	117.04
LREE/HREE	4.52	1.16	1.58	0.86	1.57	3.07	2.58	3.65
Eu/Eu^*	0.78	0.63	0.98	0.62	0.71	0.81	0.79	0.70

Elements	MK-25	MK-26	MK-27	MK-28	MK-29	MK-30	MK-31	MK-33
SiO_2	53.43	64.18	57.14	60.34	54.73	65.05	47.57	50.16
TiO_2	1.11	0.59	0.91	0.65	1.17	0.72	1.06	0.33
Al_2O_3	14.66	13.73	14.61	14.00	13.10	8.96	21.29	3.27
$Fe_2O_3^{(T)}$	16.90	8.46	13.94	9.74	16.15	9.01	11.50	10.52
MnO	0.13	0.11	0.11	0.10	0.22	0.04	0.10	0.21
MgO	7.10	4.60	7.82	6.87	6.02	6.80	15.13	26.28
CaO	0.49	1.73	1.09	0.83	2.75	0.99	0.98	5.60
Na_2O	2.29	2.22	2.10	2.59	2.29	1.75	1.38	0.09
K_2O	0.59	1.66	1.97	1.76	2.01	1.39	2.78	-
P_2O_5	0.30	0.15	0.13	0.12	0.16	0.02	0.06	0.08
Total	97.00	97.43	99.82	97.00	98.60	94.73	101.85	96.54
C.I.A	81.31	70.77	73.90	72.99	65.01	68.45	80.55	36.50
K_2O/MgO	0.08	0.36	0.25	0.26	0.33	0.20	0.18	-
K_2O/Na_2O	0.26	0.75	0.93	0.68	0.88	0.79	2.00	-
SiO_2/Al_2O_3	3.64	4.67	3.91	4.31	4.18	7.26	2.23	15.33
Sc	27.49	13.16	22.55	18.14	24.71	13.00	29.83	19.16
V	174.24	141.06	195.98	156.63	234.94	123.34	236.50	132.37
Cr	13.90	303.68	280.47	152.64	144.05	121.16	447.44	2201.72
Co	49.94	56.93	53.69	52.93	52.50	58.19	64.34	81.47
Ni	74.37	88.93	126.06	86.50	109.93	74.58	124.25	850.09
Cu	9.41	13.40	139.83	28.74	32.10	65.22	14.06	15.32
Zn	60.95	53.52	88.55	51.34	58.68	30.43	142.93	69.53
Ga	14.98	14.01	17.41	12.72	13.36	11.36	21.91	3.99
Rb	9.96	48.46	79.21	50.00	62.05	29.16	50.12	0.12
Sr	20.17	63.37	65.69	57.12	61.46	34.90	42.50	19.29
Y	35.66	6.31	9.93	18.29	11.51	12.57	28.62	5.51
Zr	315.17	78.85	107.10	163.46	131.71	94.74	128.69	7.76
Nb	6.57	2.01	2.24	6.19	6.52	5.54	6.30	1.72
Ba	97.86	117.62	105.35	96.96	120.11	128.13	126.63	-
Hf	5.71	1.35	1.86	3.07	1.99	2.28	3.06	0.09
Ta	0.82	0.24	0.18	0.43	0.23	0.61	0.53	0.06
Th	5.89	2.22	1.55	3.17	1.06	2.75	2.88	0.03
U	1.68	0.71	0.88	0.57	0.29	0.82	0.91	-
K/Rb	491.77	284.38	206.46	292.22	268.93	395.71	460.47	-
Rb/Sr	0.49	0.76	1.21	0.88	1.01	0.84	1.18	-
Cr/Ni	0.19	3.41	2.22	1.76	1.31	1.62	3.60	2.59
La	34.82	20.14	17.79	19.16	10.46	50.54	27.38	2.40
Ce	45.13	19.27	18.17	20.38	12.27	36.23	18.47	2.33
Pr	25.77	13.72	14.38	15.26	10.00	37.01	15.04	2.34
Nd	33.36	10.59	10.56	11.44	8.14	24.70	15.91	2.31
Sm	21.17	8.18	7.75	8.57	6.62	19.13	12.03	2.29
Eu	15.28	5.40	4.71	3.79	4.37	11.03	11.03	0.80
Gd	1.86	4.44	5.78	5.82	4.58	11.31	11.99	1.73
Tb	12.33	3.17	4.51	5.87	3.80	7.93	12.24	1.51
Dy	12.81	2.26	3.52	5.93	3.15	6.77	10.87	1.31
Ho	11.63	1.86	3.00	5.46	3.14	5.99	13.87	1.38
Er	10.56	1.53	2.57	5.02	3.13	6.06	11.53	1.45
Tm	12.08	1.97	3.65	5.06	4.21	7.58	14.04	0.56
Yb	12.94	2.14	3.39	7.10	4.07	7.78	11.63	1.37
Lu	15.22	1.10	3.67	7.09	4.99	7.09	11.81	1.31
ΣREE	264.96	96.77	103.45	125.95	82.93	229.15	197.82	20.69
LREE/HREE	1.51	3.69	2.28	1.58	1.53	2.60	0.91	0.87
Eu/Eu^*	0.96	0.90	0.70	0.54	0.79	0.75	0.92	0.40

Elements	MK-34	MK-35	MK-36	MK-37	MK-38	MK-39	MK-40	MK-41
SiO_2	46.37	46.46	49.73	58.86	59.46	52.83	55.43	43.78
TiO_2	0.34	0.41	0.94	0.68	0.73	0.83	0.61	1.45
Al_2O_3	4.66	3.62	14.26	14.84	14.26	14.95	13.98	18.88
$Fe_2O_3(T)$	10.69	9.66	17.19	11.73	11.65	13.98	8.21	14.74
MnO	0.21	0.22	0.16	0.11	0.12	0.10	0.08	0.11
MgO	27.52	27.89	12.04	9.63	9.63	11.13	10.91	11.73
CaO	6.43	7.22	0.82	0.55	0.60	0.67	0.44	0.50
Na_2O	0.16	1.01	2.41	2.04	1.86	2.29	3.06	2.10
K_2O	0.01	0.01	1.36	1.90	1.71	1.11	2.39	3.56
P_2O_5	0.10	0.10	0.12	0.11	0.10	0.08	0.12	0.22
Total	96.49	96.60	99.03	100.45	100.12	97.97	95.23	97.07
C.I.A	41.39	30.52	75.65	76.77	77.37	78.86	70.35	75.40
K_2O/MgO	-	-	0.11	0.20	0.18	0.10	0.22	0.30
K_2O/Na_2O	0.06	-	0.56	0.93	0.92	0.49	0.78	1.69
SiO_2/Al_2O_3	9.95	12.83	3.49	3.97	4.17	3.53	3.96	2.32
Sc	18.89	17.38	25.04	17.69	15.98	20.97	18.88	34.66
V	128.56	120.31	218.34	173.38	138.34	185.54	193.32	200.67
Cr	2432.86	1977.26	35.85	181.08	254.31	235.78	80.34	10.00
Co	83.22	98.53	58.27	48.73	52.63	51.78	56.81	46.33
Ni	936.72	1117.00	116.25	116.89	142.70	125.35	58.56	61.05
Cu	77.83	136.06	206.10	72.24	104.47	62.03	12.38	5.84
Zn	62.55	62.04	71.70	54.65	75.98	67.51	87.15	70.08
Ga	5.15	4.81	15.48	12.08	11.99	15.97	18.70	16.62
Rb	0.14	0.03	32.25	42.49	37.93	28.62	61.25	102.73
Sr	16.98	107.93	27.69	43.84	48.12	70.27	51.95	29.58
Y	6.29	6.34	7.57	7.88	7.52	6.48	7.63	7.35
Zr	7.97	6.67	86.04	99.96	85.07	89.24	89.47	127.11
Nb	1.30	1.79	2.78	3.01	2.23	2.27	2.56	2.61
Ba	-	-	99.67	67.99	57.34	73.52	330.42	115.89
Hf	0.18	0.08	1.69	1.24	0.95	1.10	2.25	1.32
Ta	0.07	0.04	0.13	0.13	0.14	0.12	0.47	0.08
Th	0.06	0.01	1.14	1.35	1.17	1.43	3.58	1.12
U	0.03	-	0.35	0.27	0.21	0.17	0.53	0.32
K/Rb	592.86	2766.77	350.08	671.22	374.27	321.98	323.93	287.70
Rb/Sr	-	-	1.16	0.97	0.79	0.41	1.18	3.47
Cr/Ni	2.60	1.77	0.31	1.55	1.78	1.88	1.37	0.16
La	2.45	2.00	8.09	8.80	23.35	7.82	53.57	10.14
Ce	2.68	2.12	9.67	9.62	16.36	10.52	48.59	16.41
Pr	2.63	2.26	7.81	8.76	12.04	10.36	35.55	10.58
Nd	2.36	2.42	7.19	6.40	9.44	6.03	32.84	7.83
Sm	2.12	2.60	6.62	4.68	7.40	3.51	21.39	5.80
Eu	1.03	1.03	2.41	2.99	4.14	2.53	16.44	3.45
Gd	1.11	1.99	4.18	3.89	3.46	2.97	13.82	4.15
Tb	1.49	1.78	2.94	2.62	2.61	2.01	7.24	3.04
Dy	1.99	1.60	2.07	1.76	1.97	1.36	5.17	2.23
Ho	1.81	1.21	1.87	1.43	1.69	1.12	3.64	1.85
Er	1.65	0.92	1.69	1.16	1.45	0.92	20.24	1.53
Tm	0.56	1.12	2.53	1.69	1.69	1.97	4.49	1.12
Yb	1.00	0.97	3.23	1.57	1.29	1.49	2.74	1.65
Lu	1.05	1.05	2.62	1.84	1.57	0.79	2.10	1.84
ΣREE	22.54	21.07	62.92	57.51	88.46	53.40	267.82	71.62
LREE/HREE	1.02	0.88	1.86	2.42	4.36	3.03	3.23	2.92
Eu/Eu^*	0.67	0.45	0.45	0.70	0.82	0.78	0.96	0.70

Elements	MK-42	MK-43	MK-44	MK-45	MK-46	MK-47	MK-48	MK-49	MK-50
SiO_2	42.06	53.78	49.41	59.64	58.75	54.75	45.84	59.82	67.78
TiO_2	1.45	0.70	1.12	0.85	1.20	1.53	0.42	1.02	0.52
Al_2O_3	18.77	15.01	16.75	14.50	12.79	15.73	4.03	10.96	12.15
$Fe_2O_3(T)$	15.39	7.25	12.85	8.65	8.72	11.30	10.06	12.13	3.46
MnO	0.10	0.07	0.13	0.13	0.16	0.22	-	-	0.06
MgO	11.73	11.14	17.01	9.83	11.56	7.91	26.69	8.77	4.25
CaO	0.44	0.29	0.82	2.12	3.57	3.17	8.80	6.62	3.27
Na_2O	1.98	3.36	1.16	2.68	0.58	3.77	0.29	2.53	4.20
K_2O	3.88	1.97	2.80	2.00	2.69	2.21	0.02	0.42	1.08
P_2O_5	0.22	0.02	0.03	0.10	0.12	0.09	0.17	0.28	0.08
Total	96.02	93.59	102.08	100.50	100.14	100.68	96.32	102.55	96.85
C.I.A	74.87	72.76	77.80	68.08	65.16	63.22	30.67	53.39	58.70
K_2O/MgO	0.33	0.18	-	0.23	0.23	0.28	-	0.05	0.25
K_2O/Na_2O	1.96	0.58	2.44	0.75	4.55	0.58	0.07	0.17	0.26
SiO_2/Al_2O_3	2.24	3.58	2.95	4.11	4.59	3.48	11.37	5.46	5.57
Sc	36.91	16.36	21.31	0.84	1.25	1.63	27.22	28.45	12.53
V	277.56	174.72	267.70	15.78	16.38	25.35	155.23	250.64	41.35
Cr	12.67	239.77	784.44	31.59	80.82	0.46	2149.10	232.96	4.86
Co	52.61	54.54	68.75	5.17	4.41	4.74	67.95	53.82	40.35
Ni	81.46	82.81	234.24	2.31	1.08	0.36	711.55	84.33	25.19
Cu	8.85	14.54	60.21	17.57	6.31	-	245.77	160.97	1.81
Zn	95.63	86.69	128.22	6.69	6.31	5.46	63.11	137.68	47.42
Ga	20.02	17.53	20.24	1.36	1.30	1.48	6.22	17.84	15.09
Rb	125.79	42.13	81.72	5.95	3.40	6.40	0.41	10.67	35.91
Sr	39.26	47.71	34.91	13.26	12.94	10.18	15.18	72.94	107.76
Y	6.73	7.89	20.10	2.31	2.52	1.81	8.69	13.32	25.59
Zr	155.96	81.16	83.96	6.84	7.26	16.54	11.00	126.57	267.75
Nb	3.60	3.23	6.16	0.57	0.61	1.10	1.05	5.79	6.72
Ba	133.18	227.77	200.58	217.71	176.41	437.85	1.70	63.02	71.65
Hf	1.09	2.30	2.22	2.08	2.40	5.03	0.49	3.01	7.30
Ta	0.14	0.44	0.64	0.69	0.65	0.86	0.14	0.44	0.79
Th	1.44	2.97	2.96	7.32	3.51	5.17	0.16	3.10	3.11
U	0.29	0.77	0.78	1.25	1.10	1.22	0.02	0.67	0.95
K/Rb	256.07	388.18	284.45	2790.59	6568.24	2866.72	404.88	326.71	249.68
Rb/Sr	3.20	0.88	2.34	0.45	0.26	0.62	0.03	0.15	0.33
Cr/Ni	0.16	2.90	3.35	13.68	17.43	1.28	3.02	2.76	0.19
La	6.57	37.00	23.41	57.98	49.37	42.86	0.68	47.68	6.49
Ce	13.10	29.63	21.11	33.53	37.73	31.18	0.92	32.07	51.88
Pr	10.29	20.29	17.30	27.96	29.27	23.43	1.61	24.53	41.46
Nd	6.84	20.73	17.36	24.98	27.00	22.76	2.50	27.40	42.06
Sm	4.55	13.46	13.46	17.23	18.05	15.11	2.51	16.62	25.41
Eu	3.68	9.54	8.62	16.21	13.79	15.06	4.14	15.98	15.75
Gd	2.88	8.56	11.54	13.07	15.75	14.74	2.97	13.66	23.20
Tb	2.09	6.03	11.72	12.41	13.10	9.31	2.76	8.97	14.83
Dy	1.52	4.38	9.53	10.71	11.36	10.63	3.44	6.54	12.20
Ho	1.35	4.94	9.64	11.75	12.34	7.76	4.11	6.70	12.57
Er	1.20	3.49	8.19	10.08	10.76	8.35	2.93	5.26	9.40
Tm	0.84	3.37	9.55	13.48	12.08	11.52	4.78	6.46	11.52
Yb	1.21	4.07	8.27	6.73	10.93	9.64	3.15	6.65	13.39
Lu	2.10	5.51	8.14	11.02	11.55	10.24	3.41	9.71	12.60
ΣREE	58.22	171.00	177.84	267.18	273.08	232.59	43.97	228.23	346.71
LREE/HREE	3.13	3.00	1.21	1.81	1.65	1.65	0.45	2.32	2.32
Eu/Eu^*	1.02	0.89	0.69	1.08	0.82	1.00	1.52	1.06	0.65

1. All major elements are in wt. percent.
2. Trace and rare earth elements are in ppm.
3. All rare earth elements are normalized to chondrite.

Fig.11.1 : Harker variation diagram, showing moderate effect of dilution by increasing SiO_2 content on several major elements components. r will stand for correlation coefficient .

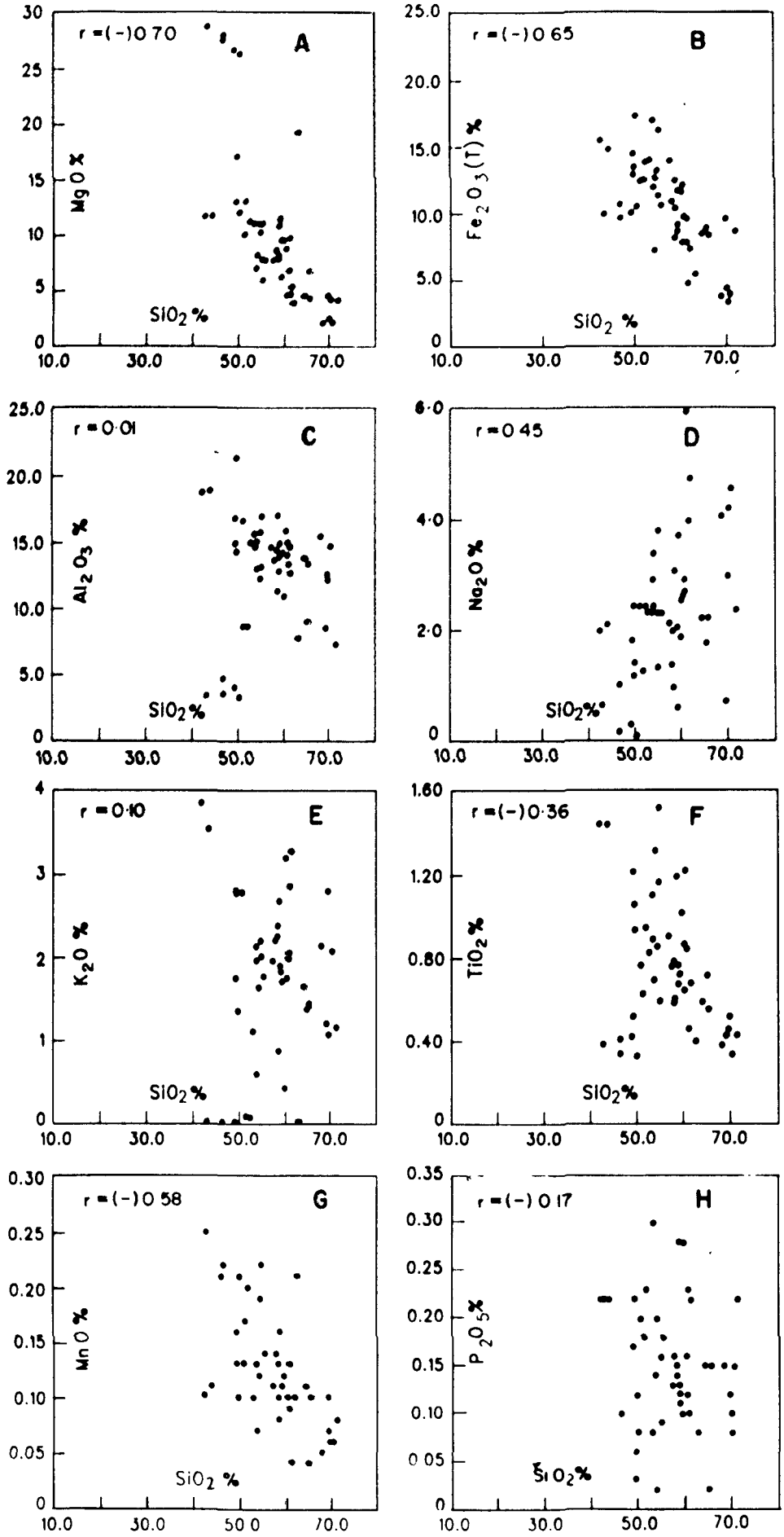
r = (-) 0 70
A
MgO %
SiO2 %
r = (-) 0 65
B
Fe2O3 (T) %
SiO2 %
r = 0·01
C
Al2O3 %
SiO2 %
r = 0 45
D
Na2O %
SiO2 %
r = 0·10
E
K2O %
SiO2 %
r = (-) 0·36
F
TiO2 %
SiO2 %
r = (-) 0 58
G
MnO %
SiO2 %
r = (-) 0 17
H
P2O5 %
SiO2 %
10.0
30.0
50.0
70.0

effect of increase of SiO_2 content in dilution of Cr, Co and Ni can also be seen (Table 11.1). Incomplete mixing and highly im mature nature of the debris is reflected in the scatters of Ni, Cr, Co and Zr content between 42-71% SiO_2 level. Contribution of the mafic-ultramafic component of the source is illustrated by Al_2O_3-MgO-CaO and CaO-Na_2O-K_2O ratios (Fig.11.2) where several samples fall in the mafic-ultramafic komatiitic field and some occupy places between TTG and thoeliitic and basaltic komatiitic field. These ratios indicate a high proportion of mafic-ultramafic rocks in the source area. The CaO-Na_2O-K_2O ratios (Fig.11.2) clearly illustrate that the feldspar content of the debris is both plagioclase and K-feldspar derived from acid plutons or gneisses. The Au content of the plagioclase of M_1 as determined at EPMA varies between An^{10-50}.

The KCM has a low maturity index averaging 0.73 (Table 11.1) and moderate chemical index of alteration (CIA, Nesbitt and Young, 1982) averaging 65.75, after exclusion of four carbonate bearing samples. A high matrix (M_2) : fragments ratio (average 1.26) and the presence of unaltered sodic plagioclase indicates that the mafic-ultramafic component has weathered, more than the feldspars. The constituents which could resist the effect of alteration like quartz and quartzite and to some extent feldspar are still present in the form of framework constituents, whereas more alteration-susceptable constituents like olivines and pyroxenes are incorporated into the matrix (M_1). Hence, most of the Fe_2O_3, MgO and other related elements are concentrated in matrix, whereas SiO_2 is present in both matrix (M_1) and framework.

Fig.11.2 : Al_2O_3-CaO-Na_2O and Na_2O-K_2O-CaO ternary ratio diagrams showing the compositional characteristics of the KCM and the effect of mixing of debris derived from multicomponent source. Most of the samples occupy their place between mafic-ultramafic and tonalite & granitic fields. It can be seen that the KCM samples are much more mafic than those of sediments of other younger schist belts.

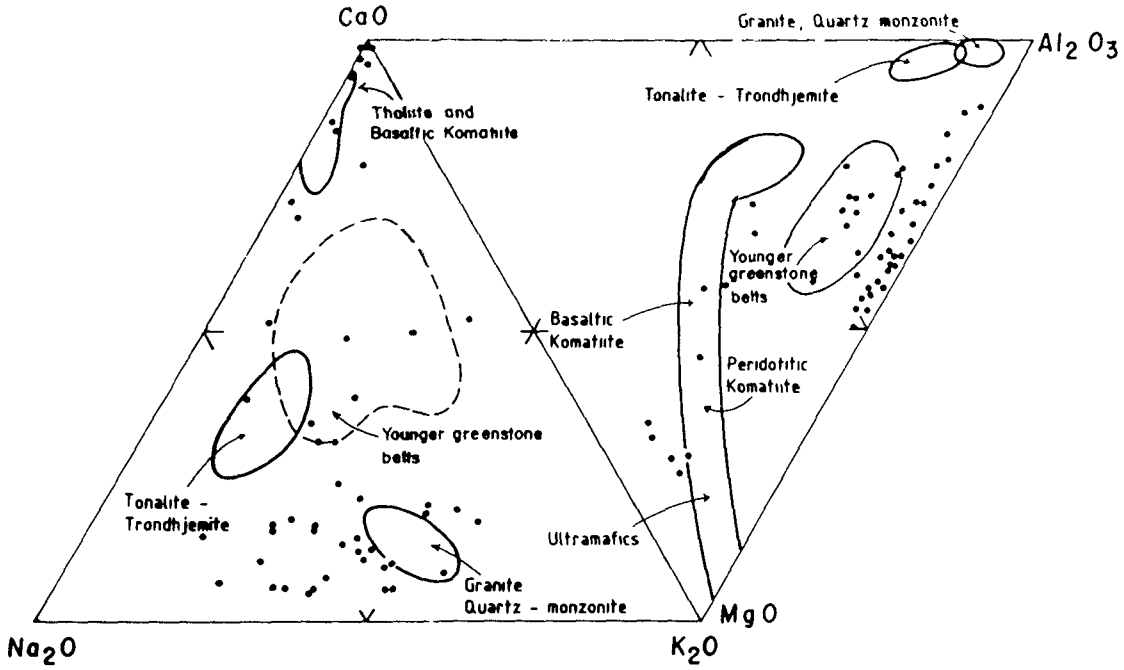
CaO
Granite, Quartz monzonite
Al_2O_3
Tonalite - Trondhjemite
Tholiste and
Basaltic Komatiite
Younger
greenstone
belts
Basaltic
Komatiite
Peridotitic
Komatiite
Younger greenstone
belts
Tonalite -
Trondhjemite
Ultramafics
Granite
Quartz - monzonite
MgO
Na_2O
K_2O

Relationship between Al_2O_3-K_2O illustrates (Fig.11.3A) that wherever K-feldspar and micaceous constituents of the samples have gone up, both the elements increase together (Fig. 11.3A). This suggests that the source area was not completely devoid of rock suites containing K-feldspar and K-rich micaceous minerals. Chickmagalur granite granodiorite and/or similar granitoids must have provided debris to the sediments of Bababudan basin. In spite of the existence of K-rich granite-granodiorite in the source area, K_2O/Na_2O (Fig. 11.3B) ratio of only eleven samples is more than one. It clearly demonstrates the predominance of sodic acid plutons over potassic ones in the source region. The K_2O/Na_2O ratio has been widely used to infer crustal evolution and secular variation in the composition of provenance of metasedimentary sequences. It is believed that for most sediments formed prior to 2.5 Ga, this ratio is generally < 1 (Engel et al., 1974; Schwab, 1978). This characteristic is supported by the observation of wide emplacement of K-rich granite near the Archaean-Proterozoic boundary which significantly increased K_2O content in younger sediments and the reversal of K_2O/Na_2O ratio. Further this aspect is reflected in the Eu depleted REE patterns of PAAS (Taylor and McLennan, 1985). However, the matrix of the Kaldurga Conglomerate shows variations in K_2O/Na_2O ratio from 0.03 to 4.55 (Fig. 11.3B), with a mean of 0.93. It indicates that K-rich granitic rocks were present as early as 3.1 Ga ago. The variations in K_2O/Na_2O are another indicator of mixed provenance. Samples with high K_2O content are also enriched in orthoclase. Hence, most of the K_2O in KCM is contributed by framework constituents. Similarly most of the Na_2O is provided by

Fig.11.3 :(A)Al_2O_3-K_2O distribution showing low order sympathetic increase of both the components, indicating that most of the K-feldspar has not been disintrigated. (B) Al_2O_3 - Na_2O distribution showing low order simalteneous increase of both the oxides, indicating that plagioclase was also not very intensely weathered before deposition. (C) K_2O - Na_2O distribution pattern showing that most of the samples fall below 1:1 ratio, only for eleven samples K_2O/Na_2O ratio is more than one. The scatter in this ratio is suggestive of mixed provenance.

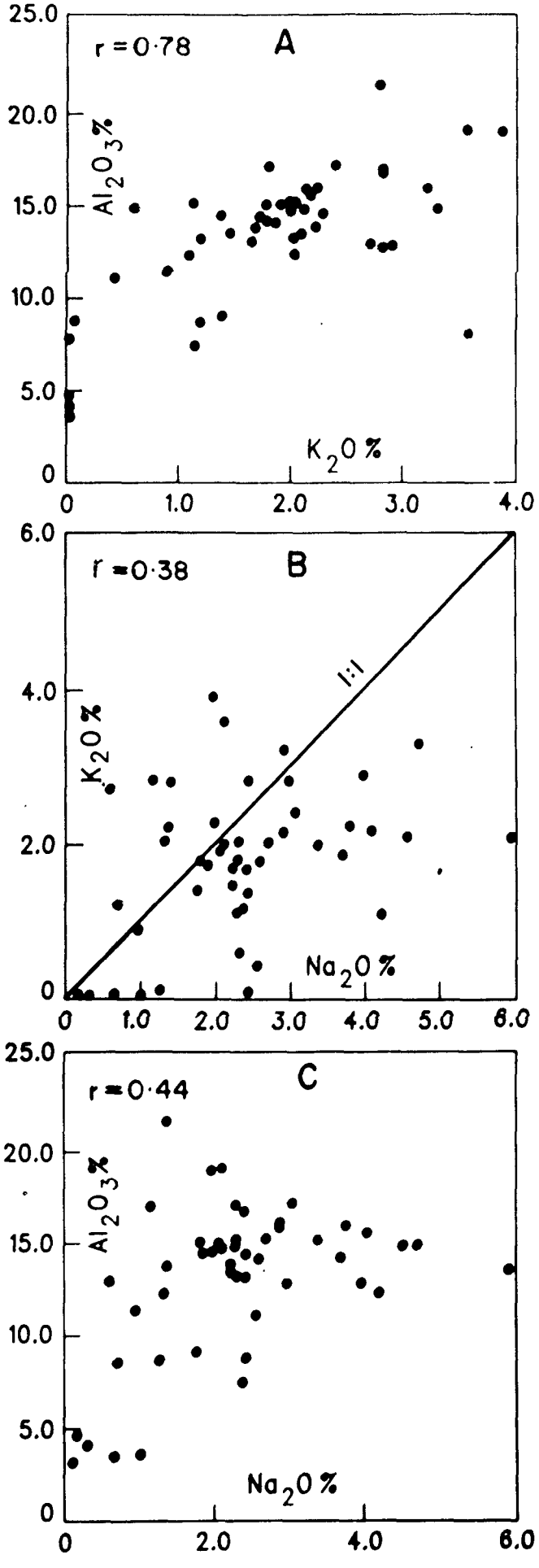
r = 0·78
A
Al_2O_3%
K_2O %
r = 0·38
B
1:1
K_2O%
Na_2O %
r = 0·44
C
Al_2O_3%
Na_2O %

plagioclase of the framework as shown by a low order sympathetic linearity in the Al_2O_3-Na_2O plot (Fig. 11.3C).

Widely scattered MgO values for the KCM samples (Fig. 11.1A) are a distinguishing feature of this conglomerate. Enrichment in MgO may be due to abundance of mafic-ultramafic rocks in the provenance area and/or contemporaneous volcanism in the basin of deposition. Underlying strata of the Bababudan group are mafic volcanic rocks but mafic volcanic rocks contemporaneous to the KCM are not found in the basin. The debris of the underlying volcanic rocks could also have contributed ferromagnesian components. Since cross bedded quartzites (form as pebbles) are interbedded with the metavolcanics and since such cross bedded quartzites have not been found in the older greenstone belts (Naqvi, 1978; 1983), it is apparent that the underlying volcanics have also contributed some debris to the conglomerate. $MgO/Fe_2O_3^{(t)}$ and MgO/K_2O (Fig. 11.4 A and B) ratios illustrate this aspect. The MgO content of these rocks falls above the MgO-$Fe_2O_3^{(t)}$ mantle curve (Fig. 11.4A). This indicates that Mg-enriched rocks were present in the source region. Such rocks are present in older schist belts and are known as high Mg basalts, ultramafic peridotitic komatiites and actinolite chlorite schists (Hussain and Naqvi, 1983). Where the contribution of Mg-rich roks is great, the samples occupy a place towards the high Mg rock field and if the BIF contribution is more, then the samples are shifted towards the BIF field (Fig. 11.4 A). High concentrations of $Fe_2O_3^{(t)}$ in these samples do not necessarily reflect magmatic source rocks. Pebbles of BIF are also found. Most probably the BIF present in the underlying sequence of the Bababudan Group has contributed a significant part

Fig.11.4 : (A) MgO - Fe_2O_3 distribution pattern showing extreme enrichment in MgO in some samples. Line shows mantle curve, MMB = High Mg basalt, BIF = Banded Iron Formation field, Predominance of ultramafic rocks in source area is clearly visualized (B) MgO-K_2O plot showing the predominance of high Mg rocks over K-bearing rocks in the source area. Both the plotes clearly illustrate the abundence of the mafic-ultramafic components in the source.

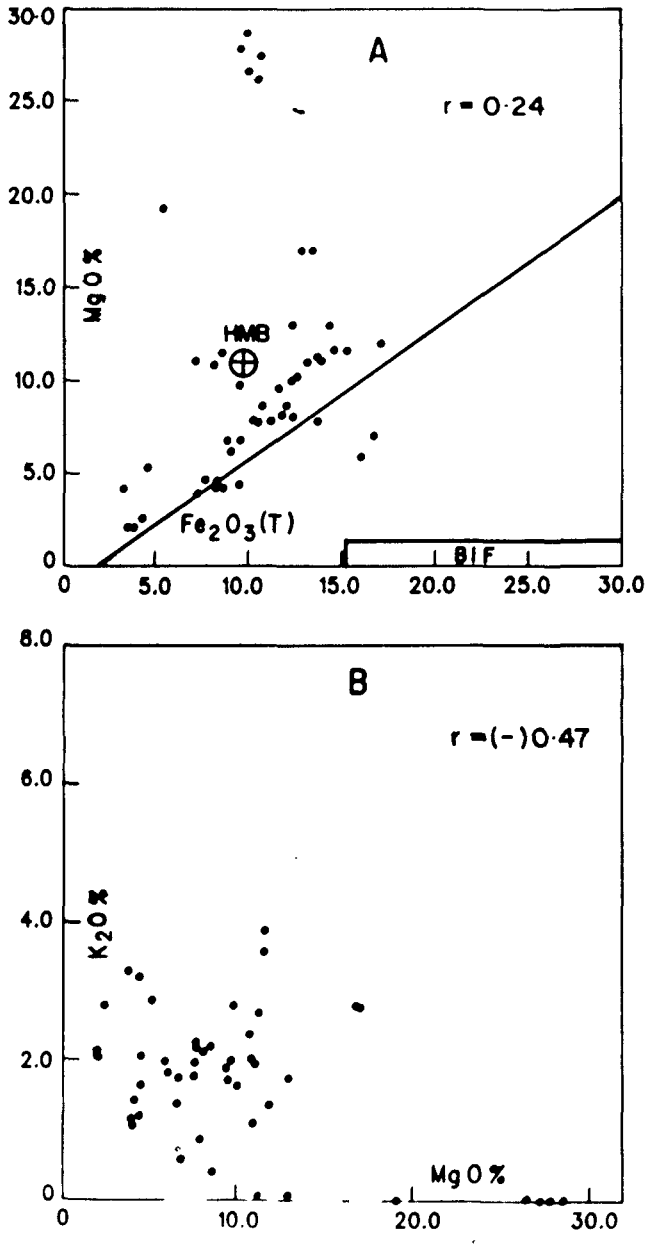
A
r = 0·24
MgO %
HMB
Fe2O3(T)
BIF
30·0
25.0
20.0
15.0
10.0
5.0
0
5.0
10.0
15.0
20.0
25.0
30.0
B
r =(-)0·47
K2O %
Mg O %
8.0
6.0
4.0
2.0
0
10.0
20.0
30.0

of $Fe_2O_3^{(t)}$. However, some part of the $Fe_2O_3^{(t)}$ present in the KCM samples must have been provided by mafic-ultramafic rocks. The older schist belts below the Kalasapura unconformity also contain high grade iron formation made up of garnet, grunerite, magnetite and quartz. This clearly indicates the multicomponent nature of the source. This is further substantiated by K_2O-MgO relationship (Fig. 11.4B). MgO enriched samples are extremely depleted in K_2O, whereas K_2O enriched samples are depleted in MgO having a scatter in between the two extremes (Fig. 11.4B). This along with K_2O-Na_2O distribution confirms that the source was dominated by Mg-Na rich and K depleted rocks. Sample No.MK-13, 40, 48 and 50 contain around 10-13% of calcite and/or dolomite which appear to have formed during diagenesis and recrystallization of matrix [M_2]. Part of the high MgO and CaO abundances of the samples present as carbonate has affected its trace elements abundance including REE. These samples are excluded from the interpretation and modelling of the source composition as the carbonates are not detrital.

11.3 TRACE ELEMENTS:

The Rb content of the matrix of the Kaldurga Conglomerate show a large scatter from 0.41 to 81.72 ppm. Low Rb content is found in the samples which are enriched in MgO and depleted in K_2O. Similarly higher Rb contents are associated with low MgO and high K_2O abundances (Table 11.1). These characteristics of the KCM are illustrated in a plot of K/Rb ratios (Fig. 11.5A) showing values between those of basic and felsic rocks. The Sr contents vary from 2.00 to 200 ppm and appear to be dependent on CaO

Fig. 11.5 : (A) K-Rb distribution pattern showing the large scale variation and sympathetic linear relationship between the Felsic and mafic end members.

K-Rb distribution shows mixing of the mafic and felsic and number of the source area (B) Distribution pattern of K-Sr showing large scale scatter in Sr concentration (C) Rb-Sr distribution showing a week sympethetic relationship between the two (D) Ba-K distribution pattern showing weak sympathetic relation between Ba and K with large scale variation.

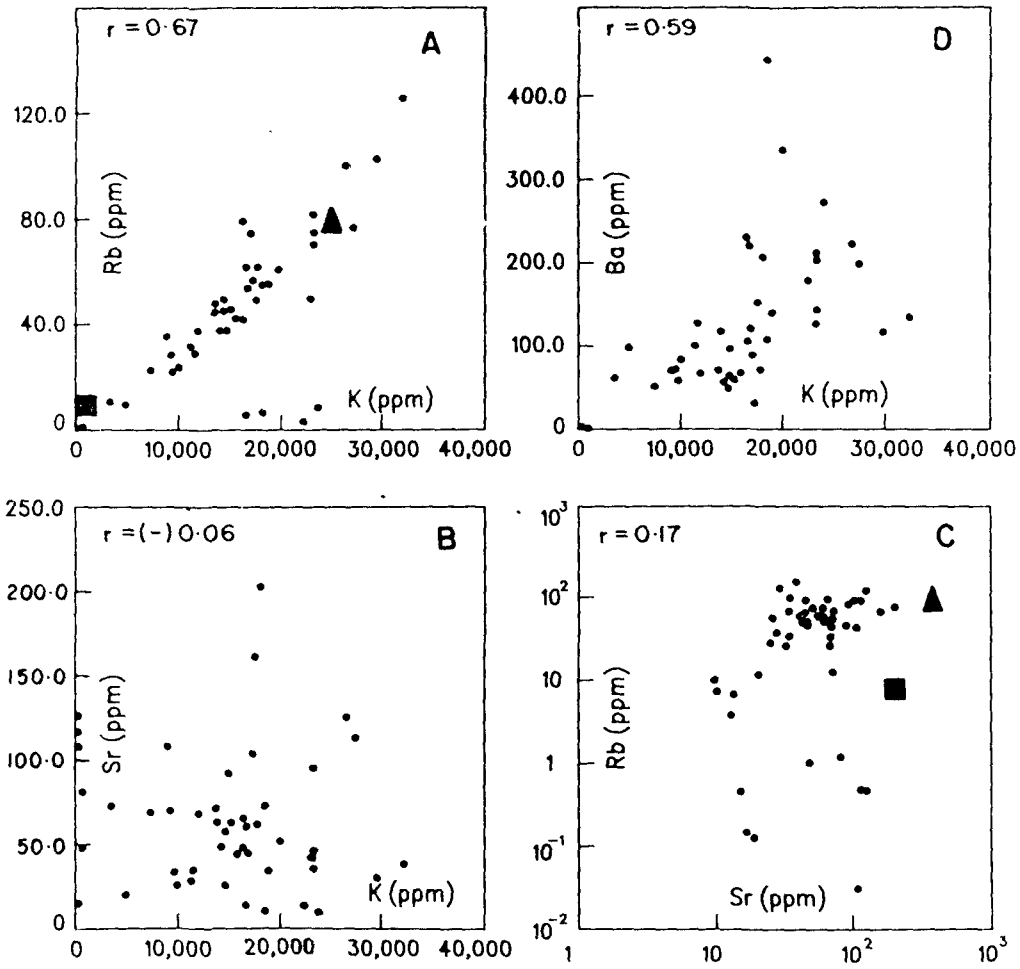
r = 0·67
A
Rb (ppm)
K (ppm)
120.0
80.0
40.0
0
0
10,000
20,000
30,000
40,000
r = 0·59
D
Ba (ppm)
K (ppm)
400.0
300.0
200.0
100.0
r = (-) 0·06
B
Sr (ppm)
K (ppm)
250·0
200·0
150·0
100·0
50·0
r = 0·17
C
Rb (ppm)
Sr (ppm)
10^3
10^2
10
1
10^{-1}
10^{-2}

content (Table 11.1). Large scale scatter in Sr content against K (Fig. 11.5B) is indicative that a multicomponent source has provided the debris. Similarly, Rb/Sr do not show a complementary increase. Random scatter of the Rb-Sr values (Fig. 11.5C) of the KCM ranging between Rb-Sr values of mafic and felsic rocks also suggest a multicomponent rock mixing, through sedimentary processes. The Ba is extremely depleted in high Mg samples and appears to be more enriched in the samples with higher K_2O (Fig. 11.5D). Ba content ranges from 0.67 to 438 ppm. This scatter and its dependence on K illustrates that the concentration of trace elements is also controlled by the source rocks and the incomplete mixing of the two extreme members of the source region. When the Rb/Sr and K/Rb ratios are compared with those of the Archaean TTG from Dharwar Craton and elsewhere, these elements and ratios fall between the elemental abundances and ratios of mafic-ultramafic rocks and TTG.

Above inferences are strongly substantiated by ferromagnesian and other trace elements like Cr, Ni, V, Sc and Zr (Fig. 11.6). Chromium content of these rocks show a large scatter from 0.46 to 2432 ppm with an average of 427 ppm (Table 11.1). In a similar way, Ni abundances range from 0.36 to 1117 ppm with an average of 191 ppm. Co shows a variation from 4.4 to 94 ppm and mean concentration is 52 ppm (Table 11.1). These Cr, Ni, Co abundances are high relative to those in TTG (average values are 21, 16 and 11 respectively) and are best explained by a contribution from ultramafic sources. The Ni and Cr concentrations of MgO-rich samples, e.g., MK-15,33,34 and MK-48, can be directly related to the ultramafic component of the provenance. MgO values higher

Fig. 11.6 : (A) MgO-Cr distribution pattern showing sympathetic relationship between MgO-Cr derived from ultramafic source. Apparent scatter between 4-12% MgO is an effect of mixing with low MgO-rocks. High Cr value rules out Mg-metasedi- mentation. High MgO and Cr values of the samples may be noted. (B) MgO-Ni distribution pattern shows the simultaneous inferences of Ni with MgO indicating that both elements have been derived from mafic-ultramafic source. Dolomite/calcite bearing samples are having low Ni-Cr contents (C) Simultaneous increase in Ni-Cr except in dolomite/calcite bearing samples which have lower Ni and Cr (D) Cr-Zr distribution pattern, showing the antipathetic relationship between the two as the samples enriched in Cr and depleted in Zr, and the sample enriched in Zr are depleted in Cr. Zr and Cr distribution is diagnostic for mixing of the mafic-ultramafic rocks and felsic components of the soruce (E) Ti-Zr distribution pattern showing a scatter as a result of mixing; the hydrodynamic processes were short lived and were not effective for concentration of heavy minerals. (F) V-Sc showing linear relationship between the two as both these elements are largely derived from felsic component of the source.

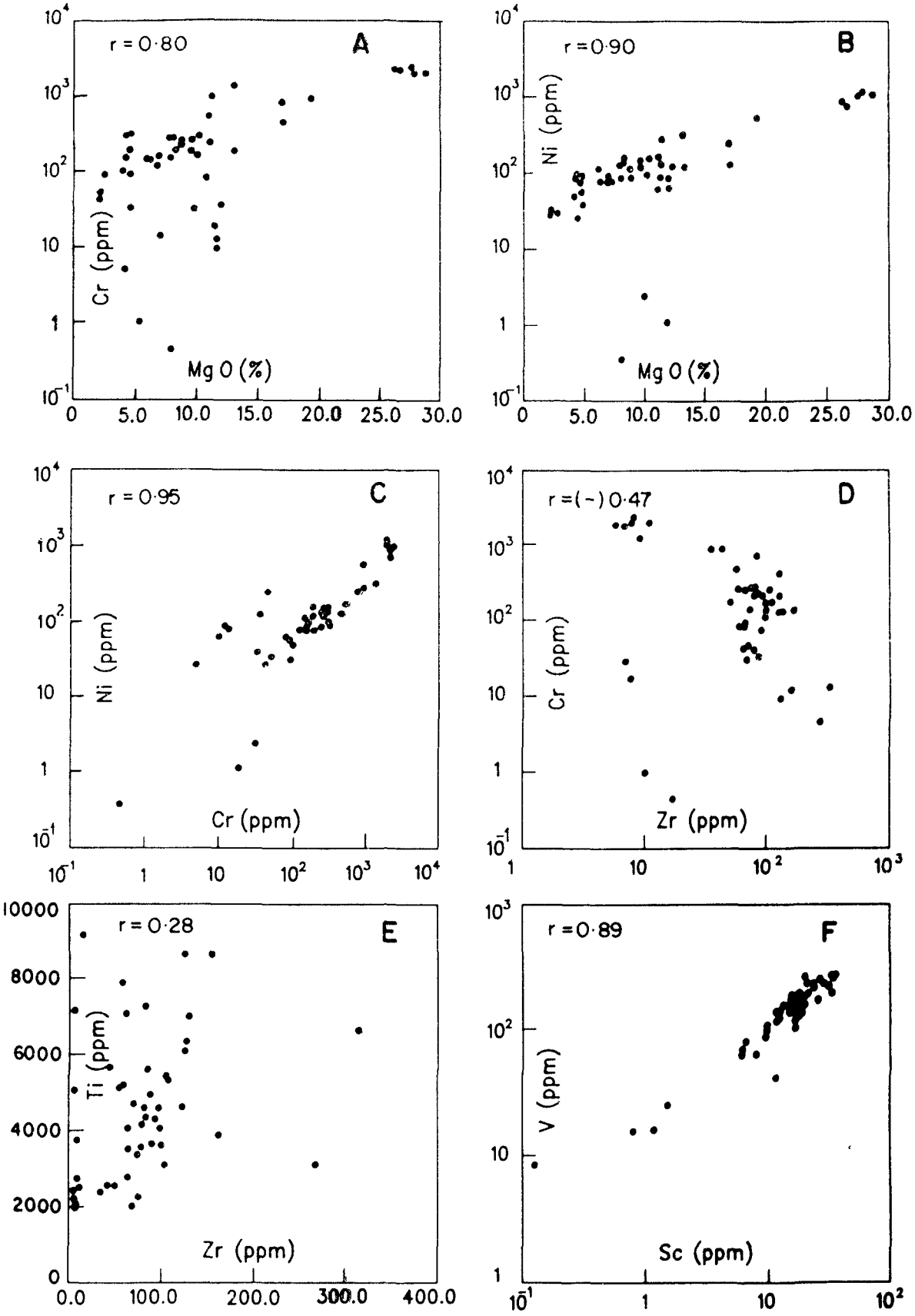
r = 0·80
A
Cr (ppm)
Mg O (%)
r = 0·90
B
Ni (ppm)
Mg O (%)
r = 0·95
C
Ni (ppm)
Cr (ppm)
r = (−) 0·47
D
Cr (ppm)
Zr (ppm)
r = 0·28
E
Ti (ppm)
Zr (ppm)
r = 0·89
F
V (ppm)
Sc (ppm)

than 10% indicate mafic-ultramafic components in the source rocks. Corresponding high Cr and Ni values together with the absence of significant amount of carbonate (except in four samples MK 13, 40, 48, 50) in the modal analysis (Table 6.3) rules out that the MgO is present mainly as dolomite. Furthermore these carbonate bearing samples except MK-48 do not contain more than 8-9% MgO. The K_2O/MgO (Fig. 11.4B) and MgO-Ni, MgO-Cr relationship (Fig. 11.6 A&B) leave no doubt that ultramafic rocks were abundant in the source area. Magnesium metasomatism is clearly ruled out by high Cr and Ni values. Sympathetic linear relationship between Ni and Cr clearly demonstrate that these elements have common ultramafic source (Fig. 11.6C). Antipathetic crude linear relationship is illustrated by the Cr-Zr plot (Fig. 11.6D). Low Zr (5.77 ppm) is found in MK-15 which contains 28.72% MgO and 1975 ppm Cr and 1010 ppm Ni, whereas highest Zr (266 ppm) is present in sample No.MK-50, which has a low MgO, Cr, Ni and high feldspar and quartz contents, as reflected in their alkalies. Al_2O_3 and SiO_2 abundances (Table 6.3 and 11.1). Scatter in the Zr and Ti plot (Fig. 11.6E) also provides evidence that the multicomponent source rocks have not been subjected to the strong hydrodynamic fractionation and the heavy minerals present in the source rocks could not be concentrated or removed from the debris. Since V and Sc both represent the mafic components an excellent linear sympathetic relationship between the two elements is illustrated (Fig. 11.6F). Similar enrichments and depletions are indicated by U and Th contents of the analysed samples.

11.4 REE DISTRIBUTION AND Eu-ANOMALIES:

On the basis of the REE distribution patterns, the KCM is divided into eight groups. Group I (Fig. 11.7A) consists of four samples of high MgO content (~25%) showing very strong negative Eu anomalies with depleted REE pattern and almost flat pattern shape. The unfractionated REE pattern with high amount of MgO is reflecting the abundance of ultramafic rocks in the source region. The negative Eu anomalies in this group are similar to those of altered komatiites (Jahn and Schrank, 1983). Group II (Fig. 11.7B) consists of sixteen samples showing relatively enriched ΣREE, moderate negative Eu anomalies and LREE/HREE~1. Group III (Fig. 11.7C_1) consists of eleven samples having depleted ΣREE, moderate to weak negative Eu anomalies and fractionated pattern shapes, reflecting LREE enrichment and HREE depletion. These samples contain MgO and $Fe_2O_3^{(t)}$ of moderate levels. Group IV (Fig. 11.7C_2) consists of three samples with negative Eu anomalies and fractionated pattern shapes, illustrated by enrichment of LREE and depletion of HREE. Group V (Fig. 11.7D) consists of nine samples with fractionated patterns exhibited by enrichment of LREE with extremely negative Eu anomalies or no anomalies. Group VI (Fig. 11.7E) consisting of three samples with almost flat patterns and no Eu anomalies. Group VII (Fig. 11.7F) consists of only one sample (MK-48) of a pattern shape illustrating depletion in LREE and relative enrichment in HREE along with positive Eu anomaly. This sample contains 26% MgO and mainly consists of amphiboles, quartz and dolomite. The REE pattern of the sample resembles to those of high Mg Basalt and pyroxenites. Group VIII (Fig. 11.7G) consists of two samples with depleted ΣREE and no Eu anomalies.

Fig. 11.7 : REE distribution pattern in various group of the KCM. Detail from A to G are given in text.

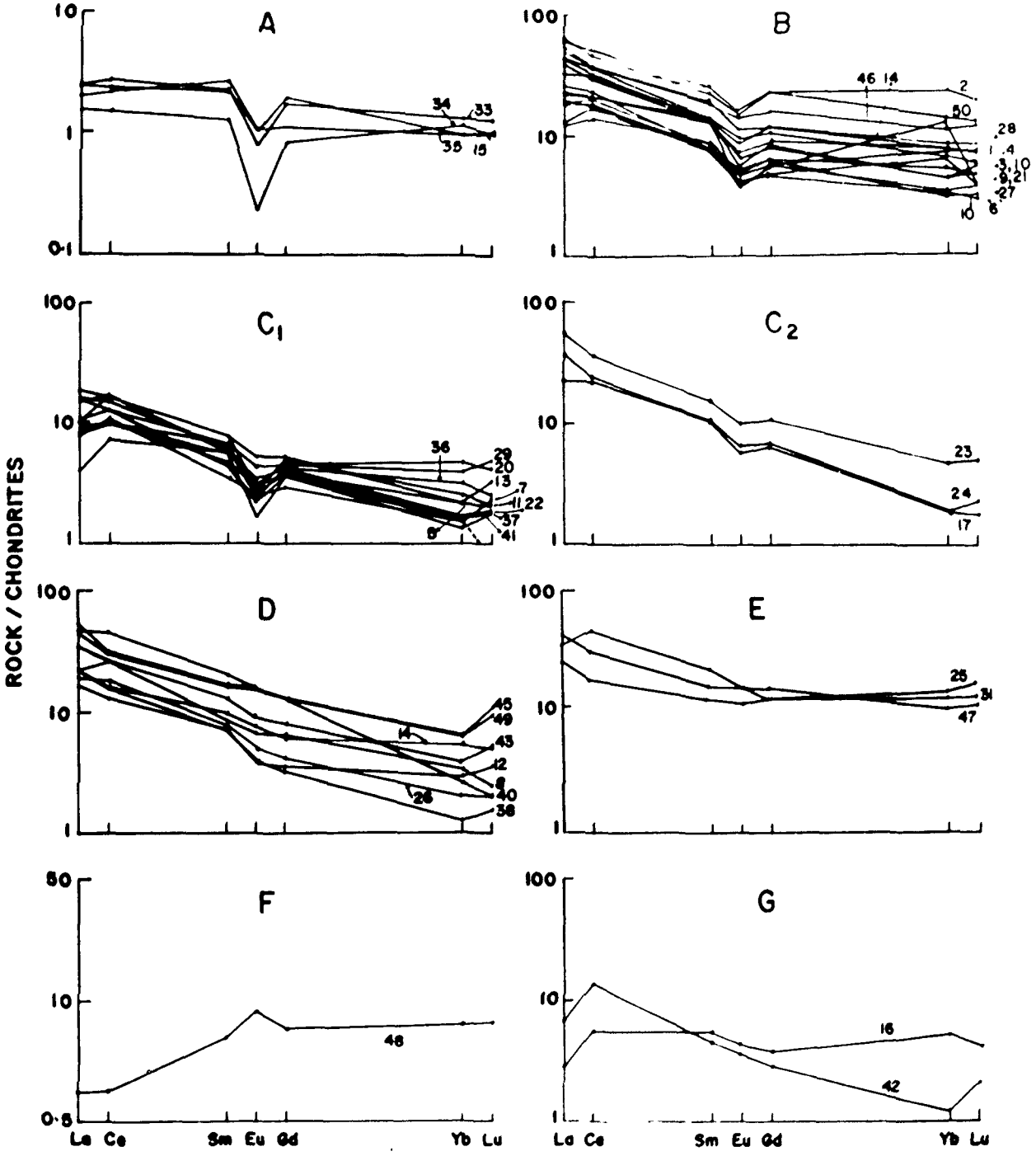
A
B
C1
C2
D
E
F
G
ROCK / CHONDRITES
La Ce Sm Eu Gd Yb Lu

Sample No.MK-16 is having almost flat pattern, whereas sample No.MK-42 shows sloping pattern of fractionation. LREE are enriched in tonalites and trondhjemites, whereas mafic-ultramafic rocks are depleted in ΣREE. Mixing of the two in different proportions would yield REE patterns as shown by the KCM (Fig. 11.8). This mixing and high Zr content has yielded a less fractionated pattern in MK-50 (Fig. 11.7B), whereas MK-23, 24 (Fig. $11.7C_2$) show a highly fractionated pattern. This highly fractionated pattern is deceptive, it does not mean that debris has been derived from highly fractionated rocks, but is a result of mixing of TTG and mafic-ultramafic rocks in a given proportion. The negative Eu anomalies in this suite of rocks are inconsistent with the model proposed by Taylor and McLennan (1985), though, a small body of K-rich granite-granodiorite is present in the source area. Negative Eu anomaly has been considered by Taylor and McLennan (1985) as a characteristic feature of PAAS, however, the work of last few years has shown that despite the abundance of sodic plutons and relative absence of K-granite from these terrains, -ve Eu anomalies are common in the Archaean rocks of India, Greenland and Africa (Naqvi et al., 1983, 1988; McLennan et al., 1983, 1984).

Considering the total population of the samples analysed the enrichment in $LREE_N$ and depletion in $HREE_N$ (Fig. 11.8) appears to be the result of two end members in the source having different REE characteristics and their mixing to variable proportions has generated the observed patterns. This aspect is very clearly demonstrated in Fig. (11.8), where the total range of the REE pattern shapes of the KCM encompass the patterns of altered

Fig. 11.8 : Overall range of REE distribution in the KCM along with the felsic and mafic end members, NASC, PAAS, AAS and altered peridotitic komatiites. This figure clearly demonstrated that observed variations in the REE are the result of mixing of multi-component source rocks. Overall effect and contribution of basic ultrabasic rocks is very pronounced.

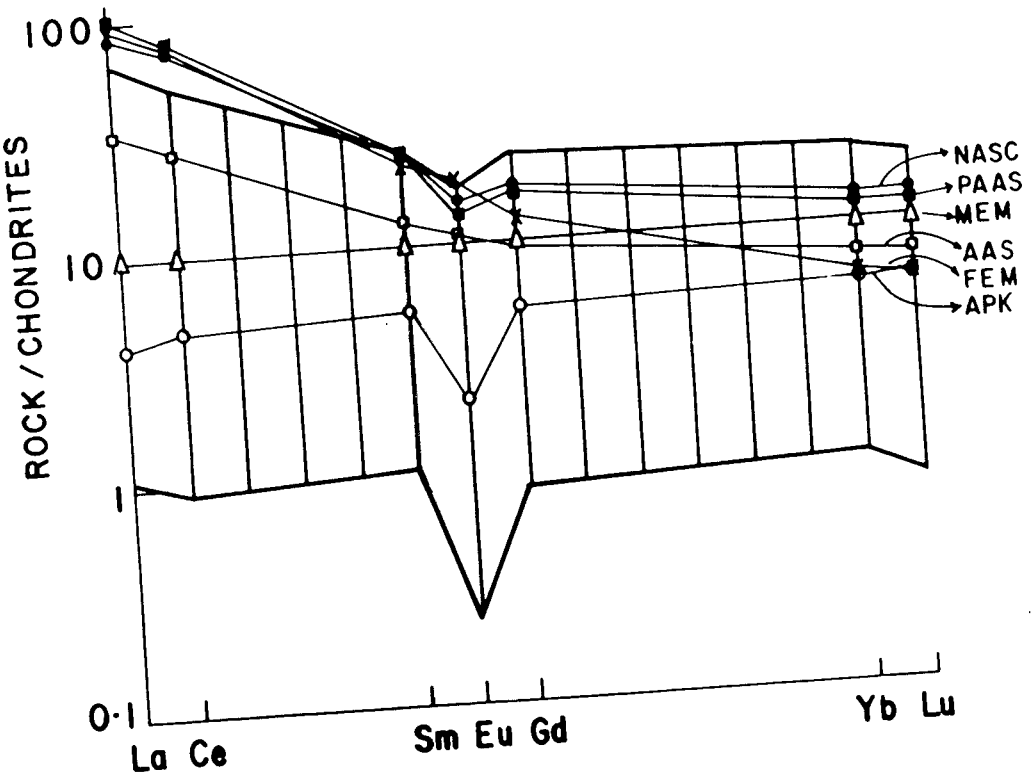
100
10
1
0·1
ROCK / CHONDRITES
La Ce
Sm Eu Gd
Yb Lu
NASC
PAAS
MEM
AAS
FEM
APK

peridotitic komatiites, mafic and felsic end members of bimodal Archaean volcanism and average Archaean sediments.

Samples with pronounced negative Eu anomalies like MK-50 and that which do not show any Eu anomaly such as MK-40, 43 and 45 contain similar amounts (around 10%) of K-feldspar. Therefore, the negative Eu anomalies in these samples (MK-50) may not be simply due to the presence or absence of K-feldspar. Sample MK-50, contains 20% plagioclase but has a negative Eu anomaly, whereas MK-40 contain 9% plagioclase but does not exhibit any Eu_N anomaly. Similarly the CaO contents of MK-50 and MK-40 being 3.27% and 0.44% respectively, do not suggest any simple relationship between the composition of feldspars and their Eu anomalies, as is widely believed (Taylor and McLennan, 1985). Both MgO and K_2O contents of the KCM appear to have some control on the overall abundances of ΣREE. Inspite of an overall scatter it is evident that samples extremely enriched in MgO and depleted in K_2O are also depleted in ΣREE, whereas the samples enriched in K_2O contain higher ΣREE except in two cases (Table 11.1). The Eu content shows a very crude relationship with MgO and K_2O. However, the alteration of the komatiitic source rocks has produced negative Eu anomalies in the MgO rich samples and thus a very clearcut relationship is not seen. A large scale scatter of the Eu content against K_2O is observed which corroborates the above inference that feldspar composition cannot be correlated with the Eu anomalies.

The geochemical data of the KCM, discussed above, show that the composition of the KCM can best be explained by a multicomponent provenance model. The inferred provenance of these

sediments was made up of TTG, mafic-ultramafic rocks and sedimentary rocks including BIF. The average composition of the KCM can be generated by mixing of 50% TTG, 35% ultramafics, 10% mafics and 5% sediments. The mafic-ultramafic rocks and sediments appear to have been derived from an older schist belt sequences and the underlying sequence of quartzite, amphibolites and BIF of Bababudan group. This debris was deposited into the basin without much reworking, sedimentary and/or chemical differentiation. The composition of the exposed crust around 2.6 Ga ago is computed to be 90% TTG and, 10% mafic-ultramafic rocks. This composition shows that during the early-middle Archaean the continental crust must have been much more mafic than it is now. Therefore, mafic-ultramafic components were formerly more prominent in the source region and have been eroded to expose a greater proportion of magmatic TTG, which were emplaced into the older schist belts. It is emphasized that older schist belts have also been intruded by 3.4 Ga old gneisses in addition to younger events (Naqvi, 1981). The gneisses in the northern region around Goa which contain significant mafic-ultramafic enclaves of variable dimensions are also dated at 3.4 Ga (Dhoundial et al., 1987). Based on these radiometric data it has been envisaged by Naqvi (1981) and Naqvi et al. (1988) that the older schist belts may be as old as 3.5 Ga. However, exact radiometric age on these belts is yet not available. Inspite of the uncertainty of the exact age of the older schist belts, it is certain that the KCM has sampled the upper crust which was younger than 3.4 Ga and older than 3.1 Ga. Presence of much older supracrustals in these 3.4 Ga. old gneisses cannot be ruled out. In view of these facts we infer

that the KCM has sampled the crust which was formed during early and middle Archaean. This crust appears to contain a very large proportion (about 45%) of mafic-ultramafic rocks. The graywackes of Shimoga and Chitradurga (2.6 Ga) also show a multicomponent source area but have only about 20% mafic-ultramafic component in their model source. Comparison of the present model crustal composition with those inferred earlier (Argast and Donelly, 1986; Naqvi et al., 1988) shows that the early-middle Archaean crust of the Karnataka Nucleus was heterogenous in composition at the exposed surface level and the percentage of mafic and ultramafic material varied greatly. Compositional Hetrogeneity and diachronous evolution of the Archaean crust have been recognised in different cratons (Young, 1978; Gibbs et al., 1986).

CHAPTER-XII

TECTONIC SETTING OF DEPOSITION

12.1 INTRODUCTION:

Tectonic setting of the deposition of Dharwar sediments has been debated for a long time (Naqvi and Hussain, 1972; Swami Nath and Ramakrishnan, 1981; Naqvi et al.,1988). The debate has been about the question of ensialic or ensimatic deposition of these sediments. Naqvi et al. (1978b) have proposed that the graywacke sedimentation has been mainly ensimatic between the continental nuclei and that the debris was supplied from juvenile cratons on both the sides. Whereas, Chadwick et al. (1981) suggest that the Peninsular Gneiss formed the basement on which sedimentation of graywacke etc. occurred in ensialic rift basins.

The concept of plate tectonics has been evolved from the earlier hypothesis of continental drift, sea floor spreading and transform faults (Bott, 1982). Conceptual unification of explanation of observed features by this concept, has revolutionised the earth science (Cloud,1980) and understanding of the processes of crustal evolution. According to plate tectonic theory all the exogenic and endogenic processes are controlled by their site of activation with respect to the plate margins. However, the applicability of this theory to the era older than 2.5 Ga is slowly gaining grounds. More and more data from the Archaean terrains are accruing which support the validity and applicability of plate tectonics in a modified form during the Archaean time (Naqvi et al.,1974; Cloud, 1980; Kroner, 1981; Sleep

and Windley,1982; Candie, 1982; Nisbet and Fowler, 1983; Abbott, 1984; Abbott and Haffman, 1984; Naqvi, 1985; Hargraves, 1986 and Chadwick et al., 1989).

Studies of sedimentary petrography and geochemistry have made important contributions to the interpretations of plate tectonic settings and estimate of average upper crustal composition. In many instance, provenance regions have been destroyed and the only record lies in the sediments derived from them. Recent data indicate that the compositional and petrographic characteristics of young graywackes and modern deep-sea sands are closely related to their tectonic settings and provenance (Dickinson and Suczek, 1979; Dickinson and Vallani, 1980; Bhatia, 1983; McLennan, 1984; Taylor and McLennan, 1985; Bhatia and Crook, 1986; Roser and Korsch, 1988).

The basic principle to discriminate various tectonic setting for a sedimentary basin is that away from the continent in an oceanic basin, continental debris is reduced, and the petrographic and chemical constituents which are diagonestic of continental provenance, are depleted.

Moorris (1974a), Dickinson (1980), Dickinson and Suczek (1979), Dickinson and Valloni (1980), Dickinson et al. (1983) and Ingersoll (1990), have studied the sandstones mineralogical composition and its relationship to the plate tectonic setting of the basin. They (ibid) have found that detrital framework modes of sandstone suites from different kind of basins are a function of provenance types governed by plate tectonics. Quartzose sands drived from continental cratons are widespread within interior basins, plateform successions, miogeoclinal wedges, and opening

ocean basins. Arkosic sands from uplifted basement blocks are present locally in rifted troughs and in wrench basins related to transform ruptures. Similarly volcaniclastic sands and recycled orogenic sands rich in quartz or chert plus other lithic fragments, are derived from magmatic arcs and subduction complexes respectively.

Bhatia (1981,1983,1985), Bhatia and Taylor (1981) and Bhatia and Crook (1986) have recognized oceanic island arc, continental island arc, active continental arc and passive margin type tectonic setting for the various sedimentary basins. Immobile trace elements, e.g. La, Ce, Nd, Th, Zr, Nb, Y, Sc, and CO have been found very useful in tectonic setting discrimination. In general, there is a systematic increase in LREE, Th, Nb, and the Ba/Sr, Rb/Sr, La/Y and Ni/Co ratios and a systematic decrease in V, Sc and the Ba/Rb, K/Th and K/V ratios in sedimentary rocks, specially in graywackes from oceanic island arc to continental island arc to active continental arc to passive margin tectonic settings. Major element indices such as $Fe_2O_3^{(t)}$ + MgO content, along with parameters that are sensitive to the presence of continental detritus like K_2O/Na_2O or Al_2O_3/SiO_2 ratios have also empirically been shown as useful discriminants of the various tectonic setting of sedimentation (Bhatia, 1983, Roser and Korsch, 1988).

For Archaean sediments, however, the above principles may not be entirely applicable (e.g. McLennan, 1983, 1984), given that K_2O was not as abundant in the upper continental crust as in the Proterozoic and Phanerozoic eras; instead Na_2O was predominant in continental rocks like tonalitic gneisses. Similarly during late

Archaean, the BIF supplied considerable debris and was recycled into graywackes of 2.6 Ga. Therefore, both the K_2O/Na_2O ratios and the total $Fe_2O_3^{(t)}$ + MgO content are of some extent misleading for discrimination purpose in the Archaean. Furthermore, major uncertainities exist in extrapolating the Phanerozoic tectonic setting to the Archaean. Despite all these complexities, Argast and Donnelly (1986), Bhatia and Crook (1986), Naqvi et al. (1988), Wronkiewicz and Condie (1987, 1989), Feng and Kerrich (1990), Condie and Wronkiewicz (1990a), Pan et al. (1991) were able to infer tectonic settings and source for Archaean graywackes sediment.

The present chapter is devoted to reconstruction of tectonic environment of the Bababudan basin at the time of deposition of (1) basal quartz pebble conglomerate with associated quartzites (quartz arenites) and (2) upper most member of the sequence namely the Kaldurga Polymitic Conglomerate. Main conclusions of geochemical investigations of intimately interstratified volcanics and overlying thick sequence of oxide facies BIF, were incorporated to infer the tectonic regime of deposition of QPC and the KCM, and then an attempt is made to propose a model for the tectonic evolution of late Archaean Bababudan basin of Dharwar Craton, KN.

12.2 PALAEOENVIRONMENTAL CONSTRAINTS AND TECTONIC SETTING:

12.2.1 QPC and Associated Quartzites:

Quartz pebble conglomerate shows well rounded pebbles of quartz with very less amount of intervoid matrix (~ 5%). Main

constituents of matrix are rounded quartz grains, fuchsitic mica, and detrital rounded grains of pyrite and other micaceous minerals with very rare presence of uraninites. A higher degree of roundness of clasts as well as framework constituents of matrix indicate the higher intensity and degree of hydrodynamic activity. This fact is further strengthened by the total absence of feldspar and other unstable minerals. Furthermore, the presence of detrital pyrite indicates the anoxic atmosphere over the provenance and reducing environment at the site of deposition. Sulpher isotopic ($\delta^{34}S$) data also support this assumption. All the sedimentalogical characters discussed in Chapter-V indicate the shallow water environment for the deposition of quartz pebble conglomerate.

Overlying facies of quartzite, which is actually quartz arenite or feldthespatic quartz arenite, show textural and mineralogical maturity. Medium grained quartzite with high degree of sorting, further indicate that sediments have undergone longer duration of reworking and winnowing processes before deposition. More reworking is possible only in shallow water condition, where wave and current action is very strong. In addition to above well preserved primary depositional sedimentary structures of various sort indicate that, these rocks were deposited in a shallow basin under the influence of mutual interaction of sediment load and water current (Potter and Pettijohn, 1972; Pettijohn, 1984). In the upper portion of depositional column, mud crackes were found (Fig. 5.2 and 5.21), which shows that at the end of this depositional cycle which constitutes various sedimentary facies of conglomerate and quartzites, the depth of water column had

become very shallow, or basin decsication had started. All these field constraints indicate the presence of plateformal succession deposited in a shallow basin within the continental crust under stable tectonic conditions.

12.2.2 The Kaldurga Polymitic Conglomerate:

As discussed in chapter V, the Kaldurga Conglomerate consists of clasts of various lithology with a difference in their size. Boulder to pebble size clasts are embedded, in fine grained chloratic to amphiobolitic matrix. Sometime these boulders and pebbles show a prefered orientation, thereby indicating flow direction. Variation in the size of the boulders and the high percentage of matrix suggest that this matrix supported conglomerate has been rapidly deposited by high viscous medium. Rather weak hydrodynamic activity, characteristic of slurries, was unable to sort the debris. Its deposition appear to have taken place due to sudden subsidence of the basin, which gave rise to "sediment gravity flow" or "mass flow" mode of transportation. High relief of provenance was responsible, for the rapid and strong physical weathering and very low chemical disintigration. These inferences are evident by the presence of big boulders and unstable framework minerals in the matrix. Systematic facies analysis suggest that enormous quantities of the boulders, cobbles and pebbles of various lithology with the floating framework in matrix, were transported by highly viscous slury or mud flow or sediment gravity flow and deposited as deep sea fans or fanglomerates (Walker, 1978, Nocita and Lowe, 1990). Occurrence of Imbrication of such unsorted sediments, also

indicates that these deposits are mass flow deposits. These observations suggest that the Kaldurga Palymetic Conglomerate was deposited in deeper water conditions, indicating the unstable mobile tectonic regime at the end of the Bababudan basin. The above characteristics indicate that the Kaldurga Conglomerate is an active continental margin turbidite.

12.3 PETROGRAPHY AND TECTONIC SETTING:

To understand the petrographic characteristics of basal quartzites and the Kaldurga Conglomerate with graywackes matrix, in terms of possible tectonic environment of their deposition, schemes proposed by Dickinson and Suczek (1979) and Dickinson et al. (1983) were applied. Triangular diagrams with the apexes of total quartz ($Q = Qm + Q_p$), total feldspar ($F = f + p$) and total rock fragments ($L = L_v + L_s$), are shown in Fig. (12.1).

12.3.1 Basal Quartzites:

It may be noted from Fig. (12.1), that most of the data points for quartzites fall into the field of continental block provenance. Detritus from nonorogenic continental blocks forms a spectrum of sand types derived from the broad positive areas of stable cratons at one extreme and from locally uplifted, commonly fault-bounded basement blocks at the other extreme (Dickinson and Suczek, 1979). In other words, these sediments came from continental interiors and uplifted cratonic blocks. This includes passive margin settings as well as other continental environments (Dickinson et al., 1983).

Fig. 12.1 : Modal quartz - feldspar - rock fragment plot for the quartzites and matrix of the Kaldurga Conglomerate. It is clear from this plot that maximum number of samples of quartzites, fall in the field of continental block provenance, which indicates that the basin developed within the continental crust. However, most of the samples of the KCM occupy the field of dissected arc zone. Five samples of the KCM are lying in recycled orogen. But in either setting unstable depositional environment is evident for the Kaldurga Conglomerate. (Fields after Dickinson et al. 1983). Open circle = KCM; Solid circle = Quartzites.

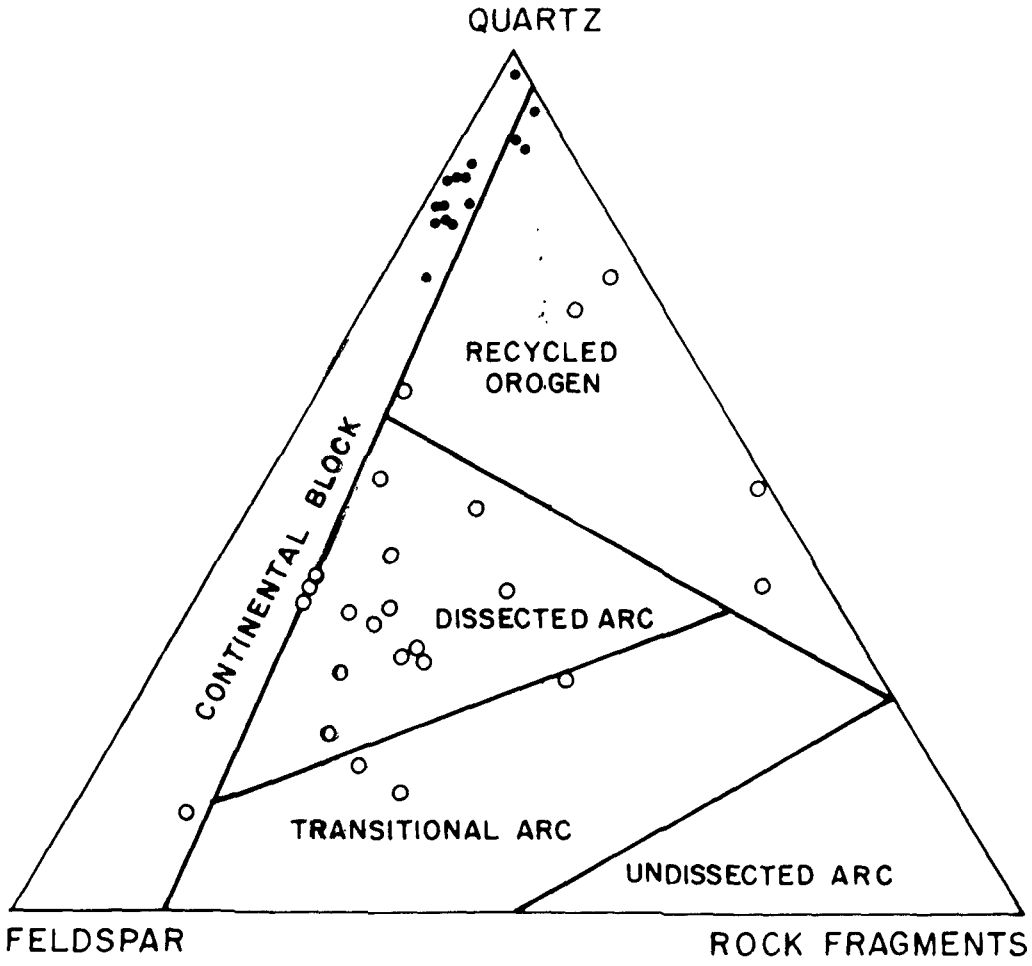
QUARTZ
RECYCLED
OROGEN
CONTINENTAL BLOCK
DISSECTED ARC
TRANSITIONAL ARC
UNDISSECTED ARC
FELDSPAR
ROCK FRAGMENTS

Continental block provenance, has again been divided into craton interior provenance and uplifted basement provenance. Well sorted quartz rich sediments, which indicate low relief and intense chemical weathering with high hydrodynamic activity, rule out the possibility of uplifted basement provenance for these quartzites. Essentially pure quartz (orthoquartzite) with minor feldspar (Table 6.2) represent especially mature detritus, which might have been accumulated in active rifted basin within platform successions or in an interior basin of the continental block (e.g. Ketner, 1966; Dickinson and Suczek, 1979). Alternatively, these quartzites might have been deposited as miogeoclinal wedge at passive continental margin.

12.3.2 The Kaldurga Conglomerate:

Three main framework constituents of graywacke matrix of the Kaldurga Polymictic Conglomerate, i.e quartz; including both mono and polycrystalline, feldspar and rock fragments of all varieties, were plotted in a QFL diagram (Fig. 12.1). Classification scheme, as shown in the figure (12.1), is proposed by Dickinson et al. (1983), mainly for the graywackes. It may be noted from the fig. (12.1) that a sizable number of data point fall into the dissected arc zone in general. Three points fall in the transitional arc field and four points occupy their place in recycled orogen sector.

Detritus eroded from arc orogens forms a spectrum of sand types including lithic rich volcaniclastic debris at one extreme and more quartzo-feldspathic detritus of largely plutonic origin at the other extreme (Duncan and Kulm, 1970; Dickinson, 1980).

The modal analysis (Table 6.3) of the matrix of the Kaldurga Conglomerate (KCM) suggests that mostly they are lithic arkosic rocks. This indicates their derivation from more mature and eroded magmatic arcs, especially those along continental margins. These derivatives might have been deposited in forearc and/or back arc basins at active continental margin (Dickinson and Rich, 1972, Dickinson et al., 1983). Field study of the Kaldurga Conglomerate also support this inference, as the Kaldurga Conglomerate has been divided into two; lower and upper units, and the clast lithologies of lower and upper unit indicate the erosional unroofing. Alternatively, recycled orogen provenance, which can be treated here as a particular type of uplifted subduction complex (Dickinson et al., 1983) could be possible tectonic nature of source area.

12.4 GEOCHEMISTRY AND TECTONIC SETTING:

12.4.1 Major Elements:

Bhatia (1983) observed a close correlation between the major element composition of sandstones and their relative tectonic settings. He classified the possible tectonic settings of sandstone deposition into oceanic island arc (OIA), continental island arc (CIA), active continental margin (ACM) and passive margin (PM). Bhatia observed that sandstones of these environments can be distinguished on the basis of following geochemical parameters: $Fe_2O_3^{(t)}+MgO$, TiO_2, Al_2O_3/SiO_2, K_2O/Na_2O, $Al_2O_3/CaO+Na_2O$ and SiO_2. These parameters are summarised in Table (12.1). First three parameters show decreasing trend from oceanic

Table 12.1: Chemical characteristics of sand size matrix of QPC, quartzite and the KCM (after Bhatia, 1983).

	$Fe_2O_3^{(t)}$ +MgO	TiO_2	Al_2O_3/SiO^2	K_2O/Na^2O	$Al^2O^3/CaO+Na_2O$	SiO^2
(OIA)	8-14 (11.73)*	0.8-1.4 (1.06)	0.24-0.33 (0.29)	0.2-0.4 (0.39)	(1.72)	(58.83)
(CIA)	5-8 (6.79)	0.5-0.7 (0.64)	0.15-0.22 (0.20)	0.4-0.8 (0.61)	(2.42)	(70.69)
(ACM)	2-5 (4.63)	0.25-0.45 (0.46)	(0.18)	(0.99)	(2.56)	(73.86)
(PM)	(2.89)	Depleted	(0.10)	(1.60)	(4.16)	(81.95)
(QPC & QTZ)	(1.05)	(2.30)	0.09-0.04	(2.05)	(7.10)	Enriched
KCM	(21.05)	(0.77)	(0.23)	(0.93)	(3.67)	(56.85)

* Numbers in ( ) indicate average values.

island arc to continental island arc to active continental margin to passive margin, whereas, the remaining three parameters indicate an increasing trend from oceanic island arc to passive margin.

Partial analysis of major elements of sand size matrix of QPC and associated quartzites suggest that according to Bhatia's (1983) classification of tectonic setting, passive margin type of tectonoregime is most likely environment for the QPC and quartzites. K_2O/Na_2O ratio varies from 11.39 to 0.30 with an average of 2.05 (Table 8.1) and $Al_2O_3/CaO+Na_2O$ has an average of 17.10. These ratios are strong evidences to assume the passive margin setting for the shallow basin in which QPC and quartzites were deposited. Since the sand size matrix of quartz pebble conglomerate (MQPC) is highly enriched with detrital pyrite, the matrix is exceptionally high in FeO (Table 8.1). Hence the FeO+MgO parameter obviously shows abnormally high values. However, the same parameter for quartzites shows a variation from 1.81 to 0.41 with a mean value of 1.05, which again suggest passive margin tectonic setting. Being mature arenite, the SiO_2 of these samples is very high (80 - 95%) and Al_2O_3/SiO_2 ratio also substantiate the inferred passive margin setting.

Major element composition and the ratios between different oxides components of graywacke matrix of the Kaldurga Conglomerate, outrightly eliminate the passive setting for their deposition. However, it was found difficult to discriminate between OIA, CIA and ACM setting. $Fe_2O_3^{(t)}+MgO$ and SiO_2 are two parameters, which indicate OIA setting, while K_2O/Na_2O ratios are closer to the range of ACM. Ojakangas (1972,1985) observed that

the graywackes with significant volcanoclastic detritus have K_2O/Na_2O generally less than one. TiO_2 and Al_2O_3/SiO_2 parameter range between the OIA and CIA setting. $Al_2O_3/CaO+Na_2O$ has a very wide range from 9.02 to 0.33 with an average value 3.67. Apparently, this parameter is not supposed to be discriminative for the graywacke sediments.

Roser and Korsch (1988), proposed another scheme for the identification of tectonic setting on the basis of SiO_2 - K_2O/Na_2O relationship (Fig. 12.2). They (ibid) divided all settings into three groups namely passive margin (PM), active continental margin (ACM) and island arc settings (ARC). It is clear from Fig. (12.2), that there is scatter in between the fields of ACM and ARC for the KCM samples analysed. However, most of the samples fall in the ACM field. On the basis of major elements alone, it is difficult to distinguish between active continental margin and island arc settings for the Kaldurga Conglomerate, whereas passive margin setting for QPC and quartzite is clearly demonstrated by these data.

12.4.2 Trace Elements:

Bhatia and Crook (1986) believed that the most useful trace and rare earth element tectonic discriminant parameters are La-Th-Sc, Th-Co-Zr/10 and Th-Sc-Zr/10 plots. These parameters are plotted in Fig. (12.3) for the sand size matrix of QPC and associated quartzites, and graywacke matrix of the Kaldurga Conglomerate (Fig. 12.4). La-Th-Sc triangular diagrame (Fig. 12.3A) of QPC and quartzites shows La enrichment, relative to Th and Sc and they occupy their place near the La apex and also show

Fig. 12.2 : K_2O/Na_2O vs. SiO_2 plot which shows that about 65 percent of total sample population of the KCM all in the field of active continental margin (ACM), and around 33 percent of total samples are lying within the zone of island arc region (ARC). Since SiO_2 content of QPC and quartzites is very high (80-90%), a narrow scatter of QPC and quartzites is found within the field of passive margin (PM). Although it is difficult to distinguish between 'ACM' and 'ARC' for the KCM on the basis of this chemical filter, the stable tectonic setting for QPC and quartzites and unstable tectonic setting for the KCM are apparent. (Field after Roser and Korsch, 1988).

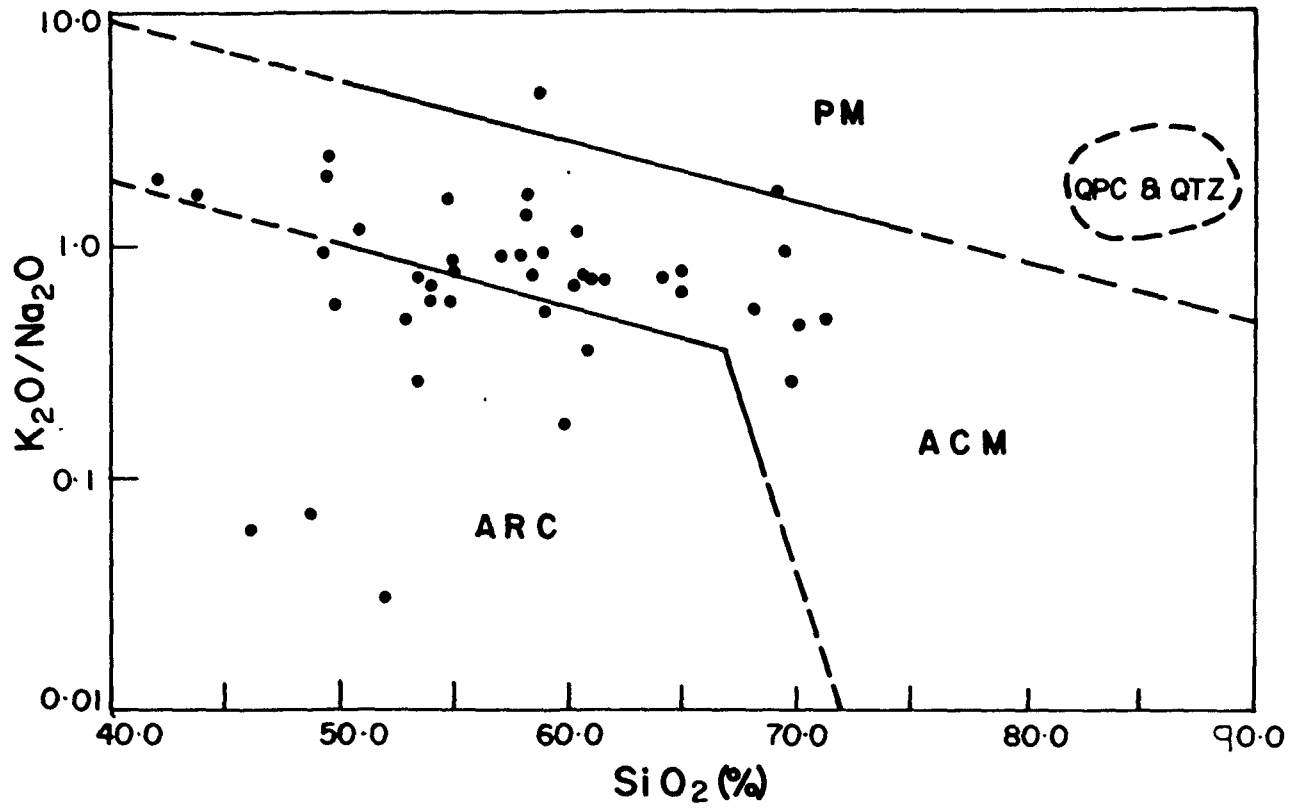
10·0
1·0
0·1
0·01
K_2O/Na_2O
PM
QPC & QTZ
ACM
ARC
40·0
50·0
60·0
70·0
80·0
90·0
SiO_2 (%)

Fig. 12.3 : (A) A ternary plot of La-Th-Sc in sand size matrix of QPC and quartzites showing La enrichment relative to Th and Sc. The plot also shows a trend of Th enrichment. Most of the samples fall above the field of PM and ACM.

(B) Co-Th-Zr/10 ratios; as a result of the exceptionally high Co value of sand size matrix of QPC and quartzites, all samples have clustered near the field of OIA.

(C) Th-Sc-Zr/10 plot showing that most of the samples of QPC and quartzites occupy the field of PM or fall above it towards the Th apex. It may be noted that QPC is not a normal sediment of platformal facies, detrital uraninite and pyrite have contributed to the composition of these rocks and their Th, Co values are not similar to those generally found along passive margins. ACM = active continental margin; CIA = continental island arc; OIA = occanic island arc, and PM = passive margin fields (After Bhatia and Crook, 1986). Open circle = quartzites; solid circle = QPC.

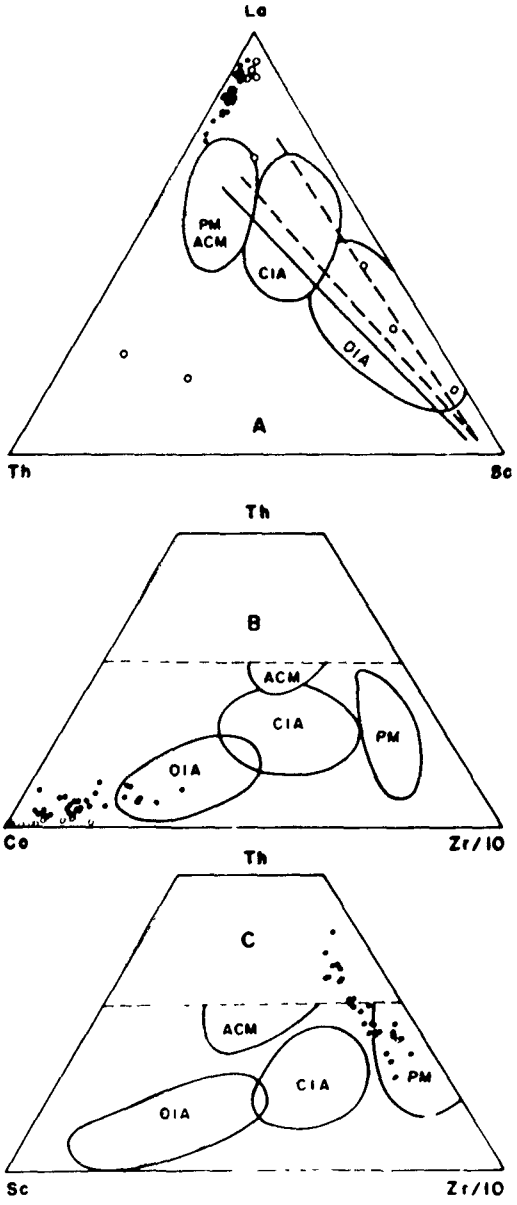
La
PM
ACM
CIA
OIA
A
Th
Sc
Th
B
ACM
CIA
PM
OIA
Co
Zr/10
Th
C
ACM
CIA
PM
OIA
Sc
Zr/10

Fig. 12.4 : (A) La-Th-Sc for the KCM triangular diagram. The points are scattered all along the La-Sc arm of the triangle. Their alignment with solid and dashed lines of mixing model is seen. All the field discussed in A, B and C diagram are given by Bhatia and Crook (1986).

(B) Ternary diagram of Co-Th-Zr/10 for the KCM. It shows that the samples fall near the Co apex indicating the oceanic island arc tectonic setting.

(C) Ternary diagram of Th-Sc-Zr/10 for the KCM showing the cluster of samples near the Sc apex. It also indicates the oceanic island arc setting.

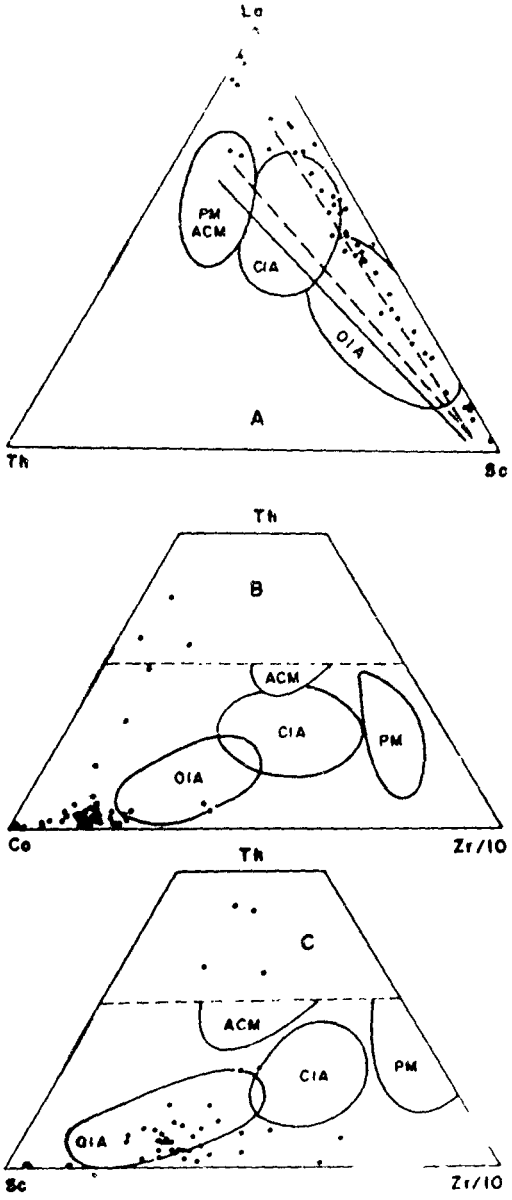
La
PM
ACM
CIA
OIA
A
Th
Sc
Th
B
ACM
CIA
PM
OIA
Co
Zr/10
Th
C
ACM
CIA
PM
OIA
Sc
Zr/10

a trend of relative Th enrichment. Most of the samples define an enrichment of La and Th due to which they fall above the passive margin field. Some of the quartzite (three) samples fall in oceanic island arc field and these samples contain higher amount of feldspar. La and Th enrichment as compared to Sc is a definite indication of passive margin tectonic setting for QPC and quartzite.The KCM samples occupy their place all along the La-Sc arm of the La-Sc-Th triangular diagram (Fig. 12.4A), which makes it difficult to discriminate between oceanic island arc, continental island arc and active continental margin tectonic setting of deposition of the KCM. However, their alignment, and the solid and dashed line of bimodal mixing trend of Taylor and McLennan (1985) and multicomponent mixing endmembers of Wronkiewicz and Condie (1987, 1989) respectively, substantiate the inference of mixed provenance of the KCM, (Chapter XI) and indicate that it has been deposited along an active plate margin.

Since Co is exceptionally high in the pyrite of the sand size matrix of QPC, it has obliterated the Co-Th-Zr/10 ratio (Fig. 12.3B). Due to the higher concentration of Co almost all samples of QPC and quartzites occupy their place near Co apex or in the field of OIA. When the Co concentration is deducted from these samples, theoretically they occupy their place in the passive margin field. (Fig. 12.3B). This aspect is substantiated when Th-Sc-Zr/10 ratios are plotted in Fig.(12.3C), where most of the data points occupy the field of PM or above it towards the Th apex. It may be noted that QPC is not a normal sediment of platformal facies. Detrital uraninite and pyrite have contributed to the composition to these rocks and their Th, Cr values are not

similar to those generally found along passive margins.

Due to elevated concentration of Cr, Co, Ni in the ultramafic-mafic source rocks, the KCM samples fall near the Co apex on Co-Th-Zr/10 triangular diagram and this indicate the oceanic island arc tectonic setting. Similarly due to same reason Sc concentration in the KCM is elevated and an oceanic island arc tectonic setting is reflected, though the field data and the pebble population of the Kaldurga Conglomerates clearly indicate an active continental margin tectonic setting. It may not be out of place to mention that the graywackes of the Chitradurga and Shimoga belts have been suggested to be deposited in an ACM tectonic setting (Naqvi et al. 1988).

Bhatia and Crook (1986) have identified many trace elements and their mutual ratios as sensitive discriminators of various tectonic setting. These indicators are Th, U, Zr/Th, La, Th/U, La/Sc, Th/Sc, Ti/Zr, La/Th, Co, and Zr etc. It is clear from the above comparative study that most of the discriminating factors indicate a passive margin related tectonic setting for the deposition of quartz pebble conglomerate and associated quartzites. Although, it is difficult to differentiate between the subduction related tectonic environments for the deposition of the Kaldurga Conglomerate, two contrasting tectonic regime are evident for these two different rock suites studied by the author. These two different rock types are completely discriminated by their Th/Sc ratios. This ratio for QPC is generally more than one and reaches upto 10, whereas for the KCM, it is mostly less than one and goes down upto 0.02. (Fig. 12.5A). Such a scatter in Th/Sc ratios as shown by the KCM is generally seen in the recent

Fig. 12.5 : (A) Th/Sc vs. Sc plot for the KCM. Field of QPC and quartzites is taken from Fig. 8.5(D). Shaded zone is the field of Archaean graywacke-shale turbidites. Th/Sc ratios and Sc abundance clearly indicate that the KCM is an active margin turbidite and QCM, and quartzites are passive margin deposites.

(B) Th/U vs Th plot for the KCM samples. The field of QPC and quartzites taken from Fig. 8.5 (E). KCM samples occupy the area of active continental margin turbidites and the region of QPC and quartzites, which is far below the average line (Th/U = 3) indicates that the tectonic regime for QPC and quartzites was drastically different from that of the KCM.

(C) Eu_N/Eu_{N*} vs. Gd_N/Yb_N plot indicating the plate margin setting and passive margin setting for the KCM and MQPC respectively.

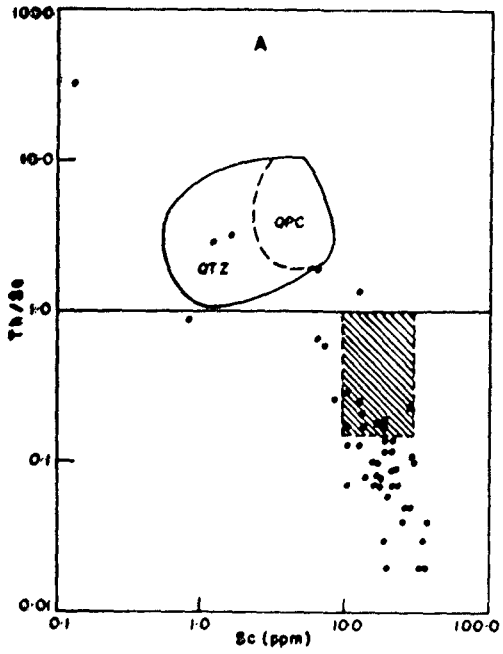
A
QPC
QTZ
Th/Sc
Sc (ppm)
1000
10·0
1·0
0·1
0·01
0·1
1·0
100
100·0

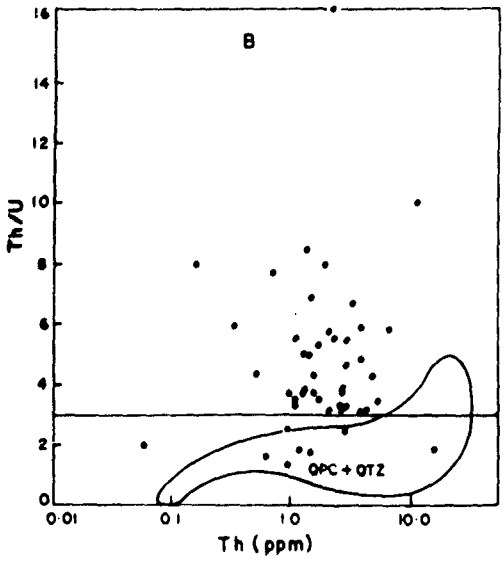
B
QPC + QTZ
Th/U
Th (ppm)
16
14
12
10
8
6
4
2
0
0·01
0·1
1·0
10·0

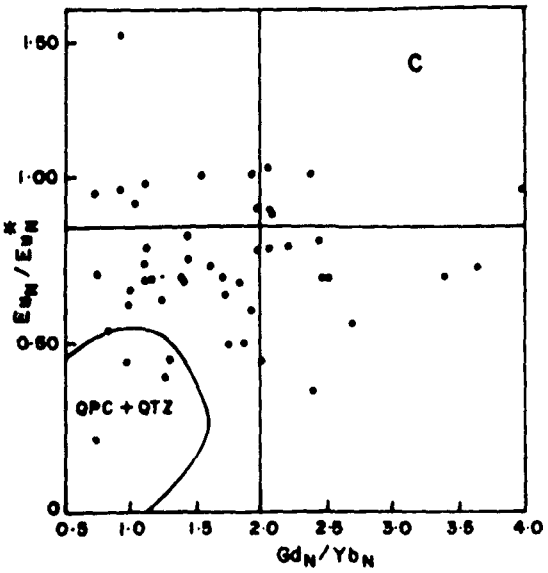
C
QPC + QTZ
Eu_N/Eu_N^*
Gd_N/Yb_N
1·50
1·00
0·50
0
0·5
1·0
1·5
2·0
2·5
3·0
3·5
4·0

and phanerozoic turbidites. (McLennan and Taylor, 1991). These Th/Sc ratios and the Sc abundance clearly indicate that the KCM is an active margin turbidite. Sc abundance are greater than 10 ppm for all Archaean turbidites (McLennan and Taylor, 1991). Though our data shows higher concentrations of Sc, it certainly substantiates the inference that the KCM is a product of active continental margin. When Th/U ratio is plotted against Th concentration (Fig. 12.5B) most of the KCM data occupy the region of active margin turbidites identified by McLennan and Taylor (1991). QPC and quartzites data fall below the average lime (3.0) and show that the processes for the generation of these two type of sediments have been drastically different. Both have been provided from the same source area but the difference in the sedimentary processes and tectonic settings have resulted in an entirely different rock type. The difference between the two i.e. QPC and KCM are clearly seen on Eu/Eu^* vs Gd_N/Yb_N plot (Fig. 12.5C). According to this parameter, turbidites from active margin tectonic setting are indistinguishable throughout the post Archaean. However, Archaean turbidites are distinctive as they tend to be considerably less depleted in Eu with Eu/Eu^* generally 0.85 (McLennan and Taylor, 1991). Since our data have great variation in Eu/Eu^* and Gd_N/Yb_N, a large scatter on Fig. 12.5C is seen. However, the conclusion that the KCM represents an active margin tectonic setting is substantiated by these data. McLennan and Taylor (1991) have concluded that a significant change in the composition of the turbidites deposited at active tectonic setting is seen at Archaean/post Archaean transition.

12.5 THE EVOLUTION OF THE BABABUDAN SCHIST BELT: TECTONIC MODEL:

It has been illustrated in earlier chapters and sections of this chapter, that each rock association of the Bababudan schist belt requires a different tectonic regime for their emplacement/deposition. For example, QPC and associated quartzites need a very shallow water environment of deposition, which may be linked with early stage of sagging within the jevunile continental crust. Furthermore, detrital pyrite suggests the anoxic atmosphere at the provenance and reducing environment of depositional basin.

Volcanic activity in the Bababudan basin ranges between ultramafic to acidic, and the occurrence of columnar basalts (Srinivasan and Sreenivas, 1971) indicate that it was often subaerial. However, its association with relatively deep water rock types also indicates that a greater part of this volcanism has taken place in deeper part of the basin or relatively deeper shelf zone. Geochemical studies of these volcanic rocks suggest their emplacement as "within plate basalt" (WPB) type to "mid oceanic ridge basalt" (MORB) type. Field and geochemical characters of these volcanic rocks indicate the advance stage of spreading across a rift, generated in the basin.

Geochemical data of oxide facies of BIF indicate that a large amount of silica, iron and REE were provided from hydrothermal vents, situated at mid oceanic ridge. Terriginous and volcaniclastic input and their incomplete mixing with the material supplied from MOR hydrothermal activity, suggest that the BIF was precipitated at relatively deeper part of shelf below the wavebase and photic zone. It was the region, where photosynthetic oxygen

became available, intermittently, to generate the Fe-rhythmites. It, indicates the activation of mid oceanic spreading ridge, and, thus, a stage of opening and spreading of the proto ocean is evident.

Field, petrographical and geochemical characteristics of the Kaldurga Conglomerate need sudden subsidence of the basin or uplifting of source area and deeper water conditions. The data presented earlier demonstrates that it is a turbidite formed at an active continental margin i.e. under the subduction regime. Therefore, Kaldurga Conglomerate represents the closing stage of the basin.

The above stated geological and geochemical data can be explained by assuming (1) the generation of a shallow basin on the juvenile sialic thin crust, in which shallow water clastic sediments were accumulated. (2) Due to tension and streaching of the lithosphere as suggested by Bott and Kuszuir (1984), along with the load pressure of accumulated sediments, a rift was generated through which magma from mantle came up and volcanic rocks were emplaced. The episodic nature of magmatic activity is evident by the alternative sequence of clastic metasedimentary and metavolcanic rocks. (3) This within plate rifting continued to generate the new oceanic crust, at mid oceanic ridge. Through this spreading ridge volcanic eruptions and fumarolic activities were continued either continuously or intermittently. The hydrothermal solutions, rich in silica and iron were supplied from MOR vents and due to thermo-chemical potential moved towards the shore line and ultimately got precipitated in the form of BIF of various types. After this stage, (4) the direction of convection

current within the asthenosphere has been reversed and compressional regime took over.The new status of geodynamic forces resulted in a unstable environment and subduction of newly generated oceanic crust has started. This sudden subduction provided the most favourable and required environment for the deposition of the Kaldurga Polymictic Conglomerate and other associated rock types. Compressional forces brought the rock suites of different tectonic settings juxtaposed. Metamorphism and deformation during this compressional orogeny produced the present geometry and configuration of the basin. By assuming the completion of wilson cycle rapidly for the smaller plates which were moving with a faster rate of spreading, almost all the geological and geochemical parameters of the Bababudan schist belt may be explained.

CHAPTER - XIII

DISCUSSION AND SYNTHESIS

13.1 ARCHAEAN PLATE TECTONICS:

Greenstone belts are fundamental tectono-stratigraphic units of Dharwar Craton, and represent one Ga of early Earth's history. The study of origin and processes, through which these volcano-sedimentary rocks were formed, shall be able to illustrate the tectonic conditions and the evolutionary processes for the continental crust. If the concept of plate tectonics is extended into the Archaean, (Abbott, 1984; Abbott and Hoffman, 1984; Hargraves, 1986; McLennan and Taylor,1991) then the search of the relics of proto oceans and conditions, prevailing during this time, has to be directed towards greenstone belts. It is very well known that the oceanic crust is not more than 200 Ma old and the most ancient part of the continents is about 3.8 Ga old (Bott 1982, Windley 1984, Wyllie, 1973) or, 3.9 Ga (Bowring et al.,1989). The processes of weathering and sedimentation have been even older than 4.0 Ga as indicated by radiometric age data of detrital zircon from the Pilbara region, Australia (Compston and Pidgeon, 1986). It is therefore, natural to ask the question: what happened to older oceanic floor, if these oceans existed? Existence of oceans as old as 3.8 Ga cannot be denied, only the dimensions of these oceans and the quantity of the water present in the ancient hydrosphere may be debated (Holland,1984; Towe, 1983, 1990; Fyfe, 1990). The nature of these oceanic floor can be studied through the sediments of greenstone belts because then no other major repositories of that time except the

volcano-sedimentary sequence of low and high grade terrains are preserved. Results of studies on the Bababudan schist belt have been presented in previous chapters and in the following pages synthesis of the data is presented in terms of processes through which these rocks have been formed. In this chapter it is suggested that with the modifications in the plate size and changes in other parameters of the modern plate tectonic concepts, the geochemical characters preserved in the Archaean greenstone belts can be explained. Through the geochemical data on the sedimentay sequence, preserved in the Bababudan schist belts, here an attempt is made to erect a model for evolution of continental crust of Dharwar Craton in this region.

13.2 COMPOSITION OF THE ARCHAEAN CRUST:

The major question which has been addressed is, which stage of continental crustal evolution is represented by the Bababudan schist belt? Has there been any change in composition of continental crust from early to late Archaean? There is no unequivocal geological record of early Archaean available in Dharwar Craton. The record of early Archaean events in DC has not been discovered as yet. Some speculations have been made by Naqvi (1978). The Gorur gneisses which have been dated around 3.4 Ga (Beckinsale et al.,1980), intrude Holenarsipur Group of older greenstone belts (Naqvi,1981). The Holenarsipur Group has been studied by many workers (Swami Nath and Ramakrishnan,1981; Naqvi and Rogers,1983, 1987). In this group silicic-clastic sediments are not recognised by Naqvi and his co-workers (Naqvi, 1982). However, Tattekere Conglomerate which is considered as autoclastic

by Srinivasan and Sreenivas (1968) and Naqvi et al.(1978), is regarded by Chadwick et al. (1978, 1979) as a basal conglomerate. The total percentage of silcic rocks in the older greenstone belts specially of Holenarsipur Group or Sargur Group (Viswanatha and Ramakrishnan, 1976) is only 1.3%, and therefore it indicates that the widespread erosion of a silicic upper crust has not occurred at that time, if at all it existed. The volcanic rocks associated with these sedimentary rocks are komatiitic with well preserved spinifex texture and komatiitic chemistry (Hussain and Naqvi, 1983; Jaffri et al., 1983; Charan et al., 1988). The tectonic setting and the process through which these older greenstone belts were formed are highly debated and controversial between various group of leading workers on Precambrian geology. Ramakrishnan and Chadwick believe that on a pre-existing sialic crust shallow basins were formed in which older greenstone belts were developed and most of the ultramafic rocks intruded them. Naqvi and his co-workers believe that older greenstone belts were deposited in basins of simatic basement, and the melting of this basement and also amphibolites of older greenstone belts resulted in the formation of TTG and thus continental nucleii were formed (Naqvi, 1982). Irrespective of this debate, which concerns early Archaean evolutionary stages, the middle and late Archaean stages are not that controversial. It is widely agreed that by 3.0 Ga ago, widespread continental crust made up of TTG and granodioritic gneisses was formed and the Bababudan Group of rocks were laid down after the formation of this crust.

13.3 CONSTRAINTS FROM QPC AND QUARTZITES:

The Bababudan Group begins with a basal quartz pebble conglomerate having a matrix of detrital pyrite and uraninite in addition to quartz and fuchsite etc. The QPC has got rounded to sub rounded pebbles of vein quartz. Formation of vein quartz pebbles requires that a large amount of quartz veins was present in the source area, which in turn indicates that TTG and granodiorite of the source area have sweated because of the change in the thermal and pressure conditions during metamorphism to form gneisses. Thus, probably at this stage a large amount of vein quartz and pegmatitic formation took place. It also needs that these vein quartz and pegmatites along with the associated gneisses were weathered both chemically and mechanically to attain mineralogical and chemical maturity which has been exhibited by the QPC and the associated quartzites. Roundness of the pebbles suggest that vein quartz has undergone abration of high order along with intense hydrodynamic processes. Both sphericity and roundness of the pebbles along with hydrodynamic sorting have given rise a contact framework. Geochemical data of the sand size matrix of QPC have very clearly illustrated that the intense chemical weathering has resulted in leaching and removing of the unstable minerals, under anoxic atmosphere. Anoxic atmosphere of the source area is evident by the presence of detrital grains of pyrite. Very strong negatiave Eu anomalies, REE pattern shape, as discussed earlier, and other geochemical data like Cr, Co, Ni, Rb, Sc, Zr, V, Hf and their interrelationships and ratios have clearly shown that at the time of formation of QPC and quartzites

at the base of the Bababudan belt, intense chemical and physical weathering has taken place. Intense chemical weathering is expected in late middle Archaean because of the corrosive nature of atmosphere, having CO_2, chlorine and other gasses in abundance (Walker 1984). This intense chemical weathering could remove the unstable minerals present in komatiities and other mafic ultramafic components of the older greenstone belts of source area. It has also effectively removed, if not completely but partially, the feldspar contents of the TTG. The sphericity and roundness of quartzose pebbles of QPC can be explained in terms of two well known causes, either the distance of transportation was very great or the duration of abrasion was very long. The palaeocurrent direction for the QPC and quartzites is found to be west to east. The presence of the upper greenschist facies and the amphibolite facies rocks in the western region and also those of amphibolitic enclaves within the TTG indicates that the source area was not buried to greater depth. Probably there was not much difference in elevation between the source area and basin of deposition, i.e. prior to the deposition of QPC. Moreover nondeposition of arkoses also suggest that elevation difference between the depository and source area was not of high order. Therefore, a longer duration and intense hydrodynamic activities are inferred to produce well rounded and spherical pebbles of QPC. This is further evident by the presence of very high proportion of terrigenous material interbedded with stratigraphically subsequent and younger BIF, which at many places have become shaly BIF and even ferruginous shales. Therefore, the sedimentological, petrological and geochemical data as discussed

in early chapters indicate that this horizon which is the first quartz pebble unconformity on Indian shield was formed under very stable conditions on land and in a shallow water basin. It was formed within a juvenile continental crust which was having very large proportion of mafic and ultramafic rocks. In addition, though the conditions in the basin and in the source area were stable; the environment and hydrodynamic conditions in the source region as well as in basin were very different and intense. During that remote period, in the absence of vegetation and existence of very different climatic and atmospheric conditions, these sediments were generated and deposited. These conditions of intense chemical weathering and hydrodynamic activities are preserved in petrographical and geochemical characteristics of the QPC and quartzites. For example, it cannot be denied, by any assumption, that mafic ultramafic rocks were very important constituents of the pre QPC crust. The chromium content of the sand size matrix of QPC is very high (266-910 ppm), but it is situated in fuchsite and not in minerals characteristic of mafic ultramafic rocks. Similarly Co concentration is also very high but it is present in pyrite. These data indicate that the elements which could react with atmospheric CO_2, Chlorine and other gasses; and also which could be affected by hydrodynamic activities were removed and the heavy minerals like chromite of mafic ultramafic rocks were left over in the source area, along with other restites. Since atmosphere was anoxic, the pyrite could also survive. It must be further noticed that the negative Eu anomalies of pyrite and other characteristics as discussed earlier, indicate that it is not a hydrothermal pyrite which was

derived from sulphide facies BIF. This pyrite appears to be a different type, probably belonging to a vein type deposit very close to the basin. Pyrite rheology does not allow to bear much physical denudation, and long distance of transport. Therefore, it is envisaged that the pyriteferous veins might have been formed at the stage of metamorphism or partial melting of the TTG, and these pyriteferous veins were situated very close to basin. Soon after the deposition of the QPC, rifting within the basin appears to have been initiated through which the magma came to the surface and a sequence of interbedded current bedded quartzites with volcanic rocks was laid down.

Some of the samples of quartzites which are interbedded with volcanic rocks contain 16% of feldspar, which shows that during the deposition of quartzites, the chemical disintegration was probably and relatively not that rapid and intense, as they were at the time of deposition of QPC. Therefore, these subarkosic sediments were deposited. Absence of feldspar from the sand size matrix of QPC and the presence of feldspar upto 16% in overlying quartzites indicate that fluctuating conditions within the period of deposition of QPC and quartzites were prevailing. This is clearly reflected by geochemical data also, as discussed in chapter VIII. In spite of having 10% of plagioclase, quartzites show strong negative Eu anomalies. Since the environment in basin was reducing at that time and the atmosphere in source area was anoxic, the negative Eu anomalies can be attributed only to the characteristics of the rocks exposed in the source area. It may be noted that many gneisses and granodiorite, present in surrounding areas, which could be provenance, show negative Eu

anomalies (Naqvi and Rogers,1983). The age of these sediments is uncertain, but they might have been formed around 2.9 Ga. They might be older as similar rock types namely current bedded quartzites which are resting on ultramafic komatiites of Holenarsipur schist belt are found to be intruded by Holekote trondhjemite which is dated at 3.1 Ga (Monrad, 1983). Based on geological correlations it is considered that northern part of Holenarsipur belt, Sigegudda and the Bababudan belt are equivalent, as they show identical development of lithologies and stratigraphic sequences. Therefore, with the available geological and geochemical informations, the basal part of the Bababudan belt could be 2.9 - 3.0 Ga old. During this geological period, there appears to be intense chemical weathering with high hydrodynamic activities to produce shallow water sediments in shallow intracratonic basin. Simultaneously at this time the basin became site of rifting and a very large and thick out pouring of lava of varying composition took place. Near the margin of basin at least at one place, undoubted columnar basalts are found. Therefore, this activity is consistent with the suggestion that in part volcanic activity was subaerial and in other part it was subaqueous.

13.4 CONSTRAINTS FROM VOLCANIC ROCKS AND BIF:

Geochemical work on these volcanic rocks of Bababudan schist belt was mainly carried out by Bhaskar Rao and as discussed in chapter IX, it clearly indicates that these volcanic rocks are by and larage within plate type with some samples having MORB affinites and appear to have been emplaced through a rift system.

These characteristics of volcanics of the Bababudan schist belt can only be explained if a continental rift is generated which gradually became MOR, along which spreading could have taken place. A modern analogous for such rift system is Red sea, where the distance between the passive continental margin and the spreading ridge is very short and the hydrothermal activity has provided mettaliferous deposits (Barrett et al.,1988). Hydrothermal solutions produced at the ridge of Red Sea have REE patterns, La and Eu anomalies similar to those found in the BIF of Bababudan group. The presence of a very thick BIF sequence in the Bababudan Group of Kudremukh and other possibly equivalent schist belt like Sandur and Kushtagi, indicate that these areas were very closely situated to MOR, where hydrothermal and fumarolic activity provided and added a huge quantity of iron and silica to the proto ocean. It has been very convincingly demonstrated that the source of iron silica is mainly hydrothermal. Extremely depleted nature in total REE, positive Eu anomalies, La enrichment and the $^{143}Nd/^{144}Nd$ ratio (~ +4.0, Goldstein and Jacobsen, 1988) clearly demonstrate that to deposit such a huge quantity of iron an upper mantle source of hydrothermal solutions is necessary and such solutions from upper mantle can be added to ocean at MOR sites, as it has been found today at EPSR, EPR, NAR and several other places. Recent work of Barrett et al. (1988), Goldstein and Jacobsen (1988), Derry and Jacobsen (1990) and others have provided extremely important and significant input for the Archaean depositional environment of BIF and associated sediments. A huge amount of ferruginous shale and SBIF are found interbedded in the Bababudan Group at all places.

These SBIF and ferruginous shale have been contributed by divergent sources viz., the terrigenous shale and the volcanic ash. This is clearly reflected in their Al_2O_3/K_2O, Al_2O_3/ REE, Zr/Hf data (Manikyamba et al.,1991; Khan et al.,1991). Any model of a basin, in which such an enormous amount of BIF is deposited , cannot be satisfactory unless it explain the genesis of BIF of that basin along with other associated rock types. Therefore, BIF of the Bababudan Group provides an important constraint on the origin and evolution of the basin and reflect the thermotectonic and thermochemical conditions at that particular state of evolution of continental crust. BIF are deposited at a shallow shelf below photic zone and wave base. They are resting on a sequence of interbedded quartzite/metavolcanics and also with some volcanic rocks. Therefore, quartzites which could have been deposited within few meters depth have subsided to a depth of below 100 mts. to allow the deposition of BIF or in other words the transgression of the sea took place towards the land so that shifting of the wave base and photic zone took place. In both the conditions, these situations and rock setting probably demand spreading along the newly formed ridge and flow of water from some other interconnected region. At this stage when the deposition of BIF, terrigenous sedimentation of shales and clays, volcaniclastic ash and pouring of lava into the basin were taking place, due to some reasons which are not understood properly as yet, the change in convection cycle direction took place in the underlying asthenosphere. Before this change in convection cycle, the main controlling factor was tension and after this change, compressional regime took over. This could have resulted by the

failure of a thin lithosphere at Archaean time and at this time, sudden subduction took place. These tectonic changes brought elevation difference between basin and source area and unstability in the basin. Under these unstable conditions which were probably consequent of change from passive margin to active continental margin setting, a very immature sediment with unsorted and angular clasts was deposited in the form of the Kaldurga Conglomerate.

13.5 CONSTRAINTS FROM THE KCM:

The mineralogical and geochemical data (Table 6.3 and 11.1) show that the composition of the KCM can best be explained by a multicomponent provenance model. The inferred provenance of these sediments was made up of TTG, mafic-ultramafic and sedimentary rocks including BIF. The average composition of the KCM can be generated by mixing of 50% TTG, 35% ultramafics, 10% mafic rocks and 5% sedimentary rocks. The mafic and ultramafic rocks and sediments appear to have been derived from an older schist belt sequences and the underlying sequence of quartzites, amphibolites and BIF of the Bababudan Group. Contemporaneous volcanism within the basin could also have provided volcanic debris for the conglomerate. Variation in the size of boulders and the high percentage of matrix suggest that the conglomerate has been deposited by a highly viscous medium. Its deposition must have taken place due to sudden subsidence of the basin which gave rise to sediment gravity flow/mass flow at the bottom of depository. However, since the boulders and cobbles of TTG are present in enormous quantity with a wide range of shapes, it appears that highly viscous mudflow in the form of deep sea fan or fanglomerate

(Nocita and Lowe, 1990) came to the basin and picked up freshly uplifted and eroded debris of quartzites, BIF, amphibolites from the margin of the basin and deposited the Kaldurga Conglomerate. Imbrication of such unsorted sediments occurs in some mass flow deposits. The composition of the exposed crust around 2.6 Ga ago is computed to be 90% TTG, 10% mafic-ultramafics and other rocks. This composition shows that during the early middle Archaean the cotinental crust must have been more mafic than it is now. Mafic ultramafic components were more prominent in the source region and have been eroded to expose a greater proportion of magmatic TTG which were emplaced into the older schist belts, which have been intruded by 3.4 Ga old gneisses (Naqvi, 1981). The gneisses in the northern region around Goa which contain significant mafic ultramafic enclaves of varying dimension are also dated at 3.4 Ga (Dhoundial et al. 1987). Based on these radiometric data, it has been envisaged by Naqvi,(1981) and Naqvi et al. (1988) that the older schist belts might be as old as 3.5 Ga. Presence of much older supracrustals in these 3.4 Ga old gneisses cannot be ruled out. In view of the above it is inferred that the KCM has sampled the crust which was formed during early and middle Archaean. The graywackes of Shimoga and Chitradurga (2.6 Ga) also show a multicomponent source area but have only about 20% mafic-ultramafic component in their modal source area. A comparison of the present modal crustal composition with those inferred earlier (Argast and Donelly, 1986; Naqvi et al., 1988) shows that the early-middle Archaean crust of the Karnataka nucleus was heterogenous in composition at the exposed surface level and the percentage of mafic- ultramafic material varied

greatly. Compositional heterogenetic and diachronous evolution of the Archaean crust have been recognised in different cratons (Young, 1978; Gibbs et al., 1986).

The above discussion and Table (13.1) shows that a change from highly stable, tectonic regime, intense chemical weathering, hydrodynamic activities gave way to a stage of unstability, intense physical weathering, less intense hydrodynamic activities, both at the source and site of deposition. The basin started as a shallow water intracratonic basin in which extremely mature sediments were deposited. It was rifted to pour "within plate volcanics" and then MOR related vent site provided the material for BIF, afterwards subsidence and subduction appears to have taken over to generate the above-stated unstable conditions which produced the present geometry of the basin.

The highly enriched nature of the Archaean crust of Karnataka nucleus in Cr and Ni was identified by Naqvi and Hussain (1972), and it is almost certain that Ni-Cr abundances change across the Archaean-Proterozoic boundary (Dia et al. 1990a & b). Middle Proterozoic is dominated by silicic sedimentation represented by basins similar to Cuddapah basin (Naqvi, 1978) all over the world. These basins have been formed on a fully cratonized and stable crust and contain highly mature sediments. Therefore, in view of the above reasons, middle and late Archaean upper continental crust, as sampled by the Kaldurga Conglomerate, represents a transitional stage of unidirectional crustal evolution from sima to sial (Naqvi,1983).

Table 13.1: Comparison of late Archaean Sediments in the Bababudan Schist Belt.

Description	QPC and Quartzites	BIF	KCM
Facies	Alluvial	Shallow shelf	Deep water turbidites (Massflow)
Associated Volcanic rosks	Calc-Alkaline	Tholeiitic and calc-alkaline	
Weathering depositional chemical environment	Reducing	Rhythematically oxydizing.	Oxydizing
Type of weathering	Intense chemical weathering with strong hydrodynamic activities		Intense and rapid physical weathering with viscous hydrodynamic medium
Environment of deposition	Shallow rifted basin within the continental crust	Spreading related rift basin	Subduction related basin
Major elements	Mobile elements are completely removed	CBIF-High $Fe_{23}O_3$ & TiO_2 SBIF-High Al_2O_3 & K_2O	High MgO, $Fe_2O_3^{(t)}$ Low CaO, $K_2O/Na_2O>1$
Cr, Ni, Co, Zr, Hf	High Cr, Co, & Zr, Moderate Ni & Hf		High Cr, Ni, Co Low Zr, & Hf
LREE/HREE	Highly to moderately fractionated		Moderately to less fractionated
Eu anomalies	Negative	Positive	Negative to no anomalies
Ce anomalies	Abscent	Positive or no anomalies	Abscent
La enrichment	Nil	High	Nil
ΣREE	High	Low	Moderate
Provenance	PG, Granodiorite, and associated older schist belts	Hydrothermal solutions, terrigenus and volcaniclastics	TTG, mafic-ultramafics, metasediments

13.6 CONSTRAINTS FROM STRUCTURE OF THE SCHIST BELTS:

Although, Chadwick et al. (1978, 1985a&b) believe in a very simple structure of the Bababudan basin, the work done by Naha and Chatterjee (1982), Naha et al. (1986) presents an entirely different picture. According to Naha and Mukhopadhyay (1990) and Naha et al. (1986), the schist belt has been intensely deformed into isoclinal tight folds which have been refolded and the southern tip of the basin is a F_1 closer. This entire structure has been refolded. Three generations of the folds have been recognised throughout the KN. If the QPC at Sigegudda, current bedded quartzite north of Holenarsipur, the QPC at Bababudan and Kudremukh represent one unconformity, then the distribution and the structure of these belts cannot be explained unless very large scale horizontal compression and movement have taken place. One of the major unsolved problems of geology of KN is the continuity of the lithology from one region to another, whether the rocks belonging to the Bababudan Group and preserved in Holenarsipur, Sigegudda, Bababudan, Chitradurga, Kudremukh belts were deposited in one basin, or these belts represent discrete and different basins of the same time? Based on the structural and limited geochronological data, it appears that at least the Bababudan Group in Holenarsipur belt, Sigegudda belt, Kudremukh belt and the Bababudan schist belt belong to one basin. If this inferance is right, there is no way but to invoke a modified form of plate tectonics with smaller plates, smaller convection currents, faster spreading and greater ridge length, to explain the observed structural and lithological similarities of these belts. Interference pattern between F_1 and F_2 has given rise to domal

structure. Similar deformational structures from small scale to map scale have been reported by Naha et al. (1986), e.g. map pattern of Kudramukh and Bababudan belts which are defined by BIF cannot be explained by simple assumption that the present pattern was the original configuration of the basin. Map pattern of the Bababudan basin does not indicate that the basin, in which BIF deposition could have taken place, is in its original structure. The depositional environment indicated by QPC, quartzites, BIF, the Kaldurga Conglomerate clearly suggest that these rock types are strongly displaced and brought into their prersent geometry as a result of compressional regime. If such a large scale event occurred its driving forces should have been the same which are driving the plates today.

13.7 SYNTHESIS AND MODEL:

Field, petrological and geochemical data presented above and the tectonic setting inferred from these data have indicated that the geological development of the Bababudan schist belt has started as a shallow sedimentary basin on a fairly stable continental crust, in which a large proportion of mafic-ultramafic rocks were present as older greenstone belt. Within this basin a rift system was developed through which the volcanic rocks of WPB and MORB charctaristics emerged and a sequence of interlayered current bedded quartzites and volcanic rocks of varying composition was formed. Spreading across this rifted region, which eventually became a MOR, took place and at the vent sites along the ridge an enormous amount of hydrothermal solutions came out which contributed Fe, Si and REE to the ancient ocean to

produce a thick sequence of CBIF. While this chemical precipitation was going on, fine grained terrigenous sedimentation (argelites) was also taking place and gave rise the SBIF. After this stage the convection direction got changed and in place of tensional forces, compressional regime took over, resulting in a tectonic setting of active continental margin. In this unstable setting, the deposition of the Kaldurga conglomerate and associate graywackes and shales occurred.

CHAPTER XIV

SUMMARY AND CONCLUSIONS

14.1 SUMMARY:

Greenstone belts of the Dharwar Craton (DC), Karnataka nucleus (KN) are one of the most important volcano-sedimentary rocks of Archaean eon for the understanding of crustal evolution of the early Earth. These belts have been divided into older and younger greenstone belts. Younger greenstone belts rest with a pronounced unconformity on an older crust made up of tonalite - trondhjemite gneisses (TTG), granodiorite and older greenstone belts comprise of mafic-ultramafic spinifex textured komatiite flows and chemogenic sediments. The volcano-sedimentary sequence in the younger greenstone belts, is subdivided into the Bababudan Group and the Chitradurga Group. The present thesis is devoted to the sedimentary constituents of the Bababudan Group exposed in the Bababudan schist belt, which is its type area. Volcanic sequence of this belt has been studied in fair detail by earlier workers (Bhaskar Rao and Naqvi, 1978; Bhaskar Rao, 1980). Sedimentary structures and depositional environment of the QPC and quartzites have been studied by Srinivasan and Ojakangas (1985). However, geochemistry of the sedimentary rocks had not been studied in detail . A comprehensive attempt has been made to study the sedimentological and geochemical characters of the quartzites and conglomerates of the belt in the present work.

The Bababudan Group in the Bababudan schist belt is divided into four formations (Viswanatha and Ramakrishnan 1981).

The subdivision has been made on homogeneity of lithologies or lithotectonic association which in ascending order are the Kalasapura, the Allampur, the Santaveri at the Mulaingiri Formations. Chadwick et al.(1985a) have enlarged the previous subdivisions and redefined the younger subdivisions in terms of an additional formation, viz. the Mundre Formation. Major emphasis in the work has been on the Kalasapura Formation and the Mundre Formation which are made up of quartz pebble conglomerate(QPC), Quartzites and the Kaldurga Conglomerate(KCM) respectively. The objectives of this work are to (1) elucidate the evolution of the basin, (2) estimate the composition of the crust exposed during middle and late Archaean and (3) infer the nature of exogenic and tectonic processes at that time.

Large scale geological mapping in selected spots of the conglomerates and quartzites, palaeocurrent measurements based on current bedding quartzites and imbrication of pebbles in the Kaldurga Conglomerate were carried out in the field. Thirty samples of the basal QPC , twenty samples of quartzites associated with QPC, and forty nine samples of the Kaldurga Conglomerate were collected from fresh and unaltered exposures. Statistical analyses of palaeocurrent data and grain size distribution of QPC and associated quartzites indicate that these are mineralogically and texturally mature sediments and that were deposited in a fluvial regime of a stable platformal environment. The presence of rounded grains of pyrite in the matrix of QPC indicates their detrital nature, derivation and transport under anoxic atmosphere and deposition in a reducing environment.

Modal analysis of the QPC, quartzites and the KCM was carried out to measure different mineral constituents. QPC mainly consists of vein quartz pebble and in its matrix, detrital pyrite, uraninite and gold along with quartz, fuchsite and other micas are found. Rounded to subrounded pebbles of vein quartz generally have contact framework and the matrix above stated is found in the voids in between these pebbles. Matrix in the quartzites of a few samples is made up of mica and feldspar. Few samples contain feldspar more than 10% as detrital grains. Fuchsite is also present in many current bedded quartzites. Zircon is not found abundant in the quartzites sampled by the author, but Fareeduddin (1988) has reported fairly good amount of zircons from these quartzites.

The Kaldurga Conglomerate is a polymictic conglomerate consisting of boulders, cobbles and pebbles of TTG, granodiorite, quartzite, BIF, amphibolite, carbonate rock, vein quartz. etc. The rock is characterised by disrupted framework texture and the matrix/pebble ratio is high. The matrix consists of angular fragments of quartz, plagioclase, K-feldspar, rock fragments set in a fine grained matrix, mainly made up of fine grained chlorite, amphibole, plagioclase and mica. Detrital kyanite and zircon are seen in secondary plagioclase and quartz, which are formed due to recrystallization of the muddy matrix . Along some horizons of the Kaldurga Conglomerate, pebbles show prefered orientation showing a palaeoflow direction from NE to SW.

Model analysis of the matrix [M_1] of the Kaldurga Conglomerate shows that it is made up of angular fragments of quartz, plagioclase, K-feldspar and rock fragments like quartzite

chert and phyllite. These fragments are set in a matrix (M_2) which is made up of fine grained quartz, plagioclase, chlorite amphibole and mica with occasional carbonate minerals.

The matrix (M_2) is recrystallized and contains secondary quartz and feldspar with inclusions of kyanite, zircon, chlorite, amphibole and mica.

Major,trace and REE analysis (42 elements) of each sample of QPC, quartzite and KCM have been carried out on XRF, AAS and ICP-MS. From ten samples of QPC, pyrite was separated and analysed for trace elements, REE and Sulphur isotopes. Composition of the plagioclase present in KCM was determined with the help of EMPA. These data, were processed on a computer for obtaining correlation coefficients between various components of each suite.

Sand size matrix of the QPC (MQPC) is characterized by enrichment in Cr, Co, Ni, Zr, Hf, V, Y and Rb; and depletion in ΣREE with pronounced negative Eu anomalies. It also contains higher U and Th. The mineralogical maturity is reflected in all geochemical data. Elevated Cr concentrations are situated in fuchsite and those of Co and Ni in detrital pyrite. K, Rb and Ba abundances reflect the micaceous content of the matrix. Most of the geochemical data indicate that QPC are the product of intense chemical disintegration and strong high energy hydrodynamic processes. Quartzites following QPC and also occuring interbedded with volcanic rocks at various stratigraphic levels are mature arenites extremely depleted in almost all trace elements and REEs. They also generally show strong negative Eu anomalies. Geochemical and mineralogical data from these quartzites also suggest their derivation from a continental crustal source which

was subjected to intense chemical weathering and strong hydrodynamic processes. Detrital pyrite of MQPC exhibits enrichment in Co, Ni, Cu, and Zn. It has depleted to moderate ΣREE with strong negative Eu anomalies. Geochemical characteristics of the pyrite are altogether different from the pyrite of sulphide facies BIF. $\delta^{34}S$ of this pyrite, from the matrix of QPC, indicate that the pyrite grains have been derived from a vein or porphyry type sulphide deposits.

Volcanic rocks of the Bababudan schist belt show geochemical characteristics of within plate type basalt or mid oceanic ridge basalt. BIFs are very important and abundant sedimentary constituents of the Bababudan Group. Geochemical work indicates that these BIF can be classified into cherty and shaly BIF (CBIEF and SBIF). They are generally characterized by low level of abundances of all elements. CBIF , in particular, are depleted in Cr, Co, Ni, Zr, Hf, Rb, Sr, V, Sc, ΣREE and exhibit strong positive Eu anomalies with enrichment in La. These data indicate that the BIFs were deposited from an ocean water in which hydrothermal solutions at MOR vent sites, brought the FeO, SiO_2 and REE. Contamination from simultaneous terrigenous clay and volcanic ash deposition has produced the observed variation. εNd = $^{143}Nd/^{144}Nd$ data from elsewhere from the BIF has indicated that these hydrothermal solutions were derived from depleted Archaean mantle.

Geochemical data like K_2O/Na_2O, Eu/Eu^*, ΣREE, HREE/LREE, La/Lu, Gd/Yb, U/Th, Th/Sc and Ni, Cr and Co abundances indicate that KCM is an active continental margin turbidite. MgO content of the KCM shoots upto 25% and the Cr content upto 1700 ppm.

These data indicate that KCM was derived from a source which consisted of about 50% TTG and 50% mafic-ultramafic and sedimentary rocks. Debris of these rocks was transported in a viscous media like slurry of mud flow or gravity flow. It indicates that at the time of deposition of the KCM , tectonic setting of the basin drastically changed from stable platformal to active continental margin type.

Structural work carried out by earlier workers and the map pattern of the belt cannot be explained unless large scale multiple deformation - folding, and crustal shortening as a result of horizontal compression is invoked. Observed geological, structural, mineralogical, sedimentological and geochemical characteristics of all rock types exposed in the belt are explained by a modified plate tectonic model with greater ridge length, faster ocean floor spreading and subduction and smaller plates. This mode is consistent with the global heat flaw data for the Archaean era, which was about 3 times more than present.

14.2 CONCLUSIONS:

On the basis of geological and geochemical work carried out on the sedimentary and volcanic rocks of the Bababudan schist belt, the following conclusions are made, which will be further strengthened with a study of palaeosols and other rock types of the adjoining areas:

i) A shallow depression was generated on the 3.0 Ga continental crust which evolved a shallow water basin. At the top of TTG and older supracrustal rocks, mature quartz pebble

conglomerate,quartzites,shales and carbonates were deposited in this basin.

ii) These conglomerates and quartzites were produced through very intense chemical (disintegration) and hydrodynamic activities operating on a middle-late Archaean crust made up of TTG and mafic-ultramafic rocks. The atmosphere in source area was anoxic, and the depositional environment was reducing shallow water not more than a few meter deep. The intense chemical disintegration leached and removed almost all mobile constituents, except restites,fuchsite mica and pyrite. Pyrite was not oxidized as oxygen was not present in the atmosphere at that time.

iii) Soon after the deposition of the basal QPC and quartzites a rift developed within the basin, through which, volcanism of "within plate" geochemical characteristics occurred. Lava was erupted into the basin in both subaqueous and subaerial conditions. At this time, spreading across the rift appears to have occurred and subsidence of the basin took place, resulting in relatively deeper shelf conditions, where deposition of CBIF, ferrugineous shale, shales and SBIF took place.

iv) The source for the silica and iron for BIF were hydrothermal solutions added to the ocean water at the site of rift which has become a mid oceanic ridge by that time. The deposition of BIF took place below wave base and photic zone, at the top of current bedded quartzites and volcanics. Volcanism continued even during the time of deposition of BIF as indicated by the interbedding of volcanic rocks with BIF.

Simultaneous and alternate deposition of terrigenous shales, SBIF and CBIF indicates transgressional conditions. Spreading continued for a while as a very thick sequence of BIF and ferruginous shales and volcanic ash was laid down.

v) After some time for which no geochemical evidence is available but which is a well recognized characteristic of "Wilson Cycle", the convection current directions were changed and compressional regime took over to produce subduction releted tectonic conditions during which the Kaldurga Conglomerate and other associated rock types were deposited. The geological, petrological and geochemical studies indicate that the Bababudan schist belt represents a geological terrain in which a shallow intracontinental basin evolved into an active continental margin related basin through a short time, and the reducing environment of basin changed into oxidizing environment. The intense chemical weathering gave way to dominant physical weathering and a transporting medium which was resposible for intense hydrodynamic activity was converted into viscous debris flow.

vi) The geochemical characteristics of the KCM suggest the multicomponent nature of the provenance, the configuration of various rock types and their mutual and probable mixing in different proportions. Transitional elements especially Cr, Ni, Rb and Sr have provided a fairly good base for computation of a mixing model of the source region and suggest a provenance area of 50% TTG, 35% ultramafic rocks, 10% mafic rocks and about 5% metasedimentary rocks, mainly quartzites. A comparative review of mafic - felsic ratios of

upper continental crust of the Dharwar Craton, KN about 2.6 Ga ago and the composition of exposed crust during the early-middle Archaean conforms that the older Archaean crust was significantly more basic. Geochemical signatures preserved in the KCM when compared with those of subsequent sedimentary strata suggest that the Bababudan schist belt represents a transitional stage in the unidirectional evolution of the Archaean continental crust from simatic to sialic.

vii) The geochemical characteristics and the structural geometry of the belt is best explained by a modified model of plate tectonics, in which smaller plates, larger ridge length (27 times), faster convection, faster production of oceanic crust and its destruction at low angle subduction zones are assumed. This model explains the observed features of all the rock types exposed in the belt. It is also suggested that during the Archaean "Wilson Cycle" was completed at a faster rate.

REFERENCES:

ABBOTT, D.H. 1984, Archaean plate tectonics revisited 2. Paleo-sea level changes, continental area, oceanic heat loss and the area age distribution of the ocean basins: Tectonics, 3: 709-722.

----------, and HOFFMAN, S.E. 1984. Archaean plate tectonics revisited. 1. Heat flow, spreading rate and their age of subducting lithosphere and their effects on the origin and evolution of continents. Tectonics, 3: 429-448.

ALAM, M.M., CROOK, K.W., and TAYLOR, G. 1985. Fluvial herringbone cross-stratification in a modern tributary mouth bar, Coonamble, New South Wales, Australia. Sedimentology, 32: 235-244.

ALLEGRE, C.J. 1987. Isotope geodynamics. Earth and Planetary Science Letters, 86: 175-203.

ALLEN, P., CONDIE, K.C., and NARAYANA, B.L. 1983. The Archaean low-to high-grade transition in the Krishnagiri-Dharmapuri area, Tamil Nadu, Southern India. In Precambrian of South India. Edited by S.M. Naqvi and J.J.W. Rogers. Geological Society of India Memoir, 4: 450-461.

ANHAEUSSER, C.R. 1981. Geotectonic evolution of the Archaean successions in the Barberton mountain land, South Africa. In Precambrian Plate Tectonics. Edited by A. KRONER. Elsevier, Amsterdam, pp. 137-160.

ARGAST, S., and DONNELLY, T.W. 1986. Composition and sources of metasediments in the Upper Dharwar Supergroup, South India. Journal of Geology, 94: 215-231.

ARORA, M., KHAN, R.M.K., and NAQVI, S.M. 1991. Composition of early and middle Archaean upper Continental Crust as sampled by Kaldurga Conglomerate, Dharwar Craton, India. Canadian Journal of Earth Sciences, (Communicated).

ARTH, J.G., and HANSON, G.N. 1975, Geochemistry and origin of the early Precambrian crust of North Eastern Minnesota. Geochimica et Cosmochimica Acta, 37: 1-18.

AURORA, S.M. 1985. Paragenesis of uraninite and associated ore minerals in the Precambrian oligomictic conglomerate from Walkunji, South Kanara District, Karnataka, India. Journal Geological Society of India, 26: 77-181.

AYRES, L.D., THURSTON, P.C., CARD, K.D., and WEBER, W. (Editors). 1985. Evaluation of Archaean supracrustal sequences. Geological Association of Canada, Special publication 28: 380 pp.

BALARAM, V., MANIKYAMBA, C., RAMESH, S.L., and SAXENA, V.K. 1990. Determination of rare earths in Japanese rock standards by Inductively Coupled Plasma-Mass Spectrometry. Atomic Spectroscopy, 11: 19-23.

BANLEY, M.E., DUNLOP, J.S.R., GLOVER, J.E., and GROVES, D.L. 1979. Sedimentary evidence for an Archaean shallow water volcanic sedimentary facies, eastern Pilbara block, Western Australia. Earth and Planetary Science Letters, 43: 64-84.

BARRETT, T.J., FRALICK, P.W., and JARVIS, I. 1988. Rare-earth element geochemistry of some Archaean iron formations north of Lake Superior, Ontario. Canadian Journal of Earth Sciences, 25: pp. 570-580.

BECKINSALE, R.D., DRURY, S.A., and HOLT, R.W. 1980. 3,360-My-old gneisses from the South Indian Craton. Nature, 283: 469-470.

BENCE, A.E., and ALBEE, A.L. 1968. Empirical correction factor for the electron micro analysis of silicates and oxides. Journal of Geology, 76: 382-403.

BHASKAR RAO, Y.J. 1980. Geology and Geochemistry of Metavolcanics and Associated Rock types from Bababudan Belt and the Later Archaean Crustal Evolution in Karnataka Craton. Unpublished Ph.D. thesis submitted to Osmania University.

----------, and NAQVI, S.M. 1978. Geochemistry of metavolcanics from the Bababudan schist belt: a late Archaean/Early Proterozoic volcano sedimentary pile from India. In Archaean geochemistry. Edited by B.F. Windley and S.M. Naqvi. Elsevier, Amsterdam, pp. 325-341.

----------, and DRURY, S.A. 1982. Incompatible trace element geochemistry of Archaean metavolcanic rocks from the Bababudan volcanic-sedimentary belt, Karnataka. Journal Geological Society of India, 23: 1-12.

----------, BECK, W.M., RAMA MURTHY, V., NIRMAL CHARAN, S., and NAQVI, S.M. 1983. Geology, geochemistry, and age of metamorphism of Archaean gray gneisses around Channarayapatna, Hassan District, Karnataka, South India. In Precambrian of South India. Edited by S.M. Naqvi and J.J.W. Rogers. Geological Society of India Memoir, 4: 309-328.

BHATIA, M.R. 1981. Petrology, geochemistry and tectonic setting of some flysch deposits. Ph.D. thesis. Australian National University, Canberra.

----------, 1983. Plate tectonics and geochemical composition of sandstones. Journal of Geology, 91: 611-627.

----------, 1985. Composition and classification of Palaeozoic flysch mudrocks of eastern Australia : implications in

provenance and tectonic setting interpretation. Sedimentary Geology, 41: 249-268.

----------, and TAYLOR, S.R. 1981. Trace element geochemistry and sedimentary provinces : a study from the Tasman geosynclines, Australia. Chemical Geology, 33: 115-125.

----------, and CROOK, K.A.W. 1986. Trace element characteristics of graywackes and tectonic setting discrimination of sedimentary basins. Contribution to Mineralogy and Petrology, 92: 181-193.

BICKLE, M.J. 1990. Archaean magmatism. (Abstract) In proceedings of third international Archaean symposium, 1990, Perth. Compiled by J.E. Glover and S.E. Ho. Geoconferences (W.A.) Inc., pp. 143-145.

----------, and NISBET, E.G. 1972. The oceanic affinities of some alpine mafic rocks based on their Ti-Zr-Y contents. Journal Geological Society, 128:-271.

BOOTHRYOD, J.C., and ASHLEY, G.M. 1975. Process, bar morphology, and sedimentary structures on braided outwash fans, northeastern Gulf of Alaska, in Glaciofluvial and Glaciolacustrine Sedimentation. Edited by A.V. Jopling and B.C. McDonald, SEPM, Special publication, 23: 193-222.

BOTT, M.H.P. 1982. The Interior of the Earth : Its structure, constitution and evolution. Second Edition, Edward Arnold, London. 403 pp.

BOUMA, A.H. 1962. Sedimentology of some flysch deposits. Elsevier, Amsterdam, 168 pp.

BOWERING, S.A., WILLIAMS, I.S., and COMPSTON, W. 1989. 3.96 Ga gneisses from the Slave province, Northwest territories, Canada. Geology, 17: 971-975.

BOWERS, T.S., VON DAMM, K.L., and EDMOND, J.M. 1985. Chemical evoltion of mid-ocean ridge hot springs. Geochimica et Cosmochimica Acta, 49: 2239-2252.

BRUCE FOOTE, R. 1888. "The Dharwar System", the Chief auriferous rocks in south India. Records Geological Survey of India, 21 (2): 1-40.

----------, 1889. Dharwar System, the chief auriferous series in south India. Records Geological Survey of India, 23: pp. 218.

----------, 1900. Geological notes on traverses through Mysore State. Memoir of Mysore Geological Department, 1: 103.

BULL, W.B. 1972. Recognition of alluvial fan deposits in the stratigraphic record. In Recognition of Ancient Sedimentary

Environments. Edited by K.J. Rigby and W.K. Hamblin. Soc. Econ. Paleontologists and Mineralogists, Special Publication, 16: 68-83.

BURKE, K., and KIDD, W.S.F. 1978. Were Archaean Continental geothermal gradients much steeper than those of today ? Nature, 272: 240-241.

---------, and ----------. 1980. Volcanism on Earth through time. In The Continental Crust and its Mineral Deposits. Edited by D.W. Strangway. The Geological Association of Canada, Special Paper, 20: 503-522.

----------, ----------, TURCOTTE, D.L., DEWEY, J.F., MOUGINIS-MARK, P.J., PARMENTIER, E.M., SENGOR, A.M.C., and TAPPONNIER, P.E. 1981. Tectonics of basaltic volcanism. In Basaltic volcanism of the terrestrial planets. Edited by W.M. Kaula. New York, Pergamon Press, pp. 804-898.

CANLSON, R.W., 1987. Geochemical evolution of the crust and mantle. Review of Geophysics, 25: 1011-1022.

CANN, J.R. 1970. Rb, Sr, Y, Zr, Nb in some ocean floor basaltic rocks. Earth Planetary Science Letters, 10: 7-11.

CHADWICK, B., RAMAKRISHNAN, M., and VISWANATHA, M.N. 1981. The stratigraphy and structure of the Chitradurga region : An illustration of cover basement interaction in the Late Archaean evolution of the Karnataka craton, Southern India. Precambrian Research, 16: 31-54.

----------, ----------, and ----------. 1985 (a). A Late Archaean intracratonic volcano - sedimentary basin, Karnataka, South India, Part I : Stratigraphy and basin development. Geological Society of India, 26: 769-801.

----------, ----------, and ----------. 1985(b). A late Archaean intracratonic volcano-sedimentary basin, Karnataka, South India, Part II : Structure. Journal Geological society of India, 26: 802-821.

----------, GORRIOCH, N.H.G., RAMAKRISHNAN, M. and VISWANATHA, M.N. 1986. Mineral composition, textures and deformation in Late Archaean Banded Iron-Formation rich in magnesioriebeckite and aegirine, Bababudan, Karnataka, Southern India. Journal Geological Society India, 28: 189-200.

CHADWWICK, B., RAMAKRISHNAN, M., VISWANATHA, M.N., and SREENIVASA MURTHY, V. 1978. Structural studies in the Archaean Sargur and Dharwar supracrustal rocks of the Karnataka Craton. Journal Geological Society of India, 19: 531-542.

----------, ----------, ----------, and -------. 1979. Foundation of the Saragur Group: Reply to the comments by A.Y. Glikson. Journal Geological Society India, 20: 252-255.

----------, ----------, VASUDEV, V.N., and VISWANATHA, M.N. 1989. Facies distribution and structure of a Dharwar volcano-sedimentary basin : evidence for Late Archaean transpression in Southern India ? Journal of Geological Society of London, 146: 825-834.

CHARAN, S.N., NAQVI, S.M., and RAMESH, S.L. 1988. Geology and geochemistry of spinifex-textured peridotite komatiite from Mayasandra schist belt, Karnataka. Journal Geological Society India, 32: 343-350.

CLOUD, P. 1980. Beyond Plate Tectonics. American Scientist, 68: 381-387.

--------. 1983. Banded Iron-Formation - A Gradualist's Dilemma. In Iron-Formation: Facts and Problems. Edited by A.F. Trendall and R.C. Morris. Elsevier, Amsterdam, pp. 401-416.

COLLINSON, J.D. 1970. Bed forms of the Tana river, Norway, Geolological Annaler, 52 A: 31-56.

----------, and THOMPSON, D.B. 1982. Sedimentary structures. George Allen and Unwin, Herts, U.K., 194 pp.

COMPSTON, W., and PIDGEON, R.T. 1986. Jack Hill evidence of more very old detrital zircon in western Australia. Nature, 321: 766-769.

CONDIE, K.C. 1976. The Wyoming Archaean Province in the Western United States. In The Early History of the Earth. Edited by B.F. Windley. J.Wiley and Sons, New York, pp. 499-510.

----------. 1981. Archaean Greenstone Belts. Elsevier, Amsterdam, 434 pp.

----------. 1982. Plate Tectonics & Crustal Evolution. Pergamon Press, New York, 310 pp.

----------. 1990. Geochemical and lithologic changes at the end of the Archaean. (Abstract). In proceedings of third international Archaean symposium, Perth. Compiled by J.C. Glover and S.E. Ho. Geoconferences (W.A.) Inc., pp. 449-450.

----------, and CROW, C. 1990. Early Precambrian within-plate basalts from the Kaapvaal Craton in southern Africa: A case for crustally contaminated Komatiites. Journal of Geology, 98: 100-107.

----------, and WRONKIEWICZ, D.J. 1990a. A new look at the Archaean-Proterozoic sediments and the tectonic constraint. In Precambrian Continental crust and its economic resources. Edited by S.M. Naqvi. Elsevier, Amsterdam, pp. 61-84.

----------, WILKS, M., ROSEN, D.M., and ZLOBIN, V.L. 1991. Geochemistry of meteasediments from the Precambrian Hapschan

Series, eastern Anabar Shield, Siberia. Precambrian Research, 50: 37-47.

COSTA, U.R., FYFE, W.S., KERRICH, R., and NESBITT, H.W. 1981. Is Ocean formation synchronus with first preservation of crust ? In Archaean Geology. Edited by J.E. Glover and D.I. Groves, Second International Symposium, Perth, 1980, 453-456.

CRAWFORD, A.R. 1969. Reconnaissance Rb-Sr dating of the Precambrian rocks of the Southern Peninsular India. Journal Geological Society of India, 10: 117-167.

CROOKSHANK, H. 1963. Geology of southern Bastar and Jeypore from the Bailadila Range to the Eastern Ghats. Geological Survey India Memoir, 87: 150 p.

DAVID, J., and LAJOIE, J. 1989. Sedimentology of an Archaean submarine channel-fill deposition in the Abitibi greenstone belt of Canada. Canadian Journal of Earth Sciences, 26: 1453-1462.

DAVIS, R.A. JR. 1983. Depositional Systems: A Genetic Approach to Sedimentary Geology. Prentic Hall, INC., New JERSEY, 669 pp.

DE LONG, S.E., HODGES, F.N. and ARCULUS, R.J. 1976. Ultramafic and mafic inclusions, Kanaga Island, Alaska, and occurence of alkaline rocks in island area. Geological Society of America Bulletin, 87: 275-288.

DE PAOLO, D.J. 1980. Crustal growth and mantle evolution : Inferences from models of element transport and Na and Sr isotopes. Geochimica et Cosmochimica Acta, 44: 1185-1196.

DERRY, L.A., and JACOBSEN, S.B. 1990. The chemical evolution of Precambrian seawater: Evidence from REEs in banded iron formations. Geochimica et Cosmochimica Acta, 54: 2965-2977.

DEVARAJU, T.C. and ANANTHA MURTHY, K.S. 1984. Carbonates of Chiknayakanhalli schist belt, Karnataka. Journal of Geological Society of India, 25: 162-174.

DREVER, J.I. 1974. Geochemical model for the origin of Precambrian banded iron formations. Geological Society of America Bulletin, 85: 1099-1106.

DEWEY, J.F., and WINDLEY, B.F. 1981. Growth and differentiation of continental crust. Royal Society of London Philosophical Transactions, Serial A. 301: 189-206.

dE WIT, M.J., and ASHWAL, L. 1986. Workshop on tectonic evolution of greenstone belts. Lunar Planetary Institute Technical Report, 86-10.Lunar and Planetary Institute, Houston. 227 pp.

DHOUNDIAL, D.P., PAUL, D.K., SARKAR, A., TRIVEDI, J.R., GOPALAN, K., and POTTS, P.J. 1987. Geochronology and geochemistry of

Precambrian granitic rocks of Goa, SW India. Precambrian Research, 36: 287-302.

DIA, A., DUBRE, B., GARIEPY, C., and ALLEGRE, C.J. 1990 (a). Sm-Nd and trace element characterization of shales from the Abitibi belt, Labrador Trough and Appalachian belt : consequences for crustal evolution through time. Canadian Journal of Earth Sciences, 27 (6): 758-766.

---------, ALLEGRE, C.J., and ERLANK, A.E. 1990 (b). The development of continental crust through geological time : The South African case. Earth and Planetary Science Letters (In Press).

DICKINSON, W.R. 1970. Interpreting detrital modes of graywacke and arkose. Journal of Sedimentary Petrology, 40: 695-707.

--------------. 1980. Plate tectonics and key petrologic associations. In The Continental Crust and its Mineral Deposits. Edited by D.W. Strangway. Geological Association of Canada, Ontario, pp. 341-360.

--------------, and RICH, E.I. 1972. Petrologic intervals and petrofacies in the great valley sequence, Sacramento Valley, California. Geological Society of America Bulletin, 83: 3007-3024.

--------------, and SUCZEK, C.A. 1979. Plate tectonics and sandstone composition. American Association of Petroleum Geologists, 63 (12): 2164-2182.

--------------, and VALLONI, R. 1980. Plate settings and provenance of sands in modern ocean basins. Geology, 8: 82-86.

--------------, BEARD, L.S., BRAKENRIDGE, G.R., ERJAVEC, J.L., FERGUSON, R.C., INMAN, K.F., KNEPP, R.A., LINDERG, F.A., and RYBERG, P.T. 1983. Provenance of North American Phanerozoic sandstones in relation to tectonic setting. Geological Society of America Bulletin, 94: 222-235.

DIMROTH, E. 1970. Evolution of the Labrador geosynclian. Geological Society of America Bulletin, 81: 2717-2742.

----------. 1972. The Labrador geosynclina revisited. American Journal of Science, 272: 487-506.

DIVAKARA RAO, V., and RAMA RAO, P. 1982. Granitic activity and crustal growth in the India shield. Precambrian Research, 16: 257-271.

----------------, ------------, GOVIL, P.K., and BALARAM, V. 1983. Geology and geochemistry of the Krishnarajpet schist belt: A greenstone belt of the Dharwar Craton. India. In Precambrian of South India. Edited by S.M. Naqvi and J.J.W. Rogers.

Geological Society of India Memoir, 4: 293-308.

----------, ----------, and SUBBA RAO, M.V. 1987. Terminal report on the first phase of the project "Geochemical and isotopic studies on acid plutonic rocks and evolution of continental lithosphere". National Geophysical Research Institute, Hyderabad (Unpublished).

----------, ----------, ----------, GOVIL, P.K., RAO, R.U.M., WALSH, J.N., THOMPSON, M., and REDDY, G.R. 1990. *Trace and rare earth element geochemistry and origin of the* Closepet granite, Dharwar Craton, India. In Precambrian Continental Crust and its Economic Resources. Edited by S.M. Naqvi. Elsevier, Amsterdam, pp. 203-222.

DRURY, S.A. 1978. Basic factors in Archaean geotectonics. In Archaean Geochemistry. Editor by B.F. Windley and S.M. Naqvi. Elsevier, Amsterdam, pp. 3-23.

----------. 1983. The petrogenesis and setting of Archaean metavolcanics *from Karnataka State, South India. Geochimica* et Cosmochimica Acta, 47: 317-329.

----------. 1988. Review on Precambrian Geology of India by S.M. Naqvi and J.J.W. Rogers. Geological Magazine, 5: 765-767.

----------, and HOLT, R.W. 1980. The tectonic framework of the South Indian craton: a reconnaissance involving LANDSAT imagery. Tectonophysics, 65: T1 - T5.

----------, HARRIS, N.B.W., HOLT, R.W., REEVES-SMITH, G.J., and WIGHTMAN, R.T. 1983. Precambrian tectonics and crustal evolution in South India. Journal of Geology, 92: 3-20.

DUNCAN, J.R., and KULM, 1970. Mineralogy, Provenance, and disposal history of late Quaternary deep-sea sands in Cascadia basin and Balanco fracture Zone off Oregon. Journal of Sedimentary Petrology, 40: 874-887.

DYMEK, R.F., and KLEIN, C. 1988. Chemistry, petrology and origin *of banded iron formation lithologies from the 3800 Ma Isua* supracrustal belt, West Greenland. Precambrian Research, 39: 247-302.

EICHLER, J. 1976. Origin of the Precambrian Iron-Formations. In Hand book of Stratabound and Stratiform Ore Deposits. II Regional Studies and Specific Deposits. Edited by K.H. Wolf. Elsevier, Amsterdam, 7: 157-201.

ENGEL, A.E.J., ITSON, S.P., ENGEL, C.G., STICKNEY, D.M., and GRAY, E.J. 1974. *Crustal evolution and global tectonics : a* petrographic view. Geological Society of America Bulletin, 85: 843-858.

ERIKSSON, K.A. 1978. Alluvial and destructive beach facies from the Archaean Moodies Group, Barberton Mountain Land, South Africa and Swaziland. In Fluvial Sedimentology. Edited by A.D. Miall. Can. Soc. Petrol. Geol. Memoir, 5: 287-311.

----------. 1980. Transitional sedimentation styles in the Moodies and Fig Tree Groups, Barberton Mountain Land, South Africa : evidence favouring a Archaean continental margin. Precambrian Research, 12: 141-160.

----------. 1981, Archaean plateform to trough sedimentation in the east Pilbara Black, Australia. Geological Society of Australia, Special Publication, 7: 236-244.

FAREEDUDDIN, JANARDHAN, A.S., and BASAVALINGU, B. 1988. Sedimentology, Mineralogy and Geochemistry of the Kalasapura Conglomerate. Journal Geological Society of India Memoir, 9: 65-82.

FAURE, G., and POWELL, J.L. 1972. Strontium isotope geology. Springer-Verlag, New York, 188 pp.

FENG, R., and KERRICH, R. 1990. Geochemistry of fine grained clastic sediments in the Archaean Abitibi greenstone belt, Canada : Implications for Provenance and tectonic setting. Geochemica et Cosmochimica Acta, 54: 1061-1081.

FOLK, R.L. 1980. Petrology of sedimentary rocks. Austin, Texas, Hemphills, 183 pp.

FRIEDMAN, G.M. 1958. Determination of sieve size distribution from thin section data for sedimentary petrological studies. Journal of Geology, 66: 394-416.

----------. 1962. On sorting, sorting coefficients and long normality of grain size distribution of sandstones. Journal of Geology, 70: 737-753.

FRIEND, C.R.L. and NUTMAN, A.P. 1991. SHRIMP U-Pb Geochronology of the Closepet granite and peninsular gneiss, Karnataka, South India. Journal Geological Society of India, 38: 357-368.

FYFE, W.S. 1978. The evolution of the earth's crust: moidern plate tectonics to ancient hot spot tectonics ? Chemical Geology, 23: 89-114.

---------. 1980. Crust formation and destruction. In The continental crust and its mineral deposits. Edited by D.W. Strangway. Geological Association of Canada, Special Paper, 20: 77-88.

---------. 1990. Reflections on the Archaean. In : Precambrian Continental Crust and its Economic resources. Edited by S.M. Naqvi, Elsevier, Amsterdam, pp. 1-11.

GHOSH, S.K., and SENGUPTA, S. 1985. Superposed folding and shearing in the western quartzite of Kolar Gold Field: Indian Journal of Earth Sciences, 12: 1-8.

GIBBS, A.K., MONTGOMERY, C.W., O'DAY, P.A., and ERSLEV, E.A. 1986. The Archaean-Proterozic transition : evidence from the geochemistry of metasedimentary rocks from Guyana and Montana. Geochimica et Cosmochimica Acta, 50: 2125-2145.

GLIKSON, A.Y. 1980. Precambrian sial-sima relations : evidence of earth expansion ? Tectonophysics, 63: 193-234.

----------. 1981. Uniformitarian assumptions, plate tectonics and the Precambrian earth. In Precambrian plate tectonics. Edited by A. Kroner, Elsevier, Amsterdam, pp. 91-104.

----------. 1984. Significance of Early Archaean mafic-ultramafic xenolith patterns. In Archaean geochemistry : the origin and evolution of the Archaean continental crust. Edited by A. Kroner, G.N. Hanson and A.M. Goodwin. Springer-Verlag, pp. 262-282.

----------, CHADWICK, B., RAMAKRISHNAN, M., VISWANATHA, M.N., and SRINIVASA MURTHY, V. 1979. Foundation of the Sargur Group; Comment and reply. Journal Geological Society of India, 20: 248-255.

GNANESWAR RAO, T. 1991. Geochemistry and genesis of BIF from Central part of Chitradurga schist belt, Karnataka Nucleus, India. Ph.D. thesis (under preparation).

GOLDSTEIN, S.J., and JACOBSEN, S.B. 1988. Rare earth elements in river waters. Earth and Planetary Science Letters, 89: 35-47.

GOODWIN, A.M. 1977. Archaean basin-craton complexes and the growth of Precambrian shields. Canadian Journal of Earth Sciences, 14: 2737-2759.

----------. 1981. Archaean Plates and Greenstone Belts. In : Precambrian Plate Tectonics. Edited by A. Kroner. Elsevier, Amsterdam, pp. 105-135.

GOVIL, P.K. 1985. X-ray fluorescence analysis of major, minor and selected trace elements in new IWG reference rock samples. Journal of Geological Society of India, 26: 38-42.

GRAHAM, S.A., INGERSALL, R.V. and DICKINSON, W.R. 1976. Common provenance for lithic grain in carboniferous sand stones from Ouchita Mountains and Black Warrior basin. Journal of Sedimentary Petrology, 46: 620-632.

GRAVENOR, C.P., and WONG, T. 1987. Magnetic and pebble fabrics and origin of the sunny brook till, Scarbarough Ontario, Canada. Canadian Journal of Earth Sciences, 24: 2038-2046.

GREEN, D.H. 1981. Petrogenesis of Archaean ultramafic magmas and implications for Archaean tectonics. In Precambrian Plate Tectonics. Edited by A. Kroner. Elsevier, Amsterdam, pp. 469-489.

GUSTAVSON, T.C. 1975. Sedimentation and physical limnology in proglacial Malaspine lake, south-eastern Alaska, In Glaciofluvial and Glaciolacustrine sedimentation. Edited by A.V. Jopling and B.C. McDonald. Society of Economic Paleontologists and Mineralogists, Special Publication, 23: 249-263.

HAND, B.M. and EMERY, K.O. 1964. Turbidites and topography of the north end of San Diego Trough, California. Journal of Geology, 72: 526-542.

HANSEN, E.C., HICKMAN, N.H., GRANT, N.K., and NEWTON, R.C. 1985. Pan-African age of "Peninsular Gneiss" near Madurai, South India (abstract). EOS, Transactiona of American Geophysical Union, 66: 419-420.

HARGRAVES, R.B. 1976. Precambrian geologic history. Science, 193: 363-371.

----------. 1978. Punctuated evolution of tectonic style. Nature, 276: 459-461.

----------. 1981. Precambrian tectonic style : A liberal uniformitarian interpretation. In Precambrian plate tectonics. Edited by A. Kroner. Elsevier, Amsterdam, pp. 21-56.

----------. 1986. Faster spreading or greater ridge length in the Archaean ? Geology, 14: 750-752.

HARMS, J.C. 1969. Hydraulic significance of some sand ripples. Geological Society of America Bulletin, 80: 363-396.

HENDERSON, J.B. 1972. Sedimentology of Archaean Turbidites at Yellow Knife, Northwest Territories. Canadian Journal of Earth Sciences, 9: 882-902.

----------. 1975. Sedimentology of Archaean turbidites at yellowknife, Northwest Territories. Canadian Journal of Earth Sciences, 9: 882-902.

----------. 1981. Archaean basin evolution in the Slave Province, Canada. In Precambrian Plate-tectonics. Edited by A. Kroner. Elsevier, Amsterdam, pp. 213-235.

HOLLAND, H.D. 1984. The chemical evolution of the atmosphere and oceans. Princeton University Press, 582 pp.

HUDLESTON, P.J., SCHULTZ-ELA, D., and SOUTHWICK, D.L., 1988. Transpression in an Archaean greenstone belt, northern

Minnesota. Canadian Journal of Earth Sciences, 25: 1060-1068.

HUMPHRIS, S.E., and THOMPSON, G. 1978. Trace-element mobility during hydrothermal alteration of oceanic basalts. Geochimica et Cosmochimica Acta, 42: 127-136.

HURLEY, P.M. 1968. Absolute abundance and distribution of Rb, K and Sr in the earth. Geochimica et Cosmochimica Acta, 32: 273-283.

----------, and RAND, J.R. 1969. Pre-drift continental nuclei. Science, 164: 1229-1242.

HUSSAIN, S.M., and NAQVI, S.M. 1983. Geological, geophysical and geochemical studies over the Holenarasipur schist belt, Dharwar Craton, India. In Precambrian of South India. Edited by S.M. Naqvi and J.J.W. Rogers. Geological Society of India Memoir, 4: 73-94.

INGERSOL, R.V. 1990. Actualistic sandstone petrofacies: Discriminating modern and ancient source rocks. Geology, 18: 733-736.

IYENGAR, S.V.P. 1976. The stratigraphy, structure and correlation of the Dharwar Supergroup. Geological Survey of India Miscellaneous Publication, 23(2): 415-455.

JACOBSEN, S.B., 1988. Isotopic and chemical constraints on mantle-crust evolution. Geochemica et Cosmochemica Acta, 52: 1341-1350.

----------, and PIMENTEL-KLOSE, M.R. 1988. A Nd isotopic study of the Hamersley and Michipicoten banded iron form ations: The source of REE and Fe in Archaean oceans. Earth and Planetary Sciences Letters, 87: 29-44.

JAFRI, S.H., KHAN, M., AHMAD, S.M., and SAXENA, R. 1983. Geology and geochemistry of Nuggihalli schist belt, Dharwar Craton, Karnataka, India. In Precambrian of South India. Edited by S.M. Naqvi and J.J.W. Rogers. Geological Society of India Memoir, 4: 110-120.

JAHN, B.M., and SCHRANK, A. 1983. REE Geochemistry of komatiites and associated rocks from Piumhi, Southeastern Brazil. Precambrian Research, 21: 1-20.

JAMES, H.L. 1954. Sedimentary facies iron-formation. Economic Geology, 49: 253-293.

JANARDHAN, A.S., RAMACHANDRA, H.M., and RAVINDRA KUMAR, G.V. 1979. Structural history of Sargur supracrustals and associated gneisses southwest Mysore, Karnataka. Journal Geological Society India, 20: 61-72.

----------, SHADAKSHARA SWAMY, N., and RAVINDRA KUMAR, G.V. 1981. Petrological and structural studies of the manganiferous horizons and recrystallized ultramafics around Gundlupet, Karnataka. Journal Geological Society of India, 22: 103-111.

JAYARAM, B. 1907. Report on the geological survey of portions of the Mysore district for the year 1906-07. Records of Mysore Geology Department, 8: 75-121.

----------. 1910. Note on the work done during the field season of 1909-10. Records of Mysore Geology Department, 11: 175-184.

JOPLING, A.V., and WALKER, R.G. 1968. Morphology and origin of ripple-drift cross-lamination, with examples from the Pleistocene of Massachusets. Journal of Sedimentary Petrology, 38: 971-984.

KETNER, K.B. 1966. Comparison of Ordovician eugeosynclinal and miogeosynclinal quartzites of the Cordilleran geosynclines. U.S. Geological Survey Professional Paper, 550-C. p. C54-C60.

KHAN, R.M.K., GOVIL, P.K., and NAQVI, S.M. 1991. Geochemistry and genesis of banded iron formation from Kudremukh schist belt, Karnataka Nucleus, India. Journal of Geological Society of India, (Communicated).

KLEIN, C., and BEUKES, N.J. 1989. Geochemistry and sedimentology of a facies transition from limestone to iron-formation deposition in the early Proterozoic Transvaal Supergroup, South Africa. Economic Geology, 84: 1733-1742.

KLINKHAMMER, G., ELDERFIELD, H., and HUDSON, A. 1983. Rare earth elements in seawater near hydrothermal vents. Nature, 305: 185-188.

KRONER, A. 1981. Precambrian plate tectonics. In : Precambrian plate tectonics. Edited by A. Kroner. Elsevier, Amsterdam, pp. 57-90.

KRUMBEIN, W.C., and PETTIJOHN, F.J. 1938. Manual of sedimentary petrology. Appleton-Century, New York. 549 pp.

KUMAR, B., VENKATA SUBRAMANIAN, V.S., and SAXENA, R. 1983. Carbon and oxygen isotopic composition of the carbonates from greenstone belts of Dharwar Craton. India. In Precambrian of South India. Edited by S.M. Naqvi and J.J.W. Rogers. Geological Society of India Memoir, 4: 260-266.

LONG, D.G.F. 1978. Proterozoic stream deposits: some problems of recognition and interpretation of ancient sandy fluvial systems. In Fluvial Sedimentology. Edited by A.D. Miall. Canadian Society of Petroleum Geologists Memoir, 5: 313-342.

LOWE, D. 1982. Comparative sedimentology of the principal volcanic sequences of Archaean greenstone belts in South Africa, Western Australia and Canada. Precambrian Research, 17: 1-29.

LOWMAN (JR.), P.D. 1989. Comparative paleontology and the origin of continental crust. Precambrian Research, 44: 171-195.

MANIKYAMBA, C., BALARAM, V., and NAQVI, S.M. 1991. Geochemical signature of polygenecity of BIFs of Archaean Sandur greenstone belt (schist belt), Karnataka Nucleus, India. Precambrian Research, (Communicated).

MAYNARD, J.B., VALLONI, R., and YU, H. 1982. Composition of modern deep-sea sands from arc-related basins. In Trench-Forearc sedimentation. Edited by J.K. Leggett. Geological Society of London, Special publication, 10: 551-561.

McCULLOCH, M.T., and WASSERBURG, G.J. 1978. Sm-Nd and Rb-Sr chronology of continental crust formation. Science, 200: 1003-1011.

McGOWEN, H., and GROAT, C.G. 1971. Von Horn Sandstone, West Texas:an alluvial fan model for mineral exploration. Report Bureau Economic Geology, University Texas, Austin, Invest. 72, 57 p.

McLENNAN, S.M. 1984. Petrological characteristics of Archaean graywackes. Journal of Sedimentary Petrology, 54: 889-898.

----------, and TAYLOR, S.R. 1991. Sedimentary rocks and crustal evolution: Tectonic setting and secular trends. Journal of Geology, 99: 1-22.

----------, NANCE, W.B. and TAYLOR, S.R. 1980. Rare earth element-thorium correlations in sedimentary rocks, and the composition of the continental crust. Geochimica et Cosmochimica Acta, 44: 1833-1839.

----------, TAYLOR, S.R., and ERIKSSON, K.A. 1983. Geochemistry of Archaean shales from the Pilbara Supergroup, western Australia. Geochemica et Cosmochimica Acta, 47: 1211-1222.

----------, ----------, and MCGREGOR, V.R. 1984. Geochemistry of Archaean metasedimentary rocks from west Greenland. Geochimica et Cosmochimica Acta, 48: 1-13.

MIALL, A.D. 1978. Fluvial Sedimentology. Canadian Society Petrology and Geology Memoir, 5: 859 pp.

----------. 1983. Glaciomarine sedimentation in the Gowganda Formation (Huroman), northern Ontario. Journal Sedimentary Petrology, 53(2): 477-491.

MICHARD, A. 1989. Rare earth element systematics in hydrothermal fluids. Geochimica et Cosmochimica Acta, 53: 745-750.

MONRAD, J.R. 1983. Evolution of sialic terranes in the vicinity of the Holenarasipur belt, Hassan district, Karnataka, India. In Precambrian of South India. Edited by S.M. Naqvi and J.J.W. Rogers. Geological Society of India Memoir, 4: 343-364.

MOORBATH, S. 1975. Evolution of Precambrian crust strontium isotopic evidence. Nature, 254: 395.

----------. 1977. Ages, isotopes and evolution of Precambrian continental crust. Chemical Geology, 20: 151-187.

----------. 1978. Age and isotope evidence for the evolution of continental crust. Philosophical Transactions of Royal Society London, A 288: 401-413.

----------, and TAYLOR, P.N. 1981. Isotopic evidence for continental growth in the Precambrian. In Precambrian Plate Tectonic. Edited by A. Kroner. Elsevier, Amsterdam, pp. 491-525.

----------, O'NIONS, R.K., PANKHURST, R.J., and MC GREGOR, V.R. 1972. Further rubidium-strontium age determinations on the very early Precambrian rocks of the Godthaab district, West Greenland. Nature, 240: 78-82.

MORRIS, R.C. 1974. Sedimentary and tectonic history of the Quachita Mountains. In Tectonics and sedimentation. SEPM Special Publication, 22: 129-142.

MUKHOPADHYAY, D. 1986. Structural pattern in the Dharwar Craton. Journal of Geology, 94: 167-186.

----------, and GHOSH, D. 1981. A tectono-stratigraphic model of the Chitradurga schist belt, Karnataka. Journal Geological Society of India, 22: 22-31.

----------, BARAL, M.C., and NEOGI, R.K. 1980. Mineralogy of banded iron formation in the southeastern Bababudan Hills, Karnataka, India. Neues Jalnab. Mineral. Abh. 139: 303-327.

MURALI, A.V., PAWASKAR, P.B., REDDY, G.R., SUBBARAO, K.V., VASUDEV, V.N., and SANKAR DAS, M. 1979. Petrogenetic significance of rare earth element patterns of selected samples of Ingaldhal metavolcanics, Karnataka State, India. Consortium studies no. 1. Journal Geological Society India, 20: 334-338.

NAGY, B., WEBER, R., GUERRERO, J.C., and SCHIDLOWSKI, M. 1983. (Eds.) Developments and Interactions of the Precambrian Atmosphere, Lithosphere and Biosphere. Elsevier, Amsterdam, 475 pp.

NAHA, K., and CHATTERJEE, A.K. 1982. Axial plane foldings in the Bababudan hill ranges of Karnataka. Indian Journal Earth Sciences, 9: 37-43.

--------, and MUKHOPADHYAY, D. 1990. Structural styles in the Precambrian metamorphic terranes of Peninsular India: A synthesis. In Precambrian Continental crust and its Economic Resources. Edited by S.M. Naqvi. Elsevier, Amsterdam, pp. 157-178.

-------, SRINIVASAN, R., and NAQVI, S.M. 1986. Structural unity in the Early Precambrian Dharwar Tectonic province, Peninsular India. Quarternary Journal Geology Mining Metallurgy Society India, 58: 219-243.

NAQVI, S.M. 1967. The banded pyritiferous chert from Ingaldhal and adjoining areas of Chitaldurg schist belt, Mysore. National Geophysical Research Institute Bulletin (Hyderabad), 5: 173-181.

----------. 1972. The petrochemistry and significance of Jogimaradi traps, Chitaldurg schist belt, Mysore. Bulletin Volcanologique, 35: 1069-1093.

----------. 1973. Geological structure and aeromagnetic and gravity anomalies in the central part of the Chitaldrug schist belt, Mysore. India. Geological Society of America Bulletin, 84: 1721-1732.

----------. 1974. Review of the present status of the geochemical work over the Precambrian mafic rocks of India. Journal Geology Society of India, 15: 380-389.

----------. 1976. Physico-chemical conditions during the Archaean as indicated by Dharwar geochemistry. In the early history of the earth. Edited by B.F. Windley. Wiley-Interscience, New York, pp. 289-302.

----------. 1978. Geochemistry of Archaean metasediments : evidence for prominent anorthosite-norite-troctolite (ANT) in the Archaean basaltic primordial crust. In Archaean geochemistry. Edited by B.F. Windley and S.M. Naqvi. Elsevier, Amsterdam, pp. 343-360.

----------. 1981. The oldest supracrustals of the Dharwar craton, India. Journal of Geological Society of India, 22: 458-469.

----------. 1982. Early Archaean evolution of Indian shield with special reference to Dharwar Craton. Revista Brasi Liera de Geociencias, 112: 223-233.

----------. 1983. Early Precambrian clastic metasediments of Dharwar greenstone belts : implications to SIMA-SIAL transformation processes. In Precambrian of South India. Edited by S.M. Naqvi and J.J.W. Rogers. Geological Society of India

Memoir, 4: 220-236.

----------. 1985. Chitradurga schist belt - an Archaean suture ? Journal Geological Society of India, 26: 511-525.

----------. 1990. Precambrian Continental crust and its economic resources. Elsevier, Amsterdam, 669 pp.

----------. and HUSSAIN, S.M. 1972. Petrochemistry of some early Precambrian metasediments from the central part of the Chitradurga schist belt, Mysore, India. Chemical Geology, 10 : 109-135.

----------. and ----------. 1973a. Geochemistry of Dharwar metavolcanics and the composition of the primeval crust of Peninsular India. Geochimica et Cosmochimica Acta. 37: 159-164.

----------. and ----------. 1973b. Relations between trace and major element composition of the Chitaldrug meta-basalts and the Archaean mantle. Mysore. India, Chemical Geology, 11: 17-30.

----------. and ----------. 1974. The protocontinental growth of the Indian shield and the antiquity of its rift valleys. Precambrian Research, 1: 345-398.

----------., and ROGERS, J.J.W. (Eds.) 1983. Precambrian of South India. Geological Society of India. Memoir, 4: 575 pp.

----------. and ----------. 1987. Precambrian Geology of India. Oxford Monographs on Geology and Geophysics. No. 6, Oxford University Press, Oxford, 223 pp.

----------., DIVAKARA RAO, V., HUSSAIN, S.M., NARAYANA, B.L., ROGERS, J.J.W., and SATYANARAYANA, K. 1978a. The petrochemical and geological implications of conglomerates from Archaean geosynclinal piles of Southern india. Canadian Journal of Earth Sciences, 15: 1085-1100.

----------., ----------., and ----------. 1978b. Primitive crust : evidence from the Indian shield. Precambrian Research, 6: 345-398.

----------, VISWANATHAN, S., and VISWANATHA, M.N. 1978c. Geology and geochemistry of Holenarasipur schist belt and its place in the evolutionary history of the Indian Peninsula. In Archaean Geochemistry: The Origin and evolution of Archaean Continental Crust. Edited by B.F. Windley and S.M. Naqvi. Elsevier, Amsterdam, pp. 109-126.

----------, NARAYANA, B.L., RAMA RAO, P., AHMAD, S.M., and UDAY RAJ, B. 1980. Geology and geochemistry of paragneisses from Javanahalli schist belt, Karnataka, India. Journal Geological Society India, 21: 577-592.

----------, GOVIL, P.K., and ROGERS, J.J.W. 1981. Chemical sedimentation in Archaean-early Proterozoic greenschist belts of the Dharwar Craton, India. In Second Internat.' Symposium on Archaean Geology. Edited by J.E. GLOVER and D.I. GROVES. Geological Society of Australia, Special Publication, 7: 245-253.

----------, ALLEN, P., and CONDIE, K.C. 1983. Geochemistry of some unusual Early Archaean metasediments from Dharwar craton, India. Precambrian Research, 22: 125-147.

----------, and 13 others. 1983. Geochemistry of gneisses from Hassan district and adjoining areas, Karnataka, India. In Precambrian of South India. Edited S.M. Naqvi and J.J.W. Rogers. Geological Society of India Memoir, 4: 401-413.

---------, VENKATACHALA, B.S., SHUKLA, M., KUMAR, B., NATARAJAN, R., and MUKUND SHARMA. 1987. Silicified cyanobacteria from the cherts of Archaean Sandur Schist belt. Journal of Geological Society of India, 29: 535-539.

----------, SAWKAR, R.H., SUBBA RAO, D.V., GOVIL, P.K., and GNANESHWAR RAO, T. 1988. Geology, geochemistry and tectonic setting of Archaean greywackes from Karnataka Nucleus, India. Precambrian Research, 39: 193-216.

NARASIMHAN, M., and VISWANATHA, M.N. 1970. Report on Kalasapura Copper investigation, Chikmagalur district, Mysore State. Geological Survey of India, Unpublished Report.

NARAYANA, B.L., NAQVI, S.M., RAMA RAO, P., UDAY RAJ, B., AND AHMAD, S.M. 1983. Geology and geochemistry of Javanahalli schist belt, Karnataka, India. In Precambrian of South India. Edited by S.M. Naqvi and J.J.W. Rogers. Journal Geological Society of India Memoir, 4: 143-157.

NELSON, C.H., NORMARK, W.R., BOUMA, A.H., and CARLSON, P.R. 1978. Thin-bedded turbidites in modern submarine canyon and fans. In Sedimentation in Submarine Canyons, Fans, and Trenches. Edited by D.J. Stanley and G. Kelling. Dowden, Hutchinson & Ross, Stroudsburg, pp. 177-189.

NESBITT, H.W., and YOUNG, G.M. 1982. Early Proterozoic climates and plate motions inferred from major element chemistry of lutites. Nature, 299: 715-717.

NESBITT, H.W., MACKOVICS, J.G., and PRICE, R.C. 1980. Chemical processes affecting alkalis and alkaline earths during continental weathering. Geochimica et Cosmochimica Acta, 44: 1659-1666.

NEWTON, R.C., and ANDERSON, A.T. 1986. The Dharwar Craton of South India : an Archaean Protocontinent. Geology, 94: 127-128.

NISBET, E.G., and FOWLER, C.M.R. 1983. Model for Archaean plate tectonics. Geology, 11: 376-379.

NOCITA, B.W., and LOWE, D.R. 1990. Fan delta sequence in the Archaean Fig Tree Group, Barberton Greenstone belt, South Africa. Precambrian Research, 48: 375-393.

OJAKANGAS, R.W. 1972. Archaean volcanogenic greywackes of the Vermillion District, North-eastern Minnesota. Geological Society of America Bulletin, 83: 429-442.

----------. 1985. Review of Archaean clastic sedimentation, Canadian shield : major felsic volcanic contributions to turbidite and alluvial fan-fluvial facies association. In Evolution of Archaean supracrustal sequences. Edited by L.D. Ayres, P.C. Thurston, K.D., Card and W. Weber. Geological Association of Canada, Special papers, 28: 23-47.

----------. 1990. Archaean sedimentation, Canadian shield. In Precambrian Continental Crust and its Economic Resources. Edited by S.M. Naqvi. Elsevier, Amsterdam, pp. 179-202.

PAN, Y, FLEET, M.E., and STONE, W.E. 1991. Geochemistry of metasedimentary rocks in the late Archaean Hemlo-Heron greenstone belt, Superior province, Ontario. Implications for provenance and tectonic setting. Precambrian Research, 52: 53-69.

PEARCE, J.A. 1973. Some relationships between the geochemistry and tectonic setting of basic volcanic rocks. Unpublished Ph.D. thesis, University of East Anglia, 319 pp.

----------. 1975. Basalt geochemistry used to investigate past tectonic environments on Cyprus. Tectonophysics, 25: 41-67.

----------. 1980. Geochemical evidence for the genesis and eruptive setting of lavas from Tellyan ophiolites. In Proc. International Ophiolite Symposium, Cyprus, 1979. Geological Survey Department, Nicosia, 261 pp.

----------. 1983. Role of the sub-continental lithosphere in magma genesis at active continental margins. In Continental Basalts and Mantle Xenoliths. Edited by C.J. Howkesworth and M.J. Norry. Nantrich, U.K. Shiva Press, pp. 230-249.

----------, and CANN, J.R. 1973. Tectonic setting of basic volcanic rocks determined using trace element analysis. Earth and Planetary Science Letters, 19: 290-300.

PETTIJOHN, F.S. 1984. Sedimentary rocks. First Indian Edition. CBS Publishers and Distributors, New Delhi, 628 pp.

----------, POTTER, P.E. and SIEVER R. 1965. Geology of sands and sandstones. Ind. University Press, Bloomington. 208 pp.

----------, ----------. and ---------. 1972. Sand and Sandstone. Springer, Berlin, 618 pp.

PICHAMUTHU, C.S. 1935a. A note on the origin of the Kaldurga conglomerates, Mysore. Current Science, 3: 431.

----------. 1935b. The conglomerates and grits of Kaldurga, Kadur district, Mysore. Proceedings of Indian Academy of Sciences, 2B: 254-279.

----------. 1935c. The Kaldurga conglomerates and the iron ore series of the Bababudan, Kadur district, Mysore. Reply to discussion by Ramachandra Rao. Current Science, 4: 417-418.

----------. 1936. On the Bababudanite, a soda amphibole from the banded ferruginous quartzites of Mysore, India. Geological Magazine, 73: 39-45.

----------. 1946. Quartz-Keratophyres from Galipuje, Kadur district, Mysore State. Quartenary Journal of Geological Mining Metallurgy Society of India, 18: 125-128.

----------. 1961. Tectonics of Mysore State. Proceedings Indian Academy Sciences, 53: 135-139.

----------. 1967. Dharwar sedimentation. Journal Geological Society, Univ. Saugar, 3: 21-29.

----------. 1976. Some problems pertaining to the Peninsular Gneissic complex. Journal Geological Society of India, 17: 1-16.

----------. 1982. Schist - gneiss relation in Dharwar Craton. Current Science, 51: 118-124.

----------, and SRINIVASAN, R. 1983. A billion-year history of the Dharwar Craton (3200 to 2100 m.y. ago). In Precambrian of South India. Edited by S.M. Naqvi and J.J.W. Rogers. Geological Society of India Memoir, 4: 121-142.

----------, and ----------. 1984. The Dharwar Craton - A Golden Jubilee Publication. Indian National Science Academy, New Delhi, 34 pp.

POTTER, P.E., and PETTIJOHN, F.J. 1972. Paleocurrents and Basin Analysis, Springer-Verlag, 296 pp.

POTTS, P.J. 1987. A handbook of silicate rock analysis. Blackie and Sun Ltd. 622 pp.

POWER, M.C. 1953. A new roundness scale for sedimentary particles. Journal of Sedimentary Petrology, 23: 117-119.

RAASE, P., RAITH, M., ACKERMAND, D., VISWANATHA, M.N., and LAL, R.K. 1983. Mineralogy of Chromiferous quartzites from South India. Journal Geological Society of India, 24: 502-521.

RADHAKRISHNA, B.P. 1940. Note on Talya Conglomerate. Records Mysore Geology Department, 37: 135-136.

----------. 1954. On the cordierite bearing granulites bordering the closepet granite of Mysore. Mysore Geology Department Bulletin, 21: 1-25.

----------. 1964. Some aspects of the stratigraphy and structure of Dharwar of Mysore State, south India. Proceedings of Symposium on Stratigraphy, age and correlation of the Archaean Provinces of India, pp. 33-34.

----------. 1967. Copper in Mysore State. Mysore Deptartment of Mines and Geology, Bangalore, 55 pp.

----------. 1983. Archaean granite-greenstone terrain of the South India shield. In: Precambrian of South India. Edited by S.M. Naqvi and J.J.W. Rogers. Geological Society of India Memoir, 4: 1-46.

----------. 1987. Introduction. In Purana Basins of Peninsular India (Middle to Late Proterozoic). Geological Society of India Memoir, 6: I-XV.

----------, and VENKOBA RAO, N. 1967. The occurrence of amosite asbestos in the iron formation of Bababudan, Chikmagalur district, Mysore State. Geological Society of India Bulletin, 4: 99-102.

----------, and NAQVI, S.M. 1986. Precambrian continental crust of India and its evolution. Journal of Geology, 94: 145-166.

----------, and RAMAKRISHNAN, M. (Eds.). 1990. Archaean greenstone belts of South India. Geological Society of India Memoir, 19: 497.

----------, DEVARAJU, T.C., and MAHABALESWAR, B. 1986. Banded iron formation of India. Journal Geological Society of India, 28: 71-91.

RAJAMANI, V., SHIVKUMAR, K., HANSON, G.N., and SHIREY, S.B. 1985. Geochemistry and petrogenesis of amphibolites, Kolar schist belt, south India. Evidence for Komatiitic magma derived by low percentage of melting of mantle. Journal of Petrology 96: 92-123.

RAMAKRISHNAN, M. 1980. Geology of the Javanahalli, Holenarsipur and Sargur schist belts of Karnataka Craton and the geochemistry of mafic rocks. Unpublished Ph.D. Thesis submitted at Indian Institute of Science, Bangalore.

----------, VISWANATHA, M.N., and SWAMI NATH, J. 1976. Basement-cover relationships of Peninsular Gneiss with high grade schist and greenstone belts of southern Karnataka. Journal of Geological Society of India, 7: 97-111.

----------, MOORBATH, S., TAYLOR, P.N., ANANTHA IYER, G.V., and VISWANATHA, M.N. 1984. Rb-Sr and Pb-Pb whole-rock isochron ages of basement gneisses in Karnataka Craton. Journal Geological Society of India, 25: 20-34.

RAMA RAO, B. 1924. Report on the revision survey work in parts of Holenarsipur taluk, Hassan district. Rec. Mysore Geology Department, 21: 146-203.

----------. 1940. Remarks on the mode of occurrence and origin of the Peninsular Gneiss of Mysore. Records Mysore Geology Department, 38: 52-72.

----------. 1964. On the classification and correlation of the ancient schistose formations of Peninsular India - a review. In Advancing Frontiers in Geology and Geophysics. Osmania University, Hyderabad.

RAMA RAO, B.V. 1974. Discovery of uraniferous Precambrian conglomerates at Chikmagalur, Karnataka State. Current Science, 44: 174-175.

RAMA RAO, P., DIVAKARA RAO, V., and SUBRAHMANYAM, C. 1979. Integrated geological, geochemical and geophysical investigations in the Peninsular Shield - a review. Geophysical Research Bulletin, 17: 361-373.

----------, NAQVI, S.M., GOVIL, P.K., and BALARAM, V. 1991. Geochemistry of Trondhjemites from Sigegudda, Hassan district, Karnataka. Journal Geological Society India, 37: 351-358.

RANGANNA, M., SHAHIDHARA, H., and RAGHU PRAKASH, T.R. 1981. Comparison of the Tarikere Valley gneiss and the gneiss pebbles in the Kaldurga conglomerate - A study in the Dharwar basement problem. Journal Geological Society of India, 22: 570-576.

READING, H.G. 1986. Sedimentary environments and facies. Blackwell Scientific Pub. London. 591 pp.

REAY, A., ROOKE, J.M. WALLACE, R.C., and WHELAN, P. 1974. Lavas from Niufo' ou Island, Tanga, resemble ocean floor basalts. Geology, 2: 605-606.

REINECK, H.E., and SINGH, I.B. 1980. Depositional sedimentary environments. Springer-Verlag, Berlin, New York, 439. pp.

REMIENGAR, A.S., DEVADU, G.R., VISWANATHA, M.N., CHAYAPATHI, N., and RAMAKRISHNAN, M. 1978. Banded chromite-fuchsite

quartzite in the older supracrustal sequence of Karnataka. Journal Geological Society of India, 19: 577-582.

ROGERS, J.J.W. 1986. The Dharwar Craton and the assembly of Peninsular India. Journal of Geology, 94: 129-144.

RONOV, A.B. 1964. Common tendencies in the chemical evolution of the earth's crust, ocean and atmosphere. Geochemical Int., 4 : 713-737.

----------, and MIGDISOV, A.A. 1971. Geochemical history of the crystalline basement and the sedimentary cover of the Russian and North America platforms. Sedimentology, 16: 137-185.

ROSER, B.P., and KORSCH, R.J. 1988. Provenance signatures of sandstone-mudstone suites determined using descriminant function analysts of major-element data. Chemical Geology 67: 119-139.

RUHLIN, D.E., and OWEN, R.M. 1986. The rare earth element geochemistry of hydrothermal sediments from the East Pacific Rise : Examination of a seawater scavenging mechanism. Geochimica et Cosmochimica Acta, 50: 393-400.

RUST, B.R. 1978. Depositional models for braided alluvium. Fluvial Sedimentology. Edited by A.D. Miall. Canadian Society Petrology and Geology Memoir, 5: 605-625.

SAMPAT IYENGAR, P. 1905. Report on the survey work in the Chitaldurg district. Records Mysore Geology Department, 6: 57-116.

----------. 1906. Report on parts of Hassan and Tumkur districts. Records Mysore Geology Department, 7: 27-42.

----------. 1908. Report on the geology of parts of Hassan and Kadur Districts. Ibid. 9.

SCHWABE, F.L. 1978. Secular trends in the composition of sedimentary rock assemblages - Archaean through Phanerozoic time. Geology, 6: 532-536.

SESHADRI, T., CHAUDHURI, A., HARINADHA BABU, P., and CHAYAPATHI, N. 1981. Shimoga belt. In Early Precambrian Supracrustals of Southern Karnataka. Edited by J. Swami Nath and M. Ramakrishnan. Geological Survey of India Memoir, 112: 163-198.

SEVIGNY, J.H., and BROWN, E.H. 1989. Geochemistry and tectonic interpretation of some metavolcanic rock units of the western North Cascades, Washington. Geological Society of America Bulletin, 101: 391-400.

SHAPIRO, L. 1975. Rapid analysis of silicate carbonate and phosphate rocks. USGS, Bulletin, 1401: 1-76.

SHEAREV, C.K., and PAPIKE, J.J. 1989. Is plagioclase removal responsible for the negative Eu anomaly in the source region of more basalts. Geochimica et Cosmochimica Acta, 53: 3331-3336.

SHIBLEY, D.F., and WILBAND, J.T. 1977. Chemical balance of earth's crust. Geochima et Cosmochemica Acta, 41: 545-549.

SHAW, D.M. 1980. Evolutionary tectonics of the earth in the light of early crustal structures. In the continental crust and its mineral deposits. Edited by D.W. Strangway. The Geological Association of Canada, Special paper, 20 : 65-76.

SLEEP, N.H., and WINDLEY, B.F. 1982. Archaean plate tectonics: Constraints and inferences. Journal of Geology, 90: 363-379.

SMEETH, W.F. 1908. Notes on a variety of ribeckite (Bababudanite) and on cummingtonite from Mysore State. Records Mysore Geology Department, 9: 85-94.

----------. 1916. Outline of the geological history of Mysore. Mysore Geology Department Bulletin, 6: 22.

SMITH, N.D. 1970. The braided stream depositional environment: Comparison of the Clatte river with some Silurian Clastic rocks, north-central Appalachians. Geological Society of America Bulletin, 81: 2993-3014.

SMITH, T.E., and HALM, P.E. 1990. The geochemistry and tectonic setting of pre-metamorphic minor intrusions of the central metasedimentary belt, Grenville Provenance, Canada. Precambrian Research, 48: 341-360.

SPENCER, D.W. 1963. The interpretation of grain size distribution curves of clastic sediments. Journal of Sedimentary Petrology, 33: 180-190.

SPRY, A. 1976. Metamorphic textures, Pergamon Press, Oxford. pp.350

SREENIVAS, B.L., and SRINIVASAN, R. 1974. Geochemistry of granite-greenstone terrain of south India. Journal Geological Society of India, 15: 390-406.

SREERAMACHANDRA RAO, K. 1977. Early Precambrian banded iron formations in the western ghats greenstone belts with special reference to Kudachadri region, Karnataka state (Abstract). UGS, UNESCO, IGCP Symp. on Archaean Geochemistry, Hyderabad, India, pp. 105.

SRINIVASAN, R., and SREENIVAS, B.L. 1968. Sedimentation and tectonics in Dharwar (Archaean) of Mysore. Indian Mineralogist 10: 282-288.

----------, and SREENIVAS, B.L. 1971. Flood basalts from Dharwars of Mysore, India. Bulletin Volcanologique. 4: 824-840.

----------, and SREENIVAS, B.L. 1972. Dharwar stratigraphy. Journal Geological Society of India, 13: 72-83.

----------, and OJAKANGAS, R.W. 1986. Sedimentology of quartz-pebble conglomerates and quartzites of the Archaean Bababudan group, Dharwar craton, South India : evidence for early crustal stability. Journal of Geology, 94: 199-214.

----------, and NAQVI, S.M. 1990. Some distinctive trends in the evolution of the early Precambrian (Archaean) Dharwar, Craton, South India. In Precambrian Continental Crust and its Economic Resources. Edited by S.M. Naqvi. Elsevier, Amsterdam, pp. 245-266.

----------, MANOJ SHUKLA, NAQVI, S.M., YADAV, V.K., VENKATACHALA, B.S., UDAY RAJ, B., and SUBBA RAO, D.V. 1989. Archaean stromatolites from Chitradurga schist belt, Dharwar Craton, South India. Precambrian Research, 43: 239-250.

----------, NAQVI, S.M., UDAY RAJ, B., SUBBA RAO, D.V., BALARAM, V., and GNANESWAR RAO, T. 1989. Geochemistry of the Archaean graywackes from the northwestern part, Chitradurga schist belt, Dharwar Craton. Journal Geological Society of India, 34: 505-516.

STANLEY, D.J., and KELLING, G. (Eds) 1967. Sedimentation patterns in the Wilmington submarine canyons area. Ocean Science & Engineering, Atlantic Shelf, Transactions National Symposium Marine Technologists Society, pp. 127-142.

STROH, P.T., MONRAD, J.R., FULLAGAR, P.D., NAQVI, S.M., and ROGERS, J.J.W. 1983. 3,000 m.y. old Holekote trondhjemite, a record of stabilization of the Dharwar Craton. In Precambrian of South India. Edited by S.M. Naqvi and J.J.W. Rogers. Geological Society of India Memoir, 4: 365-376.

SWAMI NATH, J., and RAMAKRISHNAN, M. 1981. Present classification and correlation. In Early Precambrian supracrustals of southern Karnataka. Edited by J. Swami Nath and M. Ramakrishnan. Geological Survey of India Memoir, 112: 23-38.

----------, ----------, and VISWANATHA, M.N. 1976. Dharwar stratigraphic model and Karnataka Craton evolution. Geological Survey of India Records, 107 (2): 149-175.

----------, and 13 OTHERS. 1974. The cratonic greenstone belts of southern Karnataka and their possible relation to the Charnockite mobile belt (abstract). International Seminar on Tectonics and Metallogeny of South East Asia and Far East, Calcutta. pp. 38-39.

TAYLOR, P.N., MOORBATH, S., CHADWICK, B., RAMAKRISHNAN, M., and VISWANATHA, M.N. 1984. Petrography, chemistry and isotopic ages of Peninsular gneiss, Dharwar acid volcanic rocks and the Chitradurga granite with special reference to the Late Archaean evolution of the Karnataka craton, South India. Precambrian Research, 23: 349-375.

TAYLOR, S.R., 1991. Young Earth like Venus, Nature, 350: 376-377.

----------, and McLENNAN, S.M. 1981. The rare earth element evidence in Precambrian sedimentary rocks : implications for crustal evolution. In Precambrian plate tectonics. Edited by A. Kroner. Elsevier, Amsterdam, pp. 527-548.

----------, and ----------. 1981b. The composition and evolution of the continental crust : rare earth element evidence for sedimentary rocks. Transaction of Royal Society, London, A (301): 381-399.

----------, and ----------. 1985. The continental crust : its composition and evolution. Geoscience Texts, Blacwell, pp.307.

----------, RUNDNICK, R.L., McLENNAN, S.M., and ERIKSSON, K.A. 1986. REE patterns in Archaean high grade metasediments and their tectonic significance. Geochimica et Cosmochimica Acta, 50: 2267-2279.

THURSTON, P.C., and CHIVERS, K.M. 1990. Secular variation in Greenstone Sequence Development Emphasizing Super Province Canada. Precambrian Research, 46: 21-58.

TOWE, K.M. 1983. Precambrian Atmospheric Oxygen and Banded Iron Formations : A delayed Ocean Model. Precambrian Research, 20 : 161-170.

----------. 1990. Aerobic respiration in the Archaean. Nature, 348: 54-56.

TRENDALL, A.F. 1983. Introduction. In Iron-Formation: Facts and Problems. Edited A.F. Trendall and R.C. Morris. Elsevier, Amsterdam, pp. 1-12.

UDAY RAJ, B. 1991. Geology and geochemistry of the Melukote belt, Mandya district, Karnataka. Unpublished Ph.D. thesis submitted at Osmania University. 261 pp.

VASUDEV, V.N., NAQVI, S.M., SHUKLA, M., and UDAY RAJ, B. 1989. Stromatolites from the chert-dolomite of Archaean Shimoga schist belt, Dharwar Craton. India. Journal Geological Society India, 33: 201-205.

VEIZER, J. 1976. $^{87}Sr/^{86}Sr$ evolution of seawater during geologic history and its significance as an index of crustal evolution. In The Early History of the Earth. Edited by B.F.

Windley. Wiley, London, pp. 569-578.

VENKATACHALA, B.S., NAQVI, S.M., CHADHA, M.S. and 13 others. 1989. Paleobiology and geochemistry of the Precambrian stromatolites and associated sedimentary rocks from the Dharwar Craton: constraints on Archaean biogenic processes. Himalayan Geology, 13: 1-20.

VENKATASUBRAMANIAN, V.S., and NARAYANASWAMY, R. 1974. The age of some gneissic pebbles in Kaldurga conglomerates, Karnataka State, India. Journal Geological Society of India, 15: 318-319.

VISWANATHA, M.N. 1976. Kalasapura unconformity in Chikmagalur district, Mysore State and its stratigraphic and economic significance. Geological Survey of India, miscellaneous publications, 23 (2): 465-469.

----------, and RAMAKRISHNAN, M. 1976. The pre-Dharwar supracrustal rocks of Sargur schist complex in southern Karnataka and their tectono-metamorphic significance. Indian Mineralogist, 16: 48-65.

----------, and ----------, 1981. Bababudan belt. In Early Precambrian supracrustals of southern Karnataka. Edited by J. SwamiNath and M. Ramakrishnan. Geological Survey of India Memoir, 112: 91-114.

WALKER, R.G. 1976. Facies models 2. Turbidites and associated coarse clastic deposits. Geoscience Canada, 3: 25-36.

----------. 1978. Deep water sandstone facies and ancient submarine fans: models for exploration for stratigraphic traps. American Association of Petroleum Geologists Bulletin, 62: 932-966.

----------. 1984. Turbidites and associated coarse clastic deposits. In Facies Models. Edited by R.G. Walker, 2nd edition. Geoscience Canada, reprint series 1. Toronto, Canada, pp. 171-188.

----------, and PETTIJOHN, F.J. 1971. Archaean sedimentation : Analysis of the Minnitaki Basin, North Western Ontario, Canada. Geological Society of America Bulletin, 82: 2099-2130.

WASSERBURG, G.J. 1987. Isotopic abundances : inferences on solar system and planetary evolution. Earth and Planetary Science Letters, 86: 129-173.

WEAVER, B.L., and TARNEY, J. 1979. Thermal aspects of Komatiite generation and greenstone belt models. Nature, 279: 689-692.

WENTWORTH, C.K. 1922. A field study of the shapes of river pebbles. Bulletin U.S. Geological Survey, 730-C. 114 pp.

WEST, W.S. 1980. Formation of continental crust. In the Continental crust and its mineral deposits. Edited by D.W. Strangway. Geological Association of Canada, Special paper, 20: 117-148.

WILSON, J.F., and NUTT, T.H.C. 1990. The nature and occurrence of mineralisation in the early Precambrian crust of Zimbabwe. In Precambrian Continental Crust and its Economic Resources. Edited by S.M. Naqvi. Elsevier, Amsterdam, pp. 555-591.

WINDLEY, B.F. 1977. The Evolving Continents. New York, Wiley, 385 pp.

----------. 1981. Precambrian rocks in the light of the plate tectonic concept. In Precambrian plate tectonics. Edited by A. Kroner. Elsevier, Amsterdam, pp. 1-20.

----------. 1984. The Archaean-Proterozoic boundary. Tectonophysics, 105: 43-53.

WRONKIEWICZ, D.J., and CONDIE, K.C. 1987. Geochemistry of Archaean shales from the Witwatersrand supergroup, South Africa : source area weathering and provenance. Geochimica et Cosmochimica Acta, 51: 2401-2416.

----------, and ----------. 1989. Geochemistry and provenance of sediments from the Pongola Supergroup, South Africa : evidence for a 3.0 Ga old continental craton. Geochimica et Cosmochimica Acta, 53: 1537-1549.

WYLLIE, P.J. 1973. Experimental petrology and global tectonics - pre-review. Tectonophysics, 17: 189-209.

YOUNG, G.M. 1978. Some aspects of the evolution of the Archaean crust. Geosciences, Canada, 5: 140-149.